Spring 2014

Designing Injectable Hydrogel Biomaterials with Highly-Tunable Properties

Mathew J. Patenaude

McMaster University, patenamj@mcmaster.ca

Designing Injectable Hydrogel Biomaterials with Highly-Tunable Properties

Designing Injectable Hydrogel Biomaterials with Highly-Tunable Properties

By

Mathew J. Patenaude, B.Sc.

A Thesis

Submitted to the School of Graduate Studies

in Partial Fulfillment of the Requirements

for the Degree

Doctor of Philosophy

McMaster University

DOCTOR OF PHILOSOPHY (2014) McMaster University

Department of Chemical Engineering Hamilton, Ontario

TITLE:	Designing Injectable Hydrogel Biomaterials with Highly-Tunable Properties
AUTHOR:	Mathew J. Patenaude, B.Sc. (Concordia University)
SUPERVISOR:	Professor Todd R. Hoare

ABSTRACT

Chemically cross-linked hydrogels (chemical gels) offer a number of enhanced properties over their physical counterparts, particularly in biomedical applications such as drug delivery, tissue engineering, and cell encapsulation. Conventional chemical gels are generally too elastic to be introduced into the body without requiring surgical implantation, making them challenging to use in a clinical context. In response, this thesis is focused on developing injectable analogues of conventional hydrogel-based biomaterials as well as advanced, engineered injectable hydrogels, enabling the facile use of these hydrogels in biomedical applications. Cross-linking is achieved using hydrazone chemistry, in which one precursor is functionalized with aldehyde groups and the other is functionalized with hydrazide groups. Following coextrusion of the reactive precursors, a stable hydrogel network spontaneously forms within seconds. By employing this chemistry as a standard in all of this work, a number of injectable hydrogel systems with well-defined properties (including swelling, drug loading and release, optical properties, gel formation and degradation kinetics, response to the temperature of the surrounding environment, and tissue response) have been generated that can be tuned by rationally varying the charge content in the precursor polymers, the number of cross-linking functional groups used, the reactivity of the electrophilic cross-linking units, and the length and number of hydrophobic affinity domains present within the gels. This work therefore presents a series of independent methods for customizing hydrogels so that they may be adapted to a number of different biomedical applications.

ACKNOWLEDGMENTS

This work would have been impossible without the continued support and guidance of a large number of individuals and organizations, and this document could not be considered complete without their inclusion.

My time at McMaster began with an enormous shock as I was making the transition from an undergraduate degree in biochemistry to graduate studies in engineering. Although this transition was a challenge for me, I had the unbelievably good fortune of working for Prof. Todd Hoare, whose encouragement and concern for his students made the transition more than manageable. Dr. Hoare's brilliance and devotion to his students have greatly enhanced my graduate career, and it has been an absolute honour to work for him.

I am grateful to Dr. Harald Stöver and Dr. Heather Sheardown for providing me with the support I've needed throughout graduate studies and helping to nudge my research in the right direction. I would like to thank Dr. Ryan Love and Rachelle Kleinberger for their willingness to work together on some of the most challenging projects of my graduate career. I would also like to extend a big thanks to NSERC for two USRAs, the McMaster School of Graduate Studies for the Ontario Graduate Scholarship, Clifton W. Sherman Scholarship, and the Queen Elizabeth II Scholarship, as well as the NSERC 20/20 Ophthalmic Materials Network for its financial contributions to my research.

I consider the time I have spent with friends at McMaster as valuable as the enormous opportunities for educational growth I've had during graduate studies. I am thankful to all of the members of Dr. Hoare's lab, past and present, and I consider myself blessed for

having made so many wonderful friends who have greatly enriched my time as a graduate student (and been audience to my somewhat neurotic side). In particular I'd like to thank Dr. Niels Smeets, Rabia Mateen, Scott Campbell, Daryl Sivakumaran, Emilia Bakaic, Danielle Maitland, and Trevor Gilbert. Thank you for our daily coffee breaks and lively conversations.

A great deal of thanks is owed to my parents, Ivan Patenaude, Linda Overing, Susan Woodard, and Roy Biedermann, and to my in-laws, Dr. David Lee Williams and Laurie Williams, the former of whom, in addition to making it physically possible for my academic accomplishments to reach fruition, have also guided and supported me my entire life, and the latter of whom have been more than encouraging to me in all my pursuits.

Finally, and most importantly, I must thank my wife Jessica, who has supported me immeasurably over the past five years. Thank you for being who you are. I love you.

TABLE OF CONTENTS

LIST OF FIGURES AND TABLES

LIST OF TERMINOLOGY, SYMBOLS, AND ABBREVIATIONS

"Modular" hydrogel	Hydrogels based on a PNIPAM nucleophilic precursor chain cross-linked with a pre-determined amount of an aldehyde-functionalized (i.e. electrophilic) polysaccharide (CMC and/or dextran)
^{1}HNMR	Proteum nuclear magnetic resonance
3T3	A mouse fibroblast cell line
4-hydroxy TEMPO	4-hydroxy-2,2,6,6-tetramethylpiperidin-1-oxyl
Å	Angstrom
AA	Acrylic acid
ACN	Acetonitrile
ADH	Adipic acid dihydrazide
AIBME	2,2-azobisisobutyric acid dimethyl ester
Ald	Aldehyde
AO-PEG	Aminooxy polyethylene glycol
BAC	Bisacryloylcystamine
BSA	Bovine serum albumin
$CDCl_3$	Deuterated chloroform
CMC	Carboxymethyl cellulose
CS	Chondroitin sulfate
CuAAC	Copper(I)-catalyzed alkyne-azide click reaction
D	Dextrorotatory
Đ	Dispersity

D_2O	Deuterated water
Da	Dalton
DBCO	Dibenzocyclooctyne
Dex	Dextran
DHOPMA	2,3-dihydroxypropyl methacrylate
DIBO	4-dibenzocyclooctynol
DIFO	Difluoro cyclooctyne
DIW	Deionized water
DMEM	Dulbecco's Modified Eagle Medium-high glucose
DMF	Dimethylformamide
DMSO-D_6	Deuterated dimethylsulfoxide
DTP	3,3'-dithiobis(propanoic dihydrazide)
DTT	Dithiothreitol
DxSO4	Dextran sulfate
EDC	1-Ethyl-3-(3-dimethylaminopropyl)carbodiimide
EDTA	Ethylenediaminetetraacetic acid
EtOH	Ethanol
f	Average number of charges between hydrogel cross-links
FBS	Fetal bovine serum
FITC	Fluorescein isothiocyanate
G'	Elastic modulus
G'p	Plateau modulus

G”	Loss modulus
GPC	Gel permeation chromatography
GSH	Glutathione
H&E	Hematoxylin and eosin
HA	Hyaluronic acid
HA-PD	Hyaluronic acid pyridyl disulfide
HCl	Hydrochloric acid
HEMA	2-hydroxyethyl methacrylate
HPLC	High performance liquid chromatography
HS	Horse serum
I(q)	Scattering intensity
IL	Interleukin
k'	Pseudo first-order rate constant
k_b	Boltzmann constant (1.381×10^{-23} m^2 kg s^{-2} K^{-1})
Ket	Ketone
L	Levorotatory
LCST	Lower-critical solution temperature
M	Molar (mol/L)
$M(EO)_2MA$	Di(ethylene glycol) methyl ether methacrylate
MeCe	Methyl cellulose
MEHQ	Methyl ether hydroquinone
Mn	Number average molecular weight

MSC	Mesenchymal stem cells
MTT	3-(4,5-dimethylthiazol-2-yl)-2,5-diphenyltetrazolium bromide
MWCO	Molecular weight cut-off
MWD	Molecular weight distribution
N_A	Avogadro's number (6.022×10^{23})
NaCl	Sodium chloride
NaOH	Sodium hydroxide
NMR	Nuclear magnetic resonance
N_x	Average number of monomers between hydrogel cross-links
OEGMA	Oligo(ethylene glycol methacrylate)
OLA	Oligo(lactic acid)
oxCMC	Oxidized carboxymethyl cellulose
oxDex	Oxidized dextran
oxHA	Oxidized hyaluronic acid
oxMeCe	Oxidized methyl cellulose
PBS	Phosphate buffered saline
PDI	Polydispersity index
PEG	poly(ethylene glycol)
PEG-DS	Polyethylene glycol dithiol
PEG-K	Ketone-functionalized polyethylene glycol
PEO	Poly(ethylene oxide)

PHEMA	poly(hydroxyethyl methacrylate)
PLA	Poly(lactic acid)
PLGA	Poly(lactic acid-co-glycolic acid)
PNIPAM	Poly(N-isopropylacrylamide)
PNIPAMAAm	Poly(n-isopropylacrylamide) (alternate abbreviation)
POEGMA	poly(oligoethylene glycol methacrylate)
POEGMA-PLA	Poly(oligoethylene glycol methacrylate)-PLA
Poly(NIPAM-co-ADH)	Copolymer consisting of n-isopropylacrylamide and hydrazide-functionalized repeat units
PS	Penicillin streptomycin
PVA	Poly(vinyl alcohol)
PVCL	Poly(vinyl carprolactone)
PVP	Poly(vinylpyrrolidone)
Q_m	Gel swelling ratio
R	Gas constant (8.314 J K^{-1} mol^{-1})
RI	Refractive index
RPE	Retinal pigment epithelial
SANS	Small angle neutron scattering
SEC	Size-exclusion chromatography
SMCC	4-(N-maleimidomethyl)cyclohexane-1-carboxylate
SPAAC	Strain-promoted alkyne-azide cycloaddition
T	Temperature

TGA	Thioglycolic acid
TNBS	2,4,6-trinitrobenzenesulfonic acid
UV	Ultra-violet
V_G	Gel volume
VPTT	Volume phase transition temperature
VS	Vinyl sulfones
X	Mole fraction
αCD-N3	Azido-functionalized α-cyclodextrin
η^*	Complex viscosity
π	Osmotic pressure
ρ	Cross-link density of a hydrogel (alternate abbreviation)
υ_e	Cross-link density of a hydrogel
ϕ	Volume fraction of polymer in a hydrogel
ϕ_0	Volume fraction of polymer in a hydrogel prior to swelling in aqueous media
ϕ_E	Volume fraction of polymer in a hydrogel at the maximum swollen state
χ	Flory-Huggins solubility parameter

DECLARATION OF ACADEMIC ACHIEVEMENT

The majority of the work described in this thesis was conceived, conducted, interpreted, and written by the author of this thesis, with the following exceptions:

- Chapter 1 was partially written by Niels Smeets, whose name is in the paper's list of authors. Dr. Smeets wrote the portions of the review pertaining to sections 3.1 and 3.2 along with a portion of the introduction of the article.

- Sections pertaining to *in vitro* MTT toxicity studies in chapter 3 were carried out by Scott Campbell, who is listed as an author on the paper from which chapter 3 is derived. His contributions include performing the assays, interpreting their results, and writing sections of the manuscript pertinent to the assays.

- The manuscript used for chapter 5 of this thesis was co-written by Ryan Love and myself. My contributions to this work included all material design, synthesis, and characterization. I performed some of the animal work, including resection of injected hydrogels. I also wrote the sections of the manuscript pertaining to my contributions, which spanned through the introduction, experimental, results, and discussion sections. All other work was carried out by Dr. Love.

- The manuscript for chapter 6, on which I am designated as second author, was mostly written by Niels Smeets. My contributions included small molecule (i.e. monomer) synthesis, macromolecular characterizations, including swelling and mechanical assays, and drug release assays. I wrote the original article, which was greatly expanded upon by Dr. Smeets with the inclusion of his own contributions (consisting of all remaining experimental aspects of the paper).

INTRODUCTION

The tremendous advancements in polymer science over the past few decades have provided researchers with a unique opportunity to overcome some of the most fundamental limitations facing pharmacology. In this regard, a particular challenge is achieving spatial and temporal control over the delivery of therapeutics in the body following systemic administration. Conventional routes of drug administration, including oral, nasal, intravenous, or intramuscular routes, are generally indirect and take place far removed from the drug's intended site of action within the body. Upon entering the general circulation, the drug generally reaches a distribution equilibrium with the body's tissues and may be biotransformed to an inactive state prior to reaching an effective dose at its intended site. In general, these two effects governing a drug's pharmacokinetics limit the amount of drug available at the desired site within the body, effectively diluting its effects. Of greater concern are therapeutics that can cause systemic damage following uptake by the body, such as in the case of chemotherapeutics. While such drugs are often desired to behave site-specifically, systemic administration promotes their action on tissues throughout the body. The emergence of cell-based therapies requires the entrapment of cells within a matrix in order to prevent migration away from the site of administration and support cell adhesion during the tissue repair process. These matrices may also provide a micro-environment for loaded cells to migrate through and communicate in the context of tissue engineering. On these bases, there is a clear need to

develop biocompatible systems that can be delivered site-specifically and are capable of delivering a therapeutic at a controlled rate.

Polymers have attracted particular interest in terms of addressing these pharmaceutical challenges. The chemical diversity of polymers and the ability to design them from the ground up (i.e. from simple monomer units) makes them attractive as pharmaceutical delivery vehicles since they can be adapted for use with a number of different drugs and dosing regimens. For water-soluble drugs, macromolecular drugs, and cells in particular, hydrogels have attracted specific interest. Hydrogels are water-swollen three-dimensional networks consisting of cross-linked polymer chains, with cross-linking occuring via either physical interactions or chemical bond formation between polymer chains. The chemical and mechanical similarities between hydrogels and the mammalian extra-cellular matrix[1] can impart hydrogels systems with the ability to remain undetected following placement within the body, as the body's host defenses may not deem the implanted hydrogel as being different from the body's native tissues. As a result, pre-loaded cargoes bound for a pre-determined location *in vivo* can avoid premature degradation by being protected within the matrix of the biologically inert hydrogels, potentially increasing the efficiency of cell, small molecule, or macromolecular therapy. In the context of tissue engineering, hydrogels may provide an environment for directed adhesion, spreading, growth and/or differentiation of cells into the desired tissue construct. Hydrogels made for applications in tissue engineering may potentially offer selectivity over nutrient uptake or even influence the fate of cellular growth based on the physical properties of the surrounding hydrogel environment that has been pre-seeded with precursor cells.[2,3]

While the several advantageous properties of hydrogels in biomedical applications have motivated significant research into such materials, the practical introduction of hydrogels into the body is a significant challenge limiting their routine clinical application. Materials that are difficult to introduce into the body are generally associated with high levels of patient discomfort and may therefore result in a lower degree of patient compliance. The high elasticity of conventional hydrogels has particularly limited the administration of these materials through non-invasive techniques, such as though injection. As a result, gels pre-formed outside of the body must often be introduced surgically to their target site of therapeutic application.

In previous work, this limitation has been addressed by using gels that form spontaneously *in vivo* through physical interactions between polymer chains following injection, taking advantage of unique properties of the biological environment such as ionic strength, pH, or temperature to trigger self-associations.[4,5] Physical gelation may also be triggered by using precursor polymers designed to possess latent physical inter-chain interactions, such as stereochemical,[6] electrostatic,[7] supramolecular,[8] or hydrophobic interactions.[9] These relatively weak interactions can be momentarily disrupted through the application of mechanical energy in the form of a shear force such as the force that is applied to the barrel of a syringe, enabling these precursors to be injected into the body; after, the gels may then spontaneously reform *in situ* through reassociation of physically complimentary moieties once the injection shear is removed.[10] The inherent attractiveness of this approach to gel fabrication lies not only in the ease of introduction of such materials but also in the lack of functional chemistries required for

gelation, as latent reactive functional groups are often not be well tolerated within the body.[11] However, physically cross-linked hydrogels face two major challenges that limit their overall efficacy in application. First, a reliance on physical interactions between polymer chains for gelation limits the degree of control that can be exerted over which the timescale of gel degradation within the body, with most gels susceptible to rapid dissolution by the body and subsequent dissolution (or at least rapid loss of mechanical integrity). This can be a major challenge in the biomedical context, as pre-loaded cargoes may not be secured within the context of a protective matrix throughout a pre-determined therapeutic window. For example, the thermogelling Poloxamer triblock copolymer poly(ethylene oxide)-b-poly(propylene oxide)-b-poly(ethylene oxide) has been shown to degrade and be reabsorbed by the body in a matter of hours subsequent to administration.[12] Second, the inherently dynamic nature of inter-chain physical interactions often limits the mechanical strength of these physically cross-linked gels, particularly under shear. Although this shortcoming can in part be addressed by increasing the number of polymer chains composing the physical gels, an increase in the local concentration of polymer can increase the osmotic gradient into the matrix and potentially dehydrate surrounding tissues.[13]

These limitations have encouraged the growth of a class of hydrogels formed via covalent bond formation between polymer chains. By controlling the number of complimentary reactive groups (typically electrophiles and nucleophiles) present on component precursor polymer chains, it is possible to pre-program the relative density and types of cross-links present within the hydrogel matrix.[14] In this way, the rate of hydrogel formation and

degradation and gel mechanical properties can be controlled to a degree not offered by physical gels. Unfortunately, hydrogels pre-formed in this way outside of the body generally do not possess the shear-thinning qualities of physically cross-linked hydrogels, making them difficult to introduce into the body through minimally invasive means. For this reason, there is a growing interest in hydrogels that can rapidly form under physiological conditions via chemical reactions between complimentarily functionalized precursor polymers subsequent to their co-administration at a desired site. Typically, two precursor copolymers are coinjected that possess complimentary nucleophilic and electrophilic functionality (or one polymer coinjected with a small molecule cross-linker with complimentary functionality) that spontaneously form a covalent bond *in situ* following co-injection. Chapter 1 of this thesis provides an exhaustive critical analysis of such systems and comprehensively reviews the different chemical techniques employed in the development of *in situ* forming injectable hydrogels.

In order to effectively inject complimentary precursor copolymers to the intended site of therapeutic action within the body, the injected aqueous copolymer solutions must be of sufficiently low viscosity that the reactive precursors can be injected through a standard 25G hypodermic needle.[15] More importantly, measures must be taken in order to prevent gel formation prior to the precursor solutions being introduced into the body. This may be achieved by physically separating the two reactive solutions using a double barrel syringe, in which reactive precursors are introduced into different barrels and are mixed and co-extruded into the body only after depression of the plunger (Figure 1). Although co-injection occurs rapidly, extrusion of the reactive precursors must be quicker than the

macroscopic onset of gel formation; however, gel formation must occur rapidly enough such that the reactive precursors (or their loaded cargoes) do not do not diffuse away from the site of administration *in vivo* prior to gel network formation. In this way, gel formation is temporally and spatially restricted to only occur *in vivo*.[14,16–20] The rate of gel formation depends primarily on the degree of polymer functionality (functional group concentration) and on the specific chemistries employed in the formation of covalently cross-linked *in situ* forming hydrogels and is typically targeted to occur within seconds to minutes depending on the application.

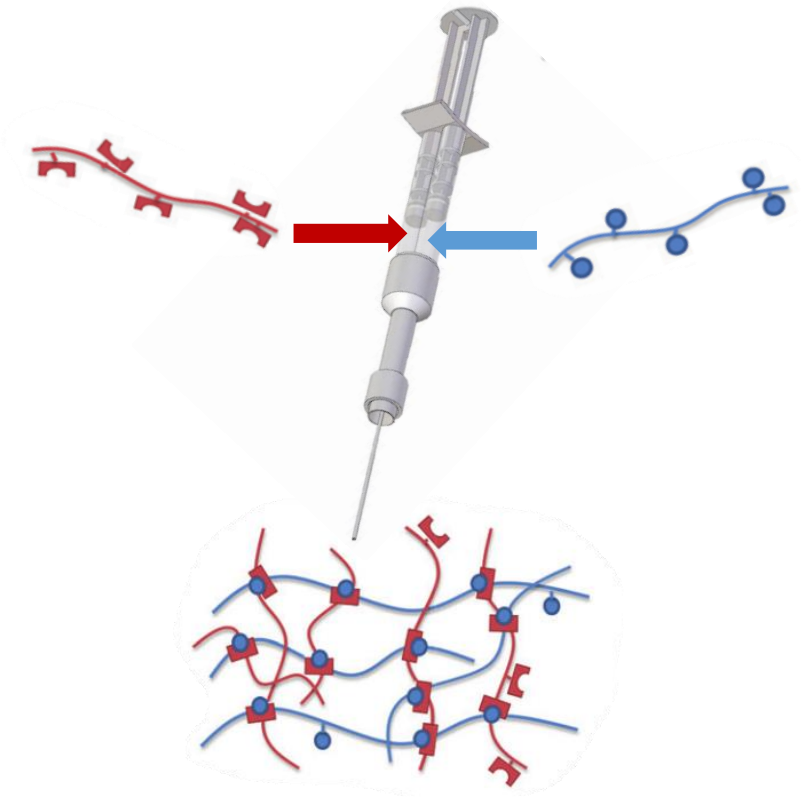

Figure I.1 – Double barrel syringe to coextrude functionalized electrophilic and nucleophilic precursor copolymer chains. The mixed polymer solution rapidly forms a stable chemically cross-linked hydrogel post-needle (i.e. in the body).

During the tenure of my Ph.D. studies, I have sought to develop novel injectable hydrogel systems that form *in situ*. A particular emphasis has been placed on developing systems with highly tunable properties that can provide a design framework that may be used to make these systems adaptable for use in a number of different biomedical applications, including drug delivery, cell encapsulation, and tissue engineering.

In this work, I begin by describing a rapidly-forming injectable, degradable, and environmentally responsive hydrogel system, which is covered in the second chapter of this thesis.

In the third chapter of this thesis, I have expanded upon the work described in the first chapter by incorporating an additional, less electrophilic, ketone monomer along with a more electrophilic aldehyde monomer within the electrophilic polymer chains. By co-functionalizing these electrophilic hydrogel precursor chains with different ratios of aldehyde to ketone groups, I have been able to fine-tune a number of gel properties, including the rates of gel formation and degradation, gel opacity, and gel mechanical properties.

I then expand on this work by demonstrating a "modular" approach to hydrogel design (presented in chapter 4 of this thesis), whereby fine-tuning different hydrogel components on either the monomeric or macromolecular level enables us to exercise fine control over a number of gel properties, including the rate of gel formation and degradation, mechanical properties, transparency, swelling, drug loading and release, and response toward the temperature of the local environment.

Chapter 5 expands upon the theme of highly-tunable injectable hydrogels by describing systems with a range of different hydrophobicities. Using this approach, the degree of gel swelling, gel mechanical properties, degradation kinetics, and protein loading and release can be rationally tuned.

CHAPTER 1

DESIGNING INJECTABLE, COVALENTLY CROSS-LINKED HYDROGELS FOR BIOMEDICAL APPLICATIONS

Authors: Mathew Patenaude, Niels M. B. Smeets, and Todd Hoare

Publication Information: Macromolecular Rapid Communications 35(6), 598-617

Accepted Date: Jan 19, 2014

Abstract: Hydrogels that can form spontaneously via covalent bond formation upon injection in vivo have recently attracted significant attention for their potential to address a variety of biomedical challenges. In this review, we discuss the design rules for the effective engineering of such materials and outline (with examples) the major chemistries used to form injectable, in situ-gelling hydrogels in the context of these design guidelines. Directions for future research in the area are addressed, noting the outstanding challenges associated with the use of this class of hydrogels in vivo.

1. Introduction

Hydrogels are three dimensional, water-swollen polymer networks formed as a result of physical or chemical cross-linking between water-soluble polymer chains.[1] Given their high water content, controllable porosity, and mechanical and (potentially) compositional similarities between hydrogels and native soft tissues in the body,[2] hydrogels have been widely investigated for tissue engineering, bioadhesives, would healing, space-filling, cell encapsulation and controlled release applications.[3–6] The design of these soft materials has benefitted greatly from recent developments in polymer science that have enabled the synthesis of polymers with unprecedented control over molecular weight, composition, topology and functionality.[7] Imparting this control on a linear polymer level to a hydrogel network has resulted in the design of novel hydrogels that can change their water content in response to one or more environmental stimuli,[8] have more uniform networks,[9,10] or can dynamically rearrange their structure.[11–13]

Successful biomedical application of conventional hydrogels, however, remains somewhat limited given that the inherent elasticity of hydrogels limits their ability to be delivered via an injection or any other minimally-invasive (i.e. non-surgical) route. Most synthetic hydrogels are prepared using free radical chemistry and/or functional group condensation chemistry, which is generally incompatible with in vivo conditions.[14] One clinical exception to this rule is in situ photopolymerization of hydrogels, which has found significant applications in conjunction with surgical interventions as adhesion prevention materials.[15] However, the need for a small molecule photoinitator as well as UV irradiation

over (in most cases) several minutes to induce gelation both pose potential safety concerns with this technique, as does the highly exothermic nature of free radical polymerization that can lead to undesirable heat generation in vivo and induce cell stress or cell death. Furthermore, the poor penetrability of UV irradiation negates the use of such materials in any non-invasive applications outside of near-surface transdermal applications.[16]

As a result of these limitations, significant research efforts have recently been invested in the design of "injectable" or "in situ gelling" hydrogels that can be delivered in vivo via injection and then rapidly gel inside the body.[17] Injectable hydrogels circumvent the need for surgery to administer the hydrogel in vivo, reducing pain while minimizing, healing time, scarring and the risk of infection. Injectability also enables effective molding of the hydrogel shape in situ by the neighboring tissue to fit cavities and/or tissue defects, of tremendous application in space filling or anti-adhesion applications.

Injectable hydrogels can be formed by exploiting a variety of physical cross-linking interactions that can be triggered by the unique pH/temperature/ionic strength environment of the body (typically driving a phase transition in all or part of the pre-gel polymers that induces physical interactions between the chains)[18,19] or by latent physical interactions between the pre-gel components (e.g. electrostatic interactions,[20] stereochemical interactions,[21] supramolecular chemistry,[22] or hydrophobic interactions[23]) that can be disrupted by shear.[24] The advantage of using physical cross-linking approaches is that no reactive functional group chemistry is required to form hydrogels in vivo, typically resulting in acceptable tissue responses to such materials over multiple types of applications.[25] However, physical in situ gelling hydrogels suffer from two significant

limitations that significantly hinder their wide-spread use in clinical settings. First, the use of physical interactions for cross-linking imparts minimal control over the clearance rate of the hydrogel in vivo and thus the therapeutic window associated with the material. For more weakly associated materials, the infinitely diluting environment of the body can significantly reduce the local polymer concentration over time, leading to (in some cases rapid) dilution of the hydrogel and a loss of mechanical integrity. For example, the widely-investigated thermogelling Poloxamer polymers (triblock poly(ethylene oxide)-*b*-poly(propylene oxide-*b*-poly(ethylene oxide) copolymers) have been observed to resorb within hours once injected in vivo even at high polymer concentrations.[26] In other cases in which the physical interaction is significantly stronger,[27] there is no clear mechanism to degrade the hydrogel outside of backbone degradation, either limiting the composition of physical gels to those with degradable polymer backbones or leading to a risk of bioaccumulation and resulting chronic inflammatory responses. Second, the mechanical strength of physically-gelled hydrogels is typically relatively low due to the often times dynamic nature of bond formation/breaking in physically-cross-linked hydrogels, particularly in the presence of even low magnitudes of shear. Improvements in mechanical strength can be achieved when extremely high polymer concentrations are used to form the gels, but this creates large osmotic gradients that can dehydrate surrounding tissues and/or further speed hydrogel degradation via dilution.[28] It must be noted that some more recent examples of physically cross-linked hydrogels (e.g. peptide assemblies) have significantly improved both the stiffness and stability achievable with physically cross-linked hydrogels[29], although such control often comes at the price of chemical versatility in the

hydrogel backbone. Overall, while physically-cross-linked injectable hydrogels may have significant advantages for shorter-term biomedical applications, they generally do not offer desirable properties for longer-term applications.

To overcome these challenges, a growing body of research is focused on the design of injectable hydrogels that are cross-linked via covalent bond formation. Typically, such gels are formed by mixing two polymers (or one polymer and one small molecule cross-linker) with complementary reactive functional groups that can lead to covalent bond formation. In this review article, we will provide a framework for the rational design of injectable and covalently cross-linked hydrogel systems. We will first discuss the design requirements of the precursors and degradation products of in situ-gelling hydrogels (as dictated by the in vivo use of these materials), followed by a discussion of different cross-linking chemistries amenable to in situ hydrogel formation in the context of currently reported injectable and covalently cross-linked hydrogel systems for controlled release and tissue regeneration. A particular focus is placed on the use of covalent chemistries that do not interfere with native biological molecules and are therefore considered toxicologically inert, a significant challenge in the field given the inherent chemical reactivity required in the precursor polymers in order to facilitate fast covalent gelation upon mixing. Due to the diversity and depth of the work published on hydrogel-based materials for biomedical applications, we have limited the focus of this review to injectable and covalently cross-linked systems; for more information on the synthesis and biomedical applications of other classes of injectable hydrogels, readers are referred to excellent earlier reviews.[17,24,30–33]

2. Designing injectable and covalently cross-linked hydrogels

Injectable hydrogels based on covalent bond formation must meet several criteria for their effective use in a clinical application. The key design requirements of injectable hydrogels are described below, with specific reference to the typical applications of such hydrogels.

2.1. Delivery mode: In order to reduce or eliminate the need for surgical procedures associated with the use of a hydrogel-based material in vivo, it is important that hydrogel precursors can be introduced into the body via a minimally invasive manner. This requires the use of precursor solutions that are either of sufficiently low viscosity or sufficiently shear-thinning that they can be extruded through at least a standard 25G hypodermic needle.[34] The maximum size of the needle may be even smaller in some applications (e.g. many ophthalmic injections routinely utilize 33G needles). As such, minimizing the viscosity of the precursor solution would facilitate use of the formulation in the maximum possible number of potential clinical settings. The delivery mechanism selected must also consider how to prevent gelation prior to administration in vivo. In most cases, this has been achieved by physically separating the two reactive polymer components in separate barrels of a double-barrel syringe, analogous to epoxy glue; co-extrusion of the two polymers through a static mixer mixes the precursor polymers on contact to induce gelation only upon delivery.[35–38] Alternately, precursor polymer solutions can be stored pre-mixed at pH conditions not amenable to cross-linking, using the body chemistry to actively titrate the mixture upon injection to physiological pH to drive gelation. In either case, for practical clinical use, the precursor polymer solutions must be stable in the pre-loaded solutions over

the course of several months at room temperature or, at minimum, under refrigerated storage without undergoing significant degradation or deactivation of the reactive functional groups.

2.2. Gelation kinetics: Gelation should occur quickly after injection, within seconds to a few minutes, under physiological conditions (aqueous, 37°C, 0.15M ionic strength, pH 7.4). Fast gelation is favorable to prevent leaching of the precursors away from the injected site, which significantly reduces the local polymer concentration and thus both volume and the ultimate mechanical strength of the resulting hydrogel. Furthermore, slow gelation would allow for diffusion of the precursor polymers (as well as any entrapped therapeutic in a drug delivery application) into surrounding tissues, leading to potentially unfavorable cross-linking reactions with surrounding tissue, potential toxicity due to high concentration of reactive polymer released locally, and (for drug delivery applications specifically) significant undesirable burst drug release. This requirement for fast gelation typically makes the pH-induced gelation mechanism described above typically less attractive than the use of a double-barrel syringe technique, as the gelation speed is in the former case inherently limited by mass transport of titrating ions into the pre-gel solution. Gelation time is in large part determined by the kinetics of the in situ gelling chemistry chosen, but can be reduced to some degree by using higher concentrations of higher molecular weight polymer precursors which require the formation of fewer bonds in order to effectively form a gel network.

2.3. Cross-linking chemistry: Most in situ-gelling hydrogels reported are cross-linked based on substitution or condensation reactions between one polymer functionalized with a

nucleophilic functional group and another polymer functionalized with an electrophilic functional group. Ideally, the cross-linking functional group pair would react both quickly (i.e. with a low activation energy) and orthogonally with functional groups normally present in biological tissues. Given the diversity of functional groups present in the body, true orthogonality is frequently difficult to achieve in injectable polymer formulations. However, many reported injectable gel systems with the potential to react with complementary functional groups on biological proteins (and thus disrupt the tertiary structure responsible for protein activity) have still been demonstrated to show good tissue responses.[37] In most cases, this positive tissue response can likely be attributed to the "kinetic orthogonality" of the cross-linking functional groups; that is, the desired cross-linking reaction occurs much faster than any competing reaction with tissue-borne functional groups such that any competing chemistries with native tissues are strongly suppressed.

2.4. Backbone chemistry: Both natural polymers (e.g. carbohydrates, polypeptides, etc.) and synthetic polymers may serve as useful backbones for the fabrication of covalently cross-linked injectable hydrogels. Natural polymers have many advantages such as biocompatibility, degradability and innate biological activity (i.e. they can play specific roles in native biological signaling and cell adhesion events);[39,40] however, their pre-defined chemistries and biological functions may also limit their utility in some applications. Consequently, many emerging hydrogel designs are based on synthetic polymers which (if non-cytotoxic and clearable) offer the advantage of outstanding control over the composition of the precursors and, therefore, the physicochemical properties of

the hydrogel. Typically, the use of synthetic polymers as injectable hydrogel precursors mandates the pre-polymerization of the monomers into a functional oligomer, typically in the presence of a chain transfer agent or in the context of a controlled radical polymerization method to limit the molecular weight of the carbon-carbon backbone.[41] Polymeric precursors are generally less cytotoxic compared to their low molecular weight analogues and benefit from a multivalency effect in that they can form hydrogels at much lower concentrations than low molecular weight molecules. Synthetic "smart" polymers that exhibit lower critical solution temperatures (LCST) in water have become of particular interest for biomedical applications and thus injectable hydrogel design. Polymers such as poly(N-isopropylacrylamide) (PNIPAM),[42] poly(vinyl caprolactone) (PVCL)[43] or poly(oligoethylene glycol methacrylate) (POEGMA)[44] are completely soluble at a temperature below their LCST but undergo a conformational change, collapse and precipitate from solution once heated above their LCST. This temperature transition can be used to trigger a macroscopic change in swelling within the hydrogel that can be applied to, for example, alter cell/protein interactions with the hydrogel in tissue engineering applications or induce pulsatile release in drug delivery applications.[35,37]

2.5. Backbone functionalization: The degree to which the precursor polymer backbones are functionalized with reactive groups must be carefully considered depending on the ultimate application of the hydrogel. Important hydrogel properties such as the cross-link density, pore size, and degree of swelling can be controlled (or at least influenced) by tuning the average number of reactive functional groups per polymer chain and thus the average molecular weight between adjacent cross-linking points (M_c). Gel swelling and

average gel pore size can be directly predicted based on M_c by applying the Flory-Huggins relationship (Equation 1),[36] where a is the gel dimension, T is temperature, χ is the solubility parameter, k_b is the Boltzmann constant, f is the average number of charges between cross-links within the gel matrix, N_x is the average number of monomers between the cross-links, and ϕ and ϕ_0 are the volume fractions of polymer in the gel at the equilibrium condition and the zero-strain condition respectively.

$$\begin{aligned}\pi_{\text{total}} &= \pi_{\text{mixing}} + \pi_{\text{elastic}} + \pi_{\text{Donnan}} \\ &= -\frac{k_b T}{a^3}(\varphi + \ln(1-\varphi) + \chi\varphi^2) + \frac{k_b T \varphi_0}{a^3 N_x} \\ &\left[\frac{1}{2}\left(\frac{\varphi}{\varphi_0}\right) - \left(\frac{\varphi}{\varphi_0}\right)^{1/3}\right] + \frac{k_b T}{a^3}\frac{\varphi_0 f}{N_x}\left(\frac{\varphi}{\varphi_0}\right)\end{aligned} \quad (1)$$

A high number of reactive groups would typically result in highly cross-linked, highly elastic hydrogels with a small pore size; conversely, a low number of reactive groups results yields a soft hydrogel with a larger pore size. Thus, to a first approximation, the number of reactive functional groups on the polymer backbone can be manipulated to modulus match stiffer soft tissues in the body, manipulate the biological responses of cells entrapped within the hydrogel,[45] reduce diffusion through the gel matrix, and/or reduce the time required for the hydrogel to cross-link. It should be emphasized that the gelation time and the cross-link density of the ultimate hydrogel are, for a given gelation chemistry, intimately linked; increasing the functional group density drives both faster gelation and higher cross-link densities. Two additional caveats must be mentioned with regard to this tunability of gel mechanics via manipulation of the precursor reactive functional group density: (1)

increasing the degree of functionalization increases potential steric effects that can limit the ability of nearby or adjacent functional groups on the polymer backbone to form cross-links with the complementary polymer, typically leading to lower numbers of cross-links per available functional group with more highly functionalized precursor polymers and (2) significantly increasing the density of reactive functional groups dilutes the effect of the principal backbone co-monomer on the hydrogel properties, potentially leading to an increased inflammatory response, a reduced magnitude "smart" response, etc. at higher degrees of chain functionalization.

2.6. Tissue interactions: Both the hydrogel as well as the hydrogel precursors, cross-linkers and degradation products must cause a minimal response from the body's innate and adaptive immune systems in order for the injectable hydrogel formulation to have potential clinical relevance. Inflammation as a response to the presence of a hydrogel in vivo may initiate the formation of granulation tissue, a foreign body response, and eventually the formation of a fibrous capsule walling-off the hydrogel from the surrounding tissue.[46] Such "walling off" responses would negate the effective use of the hydrogel in tissue engineering or cell encapsulation (no cellular access to oxygen/nutrients) and drug delivery (significantly hindered mass transport of loaded drug into the body), among other applications. The inflammatory response is in large part controlled by the interfacial properties of the hydrogel, or any other biomaterial.[47] Opsonin proteins in vivo adsorb to the surface of biomaterials to "mark" foreign materials for clearance and subsequently initiate an immune response. As highly hydrophilic and water-swollen materials, hydrogels are innately significantly less prone to opsonization compared to other classes of foreign

materials.[48,49] However, the presence of residual reactive functional groups following gelation can lead to significantly higher protein adsorption/grafting reactions in injectable hydrogels relative to conventional hydrogel systems. Thus, minimizing the number of residual functional groups following gelation (particularly those not orthogonal with protein functional groups) is generally desirable and achievable at least in part by manipulating the stoichiometry of the complementary reactive functional groups in the precursor polymer mixture. In many cases, one of the reactive functional groups is significantly more deleterious than the other in terms of inducing inflammatory responses; in such cases, preparing gels using a precursor mixture containing a large excess of the less deleterious functional group (and thereby maximizing consumption of that functional group during gelation) can significantly improve the observed tissue response. As an example, Tao *et al.* reported significantly less ophthalmic inflammation related to hydrogels prepared from methacrylate end-capped PEG and thiolated four-armed PEG as the thiol to methacrylate ratio in the precursor mixture was increased.[50]

2.7. Clearance: After injection, for most relevant biomedical applications, hydrogels should degrade into non-toxic fragments that can either be metabolized or cleared from the body at a rate matched to the intended application of the hydrogel. The use of natural polymers such as chitosan, hyaluronic acid (HA), alginate, or elastin offers the advantage that the hydrogel components are ultimately degraded and metabolized into biocompatible small molecule products in vivo at well-defined rates. Synthetic polymers based on PNIPAM, poly(ethylene glycol) (PEG), poly(hydroxyethyl methacrylate) (PHEMA), poly(vinylpyrrolidone) (PVP), or other polymers with carbon-carbon backbones cannot be

degraded into small molecule products via natural mechanisms and thus must be of sufficiently low molecular weight to allow for renal clearance. Typically, a molecular weight limit of 20×10^3 to 60×10^3 $g \cdot mol^{-1}$ has been reported for kidney clearance of macromolecules, which corresponds to the albumin excretion limit.[51] The rate of degradation is an important design criteria that can be exploited to optimize the utility of the hydrogel in a specific application.[52] For example, a fast degrading hydrogel network would result in a burst release of contained therapeutics, while a slow degrading hydrogel can provide for sustained drug release over a prolonged period of time. It should be noted that clearance is not necessarily required in all biomedical applications of hydrogels; for example, the use of hydrogels as dermal fillers may benefit from a more permanent, non-degradable matrix.

3. In situ-gelling chemistries for injectable hydrogel formulations

Based on the requirements outlined above, a variety of chemistries has been explored for the generation of injectable hydrogels cross-linked via covalent bond formation. Figure 1.1 shows the chemistry of the most common approaches to cross-link formation. The mechanisms, applications, and both benefits and drawbacks associated with each of these in situ-gelling chemistries are outlined in the sections to follow.

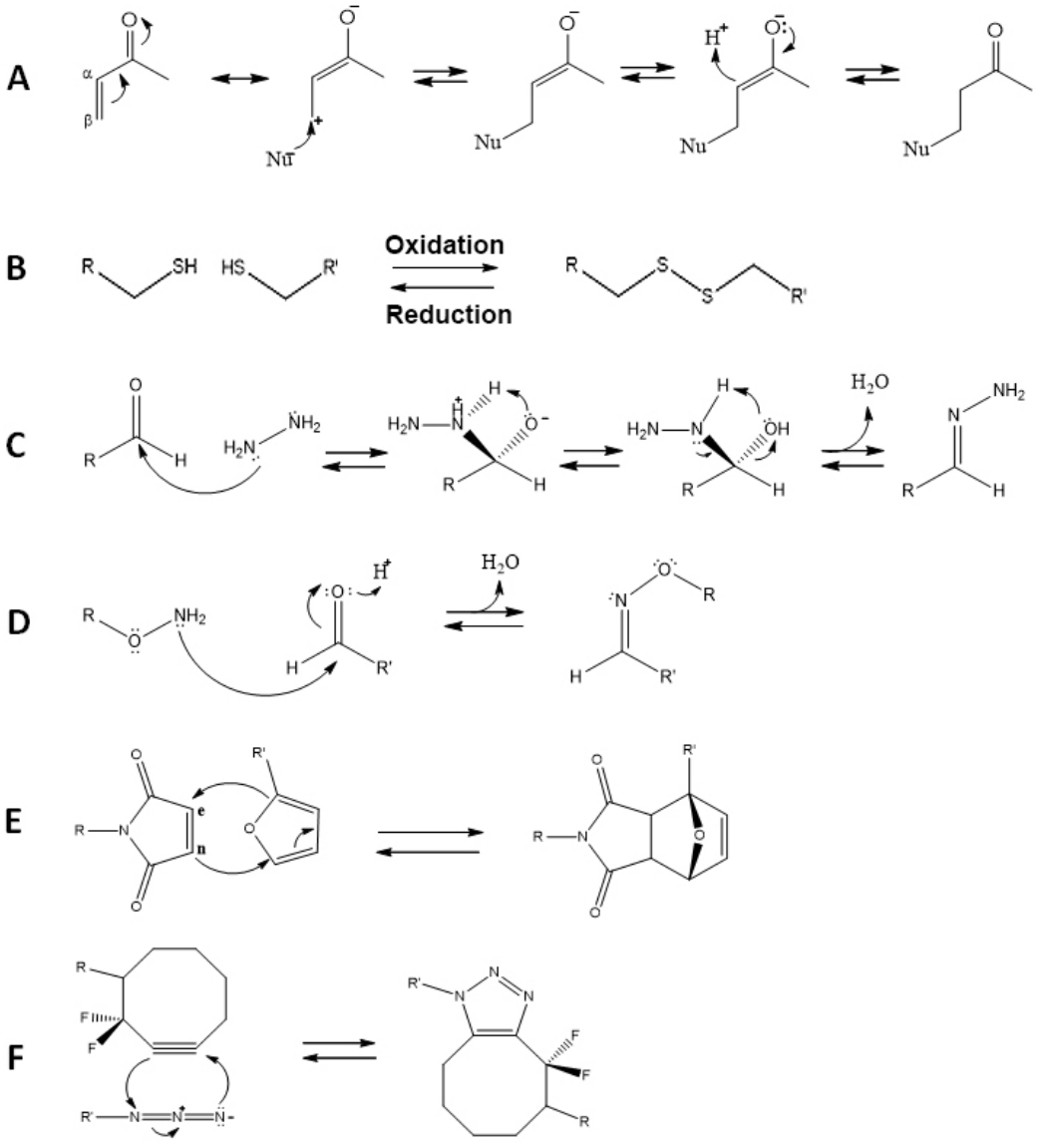

Figure 1.1. Chemistries used in forming in situ gelling, covalently cross-linked hydrogels: A - 1,4-addition (Michael-type addition); B - disulfide formation 2+4; C - hydrazone condensation; D - oxime formation; E - alkyne azide 1,3-dipolar Huisgen cycloaddition; F - Diels-Alder cycloaddition

3.1 Cross-linking via conjugate 1,4 addition (Michael-type addition): The 1,4-addition, commonly referred to as a Michael-type addition, of a nucleophile to the β position of an

α,β-unsaturated carbonyl compound such as an aldehyde or ketone is a widely-investigated approach for injectable hydrogel preparation. This reaction can occur spontaneously under physiological conditions due to the formation of a resonance-stabilized enolate ion as an intermediate following nucleophilic attack (Figure 1.1A).[53] The β position of the acceptor is made electrophilic by resonance between the α,β-unsaturated carbonyl form and the enolate form. Addition of the nucleophile to the β position then locks the acceptor into an enolate intermediate, which then tautomerizes to a ketone or aldehyde.

Nucleophiles capable of carrying out Michael-type addition include halide ions, cyanide ions, thiols, alcohols, and amines; however, only thiols, alcohols, and amines are generally suitable for use in cross-linking of biomaterial hydrogels given the relative toxicity of halides and cyanides in the body. Both secondary and primary amines have been used as nucleophilic groups;[54–56] however this chemistry requires pre-fabrication of the gels at elevated temperatures under basic conditions, limiting their utility as injectable precursors. Instead, the lower pK_a (~8) and stronger nucleophilicity of thiols relative to amines have made thiols the predominant nucleophile used for cross-linking under physiological conditions.[57,58]

The introduction of thiol groups into polymer chains is normally performed following polymerization due to the proclivity of free thiol groups to act as a chain transfer agent during free radical polymerization. The most common method of introducing thiols into polymer chains containing free amines or hydroxyl groups is to first deprotonate the amine or hydroxyl using a strong base such as NaH and react an alkene group using an allyl halide via a simple Sn2 reaction.[59,60] A radical source, commonly azobisisobutylonitrile, is then

added along with thioacetate, and the resulting thioester is deprotected with sodium hydroxide to reveal the thiol group. Alternately, functionalized thiol compounds such as thioglycolic acid,[61] cysteine[62] and *N*-acetyl-L-cysteine[63,64] can be conjugated to complementary amine or carboxylic acid-functionalized polymer backbones via carbodiimide coupling, although this method can suffer from potential cross-reactivity of the thiol with the electrophile in the thiol-containing compound to generate poorly-defined polymers. Disulfide-containing compounds can also be grafted to polymers and/or used as cross-linkers to create hydrogels and then reduced to expose free thiols[65]. For example, Vercruysse and co-workers[66] reported the synthesis of 3,3'-dithiobis(propanoic dihydrazide) (DTP) and its use as a cross-linker to for the synthesis of a HA-based hydrogel via conjugation of the dihydrazide cross-linker to carboxylic acid groups on the HA backbone. Free thiols (and linear polymer precursors) are subsequently liberated by reduction of the S-S bonds using dithiothreitol (DTT).[67] Of note, the resulting free thiols can be difficult to stabilize at physiological pH under long-term storage, frequently demanding the use of a slightly acidic carrying solution to minimize S-S bond formation over time.

The electrophile in a Michael-type addition is typically a α,β-unsaturated electrophile. Acrylates and are by far the most common electrophile used for generating injectable hydrogels[39,68–107] for both tissue engineering[76,108,109] and drug delivery[68,110,111] applications. Since the acrylate group is also common site of radical propagation in free radical based polymerizations, acrylates must also be added post-polymerization, typically via an addition-elimination reaction of a hydroxyl or amine group with acryloyl chloride.[72]

Methacrylate electrophiles have also been reported in the literature[112–122] and are typically also added to the prepolymers after polymerization using a similar approach (i.e. via nucleophilic addition-elimination of a hydroxyl or amine to methacryloyl chloride).

Michael-type chemistry typically drives gelation over time frames ranging from a few minutes to tens of minutes at physiological pH,[123] rates that may be undesirably slow in some applications. The use of slightly basic conditions to drive bond formation can significantly speed the reaction but may cause biocompatibility issues in certain applications such as cell encapsulation (although high cytocompatibility with 3T3 fibroblasts and adipose-derived stem cells was maintained in at least one study under such conditions[124]). Alternately, Michael chemistry can be combined with physical gelation strategies to create hydrogel systems that gel much faster than those based on Michael-type chemistry alone. For example, the Vermonden group reported a dual gelling system based the combination of thiolated HA with poly(N-isopropylacrylamide)-*b*-PEG-*b*-poly(N-isopropylacrylamide) triblock copolymer in which the poly(N-isopropylacrylamide) chains (capable of physically gelling rapidly once heated above the LCST of PNIPAM, ~32°C, once injected in vivo) were functionalized with methacrylate groups that could undergo Michael reactions with the thiolated HA.[115] These gels formed rapidly, degraded under physiological conditions over a period of months, and prolonged the release of a bradykinin at a rate tailored by altering the polymer concentration within the gel matrix.

Many of the more interesting Michael-type cross-linked systems reported consist of combinations of synthetic and natural polymers, combining the advantages of each component to create novel functional systems with highly biomedically-relevant properties.

For example, Dong *et al.* prepared hydrogels by cross-linking acrylate-functionalized (thermoresponsive) POEGMA hyperbranched polymers with thiolated HA that were highly cytocompatible with 3T3 fibroblast cells and adipose-derived stem cells,[124] while the Zhong group cross-linked thiolated chitosan with oligo(acryloyl carbonate)-b-poly(ethylene glycol)-b-oligo(acryloyl carbonate)[123] to form hydrogels that enzymatically biodegraded via the activity of lysozyme toward chitosan under physiological conditions.[125] Given that the Michael adduct is inherently stable under physiological conditions, incorporating an alternate method of degradation (such as that reported by Zhong) is critical to satisfy the clearance requirement of these hydrogels in vivo. Disulfide-based di(meth)acrylates[126,127] offer another alternative for hydrogel degradation in this context, as gelation can occur via a Michael reaction with the di(meth)acrylate and degradation can occur via oxidation of the S-S bond within the cross-linking moiety.

Another potential chemistry for use in in situ gelling injectable hydrogels makes use of the addition of maleimides as the electrophilic reactive partner to thiols.[128–131] Maleimides are typically incorporated into polymer chains via carbodiimide-mediated reactions of polymer-bound acid groups with nucleophilic maleimide precursors or by nucleophlic attack of polymer-bound amines to *N*-hydroxysuccinimide activated esters functionalized with maleimide groups, such as succinimidyl 4-(*N*-maleimidomethyl)cyclohexane-1-carboxylate (SMCC).[132] Thiol-maleimide cross-linking offers the advantage of increased speed of reaction over acrylates and methacrylates;[131] furthermore, maleimides do not readily undergo free radical polymerizations, which increases the simplicity of the synthetic steps required to generated maleimide functionalized polymers. Of particular note, the

Feijen group reported rapid gelation (over the course 0.5 to 5 minutes, depending on the degree of maleimide functionalization along the HA chains) of maleimide-functionalized HA cross-linked with thiol-functionalized 4-arm PEG following simple mixing at physiological pH,[133] conditions under which thiol-acrylate reactions would typically take several tens of minutes to facilitate gelation. However, the thioether bond formed remains non-degradable to normal hydrolytic or enzymatic degradation mechanisms, requiring backbone degradation if clearance is desired.

Vinyl sulfones (VS) also offer enhanced rates of gel formation relative to acrylates due to the high degree of stabilization offered by the sulfone moiety, whose reactive intermediate is more stable.[134–150] Vinyl sulfones are typically attached to polymer chains via multiple-step reactions, for example, first reacting mercaptoalkanoic acid to divinyl sulfone to yield a free carboxylic acid group and subsequently performing an esterification with hydroxyl groups on a carbohydrate via carbodiimide chemistry.[148] Single-step functionalizations are also possible via direct reactions between a polymer-bound hydroxyl or amine group and VS in the presence of a strong base[138,145] or copolymerization of a ring opening monomer possessing VS functionality that provides direct chain functionalization with VS without the need for post-polymerization reactions.[151] As an example, Peng *et al.* demonstrated the rapid gelation of VS-functionalized dextran cross-linked with 1,4-dithioerythritol, a hydrocarbon cross-linker possessing a single thiol group at each terminal carbon, to form a hydrogel intended as a bone scaffold (Figure 1.2).[136] Gels formed within 5 minutes under normal physiological conditions and were demonstrated to degrade via retro Michael addition at a rate that depended on the degree of polymer chain functionalization. The

Feijen group also demonstrated the utility of thiolated HA–vinyl sulfone PEG injectable gels in the application of cartilage repair, a notoriously challenging branch of tissue engineering.[144] These gels displayed tunable rates of gelation and degradation and were demonstrated to promote chondrocyte activity, as demonstrated by the accumulation of collagen type II, chondroitin sulfate, and additional glucosaminoglycans within the gel matrix.

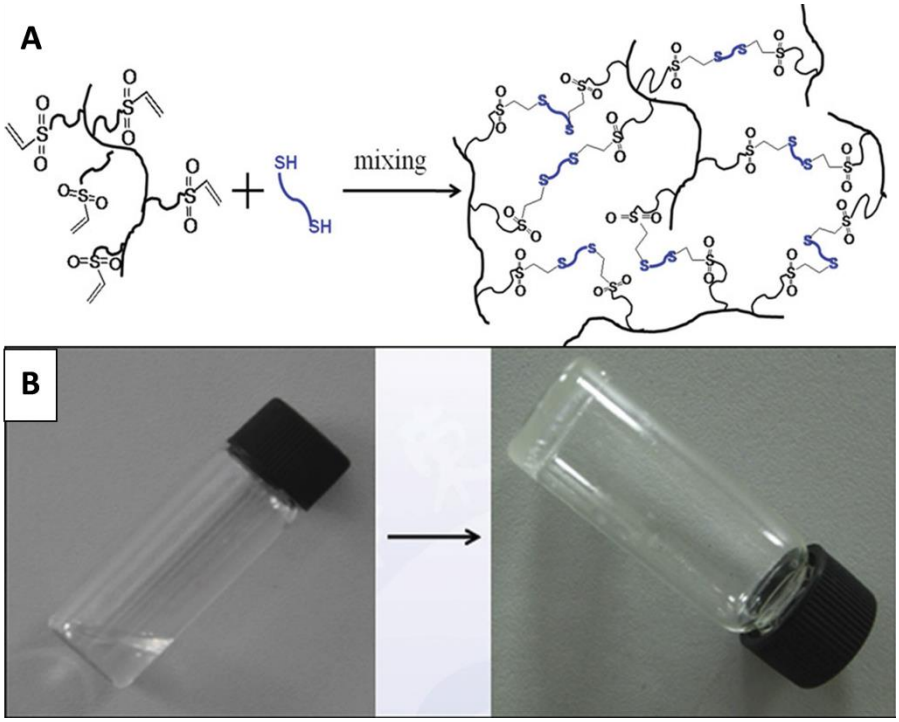

Figure 1.2. Injectable hydrogels prepared via vinyl sulfone-thiol Michael-type chemistry: A – Schematic representation of the gelation mechanism used in fabricating injectable hydrogels from vinyl sulfone functionalized dextran and 1,4-dithioerythritol; B – Gels were shown to form rapidly from by simple mixing, as is demonstrated by vial inversion test (flow to no flow). Reprinted with permission.[136] 2013, Wiley-VCH.

Quinones have also been reported for use as the Michael receptor, as reported by the Messersmith group.[152] In their work, HA was functionalized with dopamine, which can be transformed to a quinone under oxidizing conditions using EDC/NHS chemistry. Mixing of this functionalized HA with thiol end-functionalized poly(ethylene glycol)-b-poly(propylene glycol)-b-poly(ethylene glycol) (Pluronic) polymer yielded rapidly (within 5 seconds at 37 °C) reversibly thermoresponsive gels with highly tunable stability,

dependent on the amount of Pluronic added to the gel matrix. Subcutaneous injections of these gels demonstrated their stability in the body over a 21 day assay, with no significant inflammation or immune responses observed. In addition, oscillatory rheology measurements demonstrated a high degree of adhesion between unreacted catechol groups and mucin, demonstrating the effectiveness of this chemistry in generating highly tissue adhesive gels. As with other Michael adducts, however, the formed bond is functionally non-degradable via normal hydrolytic and enzymatic reactions and requires use of a backbone-degradable polymer in order to facilitate ultimate clearance.

Polymers functionalized with different Michael receptors may be mixed in a single solution in order to achieve hydrogels with intermediate properties, a strategy we refer to as "modular" hydrogel design.[36] For example, Wen *et al.* demonstrated that cross-linking of thiolated dextran by end-functionalized Pluronic was significantly slower when Pluronic was functionalized with acrylates rather than vinyl sulfones.[153]

3.2 Cross-linking via disulfide formation: The ubiquitous disulfide bond plays an essential structural and chemical role in protein folding and assembly. Disulfides are formed by the reaction of two thiol groups, which are protonated and unreactive in their reduced states (such as in the cytoplasm), but form a sulfur-sulfur bond in the presence of an oxidizing environment, such as in the endoplasmic reticulum and extracellular space (Figure 1.1B). Animal cells regulate their thiol concentration via glutathione (GSH), a tripeptide capable of reducing disulfide bonds to liberate the corresponding thiols. This biochemistry is often exploited for the design of responsive nanoparticles[154] that are destined to partially[155–157] or completely degrade[158–160] in the presence of GSH.

Dithiol-cross-linked hydrogels require the presence of an oxidation agent to form, although oxygen itself is sufficient to drive cross-linking. Vercruysse and co-workers formed hydrogels from thiolated HA in which S-S bond formation was induced in the presence of oxidation agents such as atmospheric oxygen or 0.3% hydrogen peroxide, with gels formed within 15 minutes and completely degraded upon the addition of DTT.[66] The use of these HA-based hydrogels was demonstrated for controlled drug release of dextran blue (controllable by the DTT concentration used to degrade the gels) as well as encapsulation of murine fibroblasts, which remained highly viable and proliferated inside the hydrogel over the 3 day test period. An analogous approach was reported by Swindle-Reilly and co-workers,[161] who synthesized thiolated poly(acrylamide) polymers via free radical co-polymerization of acrylamide and bisacryloylcystamine (BAC) and subsequently reduced the S-S bond in BAC by DTT. Gelation occurred within an hour in the presence of oxygen, resulting in optically clear hydrogels with a refractive index and storage modulus comparable to porcine vitreous humor. No opacity or inflammation was observed 1-7 days post-injection into a rabbit eye, suggesting the potential use of these hydrogels as vitreous substitutes.

Alternately, instead of using polymers containing free thiols and relying on auto-oxidation to drive gelation, disulfide rearrangements commonly used in nature for the formation of disulfide bonds in proteins can be exploited for the formation of hydrogels from mixtures of thiolated and disulfide-functionalized polymers.[162,163] Choh and co-workers[163] demonstrated this approach by co-extruding HA pyridyl disulfide (HA-PD) with PEG-dithiol (PEG-DS) (Figure 1.3), with simple mixing of these precursors at 37°C in PBS

resulting in gelation within 4-5 minutes. Of note, this exchange reaction facilitated gelation significantly faster than the auto-oxidation of thiols. The resulting hydrogels exhibit similar physicochemical properties to thiol-thiol cross-linked gels in that they are cleavable in the presence of hyaluronidase and/or GSH and allow for the encapsulation, protection and, in this case, release of a thiol-containing chemokine to regulate cellular processes. Fibroblasts, endothelial cells (HUVECs), and adult stem cells (pMSCs) were successfully encapsulated *in-situ* and shown to proliferate over several days, even in the presence of unreacted thiols and the low molecular weight pyridine-2-thione cross-linking by-product.

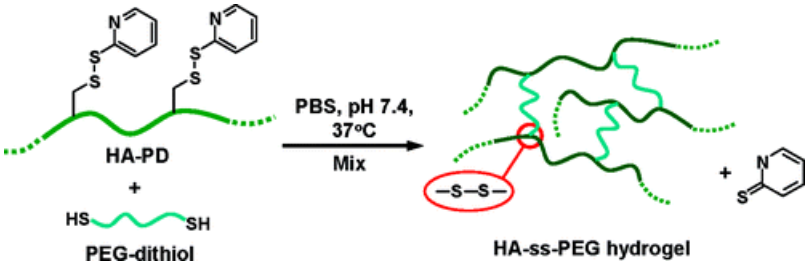

Figure 1.3. Cross-linking of HA via disulfide exchange reaction using doubly thiol terminated PEG, resulting in the in situ release of pyridine-2-thione. Reprinted with permission.[163] 2011, American Chemical Society.

A similar although more complex approach was reported by Wu and co-workers,[162] who synthesized hyperbranched polymers consisting of a hydrophilic PEG shell and a hydrophobic core containing disulfide linkages via a one-pot, two-step Michael reaction. During the Michael addition reaction, some free thiols remain unreacted which can exchange with the disulfides to form a hydrogel that remains stable for several months at physiological pH. However, gelation using this approach was only observed at high

polymer concentrations (10 w/w%) and extremely high pH (pH = 12) over a relatively long gelation time (approx. 1h), making this system less suitable for injection.

Double network hydrogels based on multiple covalent bond forming reactions and/or dual physical/chemical cross-linking can be easily introduced using dithiol cross-linking. As an example of the former, Zhang and co-workers reported the formation of a hydrogel from oxidized dextran (aldehyde-functionalized) and chitosan partially functionalized with *N*-acetyl-L-cysteine.[63] The resulting hydrogel was cross-linked by both disulfide bond formation as well as by Schiff base formation between the aldehydes and residual amine groups on chitosan, a double network structure observed to improve the long-term stability of the hydrogel. Subcutaneous injection in mice demonstrated a mild inflammatory response, with formation of only a thin fibrous capsule, and good resistance to degradation. As an example of the latter, Du and co-workers functionalized gellan gum with cysteine and observed gelation over ~4 hours in the absence of an oxidation agent.[62] Since the thiolation reacton does not alter the characteristic 3-D conformation of gellan gum, these polymers maintain their ability to form physical hydrogels typically observed upon cooling of a gellan solution in the presence of cations.[164] Gels could be formed at extremely low polymer concentrations (0.5-1 w/w%) and the resulting hydrogels displayed excellent cytocompatibility and complete degradation in the presence of reducing agents such as DTT. Such dual physical-chemical cross-linked hydrogels may be of particular interest for producing stiffer hydrogels for tissue engineering applications.

Overall, disulfide cross-linking provides a promising route to injectable hydrogel formation given that gelation can occur under mild oxidative conditions and in the absence of catalysts

or small molecules and residual thiol groups have demonstrated to not significantly impact cytocompatibility in vitro or biocompatibility in vivo. However, the relatively low gelation rates at the physiological pH in the absence of an oxidizing agent (on the order of tens of minutes to hours) limits this cross-linking chemistry to locations in the body where there is a relatively long residence time or a confined injection area (for example, inside the eye). Furthermore, it has been demonstrated that the delivery of proteins from these hydrogels may be limited due to covalent modification of the loaded protein's cysteine residues with thiol groups located on the precursor polymer chains, inducing potential protein denaturation.[165]

3.3 Cross-linking via hydrazone bond formation: The hydrazone bond is a type of Schiff base resulting from the nucleophilic addition of a nitrogen from a hydrazine group (or some derivative) to a carbonyl group (normally a ketone or aldehyde), resulting in the elimination of water. Due to the high toxicity of hydrazines, structurally-similar hydrazides, which are substantially less toxic, are normally employed as the nucleophilic group in the literature. Relative to conventional Schiff base formation between carbonyl groups and primary amines, hydrazone bonds form faster and result in a significantly more hydrolytically stable bond due to the increased nucleophilicity of adjacent lone pair-bearing amines through the alpha effect,[166] negating the need for subsequent reduction of the bond in order to impart stability in water. The most typical implementation of this chemistry is the reaction between a hydrazide group and an aldehyde group (Figure 1.1C).

The principal advantage of hydrazone bond-forming chemistry is the remarkable speed at which gelation can occur following injection, often on the timescale of seconds (indeed, in

our experience, highly functionalized polymers at higher concentrations can frequently gel in the static mixer of the double barrel syringe before they can even be extruded). In addition, the hydrolytic lability of the hydrazone bond facilitates the fabrication of hydrogels capable of degrading over time in aqueous environments to a degree that depends on the cross-link density of the hydrogel network and the pH of the surrounding environment.[167,168] The decreased electrophilicity of the sp^2 carbon attached to nitrogen over that of a carbonyl group renders the hydrazone bond less reactive than its parent carbonyl, offering prolonged residence time within the body often on the timescale of several months. In addition, again owing in part to the high driving force for cross-link formation using this chemistry, hydrazone-cross-linked hydrogels can exhibit relatively stronger mechanical properties to hydrogels prepared using other chemistries. For example, Chaikov's group observed rapid gelation (within seconds) and a maximum compressive modulus of 1MPa upon cross-linking elastin-like proteins modified with aldehyde and hydrazide functional moieties,[169] a modulus orders of magnitude higher than most reported injectable hydrogels.

Hydrazone-cross-linked hydrogels also have an excellent record of good biological performance in a variety of biomedical applications (particularly relative to other injectable hydrogel chemistries). HA based injectable hydrogels formed via hydrazone chemistry have been demonstrated by the Tan group to be effective for site-specific protein delivery while eliciting low cellular toxicity.[170] Kohane and co-workers have demonstrated the high tolerability of hydrazone-cross-linked hydrogels prepared based on a variety of carbohydrates in the peritoneum, typically a particularly challenging biological

environment for biomaterial use.[15] Varghese *et al.* demonstrated the effective use of hydrazone-cross-linked HA-based hydrogels to deliver a growth factor used in spinal fusion and promote simultaneous angiogenesis.[171] Langer *et al.* have also shown that hydrazone-cross-linked gels trigger only a mild host response following placement within vocal fold tissue.[172] It is important to note that this observed biocompatibility in multiple tissues and applications is maintained even given the potential reactivity of aldehyde functional groups toward amines on proteins via Schiff base formation, in part since many reported systems use an excess of hydrazide groups to minimize the number of residual aldehydes following gelation.

The number and identity of excess functional groups can also be manipulated to effect performance changes in the material, particularly in the context of drug delivery. For example, hydrogels made with excess hydrazide functionality have been shown to slow the release of therapeutics possessing aldehyde or ketone functional groups via the formation of reversible (covalent) hydrazone bonds between the drug and the hydrogel.[173] Similarly, Kohane and co-workers reported the use of aldehyde-functionalized dextran and hydrazide-functionalized carboxymethylcellulose with an excess of aldehydes to generate injectable reservoirs for the prolonged release of hydrophobic anti-fungal therapeutics containing an amine group, which formed a Schiff base with the excess aldehyde groups.[174] The ready reversibility of this bond in water facilitated sustained release of the hydrophobic therapeutic.

Our laboratory has also actively investigated using hydrazide-aldehyde chemistry to fabricate hydrogels based on synthetic polymers or natural-synthetic polymer mixtures with

well-defined biological properties (Figure 1.4). We have demonstrated that co-extrusion of thermally responsive poly(N-isopropylacrylamide) (PNIPAM) precursor copolymers possessing complimentary aldehyde (via copolymerization with an acetal-containing comonomer that can be acid-hydrolyzed to free aldehyde groups) and hydrazide (via carbodiimide conjugation of a large excess of adipic acid dihydrazide to a carboxylic acid-functionalized polymer) groups leads to the formation of stable gels in the body within seconds following extrusion (Scheme 1.1**)**.[175] The polymeric degradation products of these gels did not invoke any significant cytotoxic response in in vitro assays to multiple cell types even at very high polymer concentrations (2000 μg/mL) and induced an extremely mild inflammatory response and a complete absence of capsule formation even over several months when injected subcutaneously in a mouse model (Figure 1.4A). Both the biological properties and the physicochemical properties of these gels (such as the reversible swelling/deswelling at alternating temperatures above and below PNIPAM's LCST) can be precisely tuned by substituting aldehyde-functionalized PNIPAM with different aldehyde-functionalized polysaccharide "modules" composed of either carboxymethyl cellulose or dextran within the network (Figure 1.4B).[36] By using this synthetic strategy of modular hydrogel fabrication, the gel swelling, temperature-induced volume changes, drug retention, mechanical properties, and degradation kinetics can all be precisely tuned (in most cases in a manner predictable by the simple rule of mixtures) by changing the relative ratios of carboxymethyl cellulose and dextran used in gel fabrication.[36] Cell adhesion, cell spreading, and cell infiltration into the hydrogels can similarly be controlled via selection of carbohydrates with defined physical (charge, hydrophilicity) and biological properties.

Our group has also demonstrated the use of hydrazone chemistry for the design of nanocomposite materials with highly unique drug delivery properties. Soft nanocomposites have been fabricated in which acid-functionalized microgels based on PNIPAM and functionalized with hydrazide groups are co-extruded with hydrazide-functionalized carboxymethyl cellulose and aldehyde-functionalized dextran. The microgels significantly enhanced the mechanical strength of the gels and, based on ionic interactions with the cationic drug bupivacaine, could extend small molecule drug release from a few days in the absence of the microgel to over two months in the presence of the microgel (Figure 1.4C).[38,176] Inorganic nanoparticle nanocomposites have also been designed based on superparamagnetic iron oxide nanoparticles surface-functionalized with physically adsorbed hydrazide-functionalized PNIPAM.[35] Cross-linking of these nanoparticles with aldehyde-functionalized dextran resulted in nanocomposites with remarkably high elastic moduli (>60 kPa) and mechanical properties more akin to "bouncy ball" elastomers than conventional hydrogels. Furthermore, by applying an oscillating magnetic field to the nanocomposite to remotely generate heat and induce deswelling in the PNIPAM polymer coating, pulsatile "on demand" drug delivery was achieved for bupivacaine loaded within the hydrogel matrix. (Figure 1.4D).

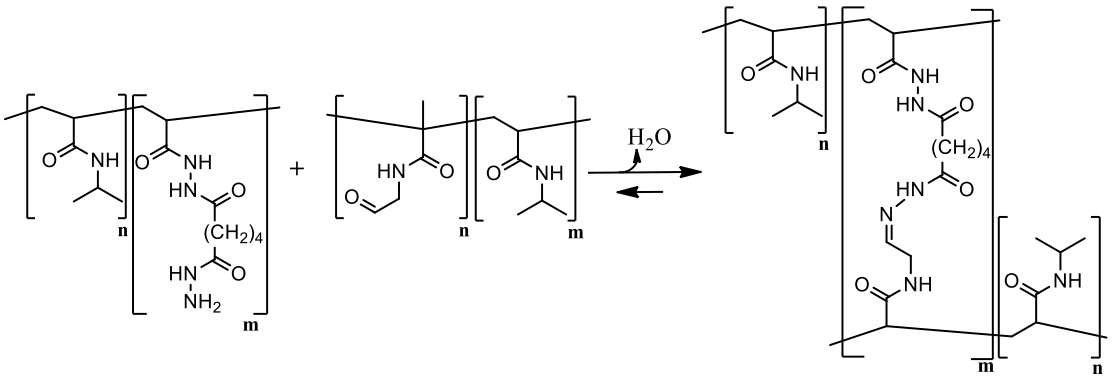

Scheme 1.1. Spontaneous chemical cross-link formation between hydrazide and aldehyde- functionalized PNIPAM precursors to generate an injectable hydrogel capable of degrading *in vivo* via reversible hydrolysis of the hydrazone bond.

On this basis, hydrazone bond formation is a highly flexible strategy for generating a range of different injectable hydrogel morphologies. However, the storage stability and potential cross-reactivity of aldehyde groups with native tissues has raised concern over wide-spread use of this chemistry (despite the positive in vivo assay results reported to date). To mitigate this potential concern, we have recently shown effective formation of hydrogels by reacting hydrazide-functionalized PNIPAM with ketone-functionalized PNIPAM.[177] Although gels form significantly slower than with aldehydes and require higher degrees of ketone functionalization in order to generate hydrogels with matched elastic moduli, ketones are significantly more stable in storage and do not react readily with any physiologically-relevant functional group, providing the advantages of hydrazone chemistry (particularly in terms of degradability) without the potential drawbacks of aldehyde groups.

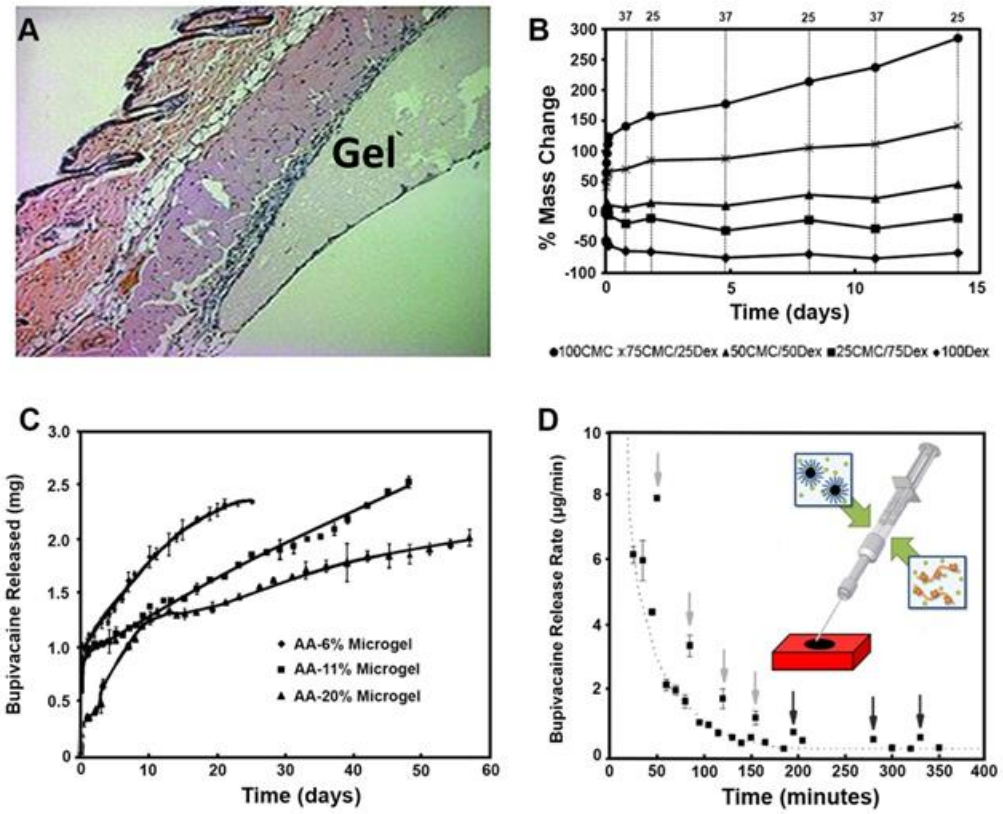

Figure 1.4. Injectable hydrogel formulations based on hydrazone bond formation. A - Subcutaneous co-injection of hydrazide and aldehyde poly(N-isopropylacrylamide)-based copolymer precursors lead to the formation of a stable gel in vivo with no apparent fibrous capsule or signs of chronic inflammatory response towards the material (Reprinted with permission.[37] 2012, American Chemical Society). B - Thermally-driven deswelling and thermoreversibility can be tuned according to the mole fraction of oxidized (aldehyde-functionalized) carboxymethyl cellulose and dextran polysaccharide precursor solutions co-extruded with hydrazide-functionalized PNIPAM precursors (fixed total polymer content of 6 wt% (m/v)) (Reprinted with permission.[36] 2012, American Chemical Society). C – Slow release of bupivacaine can be achieved by soft nanocomposite hydrogels produced by embedding or crosslinking hydrazide-functionalized PNIPAM-based microgels into a hydrogel formed by co-extruding hydrazide-functionalized carboxymethyl cellulose with aldehyde-functionalized (Reprinted with permission.[35] 2013, American Chemical Society) D - Hydrogels formed by co-extruding oxidized dextran with superparamagnetic iron oxide nanoparticles coated with hydrazide-functionalized PNIPAM can facilitate on-demand, pulsatile release of bupivacaine upon application of an external magnetic field (switched on at time points indicated by the arrows) (Reprinted with permission.[178] 2011, American Chemical Society).

3.4 Cross-linking via oxime formation: Oxime bonds form rapidly between an aldehyde or ketone and a hydroxylamine under physiological conditions. This reaction offers enhanced hydrolytic stability over Schiff base and hydrazone cross-linking strategies at the cost of

requiring an acid catalyst in order to proceed at an appreciable rate due to electron withdrawal by the adjacent oxygen (Figure 1.1D).[179,180] However, these properties make the oxide click reaction an attractive candidate for cross-linking in regions of lower pH within the body, such as ischemic tissue following myocardial infarctions, and may be compatible with less demanding biological environments such as the subcutaneous space in which the hydrogel can form and then be titrated by buffering salts in vivo prior to inducing significant tissue damage.[181]

Oxime cross-linking is a relatively new approach for the synthesis of injectable hydrogels, with the first example reported by Ossipov and co-workers in 2010.[182] HA was functionalized with a bi-functional dihydrazide compound with a cleavable 2,2'-dithiobis(ethoxycarbonyl) protective group using EDC chemistry. Subsequent treatment with dithiotreitol (DTT) liberates free unstable thiols that decompose spontaneously, liberating episulfide and carbondioxide and exposing the free aminooxy functionality. This functionalization procedure is somewhat more complex than that required for previously discussed reactions, but involves well-established aqueous chemistry that can proceed at high yields. Mixing this aminooxy-functionalized HA with an aldehyde-functionalized-HA formed an oxime cross-linked HA hydrogel within 30 seconds stable in PBS for up to 20 days but completely degraded in the presence of 500 U/mL hyaluronidase within 24 hours. No decrease in cell viability was observed when the precursor solutions were put in direct contact with the cell culture medium, suggesting that gelation is sufficiently fast to prevent exposure of the endogenous cells to the potentially toxic precursors.[182]

Grover and co-workers have significantly expanded this work into biomedical applications via the synthesis of PEG hydrogels that support cell adhesion by cross-linking 8 arm aminooxy PEG (AO-PEG) with glutaraldehyde.[183] While the use of low molecular weight cross-linkers is typically avoided for in vivo gelation due to potential toxicity issues (particularly glutaraldehyde, which is commonly used as a tissue fixative), Grover and co-workers surprisingly demonstrated that the use of glutaraldehyde did not cause any cytotoxicity in vitro to mouse mesenchymal stem cells (MSCs) mixed with the precursor solutions.[183] AO-PEG was synthesized by a Mitsunobu reaction of *N*-hydroxyphthalimde with 8 arm hydroxyl-PEG, followed by reduction with hydrazine. The mechanical properties of the hydrogels can be tuned by controlling the molar ratio of aminooxy to aldehyde groups and the AO-PEG concentration. Gelation takes approximately 20 minutes at the physiological pH but occurs within 5 minutes at pH = 6, a relatively mild acidic pH that may facilitate use of this chemistry in a broader range of biological environments. The hydrogels were further functionalized by adding a ketone-functionalized RGD signalling protein that could be grafted on residual aminooxy groups to promote MSC adhesion and proliferation.

Although rapid gelation is typically considered critical for practical use of injectable hydrogels, in certain applications a slower or a tunable gelation rate might be preferable. In a follow-up study, Grover and co-workers demonstrated such an example in vivo by cross-linking a 4-arm PEG-AO and a 4-arm ketone functionalized PEG (PEG-K) in myocardial tissue using a catheter (Scheme 1.2 and Figure 1.5).[184] The rate of gelation in vitro could be controlled by pH and ranged from 30 minutes at pH = 4 to >50 hours at pH = 7.4;

however, following subcutaneous dorsal injection in Sprague Dawley rats, gelation was observed within 20 minutes in vivo independent of the pH of the injection solution (pH 6.0-7.4), potentially as a result of the more complex biological environment (see Figure 1.5B-E). As a result, when precursor polymers were injected at physiological pH, gelation is slow within the catheter (thus allowing slow injection) but significantly faster once in vivo (thus ensuring gelation at the site of injection), which has the potential to open up more minimally invasive delivery routes that require materials to held at body temperature for an extended period of time yet gel fast once injected. Proof of principle of this controlled gelation behavior was demonstrated by injecting the PEG hydrogel in the left ventricular wall of Sprague-Dawley rats (Figure 1.5F).

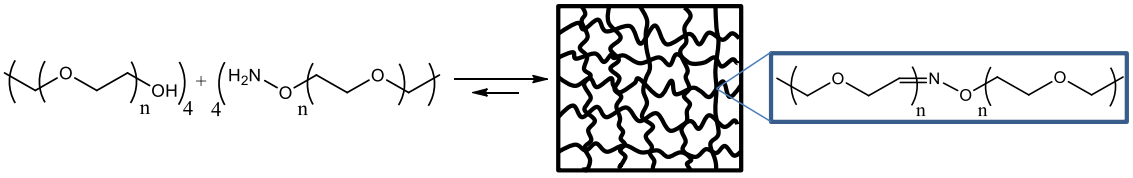

Scheme 1.2. Chemical cross-linking of 4-arm PEG precursors possessing either hydroxyl or aminoxy functionality to yield a spontaneously forming oxime cross-linked hydrogel network.

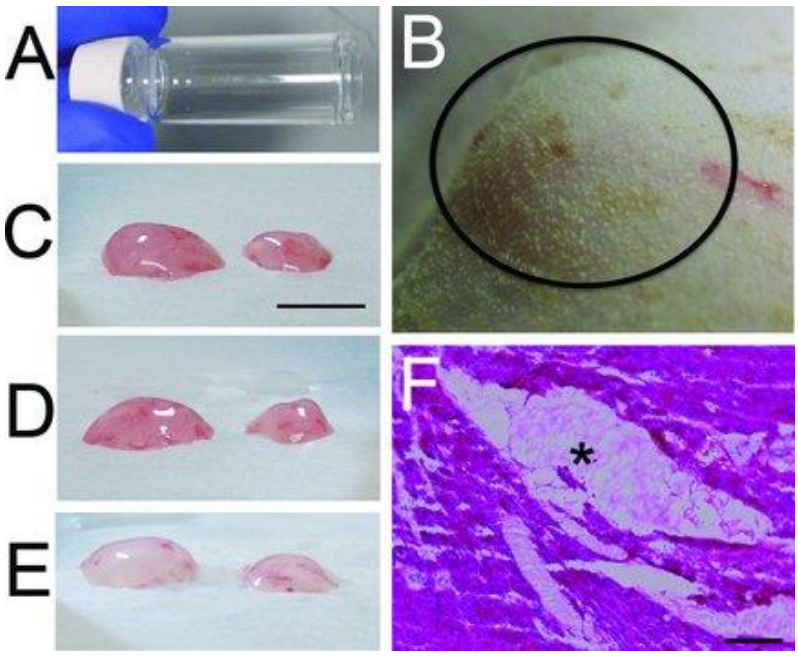

Figure 2.5. Oxime-cross-linked injectable hydrogels for catheter applications: A) PEG-oxime (pH 6.0) after injection through the inner nitinol tubing of the MyoStar catheter and subsequent incubation for 4 h at 37 °C. B) Subcutaneous injection of PEG-oxime (pH 7.4) after 20 min. C–E) 200 µL (left) and 100 µL (right) PEG-oxime gels excised after 20 min (scale bar = 1 cm): C) pH 4.0. D) pH 7.4. E) pH 10.5. F) H&E stained section of heart after injection of PEG-oxime (pH 7.4) (scale bar = 200 µm). The * denotes the region of injection of PEG. Reprinted with permission.[184] 2013, Wiley-VCH.

While this chemistry is still relatively new, functionalization of the polymers with the aminooxy functional group typically demands significantly more complex chemistries compared to the other functionalizations described herein, potentially limiting the broad appeal of the technique.

3.5 Cross-linking via 2+4 (Diels-Alder) cycloaddition: The Diels-Alder reaction is one of the only pericyclic chemistries reported in the literature that is used in the chemical cross-linking of hydrogels. In a Diels-Alder reaction, a conjugated diene reacts with an activated double bond (dienophile) in a single step, forming a new ring between the two species. The most common Diels-Alder reaction used for hydrogel formation involves the reaction

between maleimide and furan groups (Figure 1.1E). In this case, the double bond of maleimide serves as both the nucleophile and electrophile (denoted by 'e' and 'n'), performing a 1,4 addition to the conjugated double bonds of the furan group. These reactive functional groups may be conjugated to the polymers post-polymerization (for example, via attachment of amine-functionalized furans or maleimides to carboxylic acid moieties on the polymer using carbodiimide chemistry) or may be incorporated into synthetic polymer chains by copolymerizing with a monomer possessing these functionalities, as neither group is particularly reactive in a free radical polymerization environment. The relatively high selectivity of this chemistry makes it particularly attractive for use in vivo because, unlike many other cross-linking methods, its functional groups are relatively unreactive with chemical groups found within the body (with the exception of thiols present at relatively low concentrations in proteins). In addition, this reaction is spontaneous in aqueous environments and occurs spontaneously at body temperature.[185] This chemistry has been utilized in the formation of in situ-gelling hydrogels,[186] with particular success utilizing Diels-Alder chemistry to fabricate HA gels for tissue engineering,[187] and protein encapsulation.[188]

The main drawback of using Diels-Alder chemistry for injectable hydrogel formulations is that the gelation rates achieved with this chemistry are relatively slow, with hydrogels typically formed over the timescale of tens of minutes to hours instead of the seconds to minutes timescale most favored for in situ-gelling systems at physiological temperature. Again, combining physical and chemical cross-linking in a single injectable hydrogel can in part address this issue. The Zhao group reported a thermally responsive injectable

system based on dual physical and chemical cross-linking of a copolymer of N-isopropylacrylamide, N,N-dimethylacrylamide, and 2-hydroxymethacrylate functionalized with N-maleoyl alanine (dieneophile) and a copolymer of N-isopropylacrylamide, N,N-dimethylacrylamide, and furfuryl methacrylate (diene) (Scheme 1.3).[189] Below the LCST of the PNIPAM-rich chains, relatively slow gelation occurred (~50 minutes reported) based solely on Diels-Alder chemistry; above the LCST, temperature-driven physical interactions between polymer chains imparted by thermosensitive poly(*N*-isopropylacrylamide) blocks induce gel formation prior to covalent cross-linking via Diels-Alder reaction (Figure 1.6). Given the relatively slow timescale of Diels-Alder reactions at 37°C, it is likely that future injectable systems based on this chemistry will also rely on some cohesive physical interactions between polymer precursors in order to prevent diffusion away from the site of injection prior to covalent gel formation.

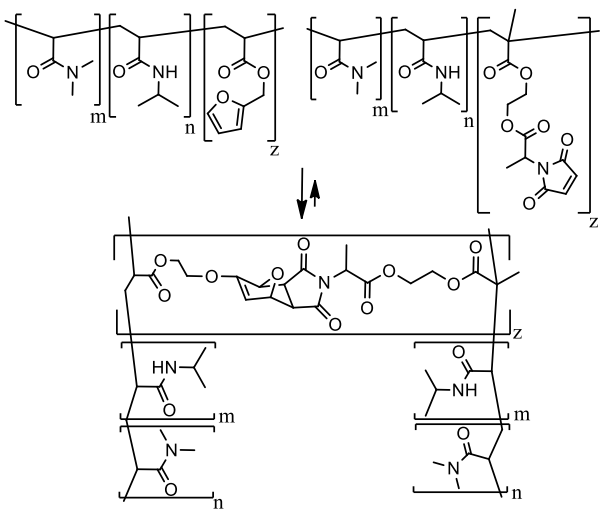

Scheme 1.3. Spontaneous formation of a Diels-Alder adduct following coextrusion of furan and maleimide functionalized precursor copolymer chains.

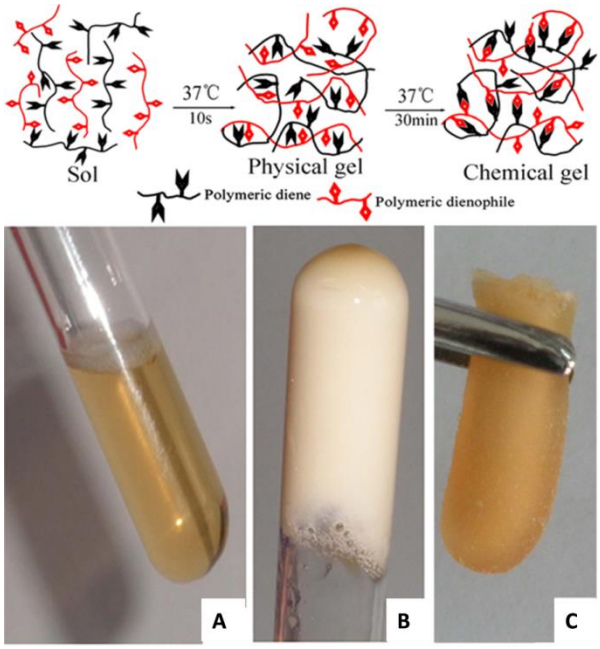

Figure 1.6. Mechanism leading to the stable formation of both physically and (subsequently) chemically cross-linked gels. Co-extrusion of the PNIPAM based precursors possessing either dieneophile or diene results in a low viscosity solution at room temperature (A). The initial volume phase transition results from thermally-driven collapse of PNIPAM moieties, bringing the diene and dienophile into proximity with one another (B), eventually forming more rigid chemically cross-linked hydrogels via Diels-Alder 2+4 cycloaddition (C). Reprinted with permission.[189] 2011**,** Springer.

3.6 Cross-linking via azide-alkyne cycloaddition: The cycloaddition between an azide and a terminal alkyne has attracted significant interest in the design of injectable hydrogels due to the high selectivity and bioorthogonality of this cross-linking chemistry. This reaction was initially described by Huisgen and in its classic form offered only limited applicability due to the requirement of high temperatures needed to drive the reaction.[190] A significant improvement was made in 2003 by Sharpless and co-workers,[191] who described a copper(I)-catalyzed alkyne-azide click (CuAAC) reaction capable of occurring at physiological temperature that quickly gained popularity for the synthesis of hydrogels. The first example of an azide-alkyne cross-linked hydrogel was reported by Ossipov and co-workers in 2006,

in which poly(vinyl alcohol) (PVA) was modified with alkyne and azide groups through carbamate linkages.[192] Transparent hydrogels could be obtained by mixing both polymeric precursors in the presence of 6 mM Cu(I), with gelation was observed in both DMSO and aqueous solutions within one minute.

As the formed trizole product of the cycloaddition is non-degradable under physiological conditions, biodegradable polymer precursors are preferred for in vivo application. Alkyne-azide cross-linked hydrogels have been synthesized using biopolymers such as polysaccharides[193–196] and peptides.[197] The Lamanna group[193,196] synthesized alkyne and azide HA (HA) precursors by EDC functionalization of the carboxylic acid groups with 11-azido-3,6,9-trioxaundecan-1-amine or propargylamine. HA hydrogels formed after mixing the functionalized HA precursors at 5 w/w% in water within a few minutes upon the addition of 1 w/v% Cu(I). Such hydrogels demonstrated sustained release of doxorubicin over the course of over 10 days and maintained the viability of over 80% of encapsulated *S. Cerevisiae* yeast cells after 24 h.[193] Similar carbohydrate-based gels have been reported by Gao and co-workers using CuAAC to cross-link both azide-functionalized HA and chondroitin sulfate (CS) with alkyne functionalized gelatin; the resulting hydrogels facilitated the formation of a confluent layer of chondrocytes within three days.[195] Peptides have also been reported as degradable backbone polymers for azide-alkyne-based hydrogels. van Dijk and co-workers[197] synthesized a protease-sensitive bis-azido peptide that was cross-linked by 4-arm PEG-alkyne in the presence of $CuSO_4$ and ascorbic acid

and could be degraded within 40-80 hours (depending on cross-link density) using 0.8 μM trypsin.

As with other in situ-gelling chemistries, both physical and chemical cross-linking can be combined to produce hydrogels with novel properties. One interesting example of this approach was reported by Tan and co-workers[198] who developed hydrogels based on α,ω-dialkyne PEG (PEG-alkyne) and azido-functionalized α-cyclodextrin (αCD-N_3). PEG and αCD can form inclusion complexes which have been extensively studied for the formation of sliding-ring hydrogels.[199] Mixing of the PEG-alkyne and αCD-N_3 in the presence of Cu(I) forms a hydrogel that is based on inclusion complexation as well as covalent cross-linking, which improves the mechanical properties of the hydrogel. Preliminary cytotoxicity studies showed excellent cell viability to HeLa and HEK293T cell lines.

While these examples demonstrate the potential of alkyne-azide cross-linking for the synthesis of hydrogels, none of these systems can be used practically as an injectable hydrogel system given the potential in vivo toxicity of copper. Indeed, most of the particularly noteworthy biological responses reported were achieved with hydrogels after removal of Cu(I) via extensive dialysis against EDTA,[193] a purification step not possible if the hydrogels are to be directly injected in vivo. As a result, the focus has shifted to the development of an uncatalyzed version of the cycloaddition reaction that can enable hydrogel formation in the body under physiological conditions. Bertozzi and co-workers have achieved such high click reactivity in the absence of Cu(I) in biologically relevant conditions by employing strained alkynes such as cyclooctyne as the reactive functional group, demonstrating selective modification of biomolecules and living cells in vitro

without any apparent toxicity,[200] Consequently, strain-promoted alkyne-azide cycloaddition (SPAAC) has emerged as one of the top choices for bioorthogonal reactions (Figure 1.1F). Lallana has described the application of this approach to generate chitosan-PEG polymeric carriers for drug delivery,[201] while Anseth and co-workers have reported hydrogels prepared from 4-arm PEG tetraazide and bis(cyclooctyne)-peptide.[202,203] In this latter example, a *gem*-difluoro cyclooctyne (DIFO) was used as the alkyne since the presence of electron-withdrawing fluoride groups adjacent to the triple bond of cyclooctyne offers faster cross-linking kinetics, facilitating gelation within a few minutes (5 min) and complete network formation within an hour.[204] The biomechanical properties of the hydrogels could be tuned by the molecular weight and the off-stoichiometric ratio of the precursors (Figure **1.7**). Interestingly, the synthetic bis(cyclooctyne)-peptide was functionalized with a pendant vinyl which allowed for further modification of the hydrogel network. Post-gelation modification with cysteine-containing peptides facilitated the creation of peptide gradients within the hydrogel network that could prove promising for 3D stem cell differentiation.[203]

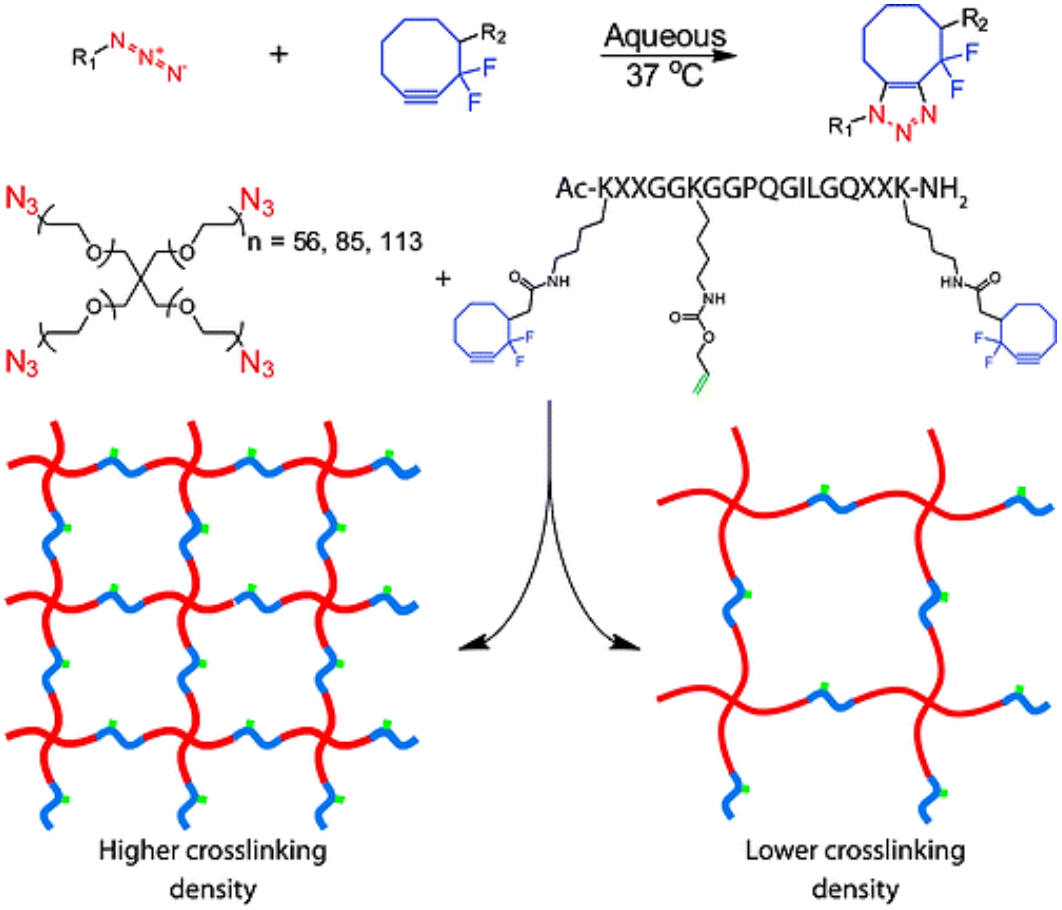

Figure 1.7. Cross-linking between azide-terminated 4-arm PEG and the fluorinated cyclooctyne DIFO bound to an RGD peptide yields a peptide cross-linked PEG based network. Further modification with thiolated proteins generates a cell matrix with tunable cell encapsulating properties. Reprinted with permission.[203] 2010, American Chemical Society.

Progress in the synthesis of functionalized cyclooctynes offer the possibility of tuning gelation kinetics to further speed the rate of gelation under physiological conditions.[205] For example, the inclusion of aromatic rings has been demonstrated to increase the degree of ring strain of a cyclooctyne, increasing its reactivity.[206] Xu and co-workers have exploited this approach to prepare hydrogels by cross-linking azido-functionalized PEG-co-poly(carbonate) with dibenzocyclooctyne (DBCO)-functionalized PEG, with gelation in this case occurring in less than one minute to form relatively strong hydrogels with shear

moduli ranging from 10^2 to 10^4 Pa.[207] The use of poly(carbonate)-based precursors ensures degradability of the hydrogel network by hydrolysis of the ester groups. Encapsulated bone marrow stromal cells exhibited higher cell viability in these hydrogel scaffolds compared to conventionally UV-cured hydrogels of similar composition. Zheng and co-workers prepared similar PEG hydrogels by cross-linking 4-dibenzocyclooctynol (DIBO) functionalized PEG with a relatively low molecular weight glycerol exytholate triazide to successfully encapsulate human mesenchymal stem cells.[208] However, the injectability of this hydrogel system in vivo may be hampered by the use of the low molecular glycerol exytholate triazide cross-linker, which is more likely to leach out of the gel than a functionalized polymer and thus runs a higher risk of inducing potential inflammatory or immune responses.

Despite the great potential of SPAAC for the synthesis of hydrogels, the high reactivity of the strained cyclooctynes makes their syntheses relatively complex, often requiring multistep reaction with poor yields. Compared to other chemistries discussed previously, which typically require a single post-polymerization reaction or even functionalization directly via comonomer incorporation, this represents a significant disadvantage of this approach. Nevertheless, the high specificity, acceptably fast cross-linking kinetics, and excellent bioorthogonality of these reactive groups makes azide-cyclooctyne chemistry a very attractive candidate for in situ forming hydrogels.

4. Summary and Outlook

Based on the examples shown here, it is clear that injectable, in situ-gelling covalently cross-linked hydrogels hold great promise for addressing a host of challenges involved with the use of hydrogels in biomedical applications. The facile delivery of the hydrogel, capacity of the precursor polymers to flow to some extent prior to gelation (to conform to biological cavities), the ability of the hydrogel lifetime in vivo to be tuned via judicious choice of cross-linking chemistry, and the absence of any external intervention or small molecules to facilitate gel formation make gels prepared using the chemistries discussed herein easier to use for clinicians, less invasive and therefore less uncomfortable for patients, and more flexible for use in multiple biological environments and multiple applications. Furthermore, the generally good biocompatibility/cytocompatibility results achieved with such hydrogels, even those gelled using functional groups which are not strictly bio-orthogonal, is promising, although rigorous in vivo evaluation of these materials remains in its infancy. However, there remain significant challenges, and thus opportunities for research, to more effectively engineer injectable hydrogels for use in multiple areas of medicine:

(1) The mechanical strength of many injectable hydrogels, at least without functionalizing the precursor polymers to a point that the favorable chemistry of the backbone polymer itself is compromised, remains below what might be desirable for modulus matching stiffer tissues in vivo or using these hydrogels as functional bioadhesives. Further development of methods to increase the potential modulus of

in situ-forming gels, via the development of dual network materials such as those discussed,[62,63,115,189] injectable interpenetrating polymer networks, or nanoparticle-reinforced hydrogel matrices, may broaden the potential applications of injectable gels.[35]

(2) For a given chemistry, there is currently a direct correlation between the kinetics of gel formation and the ultimate mechanical properties of the hydrogel. This correlation is not unexpected, given that the capacity to form more cross-links in the system would also result in more cross-links forming per unit time upon mixing. However, this correlation significantly complicates the formation of highly cross-linked injectable hydrogels (some of which form so quickly that gelation occurs in the syringe) or lower modulus gels modeling extremely soft biological tissues (in which cross-linking occurs too slowly to localize the gel at the desired injection site). Approaches to form hydrogels by mixing fast and slow reacting functional groups reactive via the same general chemical pathway (i.e. fast-gelling aldehydes and slow-reacting ketones with hydrazide groups) may address the former problem, as substituting a fraction of slower-reacting functional groups would slow down gelation without sacrificing the ultimate number of potential cross-linking functional group pairs. The latter challenge may be addressed by using native biomolecules present in vivo to compete with cross-link formation, potentially facilitating rapid hydrogel immobilization (prior to in-diffusion of the competing species) followed by effective de-cross-linking to reduce the local modulus.

(3) While the in vitro gelation and degradation rates associated with varying in situ-gelling chemistries have been largely well-documented, measurements of these parameters in vivo remain sparse. Given the complexity of the biological environment, and the example cited in the oxime cross-linking section of significant acceleration of the gelation rate in vivo relative to in PBS in vitro,[184] further studies on this point seem warranted to (1) ensure that the design rules followed based on in vitro characterization are valid in vivo and (2) ensure that the actual gelation rate in vivo instead of in vitro is optimized for any given hydrogel application.

(4) While initial results on the cytocompatibility and biocompatibility of hydrogels containing latent non-orthogonal reactive functional groups have been surprisingly positive, the development of methods to effectively consume non-reacted functional groups after gelation offers significant promise in further passivating these hydrogels in vivo. One interesting approach to address this problem is the "temporarily-reactive polyelectrolytes" reported by Stover's group, [209] in which gel formation is demonstrated by reacting amine-containing polymers with anhydride-functionalized polymers which hydrolyze in parallel to cross-linking to consume the reactive anhydride groups. However, use of such chemistries is inherently challenging given dynamic nature of many of these bond-forming chemistries as well as the need to store reactive precursor polymer solutions over extended periods for commercial or clinical use. Approaches by which quenching molecules are instead slowly released from a reservoir inside the gel may address this issue. Connecting reactive functional groups via disulfide linkages to the polymer

backbones may also offer promise in this regard, provided the small functional molecules released upon S-S reduction are themselves biocompatible. Given that to-date most in vivo investigations of these hydrogels have been relatively superficial (i.e. generally simple histological investigations of surrounding tissues), more detailed investigations into the complex biological impacts of varying concentrations of different residual functional groups at hydrogel-tissue interfaces would be highly beneficial to determine how (and to what extent) latent functional groups impact inflammatory and immunological pathways and thus the ultimate biological response to the gel.

(5) Given the likelihood that the truly bio-orthogonal hydrogel formation chemistries will ultimately provide the best performance in the widest diversity of physiological environments, developing methods by which these chemistries can be more easily implemented on a wide variety of polymer backbones (via one or maximum two step conjugation or copolymerization protocols) would significantly improve their utility as biomaterials. In particular, the alkyne-azide click reaction holds tremendous promise for injectable hydrogel development. but the chemistry required to introduce the strained alkynes remains at the present time strictly in the domain of synthetic chemists instead of biomaterials engineers.

(6) Most of the chemistries discussed in this review require the intimate mixing of two or more functionalized polymers (typically via co-extrusion in a double-barrel syringe) to drive gelation. However, the viscosities of the polymer solutions, potential misicibility mis-matches between functionalized polymers, and the

limited magnitude and length scale of mixing possible with static/mechanical mixers likely results in the formation of domains of one or both reactive polymers in many injectable hydrogel formulations (as reflected by the opacity of many of these formulations in the literature). Domain formation may significantly reduce the elastic modulus of the resulting hydrogel (limiting the potential to modulus-match stiffer tissues) as well as compromise hydrogel transparency (key in many applications such as ophthalmics). Fast-gelling polymer mixtures, in which gelation occurs faster than any diffusional mixing that may further homogenize the hydrogels, are particularly problematic in this regard, despite the fact they are typically favored for in vivo applications. However, relatively few studies have addressed the internal morphologies of injectable hydrogels, [210] an area of potentially fruitful fundamental research with direct engineering relevance.

Acknowledgements: Funding from the Natural Sciences and Engineering Research Council, 20/20: NSERC Ophthalmic Materials Research Network, and Ontario Ministry of Research and Innovation are gratefully acknowledged.

References

(1) Van Vlierberghe, S.; Dubruel, P.; Schacht, E. *Biomacromolecules* **2011**, *12*, 1387–408.
(2) Tibbitt, M. W.; Anseth, K. S. *Biotechnol. Bioeng.* **2009**, *103*, 655–663.
(3) Lee, K. Y.; Mooney, D. J. *Chem. Rev.* **2001**, *101*, 1869–1880.
(4) Drury, J. L.; Mooney, D. J. *Biomaterials* **2003**, *24*, 4337–51.
(5) Langer, R.; Tirrell, D. A. *Nature* **2004**, *428*, 487–92.
(6) Slaughter, B. V; Khurshid, S. S.; Fisher, O. Z.; Khademhosseini, A.; Peppas, N. *Adv. Mater.* **2009**, *21*, 3307–29.
(7) Matyjaszewski, K. *Science* **2011**, *333*, 1104–5.
(8) Qiu, Y.; Park, K. *Adv. Drug Deliv. Rev.* **2001**, *53*, 321–39.
(9) Yoon, J. A.; Gayathri, C.; Gil, R. R.; Kowalewski, T.; Matyjaszewski, K. *Macromolecules* **2010**, *43*, 4791–7.
(10) Ooi, H. W.; Jack, K. S.; Peng, H.; Whittaker, A. K. *Polym. Chem.* **2013**, *4*, 4788-800.
(11) Deng, G.; Li, F.; Yu, H.; Liu, F.; Liu, C.; Sun, W.; Jiang, H.; Chen, Y. *ACS Macro Lett.* **2012**, *1*, 275–9.
(12) Phadke, A.; Zhang, C.; Arman, B.; Hsu, C.C.; Mashelkar, R.; Lele, A. K.; Tauber, M. J.; Arya, G.; Varghese, S. *Proc. Natl. Acad. Sci.* **2012**, *109*, 4383–8.
(13) Murphy, W. L.; Dillmore, W. S.; Modica, J.; Mrksich, M. *Angew. Chem. Int. Ed.* **2007**, *46*, 3066–9.
(14) Klaassen, C. D. *Casarett and Doull's Toxicology: The Basic Science of Poisons*; McGraw-Hill Medical Pub. Division, 2001; pp. 254–7.
(15) Ito, T.; Yeo, Y.; Highley, C. B.; Bellas, E.; Kohane, D. S. *Biomaterials* **2007**, *28*, 3418–26.
(16) Anger, R. L. *Proc. Natl. Acad. Sci.* **1999**, *96*, 3104–7.
(17) Li, Y.; Rodrigues, J.; Tomás, H. *Chem. Soc. Rev.* **2012**, *41*, 2193–221.
(18) Crompton, K. E.; Prankerd, R. J.; Paganin, D. M.; Scott, T. F.; Horne, M. K.; Finkelstein, D. I.; Gross, K.; Forsythe, J. S. *Biophys. Chem.* **2005**, *117*, 47–53.
(19) Hoemann, C. D.; Sun, J.; Légaré, A.; McKee, M. D.; Buschmann, M. D. *Osteoarthr. Res. Soc.* **2005**, *13*, 318–29.
(20) Lim, D. W.; Nettles, D. L.; Setton, L.; Chilkoti, A. *Biomacromolecules* **2007**, *8*, 1463–70.
(21) Tsuji, H. *Macromol. Biosci.* **2005**, *5*, 569–97.
(22) Harada, A.; Li, J.; Kamachi, M. *Nature* **1994**, *370*, 126–8.
(23) Singh, S.; Webster, D. C.; Singh, J. *Int. J. Pharm.* **2007**, *341*, 68–77.
(24) Hoare, T. R.; Kohane, D. S. *Polymer.* **2008**, *49*, 1993–2007.
(25) Van Tomme, S. R.; Storm, G.; Hennink, W. E. *Int. J. Pharm.* **2008**, *355*, 1–18.
(26) Chen, P. C.; Kohane, D. S.; Park, Y. J.; Bartlett, R. H.; Langer, R.; Yang, V. C. *J. Biomed. Mater. Res. A* **2004**, *70*, 459–66.
(27) Fitzpatrick, S. D.; Jafar Mazumder, M.; Lasowski, F.; Fitzpatrick, L. E.; Sheardown, H. *Biomacromolecules* **2010**, *11*, 2261–7.

(28) Hoare, T.; Bellas, E.; Zurakowski, D.; Kohane, D. S. *J. Biomed. Mater. Res. A* **2010**, *92*, 586–95.
(29) Azagarsamy, M. A.; Anseth, K. S. *ACS Macro Lett.* **2013**, *2*, 5–9.
(30) Wieduwild, R.; Tsurkan, M.; Chwalek, K.; Murawala, P.; Nowak, M.; Freudenberg, U.; Neinhuis, C.; Werner, C.; Zhang, Y. *J. Am. Chem. Soc.* **2013**, *135*, 2919–22.
(31) Overstreet, D. J.; Dutta, D.; Stabenfeldt, S. E.; Vernon, B. L. *J. Polym. Sci. B Polym. Phys.* **2012**, *50*, 881–903.
(32) Kretlow, J. D.; Klouda, L.; Mikos, A. G. *Adv. Drug Deliv. Rev.* **2007**, *59*, 263–73.
(33) Nimmo, C. M.; Shoichet, M. S. *Bioconjug. Chem.* **2011**, *22*, 2199–209.
(34) Nguyen, M. K.; Lee, D. S. *Macromol. Biosci.* **2010**, *10*, 563–79.
(35) Campbell, S. B.; Patenaude, M.; Hoare, T. *Biomacromolecules* **2013**, *14*, 644–53.
(36) Patenaude, M.; Hoare, T. *Biomacromolecules* **2012**, *13*, 369–78.
(37) Patenaude, M.; Hoare, T. *ACS Macro Lett.* **2012**, *1*, 409–13.
(38) Sivakumaran, D.; Maitland, D.; Hoare, T. *Biomacromolecules* **2011**, *12*, 4112–20.
(39) Lei, Y.; Gojgini, S.; Lam, J.; Segura, T. *Biomaterials* **2011**, *32*, 39–47.
(40) Abdalla, S.; Makhoul, G.; Duong, M.; Chiu, R. C. J.; Cecere, R. *Interact. Cardiovasc. Thorac. Surg.* **2013**, 1–6.
(41) Ercole, F.; Thissen, H.; Tsang, K.; Evans, R.; Forsythe, J. S. *Macromolecules* **2012**, *45*, 8387–400.
(42) Schild, H. G. *Prog. Polym. Sci.* **1992**, *17*, 163–249.
(43) Imaz, A.; Forcada, J. *J. Polym. Chem. A Polym. Sci.* **2010**, *48*, 1173–1181.
(44) Lutz, J.-F. *J. Polym. Sci. Part A Polym. Chem.* **2008**, *46*, 3459–3470.
(45) Engler, A.; Sen, S.; Sweeney, H.; Discher, D. *Cell* **2006**, *126*, 667–689.
(46) Anderson, J. M. *Annu. Rev. Mater. Res.* **2001**, *31*, 81–110.
(47) Zhang, L.; Cao, Z.; Bai, T.; Carr, L.; Ella-Menye, J. R.; Irvin, C.; Ratner, B. D.; Jiang, S. *Nat. Biotechnol.* **2013**, *31*, 553–6.
(48) Seifert, L. M.; Greer, R. T. *J. Biomed. Mater. Res. 19*, 1043–71.
(49) Makarand V. Risbud, R. R. *Drug Deliv.* **2000,** *2*, 69-75.
(50) Tao, Y.; Tong, X.; Zhang, Y.; Lai, J.; Huang, Y.; Jiang, Y. R.; Guo, B. H. *Acta Biomater.* **2013**, *9*, 5022–30.
(51) Pasut, G.; Veronese, F. M. *Prog. Polym. Sci.* **2007**, *32*, 933–61.
(52) Hatefi, A.; Amsden, B. *J. Control. Release* **2002**, *80*, 9–28.
(53) Mather, B. D.; Viswanathan, K.; Miller, K. M.; Long, T. E. *Prog. Polym. Sci.* **2006**, *31*, 487–531.
(54) Han, S.; He, W.; Li, J.; Li, L.; Sun, X.; Zhang, B.; Pan, T. *J. Polym. Sci. A Polym. Chem.* **2009**, *47*, 4074–82.
(55) Liang, Y.; Jensen, T. W.; Roy, E. J.; Cha, C.; Devolder, R. J.; Kohman, R. E.; Zhang, B. Z.; Textor, K. B.; Rund, L. A.; Schook, L. B.; Tong, Y. W.; Kong, H. *Biomaterials* **2011**, *32*, 2004–12.

(56) Willis, S. L.; Court, J. L.; Redman, R. P.; Wang, J.-H.; Leppard, S. W.; O'Byrne, V. J.; Small, S. A.; Lewis, A. L.; Jones, S. A.; Stratford, P. W. *Biomaterials* **2001**, *22*, 3261–72.
(57) Dittmer, D. C.; Swain, C. G.; Benson, R. E.; Friedman, M.; Cavins, J. F.; Wall, J. S. *J. Am. Chem. Soc.* **1965**, *87*, 3672–82.
(58) Friedman, M. *J. Agricultural Food Chem.* **2003**, *51*, 4504–26.
(59) Wallace, O. B.; Springer, D. M. *Tetrahedron Lett.* **1998**, *39*, 2693–4.
(60) Goessl, A.; Tirelli, N.; Hubbell, J. *J. Biomater. Sci. Polym. Ed.* **2004**, *15*, 895–904.
(61) Sakloetsakun, D.; Hombach, J. M. R.; Bernkop-Schnürch, A. *Biomaterials* **2009**, *30*, 6151–7.
(62) Du, H.; Hamilton, P.; Reilly, M.; Ravi, N. *Macromol. Biosci.* **2012**, *12*, 952–61.
(63) Zhang, H.; Qadeer, A.; Chen, W. *Biomacromolecules* **2011**, *12*, 1428–37.
(64) Wu, Z.; Zhang, X.; Zheng, C.; Li, C. *Eur. J. Pharm. Sci.* **2009**, *37*, 198–206.
(65) Ghosh, K.; Shu, X. Z.; Mou, R.; Lombardi, J.; Prestwich, G. D.; Rafailovich, M. H.; Clark, R. F. *Biomacromolecules* **2005**, *6*, 2857–65.
(66) Vercruysse, K. P.; Marecak, D. M.; Marecek, J. F.; Prestwich, G. D. *Bioconjug. Chem.* **1997**, *8*, 686–94.
(67) Shu, X. Z.; Liu, Y.; Luo, Y.; Roberts, M. C.; Prestwich, G. D. *Biomacromolecules* **2002**, *3*, 1304–11.
(68) Pritchard, C. D.; O'Shea, T. M.; Siegwart, D. J.; Calo, E.; Anderson, D. G.; Reynolds, F. M.; Thomas, J.; Slotkin, J. R.; Woodard, E. J.; Langer, R. *Biomaterials* **2011**, *32*, 587–97.
(69) Liu, S. Q.; Yang, C.; Huang, Y.; Ding, X.; Li, Y.; Fan, W. M.; Hedrick, J. L.; Yang, Y. Y. *Adv. Mater.* **2012**, *24*, 6484–9.
(70) Li, Y.; Yang, C.; Khan, M.; Liu, S.; Hedrick, J. L.; Yang, Y. Y.; Ee, P. L. R. *Biomaterials* **2012**, *33*, 6533–41.
(71) Cho, E.; Lee, J. S.; Webb, K. *Acta Biomater.* **2012**, *8*, 2223–32.
(72) Buwalda, S. J.; Dijkstra, P. J.; Feijen, J. *Macromol. Chem. Phys.* **2012**, *213*, 766–75.
(73) Rossow, T.; Heyman, J. A.; Ehrlicher, A. J.; Langhoff, A.; Weitz, D. A.; Haag, R.; Seiffert, S. *J. Am. Chem. Soc.* **2012**, *134*, 4983–9.
(74) Dong, Y.; Hassan, W.; Zheng, Y.; Saeed, A. O.; Cao, H.; Tai, H.; Pandit, A.; Wang, W. *J. Mater. Sci. Mater. Med.* **2012**, *23*, 25–35.
(75) Biswal, D.; Wattamwar, P. P.; Dziubla, T. D.; Hilt, J. Z. *Polymer.* **2011**, *52*, 5985–92.
(76) Yu, Y.; Deng, C.; Meng, F.; Shi, Q.; Feijen, J.; Zhong, Z. *J. Biomed. Mater. Res. A* **2011**, *99*, 316–26.
(77) Gojgini, S.; Tokatlian, T.; Segura, T. *Mol. Pharm.* **2011**, *8*, 1582–91.
(78) Ouasti, S.; Donno, R.; Cellesi, F.; Sherratt, M. J.; Terenghi, G.; Tirelli, N. *Biomaterials* **2011**, *32*, 6456–70.
(79) Wang, K.; Yin, R.; Tong, Z.; Yu, Q.; Nie, J. *Int. J. Biol. Macromol.* **2011**, *48*, 753–7.
(80) Kim, D.; Kim, S.; Jo, S.; Woo, J.; Noh, I. *Macromol. Res.* **2011**, *19*, 573–81.
(81) Tong, X.; Lai, J.; Guo, B. H.; Huang, Y. *J. Polym. Sci. A Polym. Chem.* **2011**, *49*, 1513–6.

(82) Bearat, H. H.; Lee, B. H.; Valdez, J.; Vernon, B. L. *J. Biomater. Sci. Polym. Ed.* DOI:10.1163/092050610X504774
(83) Peng, K.; Tomatsu, I.; van den Broek, B.; Cui, C.; Korobko, A. V.; van Noort, J.; Meijer, A. H.; Spaink, H. P.; Kros, A. *Soft Matter* **2011**, *7*, 4881.
(84) Sui, X.; van Ingen, L.; Hempenius, M. A.; Vancso, G. J. *Macromol. Rapid Commun.* **2010**, *31*, 2059–63.
(85) Liu, S. Q.; Tian, Q.; Hedrick, J. L.; Po Hui, J. H.; Ee, P. L. R.; Yang, Y. Y. *Biomaterials* **2010**, *31*, 7298–307.
(86) Yu, H. Q.; Cong, R. *Chem. Pap.* **2010**, *64*, 619–24.
(87) Liu, B.; Liu, Y.; Lewis, A. K.; Shen, W. *Biomaterials* **2010**, *31*, 4918–25.
(88) Kim, M.; Lee, J. Y.; Jones, C. N.; Revzin, A.; Tae, G. *Biomaterials* **2010**, *31*, 3596–603.
(89) Miller, J. S.; Shen, C. J.; Legant, W. R.; Baranski, J. D.; Blakely, B. L.; Chen, C. S. *Biomaterials* **2010**, *31*, 3736–43.
(90) Wang, Z. C.; Xu, X. D.; Chen, C. S.; Yun, L.; Song, J. C.; Zhang, X. Z.; Zhuo, R. X. *ACS Appl. Mater. Interfaces* **2010**, *2*, 1009–18.
(91) Blakely, B.; Hoon Lee, B.; Riley, C.; McLemore, R.; Pathak, C. P.; Vernon, B. L. *J. Biomed. Mater. Res. B. Appl. Biomater.* **2010**, *93*, 9–17.
(92) Teng, D.; Wu, Z.; Zhang, X.; Wang, Y.; Zheng, C.; Wang, Z.; Li, C. *Polymer* **2010**, *51*, 639–46.
(93) Jukes, J. M.; van der Aa, L. J.; Hiemstra, C.; van Veen, T.; Dijkstra, P. J.; Zhong, Z.; Feijen, J.; van Blitterswijk, C. A.; de Boer, J. *Tissue Eng. A* **2010**, *16*, 565–73.
(94) Dhanasingh, A.; Salber, J.; Moeller, M.; Groll, J. *Soft Matter* **2010**, *6*, 618–29.
(95) Jo, Y. S.; Gantz, J.; Hubbell, J. A.; Lutolf, M. P. *Soft Matter* **2009**, *5*, 440-6.
(96) Lih, E. *J. Bioact. Compat. Polym.* **2008**, *23*, 444–457.
(97) Rydholm, A. E.; Held, N. L.; Benoit, D. S. W.; Bowman, C. N.; Anseth, K. S. *J. Biomed. Mater. Res. A* **2008**, *86*, 23–30.
(98) Dandan, H.; Tong, H.; Lin, Y.; Aiying, Z.; Changyong, W.; Zengguo, F. *Acta Polymerica Sinica* **2008**, *4*, 388-93.
(99) Kim, M. S.; Choi, Y. J.; Noh, I.; Tae, G. *J. Biomed. Mater. Res. A* **2007**, *83*, 674–82.
(100) Cheng, V.; Lee, B. H.; Pauken, C.; Vernon, B. L. *J. Appl. Polym. Sci.* **2007**, *106*, 1201– 7.
(101) Hiemstra, C.; A., L. J. van der; Zhong, Z.; Dijkstra, P. J.; Feijen, J. *Biomacromolecules* **2007**, *8*, 1548–56.
(102) Kim, J.; Kim, I. S.; Cho, T. H.; Lee, K. B.; Hwang, S. J.; Tae, G.; Noh, I.; Lee, S. H.; Park, Y.; Sun, K. *Biomaterials* **2007**, *28*, 1830–7.
(103) Ghosh, K.; Ren, X.-D.; Shu, X. Z.; Prestwich, G. D.; Clark, R. A. F. *Tissue Eng.* **2006**, *12*, 601–13.
(104) Metters, A.; Hubbell, J. *Biomacromolecules* **2005**, *6*, 290–301.
(105) Cellesi, F.; Tirelli, N.; Hubbell, J. A. *Biomaterials* **2004**, *25*, 5115–24.
(106) Elbert, D. L.; Pratt, A. B.; Lutolf, M. P.; Halstenberg, S.; Hubbell, J. A. *J. Control. Release* **2001**, *76*, 11–25.

(107) Liu, S. Q.; Tian, Q.; Wang, L.; Hedrick, J. L.; Hui, J. H. P.; Yang, Y. Y.; Ee, P. L. R. *Macromol. Rapid Commun.* **2010**, *31*, 1148–54.
(108) Kim, J.; Park, Y.; Tae, G.; Lee, K. B.; Hwang, C. M.; Hwang, S. J.; Kim, I. S.; Noh, I.; Sun, K. *J. Biomed. Mater. Res. A* **2009**, *88*, 967–75.
(109) Chen, C.; Wang, L.; Deng, L.; Hu, R.; Dong, A. *J. Biomed. Mater. Res. A* **2013**, *101*, 684–93.
(110) DuBose, J. W.; Cutshall, C.; Metters, A. T. *J. Biomed. Mater. Res. A* **2005**, *74*, 104–16.
(111) Cai, S.; Liu, Y.; Zheng Shu, X.; Prestwich, G. D. *Biomaterials* **2005**, *26*, 6054–67.
(112) Sekine, Y.; Moritani, Y.; Ikeda-Fukazawa, T.; Sasaki, Y.; Akiyoshi, K. *Adv. Healthc. Mater.* **2012**, *1*, 722–8.
(113) Censi, R.; Fieten, P. J.; Di Martino, P.; Hennink, W. E.; Vermonden, T. *J. Control. Release* **2010**, *148*, e28–9.
(114) Kloxin, A. M.; Kloxin, C. J.; Bowman, C. N.; Anseth, K. S. *Adv. Mater.* **2010**, *22*, 3484–94.
(115) Censi, R.; Fieten, P. J.; di Martino, P.; Hennink, W. E.; Vermonden, T. *Macromolecules* **2010**, *43*, 5771– 8.
(116) Hirakura, T.; Yasugi, K.; Nemoto, T.; Sato, M.; Shimoboji, T.; Aso, Y.; Morimoto, N.; Akiyoshi, K. *J. Control. Release* **2010**, *142*, 483–9.
(117) Marklein, R. A.; Burdick, J. A. *Soft Matter* **2010**, *6*, 136–43.
(118) Silvestri, B.; Luciani, G.; Costantini, A.; Tescione, F.; Branda, F.; Pezzella, A. *J. Biomed. Mater. Res. B. Appl. Biomater.* **2009**, *89*, 369–78.
(119) Oh, E. J.; Kim, J. W.; Kong, J. H.; Ryu, S. H.; Hahn, S. K. *Bioconjug. Chem.* **2008**, *19*, 2401–8.
(120) Wang, N.; Dong, A.; Radosz, M.; Shen, Y. *J. Biomed. Mater. Res. A* **2008**, *84*, 148–57.
(121) Hahn, S. K.; Oh, E. J.; Miyamoto, H.; Shimobouji, T. *Int. J. Pharm.* **2006**, *322*, 44–51.
(122) Noh, I.; Kim, G. W.; Choi, Y. J.; Kim, M. S.; Park, Y.; Lee, K. B.; Kim, I. S.; Hwang, S. J.; Tae, G. *Biomed. Mater.* **2006**, *1*, 116–23.
(123) Yu, Y.; Deng, C.; Meng, F.; Shi, Q.; Feijen, J.; Zhong, Z. *J. Biomed. Mater. Res. A* **2011**, *99*, 316–26.
(124) Dong, Y.; Saeed, A. O.; Hassan, W.; Keigher, C.; Zheng, Y.; Tai, H.; Pandit, A.; Wang, W. *Macromol. Rapid Commun.* **2011**, 120– 6.
(125) Shi, C.; Zhu, Y.; Ran, X.; Wang, M.; Su, Y.; Cheng, T. *J. Surg. Res.* **2006**, *133*, 185–92.
(126) Yoon, J. A.; Bencherif, S. A.; Aksak, B.; Kim, E. K.; Kowalewski, T.; Oh, J. K.; Matyjaszewski, K. *Chem. Asian J.* **2011**, *6*, 128–36.
(127) Bencherif, S. A.; Siegwart, D. J.; Srinivasan, A.; Horkay, F.; Hollinger, J. O.; Washburn, N. R.; Matyjaszewski, K. *Biomaterials* **2009**, *30*, 5270–8.
(128) Tsurkan, M. V; Chwalek, K.; Prokoph, S.; Zieris, A.; Levental, K. R.; Freudenberg, U.; Werner, C. *Adv. Mater.* **2013**, *25*, 2606–10.
(129) Koehler, K. C.; Anseth, K. S.; Bowman, C. N. *Biomacromolecules* **2013**, *14*, 538–47.
(130) Baldwin, A. D.; Kiick, K. L. *Polym. Chem.* **2013**, *4*, 133–43.

(131) Phelps, E. A.; Enemchukwu, N. O.; Fiore, V. F.; Sy, J. C.; Murthy, N.; Sulchek, T. A.; Barker, T. H.; García, A. J. *Adv. Mater.* **2012**, *24*, 64–70.
(132) Dickgreber, N.; Stoitzner, P.; Bai, Y.; Price, K. M.; Farrand, K. J.; Manning, K.; Angel, C. E.; Dunbar, R.; Ronchese, F.; Fraser, J. D.; Thomas, B.; Hermans, I. F.; Dunbar, P. R.; Ba, B. T. *J. Immunol.* **2013**, *182*, 1260–69.
(133) Jin, R.; Dijkstra, P. J.; Feijen, J. *J. Control. Release* **2010**, *148*, e41–3.
(134) Allazetta, S.; Hausherr, T. C.; Lutolf, M. P. *Biomacromolecules* **2013**, *14*, 1122–31.
(135) McGann, C. L.; Levenson, E. A.; Kiick, K. L. *Macromol. Chem. Phys.* **2013**, *214*, 203–13.
(136) Peng, G.; Wang, J.; Yang, F.; Zhang, S.; Hou, J.; Xing, W.; Lu, X.; Liu, C. *J. Appl. Polym. Sci.* **2013**, *127*, 577–84.
(137) Bearat, H. H.; Lee, B. H.; Vernon, B. L. *Acta Biomater.* **2012**, *8*, 3629–42.
(138) Yu, Y.; Chau, Y. *Biomacromolecules* **2012**, *13*, 937–42.
(139) Shikanov, A.; Smith, R. M.; Xu, M.; Woodruff, T. K.; Shea, L. D. *Biomaterials* **2011**, *32*, 2524–31.
(140) Chawla, K.; Yu, T. B.; Liao, S. W.; Guan, Z. *Biomacromolecules* **2011**, *12*, 560–7.
(141) Zustiak, S. P.; Leach, J. B. *Biotechnol. Bioeng.* **2011**, *108*, 197–206.
(142) Patterson, J.; Hubbell, J. A. *Biomaterials* **2010**, *31*, 7836–45.
(143) Lei, Y.; Ng, Q. K. T.; Segura, T. *Microsc. Res. Tech.* **2010**, *73*, 910–7.
(144) Jin, R.; Moreira Teixeira, L. S.; Krouwels, A.; Dijkstra, P. J.; van Blitterswijk, C. A.; Karperien, M.; Feijen, J. *Acta Biomater.* **2010**, *6*, 1968–77.
(145) Zustiak, S. P.; Leach, J. B. *Biomacromolecules* **2010**, *11*, 1348–57.
(146) Kong, J. H.; Oh, E. J.; Chae, S. Y.; Lee, K. C.; Hahn, S. K. *Biomaterials* **2010**, *31*, 4121–8.
(147) Hiemstra, C.; Zhong, Z.; van Steenbergen, M. J.; Hennink, W. E.; Feijen, J. *J. Control. Release* **2007**, *122*, 71–8.
(148) Hiemstra, C.; van der Aa, L. J.; Zhong, Z.; Dijkstra, P. J.; Feijen, J. *Macromolecules* **2007**, *40*, 1165–73.
(149) Rizzi, S. C.; Hubbell, J. A. *Biomacromolecules 6*, 1226–38.
(150) Lutolf, M. P.; Hubbell, J. A. *Biomacromolecules* **2003**, *4*, 713–22.
(151) Wang, R.; Chen, W.; Meng, F.; Cheng, R.; Deng, C.; Feijen, J.; Zhong, Z. *Macromolecules* **2011**, *44*, 6009–16.
(152) Lee, Y.; Chung, H. J.; Yeo, S.; Ahn, C. H.; Lee, H.; Messersmith, P. B.; Park, T. G. *Soft Matter* **2010**, *6*, 977–83.
(153) Lin, C.; Zhao, P.; Li, F.; Guo, F.; Li, Z.; Wen, X. *Mater. Sci. Eng. C* **2010**, *30*, 1236–44.
(154) Murray, B. S.; Fulton, D. *Macromolecules* **2011**, *44*, 7242–52.
(155) Aleksanian, S.; Khorsand, B.; Schmidt, R.; Oh, J. K. *Polym. Chem.* **2012**, *3*, 2138-47.
(156) Khorsand Sourkohi, B.; Cunningham, A.; Zhang, Q.; Oh, J. K. *Biomacromolecules* **2011**, *12*, 3819–25.
(157) Cunningham, A.; Oh, J. K. *Macromol. Rapid Commun.* **2012**, 1–6.

(158) Oh, J. K.; Siegwart, D. J.; Lee, H.; Sherwood, G.; Peteanu, L.; Hollinger, J. O.; Kataoka, K.; Matyjaszewski, K. *J. Am. Chem. Soc.* **2007**, *129*, 5939–45.
(159) Klaikherd, A.; Nagamani, C.; Thayumanavan, S. *J. Am. Chem. Soc.* **2009**, *131*, 4830–8.
(160) Ryu, J. H.; Chacko, R. T.; Jiwpanich, S.; Bickerton, S.; Babu, R. P.; Thayumanavan, S. *J. Am. Chem. Soc.* **2010**, 17227–35.
(161) Swindle-Reilly, K. E.; Shah, M.; Hamilton, P. D.; Eskin, T. A.; Kaushal, S.; Ravi, N. *Invest. Ophthalmol. Vis. Sci.* **2009**, *50*, 4840–6.
(162) Wu, D. C.; Joh, X. L.; Wu, J. L.; Lay, C. L.; Liu, Y. *J. Am. Chem. Soc.* **2010**, *132*, 15140–3.
(163) Choh, S. Y.; Cross, D.; Wang, C. *Biomacromolecules* **2011**, *12*, 1126–6.
(164) Grasdalen, H.; Smidsrød, O. *Carbohydr. Polym.* **1987**, *7*, 371–93.
(165) Wu, Z. M.; Zhang, X. G.; Zheng, C.; Li, C. X.; Zhang, S. M.; Dong, R. N.; Yu, D. M. *Eur. J. Pharm. Sci.* **2009**, *37*, 198–206.
(166) Garver, J. M.; Gronert, S.; Bierbaum, V. M. *J. Am. Chem. Soc.* **2011**, *133*, 13894–7.
(167) Lee, K. Y.; Bouhadir, K. H.; Mooney, D. J. *Macromolecules* **2000**, *33*, 97–101.
(168) Vetrík, M.; Přádný, M.; Hrubý, M.; Michálek, J. *Polym. Degrad. Stab.* **2011**, *96*, 756–9.
(169) Krishna, U. M.; Martinez, A. W.; Caves, J. M.; Chaikof, E. L. *Acta Biomater.* **2012**, *8*, 988–97.
(170) Zhang, R.; Huang, Z.; Xue, M.; Yang, J.; Tan, T. *Carbohydr. Polym.* **2011**, *85*, 717–25.
(171) Martínez-Sanz, E.; Ossipov, D. A.; Hilborn, J.; Larsson, S.; Jonsson, K. B.; Varghese, O. P. *J. Control. Release* **2011**, *152*, 232–40.
(172) Luo, Y.; Kobler, J. B.; Heaton, J. T.; Jia, X.; Zeitels, S. M.; Langer, R. *J. Biomed. Mater. Res. B. Appl. Biomater.* **2010**, *93*, 386–93.
(173) Buchs, B.; Fieber, W.; Vigouroux-Elie, F.; Sreenivasachary, N.; Lehn, J. M.; Herrmann, A. *Org. Biomol. Chem.* **2011**, *9*, 2906–19.
(174) Hudson, S. P.; Langer, R.; Fink, G. R.; Kohane, D. S. *Biomaterials* **2010**, *31*, 1444–52.
(175) Patenaude, M.; Hoare, T. *ACS Macro Lett.* **2012**, *1*, 409–13.
(176) Hoare, T.; Sivakumaran, D.; Stefanescu, C. F.; Lawlor, M. W.; Kohane, D. S. *Acta Biomater.* **2012**, *8*, 1450–8.
(177) Patenaude, M.; Campbell, S. B.; Kinio, D.; Hoare, T. Biomacromolecules, submitted.
(178) Sivakumaran, D.; Maitland, D.; Hoare, T. *Biomacromolecules* **2011**, *12*, 4112–20.
(179) Kalia, J.; Raines, R. T. *Angew. Chem. Int. Ed. Engl.* **2008**, *47*, 7523–6.
(180) Grover, G. N.; Maynard, H. D. *Curr. Opin. Chem. Biol.* **2010**, *14*, 818–27.
(181) Slfidek, T.; Filkuka, J.; Dole, S.; V., J.; Hartmannov, B.; Tr, J. **1984**, *349*, 344–9.
(182) Ossipov, D. A.; Piskounova, S.; Varghese, O. P.; Hilborn, J. *Biomacromolecules* **2010**, *11*, 2247–54.
(183) Grover, G. N.; Lam, J.; Nguyen, T. H.; Segura, T.; Maynard, H. D. *Biomacromolecules* **2012**, *10*, 3013–7.

(184) Grover, G. N.; Braden, R. L.; Christman, K. L. *Adv. Mater.* **2013**, 1–6.
(185) Baldwin, J. E.; Herchen, S. R.; Schulz, G.; Falshaw, C. P.; King, T. J. *J. Am. Chem. Soc.* **1980**, *70*, 7816–7.
(186) Wei, H. L.; Yang, Z.; Zheng, L. M.; Shen, Y. M. *Polymer.* **2009**, *50*, 2836–40.
(187) Nimmo, C. M.; Owen, S. C.; Shoichet, M. S. *Biomacromolecules* **2011**, *12*, 824–30.
(188) Tan, H.; Rubin, J. P.; Marra, K. G. *Macromol. Rapid Commun.* **2011**, *32*, 905–11.
(189) Wei, H. L.; Yao, K.; Yang, Z.; Chu, H. J.; Zhu, J.; Ma, C. C.; Zhao, Z. X. *Macromol. Res.* **2011**, *19*, 294–9.
(190) Huisgen, R. *Angew. Chemie* **1963**, *2*, 565–632.
(191) Wang, Q.; Chan, T. R.; Hilgraf, R.; Fokin, V. V; Sharpless, K. B.; Finn, M. G. *J. Am. Chem. Soc.* **2003**, *125*, 3192–3.
(192) Ossipov, D. A.; Hilborn, J. *Macromolecules* **2006**, *39*, 1709–18.
(193) Crescenzi, V.; Cornelio, L.; Di Meo, C.; Nardecchia, S.; Lamanna, R. *Biomacromolecules* **2007**, *8*, 1844–50.
(194) Koschella, A.; Hartlieb, M.; Heinze, T. *Carbohydr. Polym.* **2011**, *86*, 154–61.
(195) Hu, X.; Li, D.; Zhou, F.; Gao, C. *Acta Biomater.* **2011**, *7*, 1618–26.
(196) Testa, G.; Di Meo, C.; Nardecchia, S.; Capitani, D.; Mannina, L.; Lamanna, R.; Barbetta, A.; Dentini, M. *Int. J. Pharm.* **2009**, *378*, 86–92.
(197) Van Dijk, M.; van Nostrum, C. F.; Hennink, W. E.; Rijkers, D. T. S.; Liskamp, R. M. J. *Biomacromolecules* **2010**, *11*, 1608–14.
(198) Tan, S.; Blencowe, A.; Ladewig, K.; Qiao, G. G. *Soft Matter* **2013**, *9*, 5239–50.
(199) Okumura, Y.; Ito, K. *Adv. Mater.* **2001**, *13*, 485–87.
(200) Agard, N. J.; Prescher, J. a; Bertozzi, C. R. *J. Am. Chem. Soc.* **2004**, *126*, 15046–7.
(201) Lallana, E.; Fernandez-megia, E.; Riguera, R. *J. Am. Chem. Soc.* **2009**, 5748–50.
(202) DeForest, C.; Polizzotti, B. D.; Anseth, K. S. *Nat. Mater.* **2009**, *8*, 659–64.
(203) Deforest, C. A.; Sims, E. A.; Anseth, K. S. *Chem. Mater.* **2010**, *22*, 4783–90.
(204) Codelli, J.; Baskin, J. *J. Am. Chem. Soc.* **2008**, *130*, 11486–93.
(205) Sletten, E. M.; Bertozzi, C. R. *Acc. Chem. Res.* **2011**, *44*, 666–76.
(206) Ning, X.; Guo, J.; Wolfert, M.; Boons, G.-J. *Angew. Chem. Int. Ed. Engl.* **2008**, *47*, 2253–5.
(207) Xu, J.; Filion, T. M.; Prifti, F.; Song, J. *Asian Chem. J.* **2011**, *6*, 2730–7.
(208) Zheng, J.; Smith Callahan, L. A.; Hao, J.; Guo, K.; Wesdemiotis, C.; Weiss, R. A.; Becker, M. L. *ACS Macro Lett.* **2012**, *1*, 1071–1073.
(209) Gardner, C. M.; Potter, M. A.; Stöver, H. D. H. *J. Mater. Sci. Mater. Med.* **2012**, *23*, 181–93.
(210) Samiullah, M. H.; Reichert, D.; Zinkevich, T.; Kressler, J. *Macromolecules* **2013**, *46*, 6922-30.

CHAPTER 2

INJECTABLE, DEGRADABLE THERMORESPONSIVE POLY(N-ISOPROPYLACRYLAMIDE) HYDROGELS

Authors: Mathew Patenaude and Todd Hoare

Publication Information: ACS Macro Letters 1(3), 409-413

Accepted Date: 27 February 2012

Abstract:

Degradable, covalently *in situ* gelling analogues of thermoresponsive poly(N-isopropylacrylamide) (PNIPAM) hydrogels have been designed by mixing aldehyde and hydrazide-functionalized PNIPAM oligomers with molecular weights below the renal cut-off. Co-extrusion of the reactive polymer solutions through a double-barreled syringe facilitates rapid gel formation within seconds. The resulting hydrazone cross-links hydrolytically degrade over several weeks into low molecular weight oligomers. The characteristic reversible thermoresponsive swelling-deswelling phase transition of PNIPAM hydrogels is demonstrated. Furthermore, both *in vitro* and *in vivo* toxicity assays indicated that the hydrogel as well as the precursor polymers/degradation products were non-toxic at biomedically-relevant concentrations. This chemistry may thus represent a general approach for preparing covalently-cross-linked, synthetic polymer hydrogels that are both injectable and degradable.

Thermoresponsive hydrogels based on poly(N-isopropylacrylamide) (PNIPAM) that switch from a hydrated, expanded state at low temperature to a collapsed state at high temperature have been extensively investigated in the literature. The proximity of the ~32°C volume phase transition temperature (VPTT) of PNIPAM hydrogels with physiological temperature (37°C) has sparked particular interest in the biomedical applications of these hydrogels as "smart", environmentally-tunable drug delivery vehicles[1], tissue engineering scaffolds[2], cell growth/separation supports[3], and biomolecule separation and recovery matrices[4], among other applications[5].

Despite their significant potential in biomedical applications, PNIPAM hydrogels have not achieved clinical success, primarily due to concerns regarding the ultimate fate of PNIPAM inside the body. Though toxic in its monomeric form[5], poly(N-isopropylacrylamide) has been shown to be effectively non-cytotoxic at concentrations realistic to many medical applications[6]. However, possible depolymerization and/or chronic bioaccumulation of PNIPAM represent significant regulatory barriers to medical use. An additional practical barrier is the need to fabricate current PNIPAM hydrogel formulations outside of the body, as the free radical chemistry and thermal or UV initiation[216] required to form the hydrogels can induce significant cell toxicity and/or cannot be performed in deep tissues. While weakly cross-linked hydrogels may be sufficiently viscous to facilitate injection[217], injection of more highly elastic hydrogels is impractical. As a result, there is a need for mechanically-robust PNIPAM-based

hydrogels that can be introduced into the body through minimally invasive means and subsequently degrade into safe and clearable products.

While many studies have explored the formation of injectable and degradable thermoresponsive hydrogels via physical association[1, 7, 8] or space-filling[9], relatively few studies have addressed the challenge of creating injectable and degradable covalently-cross-linked PNIPAM hydrogels. Hydrolytically-degradable hydrogels have been prepared by copolymerizing NIPAM with di(meth)acrylate cross-linkers containing a hydrolyzable internal segment, including poly(caprolactone)[10, 11], poly(trimethylene carbonate)[12], acryloyloxyethylaminopolysuccinimde[13], ester linkages[14], or chitosan[15]. Reducible hydrogels have been fabricated by incorporating disulfide linkages in the cross-linker[16, 17]. Enzymatically-degradable PNIPAM hydrogels have also been reported based on peptide cross-linkers[18]. In all these cases, chain transfer or controlled radical polymerization techniques can be used to limit the molecular weight of the polymers between degradable cross-linking points to promote clearance following degradation[17]. However, none of these formulations gel *in situ* upon injection, limiting the maximum mechanical strength of a hydrogel amenable for injection. *In situ*-gelling natural polymer hydrogels have also been reported, using Michael addition[19], Schiff base formation[20], and hydrazone bond formation[21] to facilitate rapid gelation upon the mixing of reactive polymer precursors and/or functional cross-linkers. However, outside of hydrogels fabricated by mixing aldehyde and amine-functionalized Pluronic copolymers[22], no covalently cross-linked and *in situ*-gellable thermoresponsive hydrogels have been reported.

In this communication, we report the design and synthesis of covalently-cross-linked PNIPAM hydrogels that are both injectable and degradable based on PNIPAM copolymers possessing hydrazide and aldehyde functionalities. Figure 2.1 shows the chemistry used to synthesize the reactive polymeric precursors. Hydrazide-functionalized polymer precursors (poly(NIPAM-co-ADH)) were synthesized by functionalizing poly(NIPAM-co-acrylic acid) polymers with adipic acid dihydrazide via carbodiimide chemistry. Aldehyde-functionalized polymer precursors (poly(NIPAM-co- oxoethyl methacrylate) were synthesized via copolymerization of NIPAM with dihydroxypropyl methacrylate and subsequent oxidation of the diol. In both cases, use of a chain transfer agent limits the molecular weight of the polymers (M_n < 22 kDa) below the renal cut-off (~40 kDa), facilitating potential clearance of the degradation products from the body. To make a hydrogel, reactive polymers were individually dissolved in 6 wt% 10mM NaCl aqueous solutions, loaded into separate barrels of a double-barreled syringe, and co-extruded through a turbulent mixer into a silicone mould. Formation of the hydrogel network occurred in less than one minute following co-extrusion. This rapid gelation would permit the formation of a gel network before the low-viscosity linear polymer precursors are able to diffuse away from their site of introduction, a significant problem with slower-reacting *in situ* gelation chemistries.

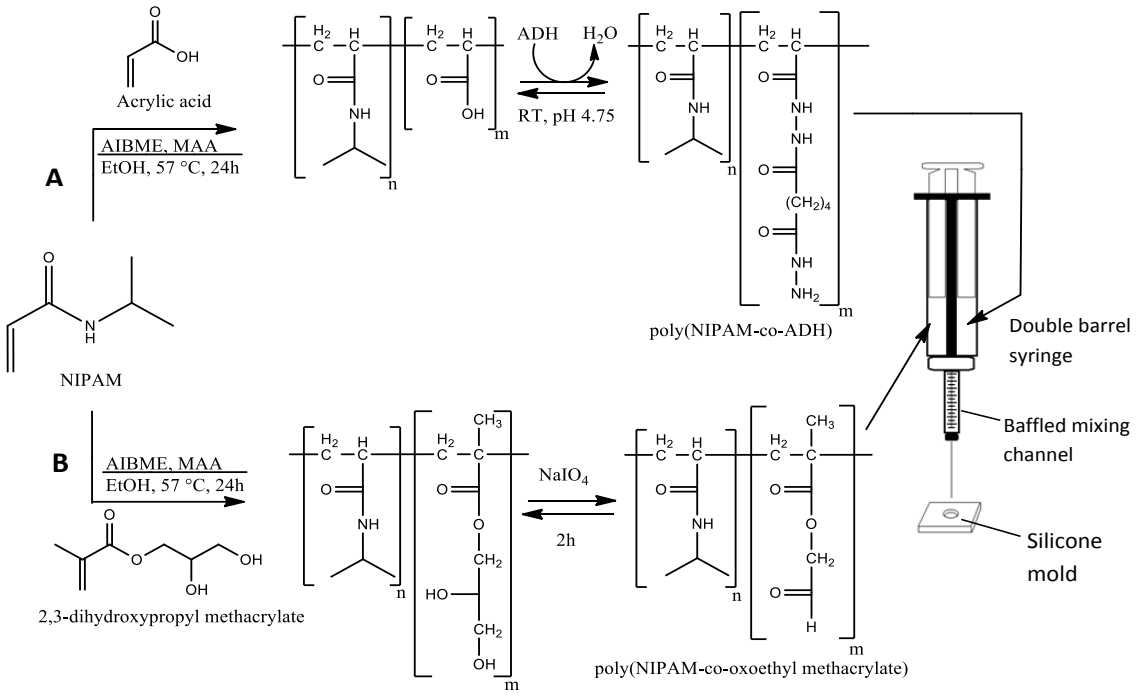

Figure 2.1. Synthesis of hydrazide-functionalized precursor copolymers (route A) and aldehyde-functionalized precursor copolymers (route B). Each precursor copolymer (dissolved at 6 wt% in 10mM NaCl aqueous solutions) was added to its respective barrel of a double-barreled syringe. Precursors are then extruded along a mixing channel into a mould, where they rapidly cross-link to form the hydrogel.

The reversible thermal response of the resulting PNIPAM hydrogel is demonstrated in Figure 2.2. Hydrogels were incubated in 10 mM PBS (pH 7.4) and were alternately placed on shaking platforms maintained at 25 °C and 37 °C for defined time intervals to assay the reversibility of the PNIPAM hydrogel phase transition.

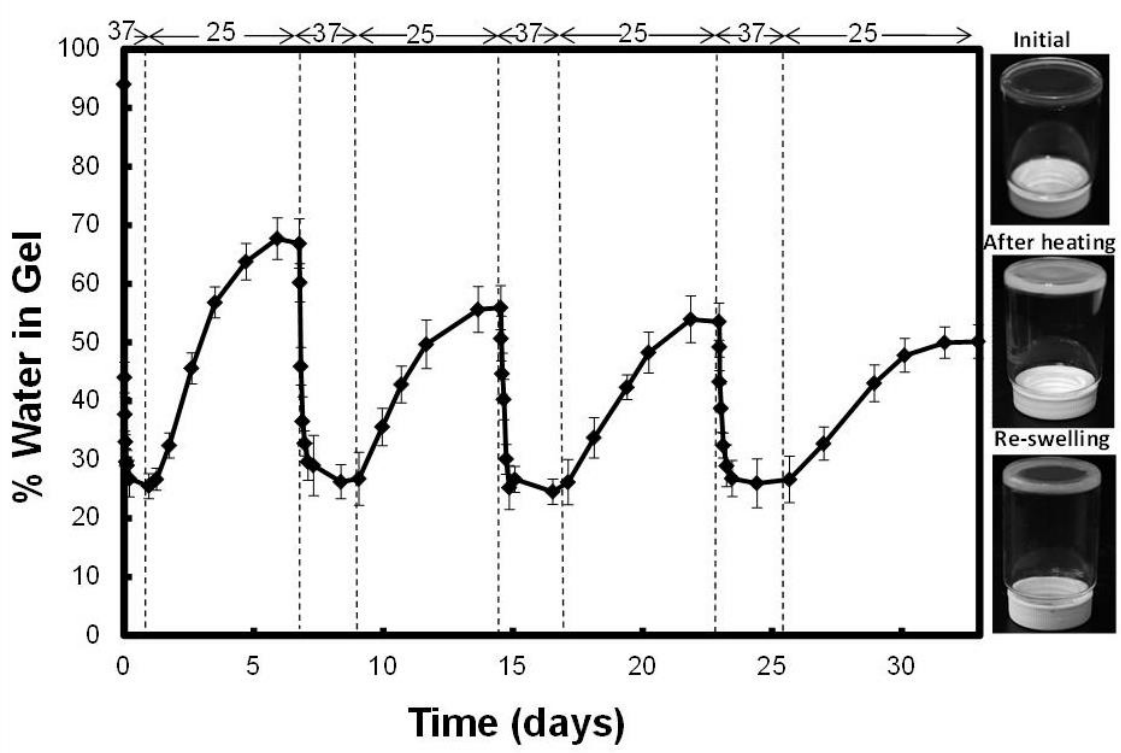

Figure 2.2. Reversible collapse/swelling of poly(NIPAM) hydrogel network incubated in 10 mM PBS (pH 7.4) at alternating temperatures of 25 °C and 37 °C (as noted at top of graph). Inset: Gel opacity resulting from a transition from the zero-strain state to 37 °C and re-swelling at 25 °C.

The initial collapse of the hydrogel network occurs more rapidly (5.1 hours) than subsequent cycles (7.7 hours on average), while re-swelling of the network takes place over a number of days before the equilibrium swelling condition is again reached. Although the hydrogels do not fully recover to the zero strain state following their first incubation at 37 $^{\circ}$C, hydrogels exhibit reversible swelling-deswelling transitions upon subsequent cycles; this is consistent with previous reports of conventional PNIPAM hydrogels[218]. The swelling response is mirrored by changes in the turbidity of the hydrogel, which switches from nearly transparent immediately following gel formation to completely opaque upon thermal collapse to semi-translucent upon re-hydration (Fig. 2.2,

side panel). The relatively long time period required for full reswelling at each cycle likely results from the high degree of cross-linking between precursor copolymers. Based on the degree of functionalization of the constituent polymers (14.3 ± 0.3 % hydrazide groups and 11 ± 3 % aldehyde groups), the average number of monomers between cross-links N_x is as high as ~12 in these injectable hydrogels, equivalent to the preparation of conventional hydrogels with ~8.5 mol% cross-linker; conventional PNIPAM hydrogels of similar cross-link densities have been reported to require several days to reswell to their equilibrium state upon a temperature change[23]. Thus, the injectable hydrogels exhibit the same thermal deswelling and scattering properties of conventional, non-degradable PNIPAM hydrogels.

Figure 2.3 demonstrates the degradability of the synthesized PNIPAM hydrogels in response to acid-catalyzed hydrolysis. The increase in degradation rate with increasing acid concentration demonstrates that bulk loss of hydrogel occurs by proton-catalyzed hydrolysis of the hydrazone cross-links (the carbon-carbon polymer backbone is not hydrolytically susceptible). It should also be noted that minimal hydrolysis of amide groups in PNIPAM residues has been observed using the same catalytic conditions[24]. Extrapolating the measured kinetics using a power law correlation that fits the data, the gel lifetime would be ~3 months at physiological pH (pH = 7.4), consistent with previously reported hydrolytic lifetimes of hydrazone cross-links[25]. Note that the maximum water content (measured gravimetrically) upon thermal cycling decreases slightly upon multiple cycles (Figure 2.2), indicating a loss of hydrogel mass as a function of time that may be related to slow degradation of the hydrogel in the PBS media used for

release studies. By degrading the hydrogels at defined chemical cross-linking points, we expect that the toxic effects observed with very low molecular weight PNIPAM chains *in vivo* may be avoided[6] without compromising the potential clearance of the polymer degradation products through the kidney. The time frame over which this degradation occurs may be tunable by altering the number of cross-links between the polymer precursors, by reducing the amount of oxoethyl methacrylate and/or acrylic acid (i.e. conjugation sites for adipic acid dihydrazide) in the base polymer used to synthesize the hydrogels, reducing the degree of oxoethyl methacrylate oxidation, or by reducing the molecular weight of the PNIPAM gel precursors.

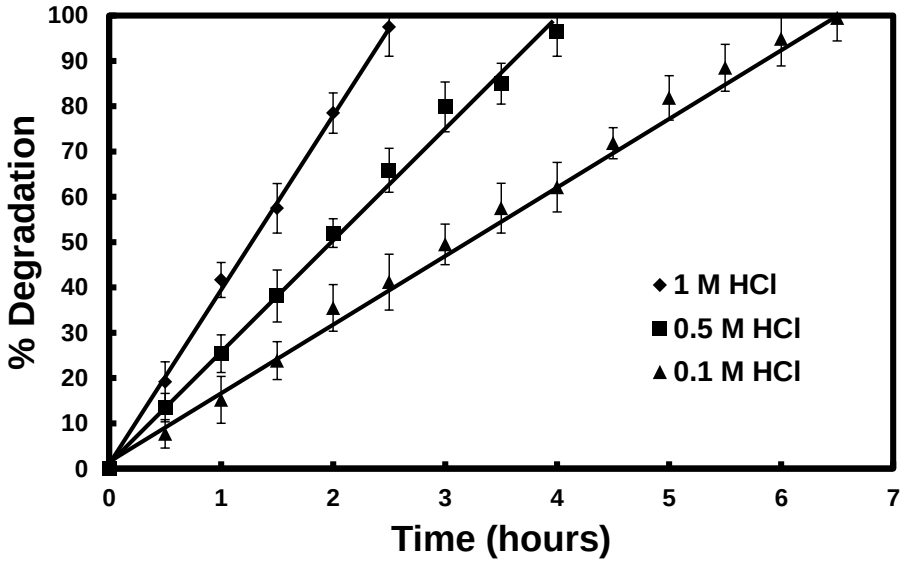

Figure 2.3. Degradation of PNIPAM hydrogels on incubation at 37 °C in 0.1 M, 0.5 M, and 1 M HCl.

In vitro and *in vivo* toxicity studies of the injectable PNIPAM hydrogels and the hydrazide and aldehyde-reactive precursor copolymers are shown in Figure 2.4. *In vitro* cell viability assays were performed using an MTT assay with 3T3 mouse fibroblasts and

retinal pigment epithelial (RPE) cells. Note that retinal pigment epithelium cells are grown in serum-free media, permitting cytotoxicity assessments both in response to the pure material (RPE cells) and a protein-adsorbed material (3T3 cells). Poly(NIPAM-co-ADH) induces a slight cytotoxic response at concentrations greater than 400 μg/mL in 3T3 cells (Fig. 2.4-A) and no significant toxicity at any tested concentration in RPE cells (Fig. 2.4-B). Poly(NIPAM-co-oxoethyl methacrylate) induces only mild cytotoxicity to both cell types at low-to-moderate concentrations but becomes more cytotoxic at very high concentrations (i.e. 2000 μg/mL, Figs. 4-A, B). Overall, any observed cytotoxicity occurs at polymer concentrations well above any local concentrations expected due to the slow hydrolytic degradation of hydrogel under physiological conditions. Similarly, 3T3 cells incubated in the presence of a PNIPAM hydrogel showed no significant decrease in cell viability relative to a cell-only control (viability = 0.99 ± 0.11 % relative to a cell-only control).

Acute (48 hours post-injection) *in vivo* toxicity assays were performed via subcutaneous injection of BALB/c mice with 0.35 mL of 6 wt% solutions of PNIPAM polymer precursors (Figs. 2.4-C and D), a 6 wt% *in situ*-formed hydrogel (Fig. 2.4-E), and a phosphate buffered saline (PBS) control (Fig. 2.4-F). Hematoxylin-eosin (H&E) staining indicates that the reactive copolymer solutions are largely cleared from the injection site 48 hours post-injection and induce only a very mild acute inflammatory response, similar to that observed with the PBS control injection (see Supporting Information, Figure 2.S2). The *in situ*-gelled PNIPAM hydrogel remains at the injection site after 48 hours and induces a mild inflammatory response at the tissue-hydrogel interface consisting

predominantly of macrophages with a few neutrophils. However, the adjacent muscle tissue maintains its polygonal, multi-nucleate structure and blood vessels remained un-occluded. Following a five-month chronic incubation of gel *in vivo* (figure 3.4F) it is observed that the gel remains at the site of introduction, although the quantity of residual gel is somewhat lower than the initial injected volume. However, minimal to no fibrous capsule formation was observed at the gel-tissue interface and no sign of a chronic inflammatory response was noted either within the residual gel or within the tissue adjacent to the gel relative to the PBS-only control (Supporting Information, Figure 2.S2). Together, these results suggest that the gel is well-tolerated within the subcutaneous space and may be amenable for practical use in *in vivo* applications.

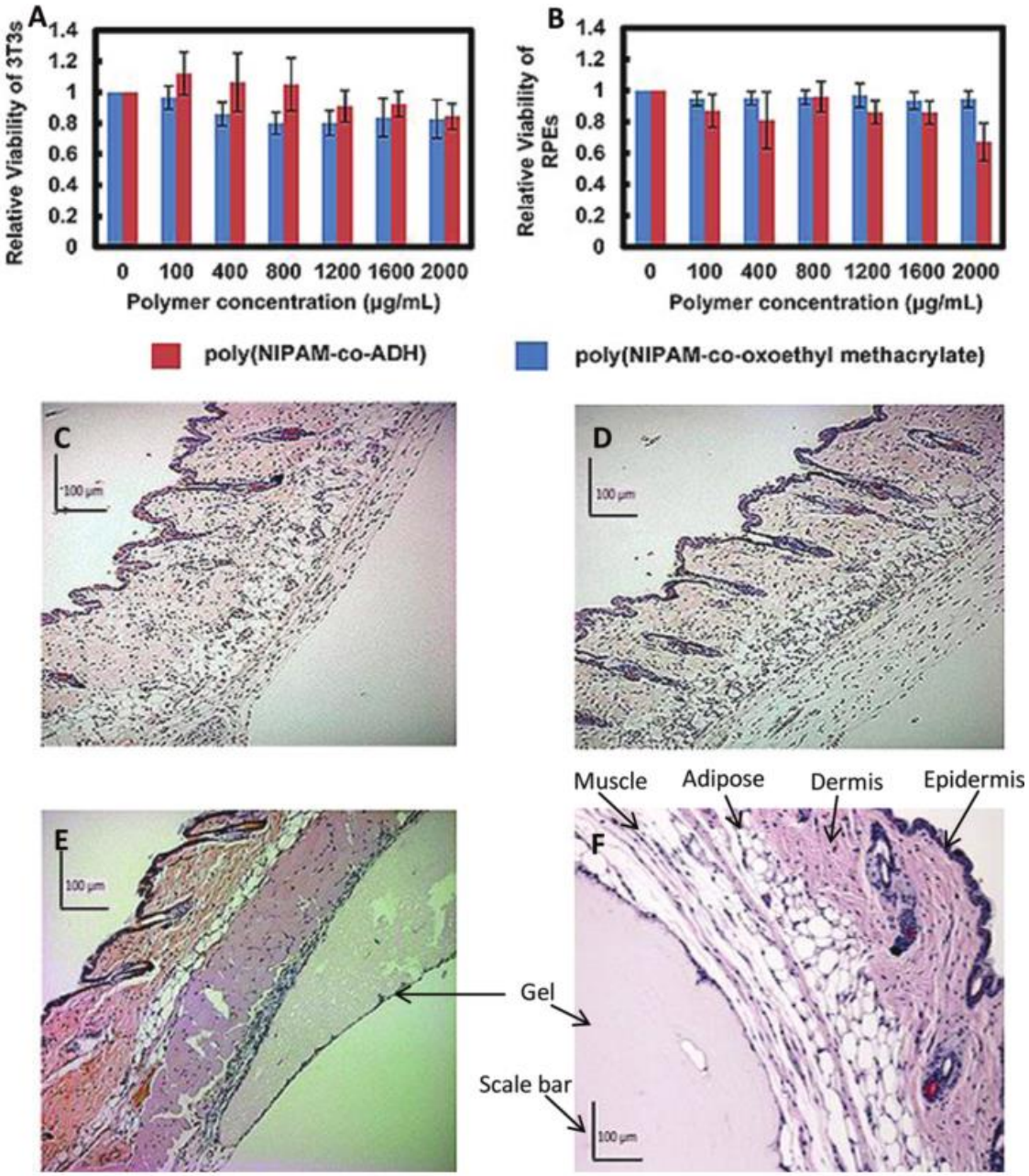

Figure 2.4. Cytotoxicity and biocompatibility of injectable hydrogels and precursor/degradation product polymers: (A) MTT viability assays of 3T3 mouse fibroblasts in the presence of both precursor copolymers at various concentrations; (B) MTT viability assays of RPE retinal pigment epithelial cells in the presence of both precursor copolymers at various concentrations; (C−F) H&E stained sections of mouse subcutaneous tissue: (C) 6 wt % poly(NIPAM-co-ADH) in PBS, after 48 h; (D) 6 wt % poly(NIPAM-co-oxoethyl methacrylate) in PBS, after 48 h; (E) PNIPAM in situ-formed hydrogel from 6 wt % polymer precursor solutions in PBS, after 48 h; (F) PNIPAM in situ-formed hydrogel from 6 wt % polymer precursor solutions in PBS, after five months. Tissue labels on (F) are pertinent to all histological samples.

In summary, we have described a novel method to synthesize covalently-crosslinked and *in situ*-gellable thermoresponsive hydrogels based on poly(N-isopropylacrylamide) using reversible and rapid hydrazide-aldehyde chemistry to link functionalized PNIPAM oligomers. The hydrogels exhibit the same thermal swelling-deswelling responses as conventional PNIPAM hydrogels but can be degraded back into the reactive polymer gel precursors via an acid-catalyzed hydrolysis process. Furthermore, the combination of rapid gelation with low toxicity observed herein suggests that this hydrazide-aldehyde oligomer cross-linking approach may be translatable to the design of injectable, degradable covalently-cross-linked hydrogels based on a range of biocompatible synthetic polymers.

Experimental

Synthesis of poly(NIPAM-co-ADH): Hydrazide-functionalized polymers were synthesized via adipic acid dihydrazide functionalization of acid-functionalized PNIPAM[219]. Poly(NIPAM-co-acrylic acid) polymers were first synthesized by reacting *N*-isopropylacrylamide monomer (4.5 g), acrylic acid (0.5 g), 2,2-azobisisobutyric acid dimethyl ester (AIBME) initiator (0.056 g), and thioglycolic acid chain transfer agent (80 μL) in 20 mL of absolute ethanol overnight at 56°C under nitrogen. Solvent was then removed under reduced pressure and the resulting viscous product was dialyzed over six cycles (12-14 kDa MWCO) against distilled deionized water. Gel permeation chromatography (GPC) indicated the product polymer had a molecular weight of M_n =

21.6 kDa (PDI 1.65), below the renal cutoff. Conductometric titration indicated that the copolymers contained 14.5 ± 0.3 mol% of acrylic acid. Hydrazide groups were then grafted to the acrylic acid residues by dissolving 0.5 g of poly(NIPAM-co-AA) and 10.15g of adipic acid dihydrazide (ADH) together with 5.58g of 1-ethyl-3-(3-dimethylaminopropyl) carbodiimide) (EDC) in 100 mL of water adjusted to pH 4.75. The pH was maintained throughout the reaction by drop-wise addition of 0.1 M HCl until no further pH change was observed (5 hours total). The resulting solution was exhaustively dialyzed for three days (12-14 kDa MWCO) against distilled deionized water. Conductometric titration showed a 99% consumption of acrylic acid groups, resulting in a 14.3 ± 0.3 mol% functionalization of polymer with ADH. ^{1}H NMR (Bruker 200 mHz) in DMSO: 1.45H - δ = 6.50-7.80 ppm, 1H - δ = 4.75-5.25 ppm, 10.82H - δ = 10.82 ppm

Synthesis of poly(NIPAM-co-oxoethyl methacrylate): *N*-isopropylacrylamide monomer (4.5 g), 2,3-dihydroxypropyl methacrylate (DHOPMA, 0.5 g), AIBME initiator (0.056 g), and thioglycolic acid chain transfer agent (80 μL) were dissolved in 20 mL absolute ethanol and reacted overnight at 56°C under nitrogen. The resulting copolymer was isolated in a similar manner to that described above. ^{1}H NMR analysis indicated that the copolymer contained 10 mol% DHOPMA. The *cis*-diol groups present in the purified copolymer were then oxidized by dissolving 1 g of the diol-containing copolymer and 1.5g sodium periodate in 150 mL H_2O for 2 hours, with 200 μL of ethylene glycol then added to stop the reaction. The oxidized copolymer was purified in the same manner as above. GPC analysis indicated M_n = 15,100 kDa (PDI 1.51), below the renal cutoff. A

tert-butyl carbazate-based aldehyde detection assay[26] indicated that 11 ± 3 mol% of total monomer residues in the polymer contained aldehyde groups. This result was confirmed by ^{1}H NMR, which gave a value of 10.5 mol% of aldehyde groups within a polymer chain. ^{1}H NMR (Bruker 200 mHz) in DMSO: 0.08H - δ = 9.45-9.6 ppm, 1H - δ = 6.75-7.75 ppm, 0.16H - δ = 5.25-4.75 ppm, 1H - δ = 3.5-4.0, 9.4H - δ = 0.0-2.25 ppm

Hydrogel synthesis and testing: 6 wt% (m/v) solutions of each precursor copolymer in 10 mM NaCl were added to separate barrels of a double barrel syringe and co-extruded into a 0.37 mL circular silicone mold (diameter 6 mm and height 2 mm) through a turbulent mixer to create hydrogel samples for testing (Fig. 2.1). Thermosensitivity assays were conducted by loading the hydrogel samples (n = 6) inside cell culture inserts (2.5 cm, 8 μm pore size) placed in 12-well cell culture plates containing 2 mL of 10 mM phosphate buffered saline (PBS, total ionic strength 0.15M) at pH 7.4. Gels were incubated in alternating cycles of 37 °C (above VPTT) and 25 °C (below VPTT) until equilibrium was reached. The change in gel mass (related directly to the water content of the gel) was determined gravimetrically at each time point indicated in Figure 2.2. Degradation assays were conducted by loading the hydrogel samples (n = 6) into the same cell culture inserts which are subsequently placed in wells containing 0.1 M, 0.5 M, or 1M hydrochloric acid (HCl). Changes in gel mass were measured gravimetrically every half hour until the bulk gels were completely degraded.

Toxicity assays: Cytotoxicity in the presence of various concentrations (0-2 mg/mL) of reactive polymers and hydrogels was tested *in vitro* in 24 hour cycles, using 3T3 *Mus musculus* mouse cells and human retinal pigment epithelial (RPE) cells as model cells. A

MTT assay was used to quantify cell viability, following published methods[220]. *In vivo* toxicity was assayed using a subcutaneous injection model, injecting $n = 4$ BALB/c mice (22-24 g, Charles River Laboratories) with 0.35 mL total of (a) 6 wt% solutions of reactive polymer precursors dissolved in 0.15 M NaCl; (b) a 6 wt% PNIPAM hydrogel prepared by mixing 6 wt% hydrazide and aldehyde-functionalized polymers (both dissolved in 0.15 M NaCl) inside a double-barreled syringe (Medimix, Switzerland); and (c) phosphate buffered saline as a control. Animals were visually observed to identify any toxic response, with two animals sacrificed 2 days following injection (acute response) and another two animals sacrificed 100 days after injection (chronic response). A tissue sample including skin, underlying tissue, and (if present) residual polymer was recovered from the animals and subjected to histological analysis using hematoxylin and eosin staining. Animals were cared for in compliance with protocols approved by the Animal Research Ethics Board at McMaster University and regulations of the Animals for Research Act of the Province of Ontario and the guidelines of the Canadian Council on Animal Care.

ACKNOWLEDGMENTS: Benjamin Greenlay and Robert Fuller are acknowledged for their help with material characterization. The Natural Science and Engineering Research Council of Canada (NSERC) and 20/20: NSERC Ophthalmic Materials Research Network are thanked for funding this work.

References

(1) Moon, H. J.; Choi, B. G.; Park, M. H.; Joo, M. K.; Jeong, B. *Biomacromolecules* **2011,** *12*, 1234-1242.

(2) Stile, R. A.; Burghardt, W. R.; Healy, K. E. *Macromolecules* **1999,** *32*, 7370-7379.

(3) Yang, J.; Yamato, M.; Shimizu, T.; Sekine, H.; Ohashi, K.; Kanzaki, M.; Ohki, T.; Nishida, K.; Okano, T. *Biomaterials* **2007,** *28*, 5033-5043.

(4) Kim, J.; Park, K. *Bioseparation* **1998,** *7*, 177-184.

(5) Schild, H. G. *Prog. Polym. Sci.* **1992,** *17*, 163-249.

(6) Malonne, H.; Eeckman, F.; Fontaine, D.; Otto, A.; Vos, L. D.; Moes, A.; Fontaine, J.; Amighi, K. *Eur. J. Pharm. Biopharm.* **2005,** *61*, 188-94.

(7) Ho, E.; Lowman, A.; Marcolongo, M. *Biomacromolecules* **2006,** *7*, 3223-3228.

(8) Lee, B. H.; Vernon, B. *Macromol.Biosci.* **2005,** *5*, 629-635.

(9) Garbern, J. C.; Hoffman, A. S.; Stayton, P. S. *Biomacromolecules* **2010,** *11*, 1833-1839.

(10) Galperin, A.; Long, T. J.; Ratner, B. D. *Biomacromolecules* **2010,** *11*, 2583-2592.

(11) París, R.; Quijada-Garrido, I. *Polym. Int.* **2009,** *58*, 362-367.

(12) Wang, F.; Li, Z.; Khan, M.; Tamama, K.; Kuppusamy, P.; Wagner, W. R.; Sen, C. K.; Guan, J. *Acta Biomaterialia* **2010,** *6*, 1978-1991.

(13) Yu, Y. Q.; Li, Z. Z.; Tian, H. J..; Zhang, S. S..; Ouyang, P. K. *Colloid Polym. Sci.* **2007,** *285*, 1553-1560.

(14) Siegwart, D. J.; Bencherif, S. A.; Srinivasan, A.; Hollinger, J. O.; Matyjaszewski, K. *J. Biomed. Mat. Res. A* **2008,** *87A*, 345-358.

(15) Yu, Y.; Chang, X.; Ning, H.; Zhang, S. *Cent. Eur. J. Chem.* **2008,** *6*, 107-113.

(16) Tsarevsky, N. V. *Macromolecules* **2005,** *38*, 3087-3092.

(17) Zhang, B. Y.; He, W. D.; Li, L. Y.; Sun, X. L.; Li, W. T.; Zhang, K. R.. *J. Polym. Sci. A* **2010,** *48*, 3604-3612.

(18) Kim, S.; Healy, K. E. *Biomacromolecules* **2003,** *4*, 1214-1223.

(19) Hiemstra, C.; van der Aa, L. J.; Zhong, Z.; Dijkstra, P. J.; Feijen, J. *Biomacromolecules* **2007,** *8*, 1548-1556.

(20) Nishi, K. K.; Jayakrishnan, A. *Biomacromolecules* **2007,** *8*, 84-90.

(21) Yeo, Y.; Ito, T.; Bellas, E.; Highley, C. B.; Marini, R.; Kohane, D. S. *Ann. Surg.* **2007,** *245*, 819-824.

(22) Nam, J. A.; Al-Nahain, A.; Hong, S.; Lee, K. D.; Lee, H.; Park, S. Y. *Macromol. Biosci.* **2011**, DOI: 10.1002/mabi.201100265.

(23) Xiao, X. C. *eXPRESS Polym. Lett.* **2007,** *1*, 232-235.

(24) Hoare, T.; Pelton, R. *Langmuir* **2004,** *20*, 2123-2133.

(25) Vetrík, M.; Přádný, M.; Hrubý, M.; Michálek, J. *Polym. Degrad. Stability* **2011,** *96*, 756-759.
(26) Maia, J.; Ferreira, L.; Carvalho, R.; Ramos, M. A.; Gil, M. H. *Polymer* **2005,** *46*, 9604-9614.

CHAPTER 2 - SUPPORTING INFORMATION

INJECTABLE, DEGRADABLE THERMOSENSITIVE POLY(NISOPROPYLACRYLAMIDE) HYDROGELS

Authors: Mathew Patenaude and Todd Hoare

Publication Information: ACS Macro Letters 1(3), 409-413

Accepted Date: 27 February 2012

Experimental

Materials: N-isopropylacrylamide (NIPAM, 99%), acrylic acid (AA, 99%), adipic acid dihydrazide (ADH, 98%), N'-ethyl-N-(3-dimethylaminopropyl)-carbodiimide(EDC, commercial grade), ethylene glycol (99.8%), sodium periodate (>99.8%), tert-butyl carbazate (≥98.0%), 2,4,6-trinitrobenzenesulfonic acid (TNBS, 5% (w/v) in H2O), thioglycolic acid (MAA) (≥98.0%), and thiazolyl blue tetrazolium bromide (MTT) were all purchased from Sigma Aldrich (Oakville, Ontario). 2,2-azobisisobutyric acid dimethyl ester (AIBME) was purchased from Wako. 2,3-dihydroxypropyl methacrylate (DHOPMA) was purchased from ABCR (Karlsruhe, Germany). 3T3 Mus musculus mouse cells and human retinal pigment epithelial cells were acquired from ATCC (Cedarlane Laboratories Ltd., Burlington, ON). Media contents, which included Dulbecco's Modified Eagle Medium-high glucose (DMEM), fetal bovine serum (FBS), horse serum (HS), and penicillin streptomycin (PS), were obtained from Invitrogen Canada (Burlington, ON). Recovery cell culture freezing and trypsin-EDTA were purchased from Invitrogen Canada (Burlington, ON). All water used was of MilliQ grade.
Gel Permeation Chromatography: Gel permeation chromatography (GPC) was run using two different solvents. Poly(NIPAM-co-ADH) molecular weights were measured using a Polymer Labs PL-GPC 50. 10 mM sodium phosphate buffer at pH 7 (1 mL/min) was used as the continuous phase and a PL Aquagel-OH mixed column was used the separation medium. Calibrations were performed using polyethylene glycol standards (Waters). Poly(NIPAM-cooxoethyl methacrylate) molecular weights were measured using a Waters 515 HPLC pump, Waters 717 Autosampler, and Waters 2414 RI detector. THF (1

mL/min) was used as the continuous phase and three Waters HR2 HR3 and HR4 columns in series were used as the separation medium. Calibrations were performed using polystyrene standards (Waters).

Conductometric Titration: The degree of acrylic acid incorporation in poly(NIPAM-co-AA) and the degree of hydrazide functionalization in poly(NIPAM-co-ADH) were measured using conductometric titration using a Burivar-I2 automatic buret (ManTech associates) with PC Titrate software (Version 2.0.0.79). Samples of 50 mg of polymer were dissolved in 50 mL of 10-3M NaCl. Titration was conducted using 0.1 M HCl and 0.1 M NaOH Acculute standards, with injections performed at a rate of 10 min/unit pH over the course of the titration. TNBS Assay: Aldehyde characterization was performed using a tert-butyl carbazate assay, taking advantage of the reaction between carbazates and aldehydes to form stable carbazones. For this assay, 5 mg of aldehyde-functionalized polysaccharide was dissolved in 1mL of a sodium acetate buffer (10mM, pH 5.2, 0.2M NaCl) containing tert-butyl carbazate (0.04 g). This solution was mixed with a defined mass of poly(NIPAM-co-oxyethyl methacrylate) polymer for 24 hours at room temperature. From this reacted solution, 0.005 mL was removed and added to 1.98 mL borate buffer (50 mM, pH 8). A further 50 µL of 5 w/v% 2,4,6-tri-nitrobenesulfonic acid solution (TNBS) was added and reacted with the borate-buffered solution at room temperature. The resulting red solution was diluted 1:1 with 0.5 M hydrochloric acid, yielding a yellow solution. From this yellow solution, 50 µL was removed and added to 1.95 mL of 0.5 M hydrochloric acid. The absorbance of the solution was measured on a DU 800 UV/Visible spectrophotometer (Beckman Coulter) at a wavelength of 334 nm.

The same dilutions with solvent were conducted above without reactive species (aldehyde, carbazate, or TNBS). The absorbance was then subtracted from the measured absorbencies of the carbazate-TNBS complex to calculate the aldehyde content of the polymers.

In vitro cytotoxicity: Cytotoxicity was assayed using 3T3 mouse fibroblasts and human retinal pigment epithelial cells. Proliferation media for 3T3 cells consisted of 500mLDulbecco's Modified Eagle Medium-high glucose (DMEM), 50mL fetal bovine serum (FBS), and 5mL penicillin streptomycin (PS). Proliferation media for RPE cells consisted of Dulbecco's Modified Eagles Media (DMEM):F12 only (no serum added). Tests were conducted in 24 well polystyrene plates (2cm2/well) containing (a) 10,000 3T3 cells and 1mL of 5% horse serum (HS) media or (b) 100,000 RPE cells and 1 mL DMEM:F12 media. A blank well containing no cells and wells containing cells but no polymer solutions were used as controls. Cells were exposed to precursor copolymer solutions at concentrations ranging from 100-2000 µg/mL. Cells were exposed to hydrogels by placing the hydrogels on top of an adhered cell layer. Each experiment was replicated 4 times, with results reported as means ±standard deviations. Thiazolyl blue tetrazolium bromide (MTT) assays were performed as previously described12. The MTT stock solution (3mL) was reconstituted in 10 mM PBS at a concentration of 40 mg/mL and sterile filtered. When applied to 3T3 mus musculuscells, the solution was diluted to 0.4mg/mL with appropriate HS containing medium. A similar dilution was made for RPE cells, but using (DMEM):F12 solution only. After 24 hour exposure to polymers, the

polymer solution was removed and fresh media was added. Cells were then exposed to 150µm of MTT solution and incubated for 4 hours. After the incubation, 250µL DMSO was added to each well to solubilize the formazan precipitate. Plates were shaken for 10-20 minutes or until formazan was dissolved. The resulting solution was transferred to a 96 well plate (200µL per plate) and read in a microplate reader at 540nm, with absorbance due to the plate and medium itself used as a control. Viability was measured as a function of formazan absorption at 540nm. Absorption was compared to a blank well, in which no polymer was exposed to cells.

EXPERIMENTAL RESULTS

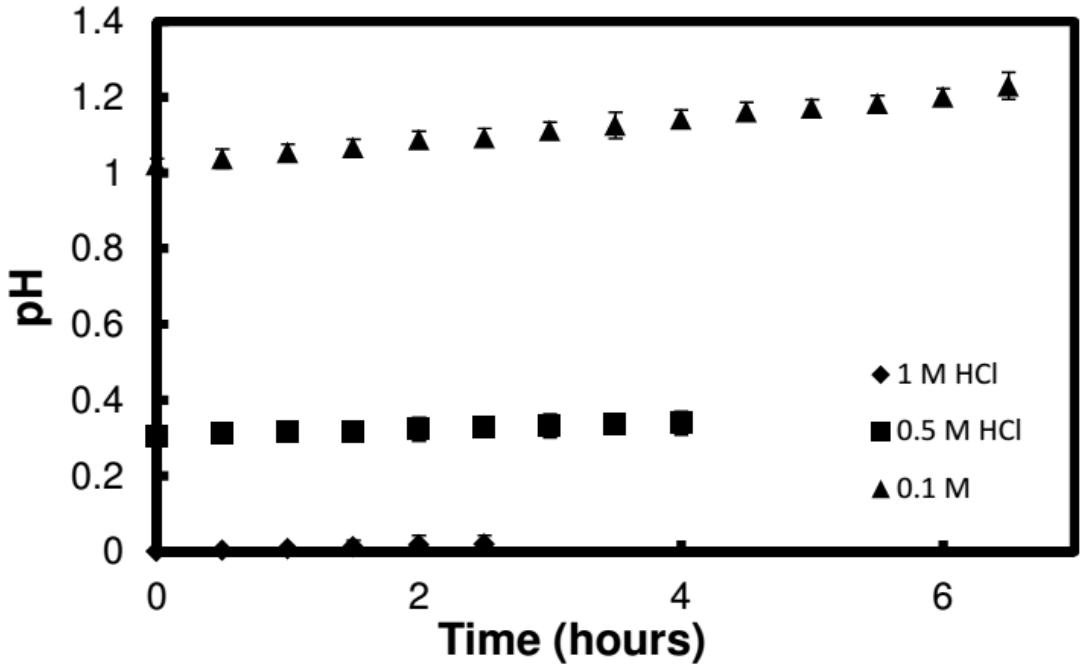

Figure 2.S1A. Changes in pH during acid hydrolysis as a function of time for acid-catalyzed gel degradation assays under 0.1 M, 0.5 M, and 1 M HCl.

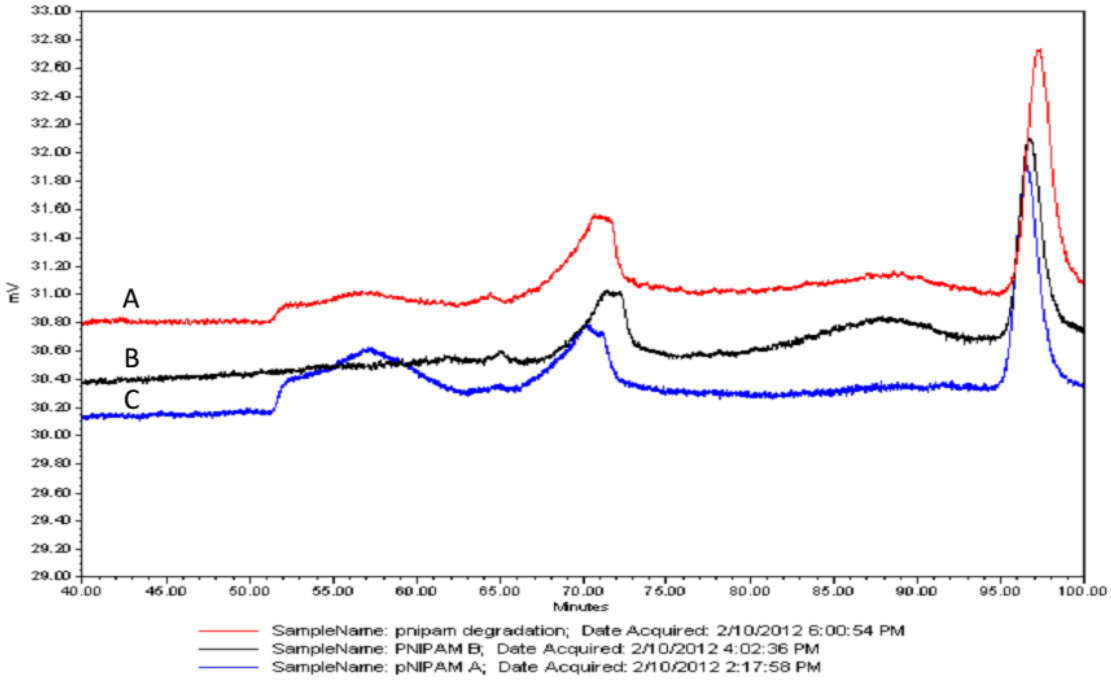

Figure 2.S1B. GPC spectra of (A) hydrogel degradation products (based on time at which 100% degradation was observed in Figure 2.3), (B) poly(NIPAM-co-oxoethyl methacrylate), and (C) poly(NIPAMco-ADH) in DMF at 30 °C. Note that the spectra were collected without presence of a charge screening molecule in the mobile phase, likely accounting forthe peak at ~70 min. retention.

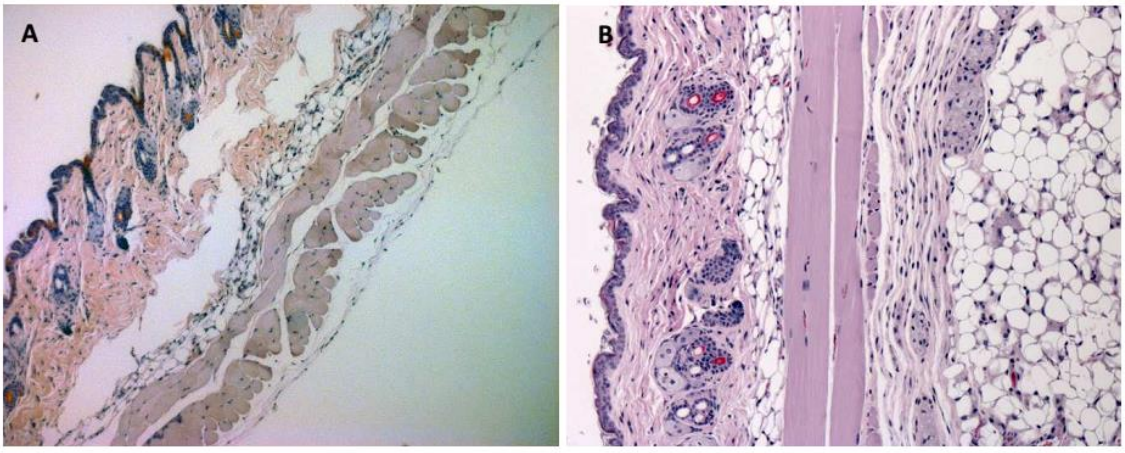

Figure 2.S2. Sub-cutaneous sections of mouse tissue followinginjection of phosphate buffered saline after (A) 2 days and (B) 150 days.

CHAPTER 3

TUNING GELATION TIME AND MORPHOLOGY OF INJECTABLE HYDROGELS USING KETONE-HYDRAZIDE CROSS-LINKING

Authors: Mathew Patenaude, Scott Campbell, Dennis Kinio, and Todd Hoare

Publication Information: Biomacromolecules 15(3), 781-790

Accepted Date: 16 January 2014

Abstract: Injectable, covalently *in situ* forming hydrogels based on poly(N-isopropylacrylamide) have been designed based on mixing hydrazide-functionalized nucleophilic precursor polymers with electrophilic precursor polymers functionalized with a combination of ketone (slow reacting) and aldehyde (fast reacting) functional groups. By tuning the ratio of aldehyde:ketone functional groups as well as the total number of ketone groups in the electrophilic precursor polymer, largely independent control over hydrogel properties including gelation time (from seconds to hours), degradation kinetics (from hours to months), optical transmission (from 1 – 85 %), and mechanics (over nearly one order of magnitude) can be achieved. In addition, ketone-functionalized precursor polymers exhibit improved cytocompatibility at even extremely high concentrations relative to polymers functionalized with aldehyde groups, even at four-fold higher functional group densities. Overall, increasing the ketone content of the precursor copolymers can result in *in situ*-gellable hydrogels with improved transparency

and biocompatibility and equivalent mechanics and stimuli-responsiveness while only modestly sacrificing the speed of gel formation.

1. Introduction

Hydrogels have attracted widespread interest as biomaterials due to their analogous interfacial, mechanical, and physicochemical properties to many soft tissues.[1] By controlling the chemistry of the monomers or linear polymers used to prepare the hydrogels, the properties of the hydrogels can readily be engineered to optimize their utility as drug storage and release depots,[2] network scaffolds for tissue engineering applications,[3–7] and biosensors.[8–10] Hydrogels cross-linked via covalent bond formation are particularly attractive in that they generally possess more elastic mechanical properties and more tunable degradation kinetics than physically cross-linked hydrogel formulations,[11] making them more suitable within the body for long-term use (especially in applications in which the gels are designed as space-filling or must bear some load). However, this enhanced elasticity makes most chemically cross-linked hydrogels unsuitable for introduction within the body through minimally invasive means such as via injection, requiring invasive surgical implantation that renders them non-ideal for routine clinical use.[12] In response, in recent years, a great deal of attention has been drawn toward the development of injectable hydrogels, including physically cross-linked shear thinning hydrogels[13] and chemically cross-linked gels that can form *in vivo* following co-injection of complimentary reactive polymer precursors.[13–16] To maintain the advantages

of chemically cross-linked hydrogels in the context of injectable formulations, a number of cross-linking chemistries that occur rapidly in water at physiological conditions have been developed, including Michael-type addition between a thiol functionalized precursor and α,β-unsaturated acid moieties of another precursor,[17–20] Diels-Alder "click" chemistry between reactive precursors functionalized with furan or maleimide groups,[21–23] oxime formation between a carbonyl group and a hydroxylamine,[24] and Schiff base formation between polymer precursors functionalized with carbonyl and amine functional groups.[25,26] Of particular interest, hydrazone bond formation, resulting from the condensation of carbonyl and hydrazide functional groups, has been widely reported for use with injectable hydrogels due to the rapid kinetics of this chemistry in aqueous environments and the hydrolytic lability of the formed hydrazone group that facilitates both *in situ* formation and biodegradation.[22] We have previously reported the use of this chemistry to prepare injectable environmentally-responsive hydrogels based on poly(N-isopropylacrylamide) (PNIPAM) that can be tailored to suit a number of biomedical applications, including drug delivery and tissue engineering.[12–14]

An ideal hydrogel chemistry for most tissue engineering or drug delivery applications would facilitate moderate to rapid rates of gel formation (preventing or minimizing undesirable diffusion of the precursor polymers away from the injection site prior to gel formation), form hydrogels with degradable linkages, and avoid reactions with biomolecules in the gel environment. In the latter case, ensuring self-gelation instead of cross-reaction of the gel precursors with biomolecules is critical to produce hydrogels

with sufficiently high cross-link densities (i.e. adequate mechanics) as well as prevent or suppress potential reactions with proteins, which can lead to significant inflammatory responses.[28] However, most if not all existing chemistries reported in the literature present limitations with respect to at least one of these criteria. For example, aldehyde groups employed in generating hydrazone cross-linked hydrogels can induce local toxicity if used at high concentrations or with sterically-hindered polymers which gel more slowly (inducing effective rapid release of aldehyde polymers into the body) due to their ability to cross-link proteins via their lysine groups.[29,30] In addition, from a fundamental engineering perspective, current gelation chemistries are inherently limited in that the cross-link density, gelation rate, mechanics, and degradation time of the hydrogel are all intimately coupled; hydrogels with higher cross-linking potential gel faster and form gels that are more elastic and degrade more slowly.[11] Gelation kinetics and the final morphology of the hydrogel are also often linked given that rapid cross-linking reactions can induce gelation faster than the timescale required for diffusional mixing of precursor polymers. As a result, depending on the type of mechanical mixing used during the gel formation process, regions of local heterogeneity may form within the polymer matrices of these gels that scatter light (significantly affecting the utility of these gels in ophthalmic applications,[31] for example), alter the diffusional properties of small molecules through the gel, and/or degrade the mechanical properties of the gel. Finding ways to decouple these variables, in particular gelation time with mechanics and degradation rate, would greatly improve our ability to engineer specific hydrogels for particular biomedical applications.

Recent approaches to this addressing this problem have involved changing the chemical characteristics of the electrophile to alter hydrogel properties. In particular, McKinnon et al. demonstrated that using an aryl aldehyde instead of an aliphatic aldehyde can be used to alter the properties of the hydrogel formed.[32] In this work, we seek to address these challenges by using ketone groups (alone or in combination with aldehyde groups) as the electrophilic reactive group used to form the hydrazone cross-link. Ketones are less reactive to hydrazone bond formation than aldehydes,[33] attributable to the presence of an extra electron-donating carbon at the alpha position of the carbonyl group as well as steric hindrance to nucleophilic attack of the carbonyl group. By adjusting the total number of ketone groups as well as the aldehyde:ketone ratio in the electrophilic precursor polymer, we aim to engineer the gelation time to produce a range of hydrogels with tunable properties. To demonstrate this phenomenon, we have chosen poly(N-isopropylacrylamide) (PNIPAM) as the backbone polymer for gel formation. PNIPAM has attracted significant interest in the biomedical literature due to its ability to respond to the temperature of its local environment; PNIPAM hydrogels undergo a reversible volume phase transition at ~32 °C that results in significant and reversible dewelling within the hydrogel matrix.[34] This environmental sensitivity allows for the design of gels that can both reduce their pore size as well as switch from highly hydrophilic to partially hydrophobic on demand to (for example) entrap pre-loaded drug and slow its release[35] or adhere and then release cells for regenerative medicine applications.[36] We have previously demonstrated the fabrication of PNIPAM hydrogels using aldehyde-hydrazide chemistry.[16]

While gels with suitable mechanical and thermoresponsive properties were produced, the gels formed very quickly (~10-30 seconds, problematic in some surgical contexts) and were extremely opaque. Herein, by using ketone groups to tune the gelation kinetics, we demonstrate the potential to create transparent but still mechanically strong and highly thermoresponsive hydrogels based on PNIPAM precursors.

2. Experimental

Materials: N-isopropylacrylamide (NIPAM, 99%), acrylic acid (AA, 99%), adipic acid dihydrazide (ADH, 98%), N′-ethyl-N-(3- dimethylaminopropyl)-carbodiimide (EDC, commercial grade), ethylene glycol (99.8%), thiolglycolic acid (MAA, ≥98.0%), toluene (99.8%), acetone (anhydrous, ≥99.9%), chloroacetone (95%), phthalimide potassium salt (≥98%), methacryloyl chloride (≥97.0%), aminoacetaldehyde dimethyl acetal (99%), 4-hydroxy-TEMPO (97%), and para toluenesulfonic acid (≥98.5%) were all purchased from Sigma Aldrich (Oakville, ON). Dimethyl sulfoxide (DMSO, reagent grade) was purchased from Caledon Laboratory Chemicals (Georgetown, ON). 3T3 *Mus musculus* mouse cells were obtained from ATCC: Cederlane Laboratories (Burlington, ON). Cell proliferation media (which includes Dulbecco's modified Eagle's medium-high glucose (DMEM), fetal bovine serum (FBS), and penicillin streptomycin (PS)), trypsin-EDTA, and recovery media were all acquired from Invitrogen (Burlington, ON).

Synthesis of an acetal-protected aldehyde monomer (N-(2,2-dimethoxyethyl)methacrylamide): Aminoacetaldehyde dimethyl acetal (50 mL, 46 mmol)

was added to a 120 mL stirred solution of 20 % NaOH (w/v). This solution was then cooled to 0 °C in an ice bath. 4-hydroxy TEMPO (10 mg, 0.06 mmol) was then added to this solution as a stabilizer and stirred until it was fully dissolved in solution. Methacryloyl chloride (47 mL, 48 mmol) was next added drop-wise over the course of 2 hours under nitrogen flow, after which the ice bath was allowed to warm to room temperature and the reaction was left to stir overnight in darkness. The reaction mixture was then extracted with 150 mL petroleum ether. Subsequently, the aqueous phase was saturated with sodium chloride and was extracted three times with tert-butyl methyl ether. Additional 4-hydroxy TEMPO was added to this phase to prevent premature polymerization of the monomer. The organic phase was then dried over magnesium sulfate, filtered, and concentrated in a rotary evaporator, yielding the acetal-protected aldehyde monomer. The monomer was stored in the darkness at -20 °C until use. ^{1}H NMR (600 MHz) in DMSO-d_6: $CH_2CC\mathbf{H_3}COONHR'$, 1.75 ppm, singlet, 3H; $RNHCH_2C\mathbf{H}(OCH_3)_2$, 3.25 ppm, triplet, 1H; $RNHCH_2CH(O\mathbf{CH_3})_2$, 3.35 ppm, singlet, 6H; $RNHC\mathbf{H_2}CH(O\mathbf{C}H_3)_2$, 4.41 ppm, doublet, 2H; $C\mathbf{H_2}CCH_3COONHR'$, 5.35-5.65 ppm, doublet, 2H; RN**H**R', 8 ppm, singlet, 1H (see Supporting Information, Scheme 3.S1).

Synthesis of a ketal-protected ketone monomer (N-((2-methyl-1,3-dioxolan-2-yl)methyl)methacrylamide): Synthesis of the protected ketone monomer was conducted based on a modification of a previously reported protocol.[37] Chloroacetone (10 mL, 12.5 mmol) and the potassium salt of phthalimide (25.5 g, 13.8 mmol) were added to 150 mL of stirred dry acetone. The solution was then heated to 80 °C for 20 hours, after which it

was cooled to room temperature and the acetone was removed in a rotary evaporator. The resulting solid was then redissolved in methylene chloride and washed repeatedly with water. The methylene chloride layer was dried over magnesium sulfate, filtered, and removed using a rotary evaporator. The resulting yellow crude solid was washed with diethyl ether several times until the solid became white; this solid was subsequently dried in a vacuum oven to yield purified intermediate A (Scheme 3.1A). Intermediate A (10 g, 50 mmol) was then added to 180 mL of toluene along with ethylene glycol (5.85 mL, 100 mmol) and dry para-tolenesulfonic acid (934 mg, 5 mmol) and refluxed for 15 hours. The reaction mixture was cooled to room temperature and the ethylene glycol layer was extracted three times with diethyl ether. The toluene and ether fractions were combined and washed three times with 5 % (w/v) NaOH followed by deionized water. The organic layer was dried over magnesium sulfate and solvent was removed in a rotary evaporator. The crude was recrystallized from ethanol to yield pure intermediate B (Scheme 3.1B). Intermediate B was subsequently added to 100 mL of deionized water along with 15 g of NaOH and refluxed for 2 days, with an additional 60 g of NaOH added slowly over the course of the reflux. Afterwards, the reaction mixture was cooled to room temperature and extracted three times with 50 mL dichloromethane. The organic layers were then combined and dried over magnesium sulfate, filtered, and concentrated in a rotary evaporator to yield pure product C (Scheme 3.1C), a slightly yellow oil. Finally, the monomer was prepared by adding product C (21.1 mL, 180 mmol) to a 20 % (w/v) NaOH solution (in water) containing 4-hydroxy TEMPO (10 mg, 0.06 mmol). This reaction mixture was brought to 0 °C in an ice bath and methacryloyl chloride (16.5 mL, 174

mmol) was added drop-wise over 2 hours under nitrogen flow. The ice bath was then allowed to warm to room temperature and the reaction left to stir overnight in darkness. After this time, stirring was halted and the product was allowed to collect at the top of the reaction flask. The pure monomer product (along with inhibitor) (shown in Scheme 3.1D) was then isolated using a separatory funnel. The monomer was stored in the darkness at -20 °C until use. ^{1}H NMR (600 MHz) in DMSO-d_6: RNHCH_2C(OCH_2CH_2O)C**H$_3$**, 1.3 ppm, singlet, 3H; CH_2CC**H$_3$**CONHR', 2 ppm, singlet, 3H; RNHC**H$_2$**C(OCH_2CH_2O)CH_3, 3.5 ppm, doublet, 2H; RNHC**H$_2$**C(OC**H$_2$**C**H$_2$**O)CH_3, 4 ppm, singlet, 4H; C**H$_2$**CCH_3CONHR', 5.35-5.65 ppm, doublet, 2H; CH_2CCH_3CON**H**R', 6 ppm, singlet, 1H. See Supporting Information, Figure 3.S1 for ^{1}H NMR spectrum.

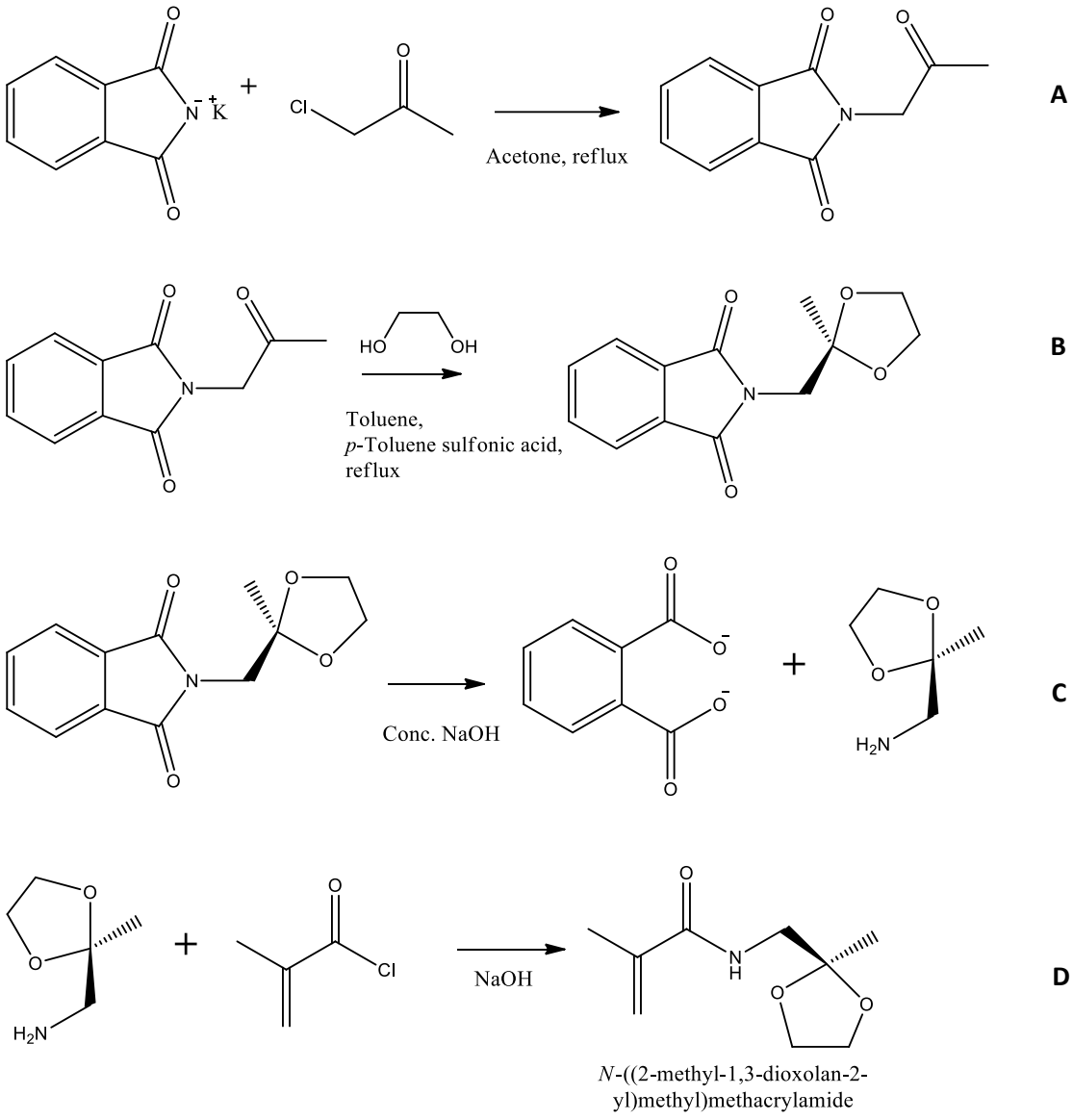

Scheme 3.1. Synthesis of a ketal-protected ketone monomer

Synthesis of hydrazide-functionalized PNIPAM copolymer: The synthesis of this nucleophilic copolymer was performed as previously described[16] (see also Supporting Information, Scheme 3.S2). Briefly, *N*-isopropylacrylamide (4 g, 35 mmol), acrylic acid

(1 mL, 14 mmol), and thioglycolic acid (87 µL, 1.25 mmol) were dissolved in 20 mL of absolute ethanol and heated to 56 °C. Following degassing with nitrogen, dimethyl 2,2′-azobis(2-methylpropionate) (AIBME) (56 mg, 2.4 µmol) was added, and the solution was allowed to stir overnight under nitrogen. The solvent was then removed in a rotary evaporator and the crude product was redissolved in deionized water and subjected to exhaustive dialysis followed by lyophilisation. Conductometric titration (ManTech, Inc.) indicated that the copolymer contained 15.2 ± 0.4 mol% acrylic acid residues per chain. The acrylic acid residues were then converted to hydrazide groups by dissolving the polymer in deionized water along with a 10-fold molar excess of ADH and adjusting the solution pH to 4.75 using 0.1 M HCl. A 2-fold molar excess of EDC (pre-dissolved in 10 mL deionized water) was then added to the solution and the reaction was allowed to continue (maintaining a constant pH of 4.75 throughout the reaction via addition of 0.1 M HCl) until no change in pH was observed, typically on the order of ~4 hours. At this point, the solution was neutralized using 0.1 M NaOH and subjected to exhaustive dialysis and subsequent lyophilisation. Conductometric titration indicated that 97 ± 3 % of acrylic acid groups had been converted to hydrazide groups, resulting in ~14.7 mol% hydrazide groups per PNIPAM copolymer chain. DMF gel permeation chromatography was conducted using a Waters 590 HPLC pump along with three Waters Ultrastyragel Linear columns operating in series and a Waters 410 refractive index detector. GPC indicated a number average molecular weight of 26.5 kDa (polydispersity 1.55) for this hydrazide-functionalized copolymer based on narrow molecular weight polyethylene glycol standards (Waters).

Synthesis of aldehyde and/or ketone functionalized PNIPAM copolymers: N-isopropylacrylamide (4 g, 35 mmol) was copolymerized with various ratios of protected aldehyde to protected ketone monomer (Scheme 3.2), keeping the total mole percent of these protected functional groups (and thus electrophilic reactive groups for covalent gelation) constant. The recipes used to prepare these ketone and/or aldehyde-functionalized copolymers are given in Table 3.1. The polymerizations were carried out as described for the hydrazide-containing copolymer. Following removal of ethanol with a rotary evaporator, the protecting acetal and ketal groups were removed by re-dissolving the obtained crude polymer in 3 M HCl and allowing the resulting solution to stir at room temperature for 24 hours. This solution was then exhaustively dialyzed and lyophilized to isolate the purified copolymers. Aldehyde and ketone group content was quantified via NMR by measuring the relative peak intensity at 9.5 ppm (RCO**H**, aldehyde) and 2.1 ppm (RCOC**H**$_3$, ketone) relative to a tetramethylsilane internal standard. GPC was performed as previously described for the hydrazide-functionalized copolymer.

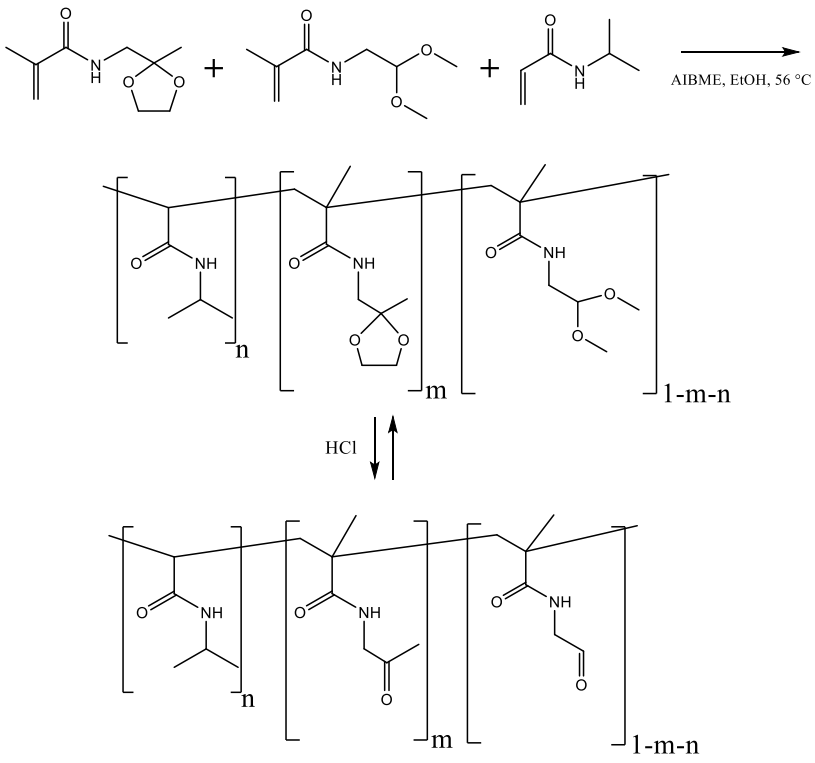

Scheme 3.2. Synthesis of protected ketone and/or aldehyde monomers with NIPAM and subsequent deprotection to reveal the electrophilic ketone and/or aldehyde moieties

Table 3.1. Compositions and properties of electrophilic PNIPAM copolymer chains. The gel identification codes represent the anticipated mole fractions of the aldehyde:ketone monomers based on the recipe while the actual mole fractions of aldehyde and ketone functional groups within the polymer chains (as determined by ^{1}H NMR) are given as X_{na} and X_{nk}, respectively. The mole fractions of monomer types, either electrophilic monomer or NIPAM, are given as X_n and X_{nip}, respectively. GPC results are reported relative to a poly(ethylene glycol) standard curve.

Gel Identification	**Aldehyde Content (X_{na})**	**Ketone Content (X_{nk})**	**Total Electrophile Content (X_n)**	**Total NIPAM Content (X_{nip})**	**M_w (kDa)**
100 Ald/0 Ket	1	0	0.12 ± 0.03	0.88 ± 0.03	21.2 ± 3.2
75 Ald/25 Ket	0.72 ± 0.05	0.28 ± 0.05	0.11 ± 0.02	0.89 ± 0.02	20.4 ± 2.3
50 Ald/50 Ket	0.45 ± 0.07	0.55 ± 0.07	0.11 ± 0.04	0.89 ± 0.04	21.8 ± 3.3
25 Ald/75 Ket	0.23 ± 0.03	0.77 ± 0.03	0.13 ± 0.03	0.87 ± 0.03	22.5 ± 2.1
0 Ald/100 Ket	0	1	0.12 ± 0.05	0.88 ± 0.05	20.6 ± 1.9
0 Ald/100 Ket*	0	1	0.42 ± 0.05	0.58 ± 0.05	19.5 ± 2.6

Hydrogel Formation, Gelation Time, and Transparency Assays: Hydrazide (nucleophilic) and aldehyde/ketone (electrophilic) functionalized polymer precursors were dissolved separately in PBS at 25 °C at a concentration of 6 % (m/v) for each precursor polymer and added to separate barrels of a double barrel syringe (Scheme 3.3). Depressing the plunger of the syringe caused the polymer precursors to mix along a baffled channel and co-extrude out of the tip of a needle. The time required to form a

stable gel was assessed using a standard vial inversion technique following co-extrusion of the reactive polymer precursors into a 20 mL glass scintillation vial.[21,38,39] The time required to form a gel (i.e. the time required such that the polymer did not flow within 5 seconds following vial inversion) was noted for each gel type. In order to assess the potential formation of microdomains and/or phase separation, gels were formed in polystyrene cuvettes (1 cm path length) and the transparency of the resulting gels was measured at 550 nm using a DU 800 UV/visible spectrophotometer (Beckman Coulter) following 24 hours of incubation at room temperature. The phosphate buffer maintained the pH at 7.4 in all gelation experiments. A total of n=4 replicates were performed per sample in each assay, with the reported error bars representing the standard deviation of the measurements.

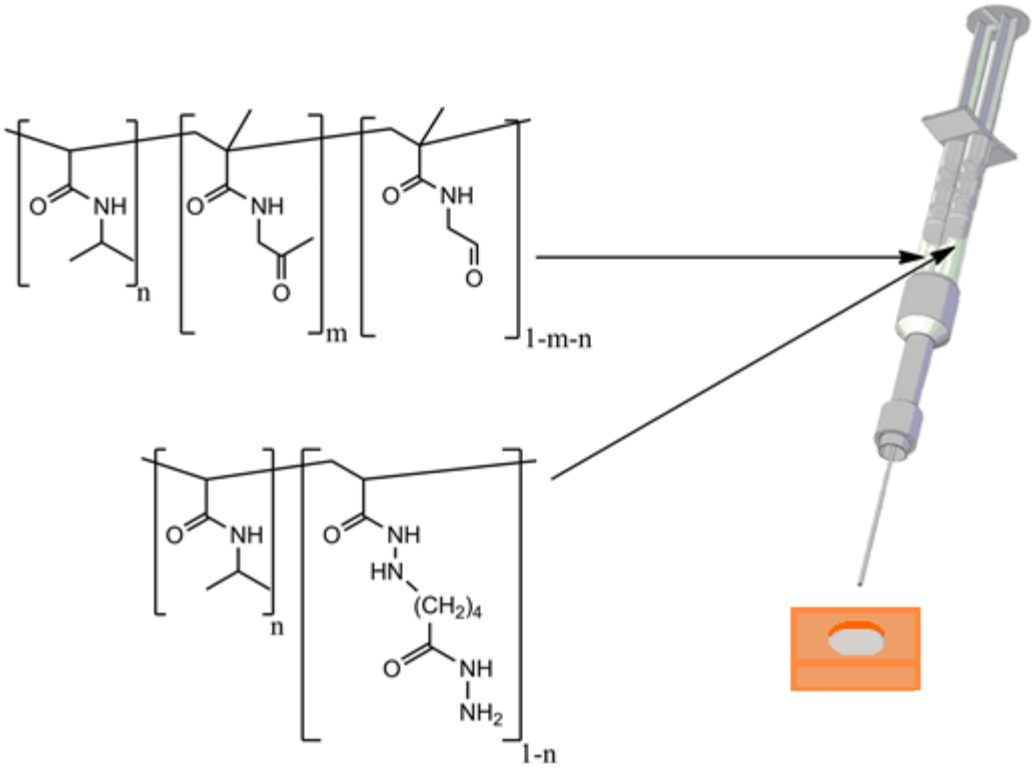

Scheme 3.3. Co-injection of hydrazide and aldehyde/ketone complimentary PNIPAM precursors into a silicone mold using a double barrel syringe to form a hydrazone cross-linked hydrogel

Hydrogel Cross-linking Efficiency: Polymer precursors 100Ald/0Ket, 50Ald/50Ket, 0Ald/100Ket, and 0Ald/100Ket* were dissolved in D_2O at 6 % (m/v) and were added to one barrel of different double barrel syringes. A 6 % (w/v) solution of hydrazide-functionalized PNIPAM in D_2O was then added to the second barrel of each of these syringes, and hydrogels were made by co-extruding each polymer pair into different NMR tubes. Spectral measurements were taken immediately following co-extrusion into the tubes for each gel type as well as 48 hours after co-extrusion (allowing cross-linking to occur). Changes in peak intensity corresponding to aldehyde protons (CO**H**, ~9.5 ppm) and terminal methyl groups of ketone moieties (C**H**$_3$, ~2.15 ppm), both of which decrease

following hydrazone bond formation, were tracked relative to spectra of polymer precursors alone at a total concentration of 3 % (matching the concentration of each precursor in each final gel) in D_2O . 16 scans were taken for each sample type at a relaxation delay of 4 seconds per scan. The ratio of peak integrations relative to the isopropyl group intensity of NIPAM moieties was measured for both precursor alone and co-extruded polymer solutions and compared at different time points in the experiment (initially and at 48 hours). For 50Ald/50Ket gels, measurements were taken for both aldehyde and ketone functional groups independently of each other, allowing for the calculation of the total residual electrophilic group content in the gel. Quantification of the number of electrophilic groups (of a given type) consumed through cross-linking was made according to Eq. 1

$$\%\ electrophilic\ groups\ consumed = \left(1 - \frac{I_{e,g}/I_{i,g}}{I_{e,s}/I_{i,s}}\right) \times 100\%$$

(Eq. 1)

where $I_{e,g}$, $I_{i,g}$, $I_{e,s}$, $I_{i,s}$ are the integrations corresponding to the electrophilic (ketone or aldehyde) peaks of the gel after 48 hours, the isopropyl groups of the gel after 48 hours, the electrophilic peaks of the polymer precursor solution initially (t = 0), and the isopropyl groups of the polymer precursor solution initially (t = 0), respectively.

Hydrogel Degradation: Hydrogel precursor solutions were co-extruded into 0.44 mL silicone molds as shown in Scheme 3.3. The solution-containing molds were then covered with silicone slabs and left for 48 hours at room temperature in order to ensure

equilibrium cross-linking of the polymer networks. Hydrogels were then placed in cell culture inserts (12 well format, Falcon) and were subsequently submerged in PBS at pH 7.4. The rates of degradation for each gel type were determined gravimetrically at pre-determined time intervals after drawing off excess (unbound) water from the surface of the gels using a Kimwipe. A total of n=4 replicates are performed on each sample, with the reported error bars representing the standard deviation of the measurements.

Hydrogel Mechanical Properties: The mechanical properties of hydrogels formed by co-extruding hydrazide-functionalized PNIPAM and PNIPAM functionalized with different ratios of ketones to aldehydes were determined using oscillatory rheology with an ARES rheometer (Texas Instruments). The storage modulus (G') of each gel type was determined using parallel plate geometry with a plate diameter of 7 mm and a plate spacing of 1 mm. An initial strain sweep was first conducted between 1-100 % at 1 Hz in order to identify the linear viscoelastic range of these gels. A strain within this linear viscoelastic range was then selected and maintained constant during a frequency sweep from 1-100 rad/s to measure G'. Measurements were performed on gels initially incubated at room temperature and at 37 °C. A total of n=4 replicates are performed on each sample, with the reported error bars representing the standard deviation of the measurements.

Cytocompatibility Assays: The cytocompatibility of the hydrogel precursors (which are also the degradation products)[16] were assessed using an *in vitro* MTT assay with 3T3 *Mus*

musculus mouse cells similar to that described by Campbell et al.[14] Briefly, 24-well polystyrene plates were cultured with 10,000 3T3 cells within 1 mL of proliferation media. After 24 hours, the cells were exposed to various concentrations of hydrogel precursor polymers (0.1, 0.4, 0.8, 1.2, 1.6, and 2 mg/mL for the lower concentration sets and 2, 4, 8, 12, 16, and 20 mg/mL for the higher concentration set, n = 4 per concentration) and incubated for an additional 24 hours. The media and polymer solutions were replaced with 1 mL of a 0.4 mg/mL MTT solution in proliferation media for the last 3 hours of incubation. After this, the MTT solution was aspirated off and the formazan produced by the cells was dissolved in 400 μL of DMSO. The absorbance of the formazan solution was read using a Biorad microplate reader (model 550) at 570 nm against a 630 nm baseline (accounting for media absorbance) and compared to the absorbances measured in cell-only wells in which no material (i.e. only media) was added to calculate the relative cell viabilities according to Eq. 2.

$$cell\ viability\ (\%) = \frac{(absorbance_{polymer-exposed,570\ nm} - absorbance_{polymer-exposed,630\ nm})}{(absorbance_{blank,570\ nm} - absorbance_{blank,630\ nm})}$$

(Eq. 2)

Error bars for each polymer tested represent the standard deviation of the cell viability percentages measured for the 4 replicates performed. A Student's t-test (at 95% confidence) is performed to assess statistical significance of differences between cell viability results.

3. Results

Reactive Precursor Polymer Synthesis: As per Table 3.1, an approximately stoichiometric incorporation of monomers at their desired mole fractions within each polymer chain was obtained for both the ketal and acetal-protected monomers, resulting in electrophilic polymer chains with statistically equal functional group contents (and therefore cross-linking potential) in all hydrogels studied. For an equal mass mixture of the polymers (each at 6 %), the hydrazide polymers contain functional groups in approximately a 1.5-fold excess over electrophilic groups on complimentary precursor polymer chains, advantageous biologically given that hydrazides are functionally bio-orthogonal with biomolecule functional groups whereas aldehydes and, to a much lesser extent, ketones are not. The ~42 mol% 0Ald/100Ket* electrophilic polymer is the exception to this relationship and is designed to offer enhanced gel formation kinetics and cross-link density relative to the other precursor polymers prepared. The molecular weight each electrophilic precursor polymers was maintained at ~20 kDa (independent of functional group incorporation, Table 3.1) while the nucleophilic chain had a molecular weight of 26.5 kDa. Considering that hydrazone bond hydrolysis regenerates the precursor polymers (i.e. the precursor polymers are the degradation products), each tested polymer has a molecular weight below the lower molecular weight cut-off of the glomerulus basement membrane of the renal excretory system (~40 kDa) and thus has the potential to be cleared following degradation.

Hydrogel Formation Kinetics: Hydrogels prepared with any combination of aldehyde/ketone functionalization could be easily co-extruded from a double-barrel syringe, and all combinations tested successfully gelled within the silicone moulds to form elastic hydrogels within the 24 hour gelation period used for screening. Results of the vial inversion assay, shown in Table 3.2, indicate that an increase in ketone content of the electrophilic polymer leads to an increase in the time required to form a gel, with the gelation time increasing dramatically when the ketone concentration is increased to >50 mol%.

Table 3.2. Time required to form a hydrogel for the various gel types assayed according to the vial inversion test

Gel ID	Gel formation time (minutes)
100Ald/0Ket	0.09 ± 0.02
75Ald/25Ket	0.4 ± 0.1
50Ald/50Ket	24 ± 2
25Ald/75Ket	45 ± 6
0Ald/100Ket	65 ± 13
0Ald/100Ket*	2.0 ± 0.5

This increased gelation time associated with ketone-rich polymers can be attributed to the lower electrophilicity of the ketone group relative to the aldehyde group, making ketones less susceptible to nucleophilic attack by the hydrazide-functionalized PNIPAM chains. When the number of ketone groups in the precursor polymers is quadrupled to ~42 mol% (0Ald/100Ket*), gelation occurs 30-fold faster than when a ~12 mol% ketone functionalized precursor polymer is used (0Ald/100Ket). Interestingly, the gelation time observed using the ~42 mol% ketone-functionalized precursor is still ~20-fold slower

than that observed when using an aldehyde-functionalized polymer with ~12 mol% functional groups to form gels.

Hydrogel Cross-linking Efficiency: By comparing the aldehyde and ketone group NMR spectral intensities immediately following co-extrusion and 48 hours post-extrusion, an estimate of the cross-link density of the respective hydrogels can be made. Changes in peak intensities were measured relative to 3 % (w/v) solutions of precursor only in D_2O (see representative raw data spectra in Supporting Information, Figures 3.S2 and 3.S3). Table 3.3 shows the percentage of ketone and/or aldehyde functional groups consumed in each gel as a function of precursor chemistry and the total cross-link density of each hydrogel following 48 hours of gel formation.

Table 3.3. Electrophilic functional group consumption and cross-link density for hydrogels prepared with different aldehyde:ketone ratios and total ketone contents as determined by ^{1}HNMR.

Hydrogel ID	% Electrophilic functional groups consumed	# Electrophilic functional groups consumed (x 10^{18})	Cross-link density (x 10^{18} cm^{-3})
100Ald/0Ket	74 ± 6	22.4 ± 1.8	11.2 ± 0.9
50Ald/50Ket	42 ± 5	12.3 ± 1.4	6.1 ± 0.7
0Ald/100Ket	14 ± 3	3.9 ± 0.5	1.9 ± 0.2
0Ald/100Ket*	17 ± 5	19.3 ± 1.4	9.6 ± 0.7

Hydrogels prepared with aldehyde-rich precursor polymers contain significantly more cross-links relative to those prepared with ketone-rich precursor polymers at the same total electrophile content (~12 mol%), consistent with the higher reactivity of aldehyde groups relative to ketone groups that would shift the equilibrium of hydrazone bond formation/breaking toward the product (cross-linked) side. However, the cross-link

density of a gel prepared with an aldehyde-functionalized precursor polymer can be matched using a ketone-functionalized polymer precursor functionalized with a higher total mole fraction of ketone functionality (Table 3.1). The percentage of available ketone groups cross-linked is approximately equal between the 0Ald/100Ket (~12 mol% ketone) and 0Ald/100Ket* (~42 mol% ketone) precursors, consistent with an equilibrium driving hydrazone bond formation; however, the 4-fold increase in the total electrophilic functional group content of 0Ald/100Ket* relative to 0Ald/100Ket gels results in formation of ~4-5-fold more cross-links in the hydrogel. While it is possible that the absolute extent of cross-linking in (unbuffered) D_2O will differ from that in (buffered) H_2O, it is clear from this data that the cross-link density of the hydrogel can be scaled directly by the number of reactive functional groups in the precursor polymers.

Hydrogel Mechanics: The results of oscillatory rheometry conducted on a range of hydrogels prepared with precursor polymers containing varying ratios of aldehyde and ketone groups are shown in Figure 3.1. A clear relationship exists between the elastic modulus (*G'*) and the ratio of aldehyde to ketone groups of the electrophilic precursor polymers used to synthesize the hydrogels, with an increasing aldehyde to ketone ratio yielding gels with an increased *G'*. This suggests that aldehydes are significantly more effective at forming cross-links than ketone groups following co-extrusion, consistent with the NMR result (Table 3.3) and the lower reactivity of ketone functional groups. Interestingly, the 0Ald/100Ket* hydrogels (prepared with ~42 mol% ketone precursor polymers as opposed to ~12 mol% total electrophilic comonomer precursor polymers

used to prepare the other hydrogels) exhibited analogous mechanical properties to the 100Ald/0Ket hydrogel, with the additional available ketone functional groups facilitating in increase in cross-link formation; again, this result matches that of the NMR experiment (Table 3.3). Thus, while the use of ketone-functionalized polymers results in a significant decrease in the elastic modulus of the resulting hydrogels at equal functional group contents, modulus matching can still be performed independent of the aldehyde:ketone ratio of the reactive copolymers by changing the total ketone content in the electrophilic hydrogel precursor polymer.

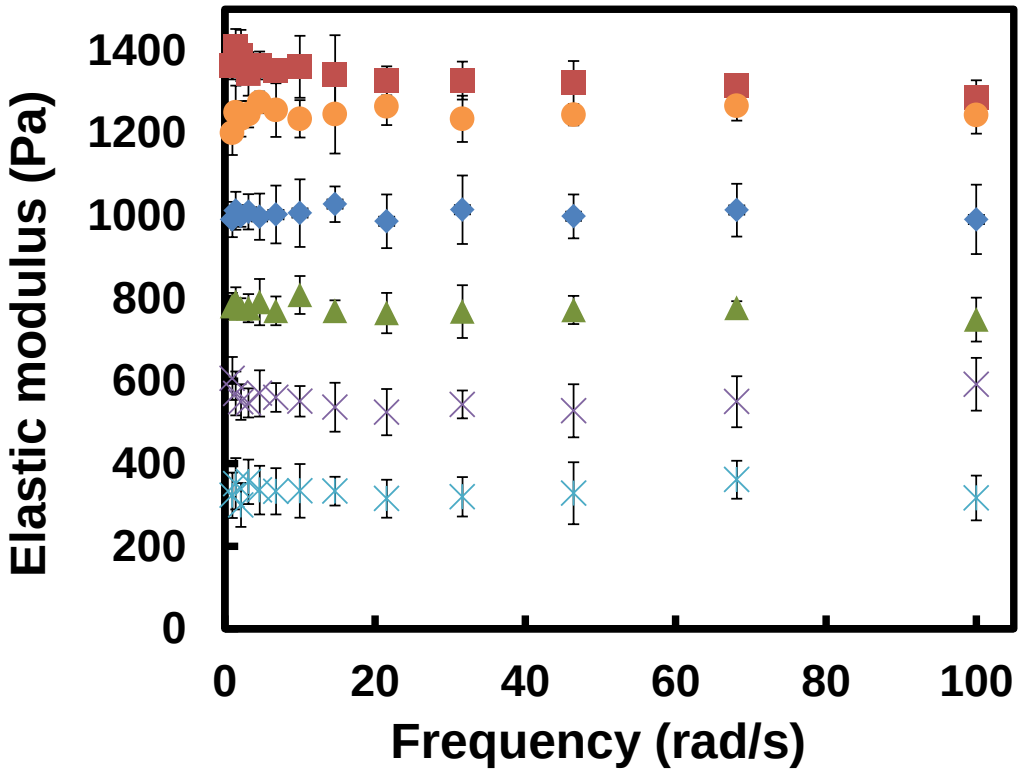

Figure 3.1. Elastic moduli versus frequency for PNIPAM hydrogels prepared with precursor polymers containing different aldehyde:ketone functional group ratios and different ketone functional group mole fractions (0Ald/100Ket* = ~42 mol% ketones; all other hydrogels ~ 12 mol% electrophile)

Hydrogel Transparency: UV/VIS absorbance measurements performed at 550 nm were used to assess the transparency of the hydrogels prepared with the different precursor polymers. A lack of transparency at this wavelength indicates the presence of micro-domains of a size similar to the wavelength of the incident light. Figure 3.2 indicates that increasing the aldehyde content of the precursor polymers results in significantly less transparent hydrogels, indicating the presence of micro-domains and regions of heterogeneity within the bulk gel. Conversely, gels prepared with precursors containing a high fraction of ketone groups remain transparent, with the higher transparency largely preserved as the number of ketone functional groups is increased (comparing 0Ald/100Ket with ~12 mol% ketones and 0Ald/100Ket* with ~42 mol% ketones); this result suggests that the ketone group itself plays a role in maintaining the gel transparency even independent of the gelation time, since the 0Ald/100Ket* gel forms 10-fold faster than the 50Ald/50Ket gel but maintains significantly higher transparency.

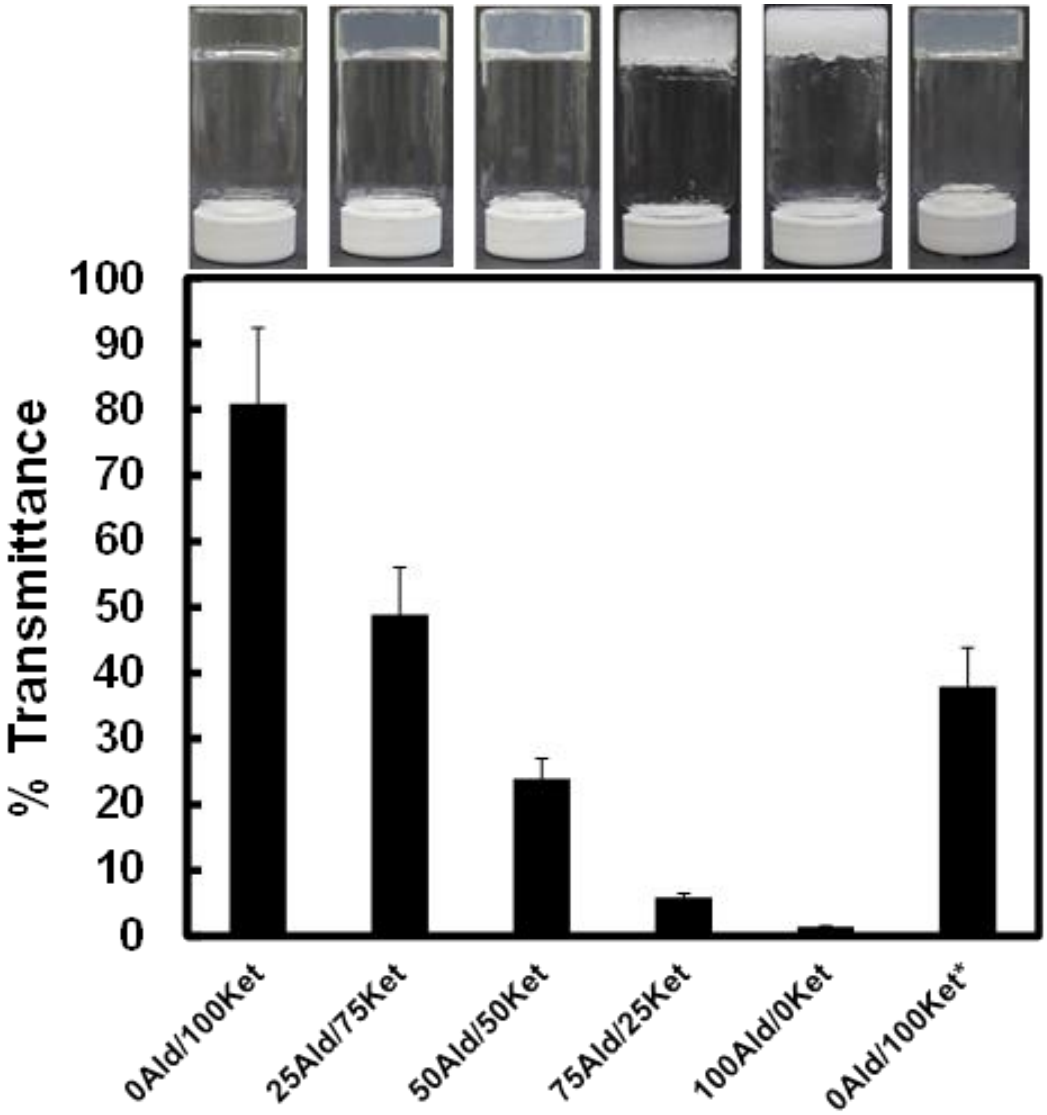

Figure 3.2. Transmittance of 550 nm light through hydrogels prepared with precursor polymers containing aldehyde:ketone functional group ratios and different ketone functional group mole fractions (0Ald/100Ket* ~ 42 mol% ketones; all other hydrogels = 12 mol% electrophile). Pictures of each hydrogel are provided above each transparency result for reference.

Hydrogel Phase Transition: Incubation of the hydrogels in PBS at 37 °C induced deswelling in all gels, consistent with the phase transition behavior of PNIPAM (Figure 3.3). Of note, while the precursor polymers themselves are significantly more

hydrophilic than PNIPAM (with LCST values of 78°C for PNIPAM-hydrazide, 45°C for PNIPAM-aldehyde, and 37°C for PNIPAM-ketone, with both electrophilic chains possessing ~12 mol% functionalization), the phase transition of the hydrogel occurs at a temperature analogous to that of PNIPAM prepared via standard free radical processes. Similar degrees and kinetics of deswelling are observed across each gel type; however, an increase in ketone content leads to a somewhat higher degree of thermal collapse of the polymer network. This discrepancy between different gel types can be attributed primarily to differences in cross-link density, by which the higher degree of cross-linking in aldehyde-rich gels elastically restricts gel deswelling. Interestingly, the highly functionalized 0Ald/100Ket* gels retain their ability to thermally deswell at 37°C to roughly the same degree as hydrogels prepared with ~12 mol% electrophilic group precursors despite the ~42 mol% ketone monomer functionalization of this precursor polymer (i.e. only ~58 mol% of the total monomer units are NIPAM). The slightly lower phase transition temperature of ketone-functionalized polymers relative to aldehyde polymers likely offsets the lower NIPAM content in this case. As such, based on Figure 3.3, the thermal phase transition can be maintained independent of the cross-link density and opacity of the hydrogel by varying both the ratio of aldehyde:ketone groups as well as the mole percentage of ketone groups in the electrophilic precursor polymer.

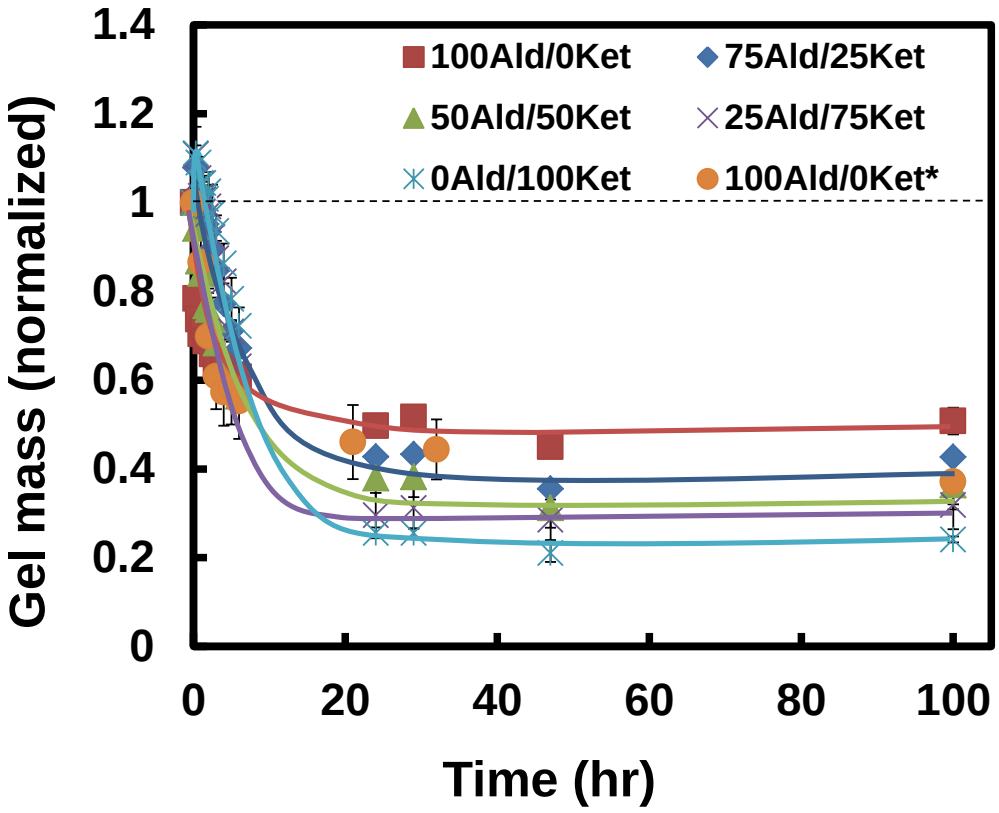

Figure 3.3. Temperature-dependent thermal collapse following gel incubation at 37 °C for PNIPAM hydrogels prepared with precursor polymers containing different aldehyde:ketone functional group ratios and different ketone functional group mole fractions (0Ald/100Ket* ~42 mol% ketones; all other hydrogels ~12 mol% electrophile). The dashed line represents the initial mass of each hydrogel tested.

Hydrogel Degradation: Hydrogels prepared by hydrazide-ketone/aldehyde chemistry can degrade via the hydrolysis of the hydrazone cross-linking moieties, as previously demonstrated.[14–16] Figure 3.5 indicates that the rate of hydrogel degradation (as measured in PBS at 37°C) can be tuned based on the aldehyde to ketone ratio used to prepare the electrophilic precursor polymers. 0Ald/100Ket gels (containing ~12 mol% ketone groups and no aldehydes) degrade rapidly (~18 days) after gel formation; in contrast, 100Ald/0Ket gels (containing ~12 mol% aldehyde groups and no ketones) degrade over a much longer time period (~93 days). This difference between these two hydrogel types is

likely attributable to the large observed variation in cross-linking between the two gels (Table 3.3), with the aldehyde-functionalized precursor polymers producing hydrogels with significantly higher cross-link densities. Of note, the 0Ald/100Ket* hydrogel degrades more slowly than the 100Ald/0Ket hydrogel with the same cross-link density (as per *G'* measurements, Figure 3.2, and NMR, Table 3.3), as the extra alpha carbon makes the hydrazone group less reactive to water hydrolysis. As such, by varying both the aldehyde:ketone ratio and the total number of ketone functional groups, the gel degradation rate can be tuned independently of the cross-link density, typically not possible with other reported injectable hydrogel formulations. Interestingly, while the 0Ald/100Ket gels undergo a nearly linear degradation profile following the onset of degradation, 100Ald/0Ket gels exhibit an additional secondary degradation profile, with a very slow degradation rate initiated at ~78 days (following >90% degradation) until complete gel degradation is achieved. These hydrogels remained as small spherical opaque samples during this secondary degradation step. This phenomenon may be attributable to the presence of inhomogeneities in these highly opaque hydrogels (see Figure 3.2), in which regions of higher and lower cross-link densities may be present; secondary hydrolysis may be attributable to the slower degradation of the more highly cross-linked pockets in the hydrogel. A similar secondary degradation rate was observed for gels possessing intermediate aldehyde to ketone ratios, with the effect decreasing as the ketone content is increased (and the transparency of the gel improves, see Figure 3.2). Furthermore, the 0Ald/100Ket* gel that has a matched cross-link density to 100Ald/0Ket but significantly higher transparency exhibits no secondary linear region in its

degradation profile, again supporting the hypothesis that an increase in ketone content in the precursor polymers leads to a greater degree of gel homogeneity and therefore a more uniform gel degradation profile.

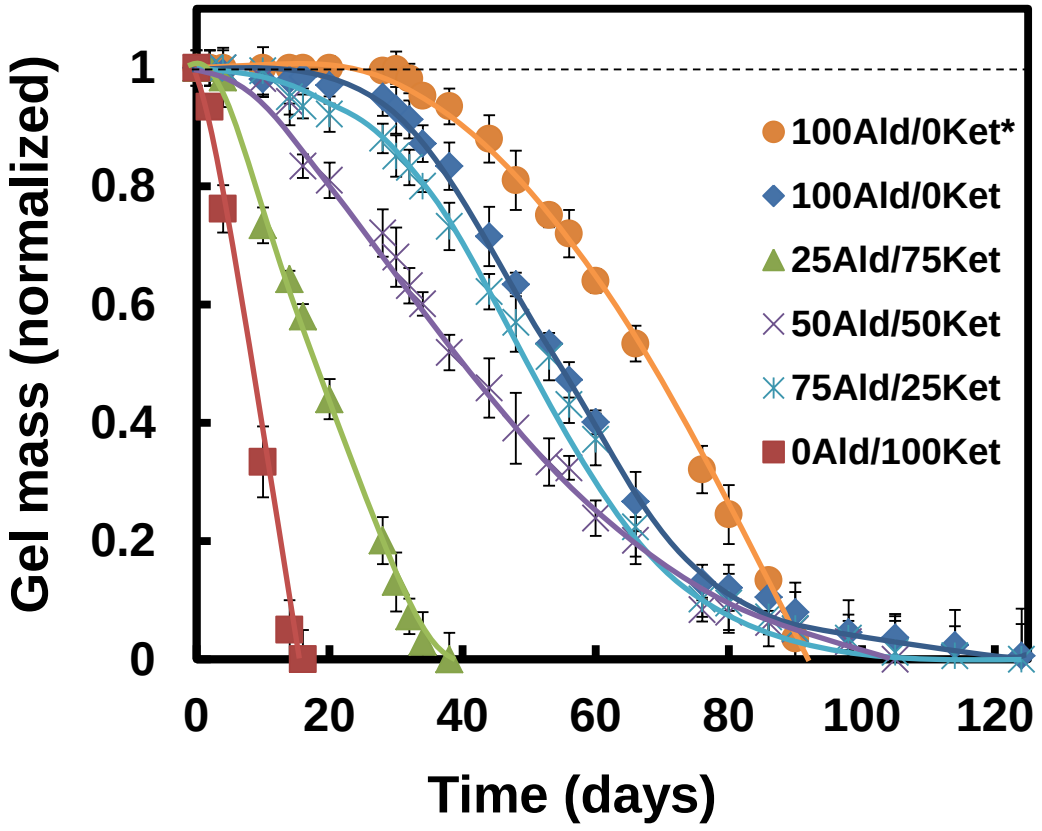

Figure 3.4. Hydrogel degradation profiles (expressed in terms of the gel mass at different time points normalized to the initial mass of the gel following co-extrusion) following gel incubation at 37 °C for PNIPAM hydrogels prepared with precursor polymers containing different aldehyde:ketone functional group ratios and different ketone functional group mole fractions (0Ald/100Ket* ~42 mol% ketones; all other hydrogels ~12 mol% electrophile). The dashed line represents the initial mass of each hydrogel tested.

Polymer Cytocompatibility: The *in vitro* cytotoxicity of the hydrogel precursor polymers, which are also the degradation products of the hydrogels,[16] was screened using an MTT assay with 3T3 mouse fibroblasts. Numerous previous studies from our group have

shown that the PNIPAM-hydrazide component exhibits no significant cytotoxicity at the typical concentrations used in cell culture assays as well as *in vivo* in subcutaneous mouse models.[14–16] Therefore the *in vitro* study herein was focused on a comparison of the cytotoxic effects of the PNIPAM-aldehyde and PNIPAM-ketone polymers, along with polymers containing a combination of aldehyde and ketone components. MTT assay results for polymers prepared with different aldehyde:ketone ratios indicated cell viabilities of at least 80% for all polymer ratios tested at concentrations up to 2 mg/mL (see Supporting Information, Figure 3.S4), viabilities that have been associated with little to no practical cytotoxicity[1]. Notably, the maximum concentration tested (2 mg/mL) is expected to be greater than the concentration of free polymer that the body would be exposed to given the relatively rapid gelation process of the hydrogels along with their slow degradation.

Figure 3.5 shows the results of an MTT assay performed on the 100Ald/0Ket (~12 mol% aldehydes) and 0Ald/100Ket* (~42 mol% ketones) precursor polymers at concentrations as high as 20 mg/mL (2 %), a concentration typically far in excess of those screened in an *in vitro* cell culture assay. At these higher concentrations, and particularly in the range of 4-12 mg/mL, the PNIPAM-ketone polymer exhibited significantly less cytotoxicity than the PNIPAM-aldehyde polymer ($p < 0.05$). The PNIPAM-aldehyde polymer started to exhibit significant cytotoxicity (< 80% relative viability) at concentrations above 4 mg/mL, whereas the PNIPAM-ketone polymer only exhibited equivalent cytotoxicity at a concentration of 20 mg/mL despite containing quadruple the mole fraction of electrophilic reactive functional groups. This result suggests that the use of ketones in

partial or complete place of aldehydes significantly reduces the potential cytotoxicity of the precursor polymer as well as the degradation products.

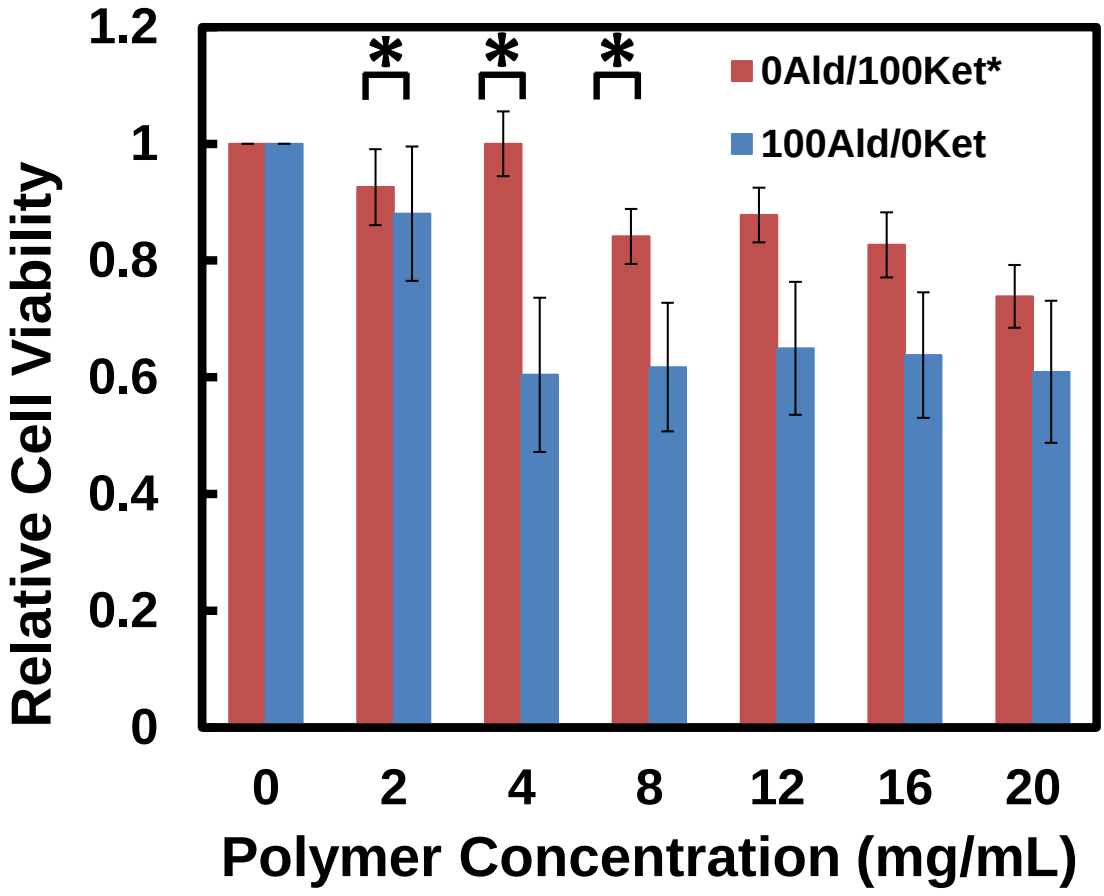

Figure 3.5. Comparison of cell viability (relative to a cell-only control) of 3T3 mouse fibroblast cells in the presence of high concentrations (> 2 mg/mL) of 0Ald/100Ket* (~42 mol% ketones) and 100Ald/0Ket (~12 mol% aldehydes). The asterisk indicates that the difference in the viabilities of the two polymers at a given concentration is statistically significant ($p < 0.05$).

4. Discussion

By changing the ratio of ketone to aldehyde groups in the electrophilic polymer involved in the formation of hydrazone cross-linked injectable hydrogels, significant control can be

exerted over several key engineering properties of these hydrogels. The slower reactivity of ketones relative to aldehydes significantly slows the rate of gelation, increasing the time required for gel formation from several seconds in the case of aldehyde-functionalized polymers to over one hour in the case of only ketone-functionalized polymers (Table 3.2). We anticipate that copolymers containing between 25-50 mol% ketones (yielding gelation times on the order of several minutes) may be ideal for many biomedical applications in this respect, allowing surgeons sufficient time to administer the gel at the site(s) desired while avoiding premature gelation inside the syringe. Ketone-functionalized precursor polymers also resulted in significantly more transparent hydrogels (Figure 3.2), a phenomenon also attributable to the slower gelation rate with these copolymers. Slower gelation allows more time for diffusional mixing of the (miscible) precursor polymers before the matrix is fixed by cross-link formation, decreasing the number of micro-domain inhomogeneities within the matrix and thus leading to more transparent gels. The uniformity of hydrogels has two significant advantages in biomedical applications. First, transparency is required in some applications of hydrogels, particularly ophthalmic applications (e.g. eyedrop formulations, intraocular lenses, or vitreal substitutes) that are particularly attractive for injectable hydrogel formulations. Second, gel uniformity reduces confounding intramatrix morphologies that may serve to complicate drug diffusion throughout the gel and simplifies the development of mathematical expressions governing drug release, improving the predictability of hydrogel performance in a drug delivery application. Similarly, if the inhomogeneities are on the same length scale as cells, local differences in

cell responses to the hydrogel may result, leading to typically undesirable non-uniform cell distributions or cell behaviors within a tissue engineering matrix.

Hydrogel properties can be tuned by varying both the ratio of aldehyde:ketone groups as well as the total number of either functional group, with varying the amount of ketone groups of particular interest. Hydrogels prepared with ~42 mol% ketone functionalized precursor polymers (0Ald/100Ket*) maintain relatively high transparency (Figure 3.2) even though they gel much more quickly than even some of the more opaque hydrogels prepared using aldehyde-ketone mix precursor polymers (Table 3.2) and exhibit both analogous mechanical (Figure 3.1) and thermoresponsive properties (Figure 3.3) as well as slower degradation rates (Figure 3.4) relative to hydrogels prepared with ~12 mol% aldehyde-functionalized precursor polymers. In this way, manipulating the total number of fast (aldehyde) and slow (ketone) gelling functional groups can result in largely independent control over gelation time, gel degradation kinetics, gel transparency, hydrogel mechanics, and phase transition behavior to a degree not currently possible with existing injectable hydrogel approaches. Specifically, for all currently reported injectable hydrogel chemistries, gelation times and hydrogel degradation rates are both directly linked to the ultimate cross-link density of the hydrogel; the use of mixtures of ketones and aldehydes for hydrogel preparation decouples these parameters to provide largely independent control over multiple key hydrogel properties. This degree of control significantly improves the potential translatability of these materials in a surgical context, since hydrogels with desired mechanical properties (i.e. for matching elastic moduli of

native tissues) can be delivered with a gelation time chosen by the surgeon administering the hydrogel that is most suitable to the procedure to be conducted.

Maximizing the ketone content of the precursor polymers also has demonstrated advantages in terms of maintaining high cell tolerance to the precursor polymers. Aldehyde groups can react with amine-containing cellular components via Schiff base formation, potentially disrupting regular cellular processes necessary for cell survival and proliferation (particularly at higher polymer concentrations); in comparison, ketones are inherently less reactive due to the presence of two adjacent alpha carbons instead of one, which reduces the electrophilicity of the carbonyl group and renders ketones significantly more bio-orthogonal to typical functional groups found *in vivo.*[40] Thus, while care must be taken not to slow the gelation time to the point where the precursor polymers diffuse away prior to gelling once injected *in vivo*, the ability to precisely tune the gelation time using ketone-aldehyde copolymers of defined compositions offers control over multiple hydrogel properties of interest. Note that all hydrogels studied in this paper are prepared with the same total mass concentration of precursor polymers (6 %), a parameter that if varied would provide an additional mechanism to control the properties of the final hydrogels.

5. Conclusions

Injectable hydrogels prepared by mixing hydrazide-functionalized PNIPAM with electrophilic PNIPAM precursor polymers containing mixtures of aldehyde and ketone groups can be tuned to exhibit desired gelation rates, degradation rates, opacities, and mechanical properties. Specifically, by changing the aldehyde:ketone ratio in the electrophilic polymer used for gelation and/or the mole percentage of ketones incorporated in the polymer, largely independent control over the gelation rate, opacity, degradation rate, and cross-link density can be achieved, unlike in currently reported *in situ* gelling chemistries. The hydrogels maintain their volume phase transition properties irrespective of the composition of the electrophile precursor polymer; furthermore, the presence of higher ketone fractions significantly improves the cytocompatibility of the precursor polymers (and, by extension, the degradation products) at even extremely high polymer concentrations, facilitating the use of such hydrogels in switchable biomedical applications. This chemistry approach could be applied to any synthetic or natural polymer backbone to produce highly tunable hydrogel compositions by simple mixing of well-defined precursor polymers applicable to a variety of different biomedical challenges.

Acknowledgements: Funding from the 20/20: NSERC Ophthalmic Materials Research Network, the Natural Sciences and Engineering Research Council of Canada (Discovery Grants Program), and the Ontario Graduate Scholarship Program (MP) is gratefully acknowledged.

References

(1) Geckil, H.; Xu, F.; Zhang, X.; Moon, S.; Demirci, U. *Nanomedicine* **2010**, *5*, 469–84.

(2) Hoare, T. R.; Kohane, D. S. *Polymer* **2008**, *49*, 1993–2007.

(3) Lee, K. Y.; Mooney, D. J. *Chemical Reviews* **2001**, *101*, 1869–80.

(4) Galperin, A.; Long, T. J.; Ratner, B. D. *Biomacromolecules* **2010**, 2583–92.

(5) Van Vlierberghe, S.; Dubruel, P.; Schacht, E. *Biomacromolecules* **2011**, *12*, 1387–408.

(6) Tan, H.; Marra, K. G. *Materials* **2010**, *3*, 1746–67.

(7) Nicodemus, G. D.; Bryant, S. J. *Tissue Engineering Part B: Reviews* **2008**, *14*, 149–65.

(8) Yang, W.; Xue, H.; Carr, L. R.; Wang, J.; Jiang, S. *Biosensors & Bioelectronics* **2011**, *26*, 2454–9.

(9) Toma, M.; Jonas, U.; Mateescu, A.; Knoll, W.; Dostalek, J. *The Journal of Physical Chemistry Part C: Nanomaterials and Interfaces* **2013**, *117*, 11705–12.

(10) Khimji, I.; Kelly, E. Y.; Helwa, Y.; Hoang, M.; Liu, J. *Methods* **2013**, *64*, 292-8.

(11) Hiemstra, C.; van der Aa, L. J.; Zhong, Z.; Dijkstra, P. J.; Feijen, J. *Biomacromolecules* **2007**, *8*, 1548–56.

(12) Azab, A. K.; Doviner, V.; Orkin, B.; Kleinstern, J.; Srebnik, M.; Nissan, A.; Rubinstein, A. *Journal of Biomedical Research Part A* **2007**, *2*, 414–22.

(13) Guvendiren, M.; Lu, H. D.; Burdick, J. A. *Soft Matter* **2012**, *8*, 260.

(14) Campbell, S. B.; Patenaude, M.; Hoare, T. *Biomacromolecules* **2013**, *14*, 644–53.

(15) Patenaude, M.; Hoare, T. *Biomacromolecules* **2012**, *13*, 369–78.

(16) Patenaude, M.; Hoare, T. *ACS Macro Letters* **2012**, *1*, 409–413.

(17) Pritchard, C. D.; O'Shea, T. M.; Siegwart, D. J.; Calo, E.; Anderson, D. G.; Reynolds, F. M.; Thomas, J.; Slotkin, J. R.; Woodard, E. J.; Langer, R. *Biomaterials* **2011**, *32*, 587–97.

(18) Yu, Y.; Deng, C.; Meng, F.; Shi, Q.; Feijen, J.; Zhong, Z. *Journal of Biomedical Materials Research Part A* **2011**, *99*, 316–26.

(19) Sekine, Y.; Moritani, Y.; Ikeda-Fukazawa, T.; Sasaki, Y.; Akiyoshi, K. *Advanced Healthcare Materials* **2012**, *1*, 722–8.

(20) Censi, R.; Fieten, P. J.; Di Martino, P.; Hennink, W. E.; Vermonden, T. *Journal of Controlled Release: Official Journal of the Controlled Release Society* **2010**, *148*, 28–9.

(21) Wei, H. L.; Yang, Z.; Zheng, L. M.; Shen, Y. M. *Polymer* **2009**, *50*, 2836–40.

(22) Nimmo, C. M.; Owen, S. C.; Shoichet, M. S. *Biomacromolecules* **2011**, *12*, 824–30.

(23) Tan, H.; Rubin, J. P.; Marra, K. G. *Macromolecular Rapid Communications* **2011**, *32*, 905–11.

(24) Grover, G. N.; Lam, J.; Nguyen, T. H.; Segura, T.; Maynard, H. D. *Biomacromolecules* **2012**, *13*, 3013–3017.

(25) Vetrík, M.; Přádný, M.; Hrubý, M.; Michálek, J. *Polymer Degradation and Stability* **2011**, *96*, 756–59.

(26) Sivakumaran, D.; Maitland, D.; Hoare, T. *Biomacromolecules* **2011**, *12*, 4112–20.

(27) Ito, T.; Yeo, Y.; Highley, C. B.; Bellas, E.; Kohane, D. S. *Biomaterials* **2007**, *28*, 3418–26.

(28) Beauchamp, R. O.; St Clair, M. B.; Fennell, T. R.; Clarke, D. O.; Morgan, K. T.; Kari, F. W. *Critical Reviews in Toxicology* **1992**, *22*, 143–74.

(29) Gough, J. E.; Scotchford, C.; Downes, S. *Journal of Biomedical Raterials Research* **2002**, *61*, 121–30.

(30) O'Brien, P. J.; Siraki, A. G.; Shangari, N. *Critical Reviews in Toxicology* **2005**, *35*, 609–62.

(31) Meid, J.; Friedrich, T.; Tieke, B.; Lindner, P.; Richtering, W. *Physical Chemistry Chemical Physics* **2011**, *13*, 3039–47.

(32) McKinnon, D. D.; Domaille, D. W.; Cha, J. N.; Anseth, K. S. *Adv. Mater.* **2013**, DOI: 10.1002/adma.201303680

(33) Uzu, S.; Kanda, S.; Imai, K. *Analyst* **1990**, *115*, 1477–1482.

(34) Cai, S.; Suo, Z. *Journal of the Mechanics and Physics of Solids* **2011**, *59*, 2259–78.

(35) Kang Derwent, J. J.; Mieler, W. F. *Transactions of the American Ophthalmological Society* **2008**, *106*, 206–13.

(36) Hou, Y.; Matthews, A. R.; Smitherman, A. M.; Bulick, A. S.; Hahn, M. S.; Hou, H.; Han, A.; Grunlan, M. *Biomaterials* **2008**, *29*, 3175–84.

(37) Adachi, J.; Sato, N. *The Journal of Organic Chemistry* **1972**, *37*, 221–5.

(38) Motokawa, R.; Morishita, K.; Koizumi, S.; Nakahira, T.; Annaka, M. *Macromolecules* **2005**, *38*, 5748–60.

(39) Dong, Y.; Hassan, W.; Zheng, Y.; Saeed, A. O.; Cao, H.; Tai, H.; Pandit, A.; Wang, W. *Journal of Materials Science: Materials in Medicine* **2012**, *23*, 25–35.

(40) Sletten, E. M.; Bertozzi, C. R. *Angewandte Chemie Int. Ed.* **2009**, *38*, 6974-98.

CHAPTER 3 - SUPPORTING INFORMATION

TUNING GELATION TIME AND MORPHOLOGY OF INJECTABLE HYDROGELS USING KETONE-HYDRAZIDE CROSS-LINKING

Authors: Mathew Patenaude, Scott Campbell, Dennis Kinio, and Todd Hoare

Publication Information: Biomacromolecules 15(3), 781-790

Accepted Date: 16 January 2014

Schemes for Monomer and Polymer Preparation

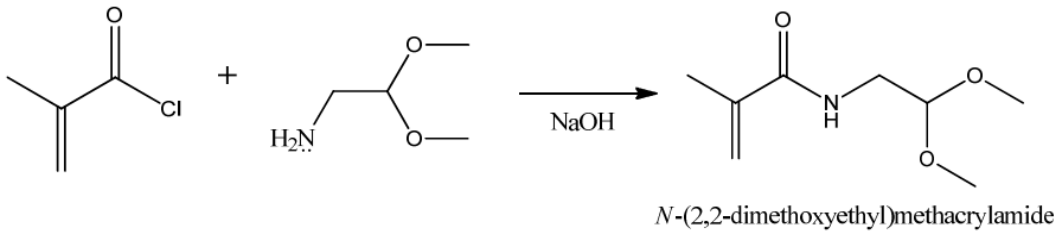

Scheme 3.S1. Preparation of acetal-protected aldehyde monomer

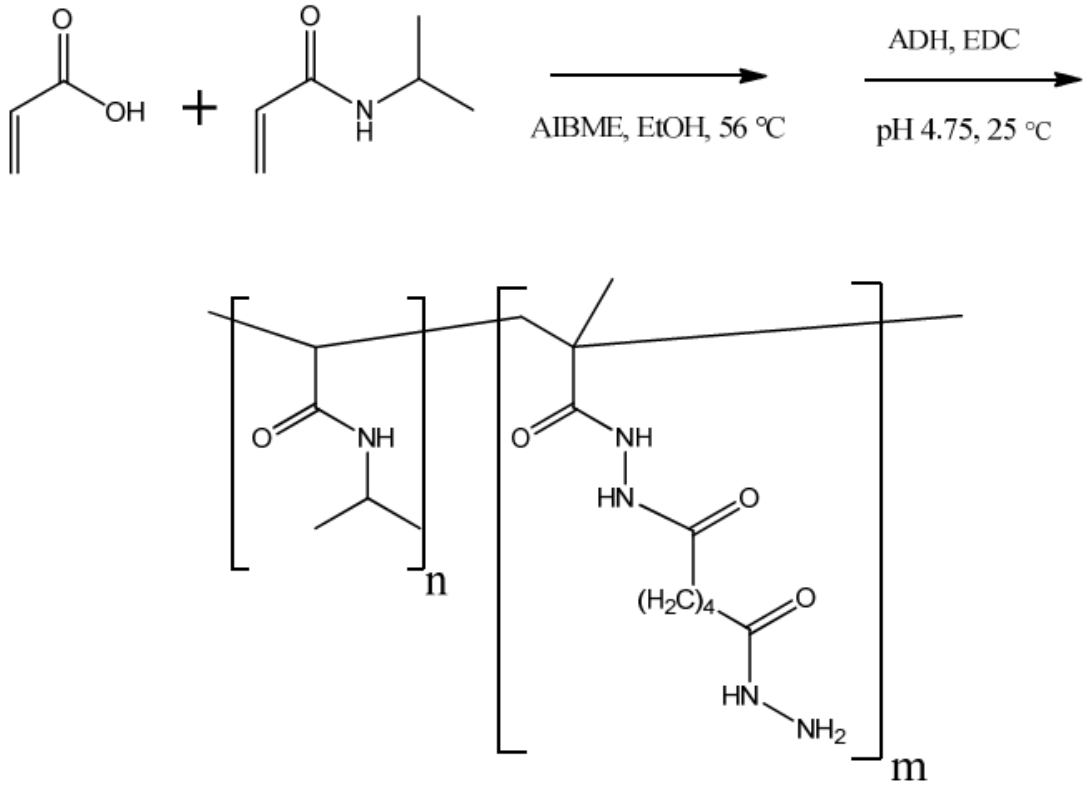

Scheme 3.S2. Preparation of hydrazide-functionalized polymers

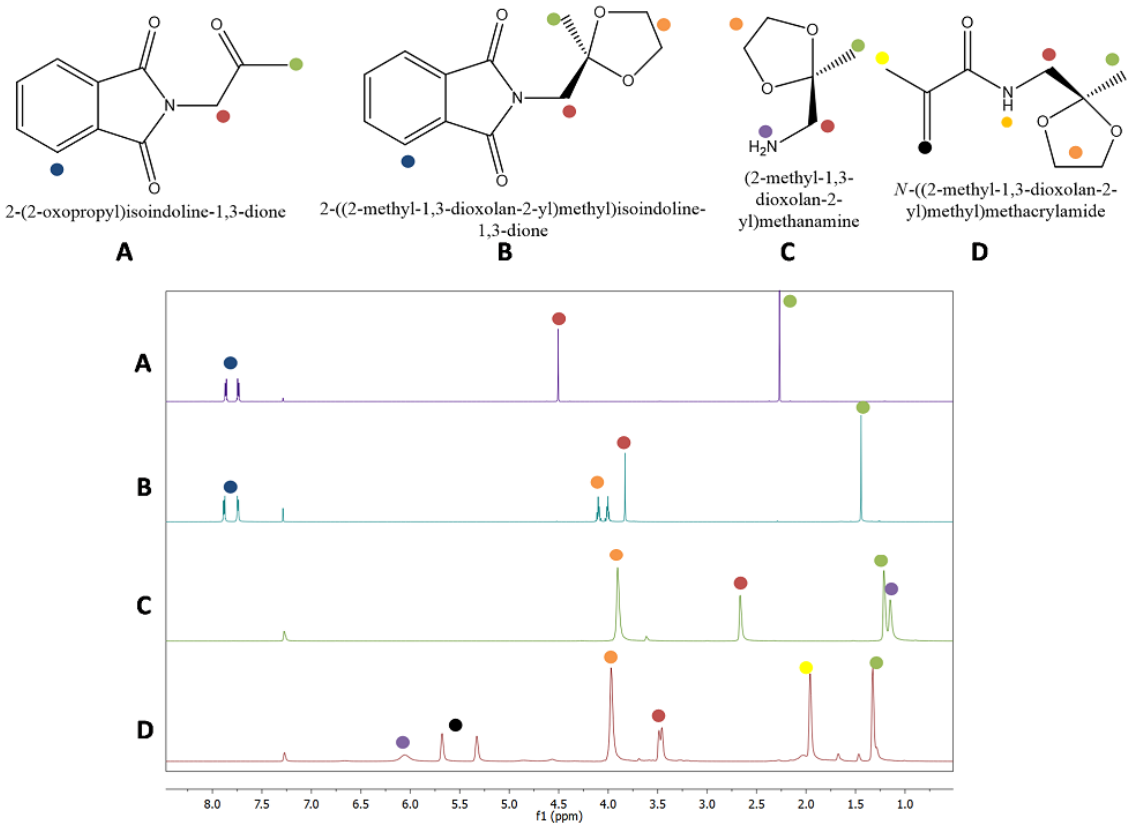

Figure 3.S1. ^{1}H NMR (600 MHz, Bruker) of isolated intermediates in the synthesis of the protected ketone monomer. The peak at ~7.25 ppm is the solvent (chloroform).

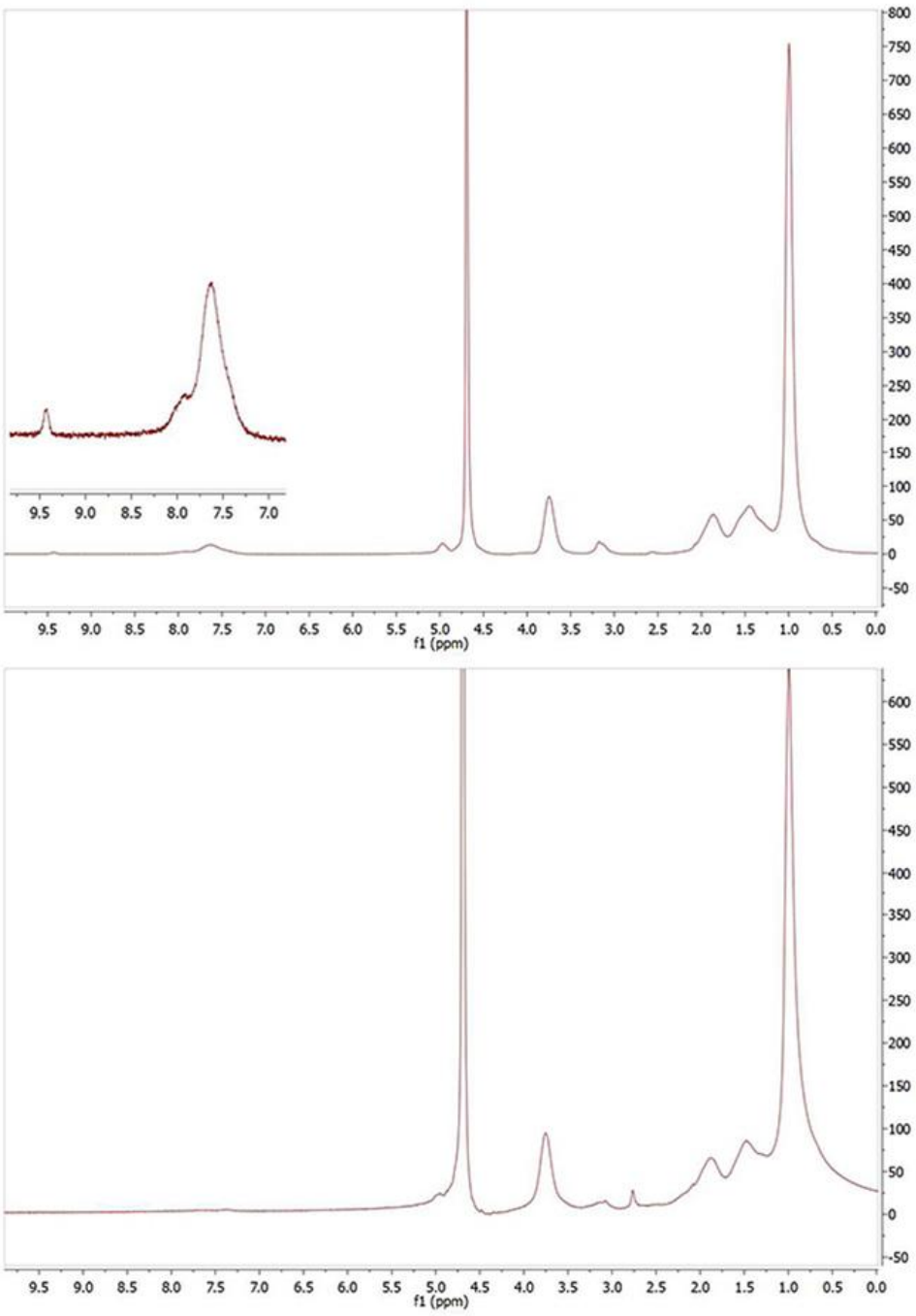

Figure 3.S2. ^{1}H NMR spectrum (200 MHz, Bruker) of 100Ald/0Ket polymer in D_2O at 3 % (w/v) (top) and 100Ald/0Ket 6 % (w/v) in D_2O cross-linked with a solution of PNIPAM-hydrazide at 6 % (w/v) in D_2O (bottom). The disappearance of the aldehyde peak at ~9.5 ppm is observed as the gel forms.

CHAPTER 4

Desig

Authors: Mathew Patenaude and Todd Hoare

Publication Information: Biomacromolecules 13(2), 369-378

Accepted Date: 17 January 2012

ABSTRACT

A series of synthetic oligomers (based on the thermosensitive polymer poly(*N*-isopropylacrylamide) and carbohydrate polymers (including hyaluronic acid, carboxymethyl cellulose, dextran, and methylcellulose) were functionalized with hydrazide or aldehyde functional groups and mixed using a double-barreled syringe to create in situ-gelling, hydrazone-crosslinked hydrogels. By mixing different numbers and ratio of different reactive oligomer or polymer precursors, covalently-crosslinked hydrogel networks comprised of different polymeric components are produced by simple mixing of reactive components, without the need for any intermediate chemistries (e.g. grafting). In this way, hydrogels with defined swelling, degradation, phase transition, drug binding, and mechanical properties can be produced with properties intermediate to those of the mixture of reactive precursor polymers selected. Using this modular, mixing approach, one property can (in many cases) be selectively modified while keeping other properties constant, providing a highly adaptable method of engineering injectable, rapidly-gelling hydrogels for potential in vivo applications.

1. Introduction

Hydrogels have attracted considerable attention in biomedical engineering applications due to their many favorable and, in some cases, biomimetic properties. Mechanically, hydrogels can be designed to have elastic and loss moduli similar to those of soft tissues, enabling their effective use in tissue engineering applications or as biological lubricants. Physically, hydrogels have high internal void fractions facilitating effective control of the molecular weight-dependent diffusion both out of the hydrogel phase (for drug delivery) or into the hydrogel phase (for sensor or tissue engineering applications). Chemically, hydrogels can be engineered to contain different charges or affinity domains that enable binding of particular classes of drugs or biological compounds to the hydrogel phase. Biologically, hydrogels typically exhibit low protein adsorption due to their high water content and thus low interfacial energy. Hydrogels based on proteins or carbohydrates native to the body can also function as effective extracellular matrices to direct cellular behavior. Given this diversity of tunable properties, hydrogels have found use in a number of applications, such as in the formation of scaffolds in tissue engineering[1,2,3], in wound care[4] , as adhesion prevention barriers following surgery[5], in biosensors[6,7], as well as in a number of drug delivery systems[8,9].

Hydrogels based on naturally-occurring carbohydrates, synthetically-modified carbohydrates, and a range of different types of synthetic polymers have been widely reported in the literature. Naturally-occurring carbohydrates such as dextran and hyaluronic acid (or other glycosaminoglycans) offer the inherent advantages of being biodegradable under physiological conditions (via enzymatic[10] or oxidative[11] cleavage)

and having defined interactions with cells to induce spreading, differentiation, or other biological responses[12]. However, a relatively limited number of natural polymers are available, restricting the range of physical and mechanical properties that can be achieved in such hydrogels. Synthetically-modified carbohydrates such as carboxymethyl cellulose or methylcellulose broaden the range of achievable properties but also are offer limited compositional diversity. Furthermore, depending on the source of the polymer, molecular weights, compositions, or architectures can differ significantly, both batch-to-batch and even within batches.

In contrast, while synthetic polymers based on carbon-carbon backbones are not inherently degradable in vivo, synthetic polymers offer exceptional control over polymer composition, architecture, and physical properties not fully accessible with natural polymers. Of particular interest in biomedical applications are synthetic polymers that possess "smart" properties; that is, the polymers undergo a discontinuous change in one or more physical properties upon the application of a stimulus. Such materials have potential to reversibly control cell adhesion[13], swelling[14], and drug diffusion coefficients[9], among other properties, as triggered by changing local biological environments and/or externallyapplied stimuli. Hydrogels based on poly(N-isopropylacrylamide) (PNIPAM) have in particular been the subject of intense investigation due to their ability to undergo a thermally-induced phase transition at 32 °C that induces deswelling in the polymer network[15]. The phase transition temperature can be tuned via copolymerization of more hydrophilic or hydrophobic comonomers to achieve desired transitions in relevant in vivo environments[16].However, the lack of a clear degradation pathway for such hydrogel

materials has significantly limited their ultimate use in the body. Materials that combine the facile degradation and biological properties ofnatural polymers with the compositional diversity and "smart" properties of synthetic polymers would offer significant benefits in a range of potential biomedical applications. Facile biomedical application of hydrogels is also significantly enhanced when hydrogels are designed to gel in situ upon injection from low-viscosity solution precursors.

Conventional bulk hydrogels of biomedical use are highly elastic and are thus difficult to introduce directly into the body without surgical intervention[17], which is inefficient and undesirable for routine clinical use. In response,a range of in situ-gellable hydrogel formulations have been developed, applying Michaelchemistry[18], imine formation[19], hydrazide-aldehyde chemistry[20] or other fast, aqueous reactions that occur at ambient conditions to form the crosslinks in situ following mixing of reactive precursors. Some of these chemistries offer the additional advantage ofgenerating a hydrolyzable crosslink which can lead to programmed degradation of the hydrogels under specific physiological environments[21]. To this point, however, reports of such injectable hydrogels in the literature have been limited to natural polymers.

In this paper, injectable, mixed natural-synthetic polymeric hydrogel systems with "smart" responsive properties and cross-linked with hydrolyzable chemical bonds are reported. The rapid gelation of the hydrogels and their subsequent degradation via hydrolysis is made possible through the use of hydrazone chemistry in the formation of chemical crosslinks[22]. By crosslinking thermoresponsive PNIPAM oligomers of a molecular weight below the kidney clearance limit (~40 kDa) with different combinations

of oxidized polysaccharide precursors (based on hyaluronic acid[23,24], dextran[25,26], and carboxymethyl cellulose[27,28]), we show that it is possible to alter hydrogel properties in an additive or combinatorial way based on the properties of each component polymer, in some cases facilitating simultaneous independent tuning of different hydrogel properties. Using this modular, mix-and-match approach to hydrogel development, a range of hydrogels with designed physical, chemical, mechanical and/or biological properties can be produced simply by mixing different numbers and/or ratios ofnatural or synthetic polymers functionalized with the same reactive functional groups, enabling the facile optimization of hydrogels for various potential biomedical applications.

2. Experimental

Materials: N-isopropylacrylamide (NIPAM, 99%), acrylic acid (AA, 99%), sodium carboxymethyl cellulose (CMC) [MW 700,000, DS = 0.9], adipic acid dihydrazide (ADH, 98%), N'-ethyl-N-(3-dimethylaminopropyl)-carbodiimide (EDC, commercial grade), dextran from Leuconstroc spp(Dex) [Mr– 500,000], ethylene glycol (99.8%), sodium periodate (>99.8%), bupivacaine hydrochloride (99%), tert-butyl carbazate (≥98.0%), 2,4,6-Trinitrobenzenesulfonic acid (TNBS, picrylsulfonic acid solution, 5% (w/v) in H_2O, Thioglycolic acid (MAA) (≥98.0%), and methyl cellulose (viscosity 400 cP, 2% in water) were all purchased from Sigma-Aldrich (Oakville, Ontario). 2,2-azobisisobutyric acid dimethyl ester (AIBME) was purchased from Wako. Hyaluronic acid (MW 176kDa-350kDa) was purchased from Lifecore Biomedical. All water used was of MilliQ grade.

Synthesis and Characterization of Poly(NIPAM-co-ADH): Co-polymers of NIPAM and acrylic acid were prepared via chain transfer polymerization (Figure 4.1)[29]. N-isopropylacrylamide (4 g, 35 mmol), acrylic acid (0.952 g, 13 mmol), AIBME initiator (0.056 g, 0.243 mmol), and thioglycolic acid chain transfer agent (80 µL, 1.15 mmol) were added to 20 mL of absolute ethanol at 56°C. The reaction was allowed to proceed overnight at 56 °C. Solvent was then removed under reduced pressure using a Rotavap at 50 °C. The resulting viscous product was then dissolved in 200 mL of diH_2O and dialyzed over six cycles using a 12-14 kDa MWCO membrane, each cycle lasting six hours. The purified polymer solution was lyophilized to dryness. The acid content of the polymer was determined using base-into-acid conductometric titration (ManTech Associates), using 50 mg of polymer dissolved in 50 mL of 1 mM NaCl as the analysis sample and 0.1 M NaOH as the titrant. Polymer molecular weight was determined with aqueous gel permeation chromatography (Agilent), using a pH 7.4 sodium acetate buffer as the eluent and polyethylene oxide standards for calibration.

Carboxylic acid groups from AA residues were then converted to hydrazide groups by adding adipic acid dihydrazide (10.15 g, 58.26 mmol) to a 0.5% wt/vol solution of 20 wt% poly(NIPAM-co-AA). The pH of this solution was thenadjusted to 4.75 with 0.1 M HCl. EDC (5.58 g, 35.94 mmol) was then added to this solution and the pH was maintained at 4.75 by drop-wise addition 0.1 M HCl for about 5 hours until no further change in pH was observed. The reaction was left to stir overnight, at which point the pH of the solution was raised to 7.00 by the addition of 0.1 M NaOH. The resulting solution was exhaustively dialyzed for three days using a 12 – 14 kDa MWCO membrane, after

which the polymer solution was lyophilized to dryness. The degree of functionalization was determined by a conductometric titration by assaying the number of unreacted acid groups. Note that the pKa of a hydrazide group (2.5-3.5) is significantly lower than the pKaof the residual carboxylic acid groups (4.5 – 6.5), permitting isolation of the carboxylic acid signal in the titration. ^{1}H NMR in DMSO: 0.24H - δ= 10-10.5 ppm, 0.12H - δ= 8.5-9.0 ppm, 1.12H - δ= 6.65-7.88 ppm, 1.6H - δ= 3.0-3.7, 9.72H - δ= 0.0-2.5 ppm.

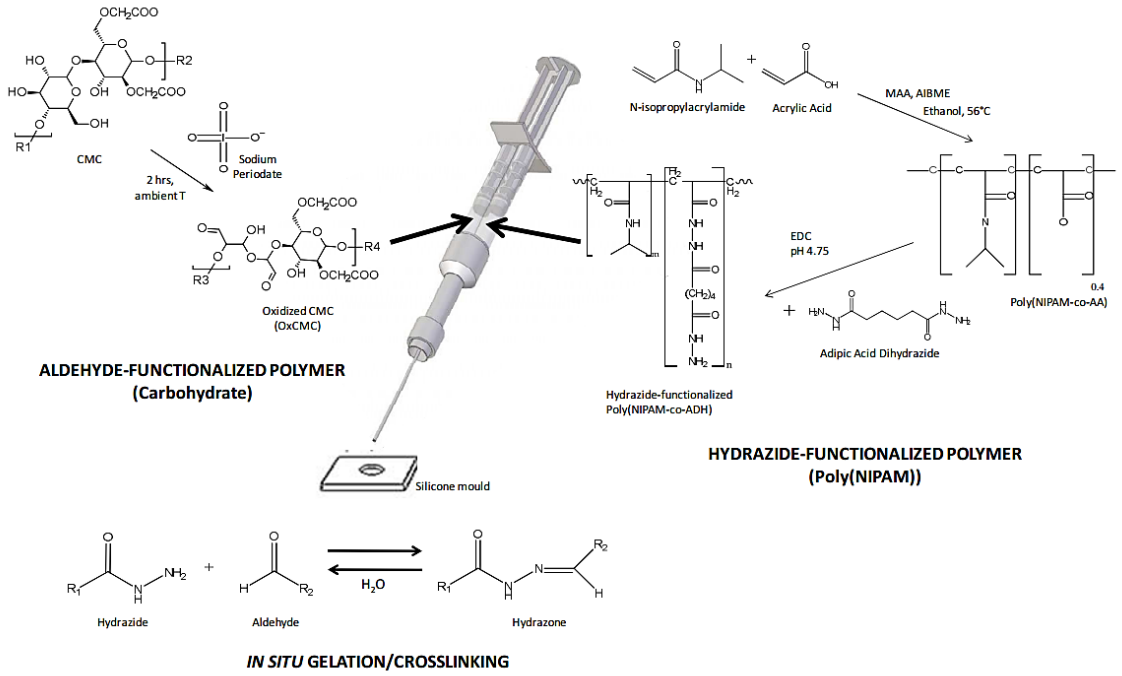

Figure 4.1. Schematic diagram of the synthesis of aldehyde-functionalized carbohydrates (shown for CMC; same chemistry used for other carbohydrates tested) and hydrazide-functionalized poly(NIPAM-co-ADH) and the formation of an in situhydrazone-crosslinked hydrogel using a double-barrel syringe.

Synthesis and characterization of aldehyde-functionalized polysaccharides: The selective oxidation of polysaccharides, including CMC, dextran, hyaluronic acid, and methyl cellulose, to form aldehyde groups was conducted using sodium periodate as the oxidizing agent (Figure 4.1). Sodium periodate (0.8 g, 3.74 mmol) was added to 150 mL of deionized H_2O containing 1.5 g of polysaccharide and oxidation was allowed to proceed with stirring for two hours at room temperature. 0.4 mL of ethylene glycol was then added to stop the reaction, at which point the mixture was stirred for an additional hour. The reaction solution was purified by exhaustive dialysis for three days using a 3500 MWCO membrane and the purified oxidized polysaccharide was freeze dried for storage. The degree of aldehyde functionalization of oxidized hyaluronic acid (oxHA),

carboxymethyl cellulose (oxCMC), dextran (oxDex), and methyl cellulose (oxMeCe) was determined using a carbazate-based aldehyde detection assay[30]. 0.005 g of oxidized polysaccharide was dissolved in 1 mL sodium acetatebuffer (10 mM, pH 5.2, 0.2 M NaCl) containing tert-butyl carbazate (0.04 g, 0.3 mmol) and allowed to react for 24 hours at room temperature. 0.005 mL of this solution was then added to 1.98 mL borate buffer (50 mM, pH 8.00) and 50 µL of 5 % (w/v) 2, 4, 6-trinitrobenesulfonic acid solution, at which point the reaction was allowed to proceed for 2 hours at room temperature. The resulting deep red solution was diluted 1:1 with 0.5 M hydrochloric acid. 50 µL of the resulting yellow solution was then added to 1.95 mLof 0.5 M hydrochloric acid. The absorbance of this resulting carbazate-TNBS complexwas measured at 334 nm using UV/VIS spectrophotometry. Concentrations of the t-butyl carbazate-TNBS complex were measured based on a calibration curve prepared using t-butyl carbazate standard solutions produced in the same manner, but without polysaccharide. Blank measurements were made using the same experimental procedure, but without tBC or TNBS.

Hydrogel preparation: Hydrogels were made by cross-linking the precursor oxidized polysaccharides with poly(NIPAM-co-ADH), the mass concentrations of each component being held constant in each gel. Gels were synthesized by dissolving 0.06 g of each reactive polymer in 1 mL 0.15 mM NaCl solutions andthen co-extruding each component through a double barrel syringe (in which the hydrazide-functionalized polymer and aldehyde functionalized polymer(s) are loaded into separate barrels, Figure 4.1) into a 0.23 cm^3 cylindrical silicone rubber mold. In cases where mixtures of aldehyde-

functionalized polymers are used, the overall mass concentration is maintained constant (6 wt% total polymer) (Table 4.1); the percentages indicated in the hydrogel codes in Table 4.1 (xCMC/yDex) in the results represent the mass percentages of each carbohydrate loaded into the syringe to make a 6 wt% total carbohydrate solution.

Table 4.1.Concentrations of poly(NIPAM-co-ADH) and oxidized polysaccharide in solutions used to fabricate hydrogels.

Hydrogel	Poly(NIPAM-co-ADH) (g/mL)	OxCMC (g/mL)	OxDex (g/mL)	OxHA (g/mL)	OxMeCe (g/mL)
100HA	0.06	0	0	0.06	0
100MeCe	0.06	0	0	0	0.06
100CMC	0.06	0.06	0	0	0
75CMC/25Dex	0.06	0.045	0.015	0	0
50CMC/50Dex	0.06	0.03	0.03	0	0
25CMC/75Dex	0.06	0.015	0.045	0	0
100Dex	0.06	0	0.06	0	0

Hydrogel swelling: In situ-gelled hydrogel disks were loaded into cell culture inserts, placed in 12 well plates, and allowed to incubate in 2 mL of 10 mM PBS at 37°C. Hydrogel mass was measured at various times to determine the swelling kinetics. Reported swelling ratios represent the average of four samples, with experimental uncertainties representing the standard deviation of the measurements. A relationship expressing the degree of swelling as a function of cross-link density can be obtained through the thermodynamics of hydrogel swelling, using the Flory-Huggins model to evaluate the net osmotic pressure at equilibrium (Equation 1)[31].

$$\pi_{total} = \pi_{mixing} + \pi_{elastic} + \pi_{Donnan}$$

$$= -\frac{k_b T}{a^3}(\phi + \ln(1-\phi) + \chi\phi^2) + \frac{k_b T}{a^3}\frac{\phi_0}{N_x}\left[\frac{1}{2}\left(\frac{\phi}{\phi_0}\right) - \left(\frac{\phi}{\phi_0}\right)^{\frac{1}{3}}\right] + \frac{k_b T}{a^3}\frac{\phi_0 f}{N_x}\left(\frac{\phi}{\phi_0}\right) \quad (1)$$

Here, T is the temperature, α is the gel dimension, χ is the Flory-Huggins solubility parameter, k_b is the Boltzmann constant, f is the average number of charges between cross-links, N_x is the average number of monomers between cross-links, and ϕ and ϕ_0 are the volume fractions of polymer in the gel and polymer volume fraction at zero-strain, respectively. At swelling equilibrium, i.e., when $\pi_{total} = 0$, equation (1) can be solved for the number of monomers between cross-links, N_x, providing an estimate of the crosslink density of the hydrogel (Equation 2).

$$N_x = -\frac{\phi_0\left[\left(\frac{\phi_E}{\phi_0}\right)^{\frac{1}{3}} - \left(\frac{0.5\phi_E}{\phi_0}\right)\right]}{\left[\phi_E + \ln(1-\phi_E) - \frac{0.27\phi_E}{\chi} + \chi\phi_E^2\right] - 0.15\phi_E} \quad (2)$$

Equation (2) was evaluated by estimating χ according to group contribution methods[32] while f was solved in terms of N_x based on the known number of ionizable functional groups present per repeat unit in each constituent polymer of the hydrogel (measured via conductometric titration). The volume fractions ϕ_E and ϕ_0 were determined according to the volume of polymer with respect to total gel volume at equilibrium and under zero

strain (i.e. the initial volume fraction of the hydrogel in the silicone mould-templated preparation conditions) respectively.

Hydrogel thermosensitivity: Hydrogels were incubated in 10 mM PBS (pH 7.4) and were alternately placed on shaking platforms maintained at 25 °C and 37 °C respectively for defined time intervals ranging from 30 minutes to 4days in order to determine the effect of polysaccharide content on hydrogel thermosensitivity. The impact of charge content on hydrogel thermosensitivity properties was determined by repeating the experiment in 2 mL of 10 mM citrate buffer at pH 3 (conditions under which all –COOH groups are protonated).

Hydrogel drug retention: Hydrogels containing 10 mg/mL bupivacaine-HCl were synthesized by dissolving bupivacaine into each of the poly(NIPAM-co-ADH) gel precursor solutions. The bulk gelation of the entire gel volume enabled facile drug entrapment inside the in situ-formed hydrogel. Drug-loaded hydrogels were subsequently incubated in 2 mL of 10 mM PBS for various time periods, after which they were placed in fresh buffer. Buffer was collected after each time period and drug concentration was analyzed with high performance liquid chromatography in an isocratic flow of 35:65 (v/v) 10 mM PBS and acetonitrile until the drug concentration in the collected buffer was effectively zero (below the sensitivity of HPLC detection) over a 24-hour period; the remaining concentration of drug inside the hydrogel represented the drug retention. A total of four hydrogels were analyzed for each composition tested, with reported drug retentions representing the mean plus or minus the standard deviation of the repeat measurements.

Hydrogel drug partitioning: Hydrogels were incubated in 2 mL of 10 mM PBS at 37°C for 24 hours in order to ensure that equilibrium swelling of the gels was achieved. The hydrogels were then incubated at 37 °C in 0.15 mM NaCl containing 10, 5, 2.5, and 0 mg/mL bupivacaine hydrochloride for three days under gentle agitation in order to ensure equilibrium drug uptake had been achieved (n= 4 as described for hydrogel drug loading). The concentration of remaining (unbound) drug in the saline solution was determined using high performance liquid chromatography (Waters, 35:65 phosphate buffer (pH 7.4):acetonitrile) to determine the partitioning coefficient of bupivacaine for the polymer phase relative to the aqueous environment.

Hydrogel degradation: Hydrogel degradation via acid-catalyzed hydrolysis was assessed in accelerated, acidic conditions to assess the relative rates of hydrazone bond hydrolysis in different hydrogel formulations. Hydrogels wereincubated in 2 mL of 1 M, 0.5 M, and 0.1 M HCl using the same procedures outlined above,with hydrogel mass measured at predetermined time intervals (n =4). Scaling principles were applied to estimate hydrolysis rate constants under physiological and endosomal pH conditions, using the assumption that the hydrolysis rate is directly proportional to the acid (catalyst) concentration. Hydrazone bond degradation was written as a first-order kinetic process according to Equation 3:

$$\frac{d[Hydrazone\ ]}{dt} = k'[Hydrazone] \quad (3)$$

where [Hydrazone] is the concentration of cross-links in the hydrogels and k' is the pseudo first order rate constant ($k' = k[H_2O][H^+]$, assuming that water and proton catalyst remain constant throughout hydrolysis). Solving the equation with respect to time yields an expression for the remaining hydrazone cross-link concentration in the hydrogel [Hydrazone] at any given time t (Equation 4):

$$ln\frac{[Hydrazone\ ]}{[Hydrazone\ ]_0} = -k'(t - t_0) \quad (4)$$

The enzymatic degradation of 100CMC and 100HA hydrogels was assayed by incubating these hydrogels at 37 °C in 2 mL of 10 mM PBS (pH 7.4) containing 0.1 mg/mL hyaluronidase. The mass of the incubated gels was measured over a number of days to monitor the degree of gel degradation (n = 4).

Hydrogel rheology: Mechanical properties of the in situ-gelled hydrogel systems were measured using oscillatory rheology. Storage (G') and loss (G") moduli, as well as complex viscosity (η*), were measured using an ARES rheomoter (Texas Instruments) operating under parallel-plate geometry with a plate diameter of 7 mm and a plate spacing of 1 mm. A strain sweep was first conducted at strains between 0.1 - 100 % at 1 Hz in order to identify the linear viscoelastic range of the hydrogels. A strain was then selected from within this linear range and set as a constant to perform a frequency sweep from 0.1 - 100 rad/s to measure the complex viscosity, elastic modulus, and loss modulus. All measurements were conducted at 21 °C. The cross-link density of the hydrogel networks tested was estimated based on rubber elasticity theory (Equation 5)[33,34].

$$\nu_e = \frac{G'_p N_A}{RT} \quad (5)$$

where G'_p is the plateau modulus, R is the gas constant, T is temperature in Kelvin, and N_A is Avogadro's number.

3. Results

Characterization of Reactive Polymers: The copolymer of NIPAM and acrylic acid was demonstrated to be of high purity by proton NMR. Conductometric titration indicated that the acrylic acid content of the copolymer was 19.5 wt%, or roughly 40 mol% of the monomers along each polymer chain. Gel permeation chromatography yielded an M_n value of 21.6 kDa for these copolymers with a polydispersity of 1.65. Following conjugation with adipic acid dihydrazide, the residual acrylic acid content was determined to be 2 % of total monomer groups, meaning that 38 % of the total monomer residues (95 mol% of acrylic acid residues) were successfully grafted with hydrazide functional groups. While this characterization does not definitively rule out the possibility of hydrazide cross-link formation as opposed to hydrazide grafting, the large excess of both ADH and EDC used (10x excess) and the lack of an observed viscosity increase upon grafting both suggest minimal if any cross-linking during the grafting reaction. The

TNBS assay determined that the degree of oxidative cleavage for polysaccharides was 13 ± 3 % for CMC, 37 ± 6 % for dextran, and 27 ± 5 % for hyaluronic acid, where the degree of oxidation refers to the percentage of repeat units that underwent oxidative cleavage (resulting in the formation of two aldehyde groups for each cleaved ring). Based on these

analyses, the ratio of hydrazide to aldehyde functionality within the tested hydrogels was determined to be 3.4 for 100CMC, 2.5 for 75CMC/25Dex, 2.1 for 50CMC/50Dex, 1.7 for 25CMC/75Dex, and 1.4 for 100Dex. As such, the hydrazide groups from the constant poly(NIPAM-co-ADH) wt% used to synthesize each hydrogel are in excess in each tested hydrogel, such that complete aldehyde consumption (i.e. a fixed constant crosslinking density) is stoichiometrically possible in each hydrogels evaluated.

Modular Hydrogel Swelling: Incubating hydrogels composed of different oxidized polysaccharide precursors in 10 mM PBS solution at 37 °C shows how the choice of precursor carbohydrate can influence the equilibrium swelling of the in situ-gelled hydrogel (Figure 4.2). Both hyaluronic acid and CMC introduce anionic functional groups into the gel network, resulting in significant gel swelling over time due to Donnan equilbirum contributions to swelling (see Equation 1). Methyl cellulose, while possessing an overall similar structure to CMC, lacks carboxylate functionality, eliminating the Donnan equilibrium osmotic pressure contribution and resulting in only minimal swelling over time; furthermore, as a polymer with a phase transition temperature itself (40-50°C), hydrophobic interactions between methyl cellulose and PNIPAM cannot be discounted in accounting for hydrogel swelling. In contrast, hydrogels cross-linked with dextran undergo a significant phase transition under the same conditions, likely owing to the lower hygroscopicity of dextran relative to the other carbohydrates tested and/or the potential for competitive hydrogen bonding between dextran and PNIPAM residues that restricts water uptake. Thus, by selecting aldehyde-functionalized carbohydrates with different physical properties, injectable hydrogels with significantly different swelling

profiles can be produced.

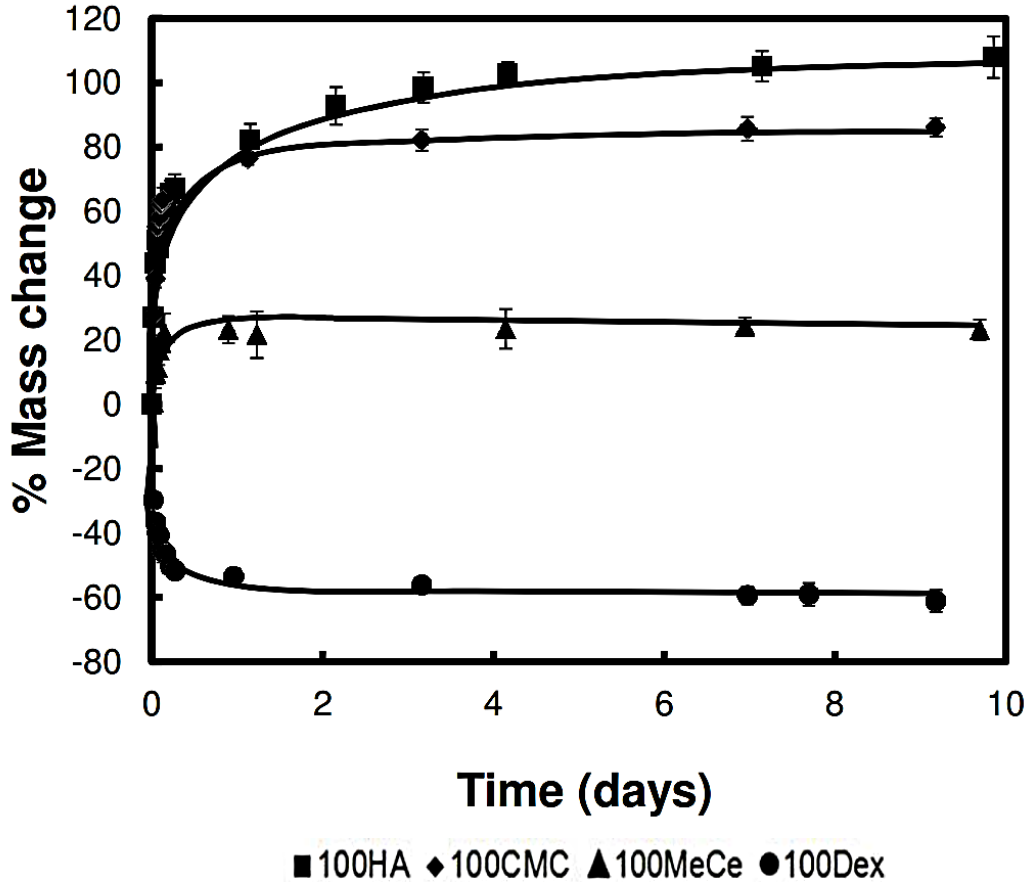

Figure 4.2. Swelling kinetics of hydrogels formed by cross-linking hydrazide-functionalized poly(NIPAM) with aldehyde-functionalized hyaluronicacid (100HA), CMC (100CMC), methyl cellulose (100MeCe), and dextran (100Dex).

Owing to these significantly swelling properties observed when injectable hydrogels were prepared using our different library carbohydrates,we proceeded to investigate whether swelling (and, by extension, the phase transition behavior of the injectable poly(NIPAM)-containing hydrogels) could be modulated by mixing different carbohydrates together in the aldehyde fraction while maintaining the same total mass concentration of carbohydrate. In this respect, within limits, hydrogels could be engineered that have

swelling responses independent of other properties (e.g. degradation, biological interactions, etc.). By increasing the CMC content in poly(NIPAM)-based hydrogels relative to dextran content, it is possible to switch the gel from one that deswells to one that swells under physiological conditions, effectively silencing the thermally-responsive collapse that is characteristic of hydrogels composed solely of poly(NIPAM) (Figure 4.3). Indeed, the degree of swelling in these systems is nearly predictable according to the rule of simple mixtures (dashed lines on Fig. 4.3), in that the overall degree of swelling achieved can be well-approximated by a weighted average of the degrees of swelling achieved in the two single-carbohydrate hydrogels. As such, hydrogels with high swelling (100CMC), high deswelling (100Dex), effectively zero swelling (50CMC/50Dex), or any intermediate swelling characteristic can easily be synthesized by simple mixing of different library carbohydrates. However, it should be emphasized that swelling in the 75CMC/25Dex hydrogel, while following the general trend, was not well-predicted by the rule of mixtures, suggesting that charge density-related swelling effects may complicate the predictive value of the rule of mixtures in this regard.

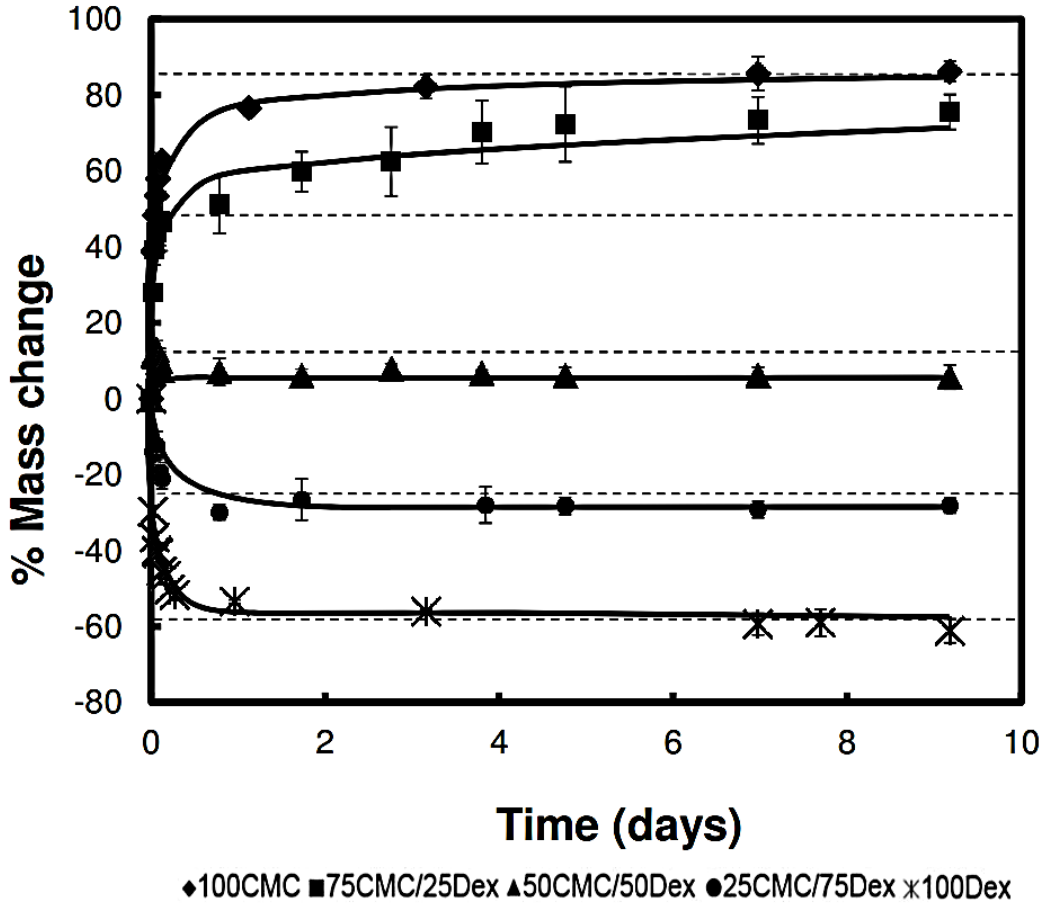

Figure 4.3. Modulating hydrogel swelling by varying CMC/dextran content in poly(NIPAM)- based hydrogels. Dashed lines depict predicted swelling from rule of simple mixtures for the different hydrogel systems.

By applying Flory-Huggins theory to the measured swelling results, the effective crosslink density of each of the hydrogels tested can be assessed. The result of applying Equation 2 to swelling data in the determination of network parameter *Nx*, along with corresponding pore size, is shown in Table 4.2.

Table 4.2. Flory-Huggins interaction constant (from group contribution theory), polymer mass fractions at equilibrium swelling (measured), average number of monomer units between crosslinks (from Flory-Huggins theory), and estimated pore size for modular injectable hydrogels prepared with poly(NIPAM)-hydrazide and mixtures ofoxCMC and oxDex.

Hydrogel	χ	ϕ_0	ϕ_E	N_x (avg.)	*Pore size (nm)*
100CMC	0.452	0.0494	0.0267	10.043	11.851
75CMC/25Dex	0.469	0.05	0.0303	8.057	10.337
50CMC/50Dex	0.531	0.0503	0.0479	4.877	6.759
25CMC/75Dex	0.776	0.05065	0.0673	3.519	5.239
100Dex	0.998	0.051	0.1275	1.319	1.556

Group contribution methods were used to predict the Flory-Huggins interaction parameter χ of each modular hydrogel; relative to the random-coil, theta condition (χ = 0.5) hydrogels that swelled when placed in PBS exhibited χ parameters below 0.5 (i.e. the solvent is of higher quality and the hydrogel expands) while hydrogels that deswelled in PBS exhibited χ parameters above 0.5 (i.e. the solvent is of lower quality and the hydrogel shrinks). This is consistent with the swelling data observed in Figure 4.2 for each of the modular hydrogels tested. The calculated N_x values also follow anticipated trends given the significantly lower degree of aldehyde functionalization in oxCMC (13 ± 3 %) relative to oxDex (37 ± 6 %). Note that the N_x value calculated represents an average between poly(NIPAM-co-ADH) (in which ~38% of the monomer units have a reactive crosslinking group) and the oxidized carbohydrates (in which each repeat unit may have two adjacent aldehyde groups), accounting for the low N_x values reported for 100Dex hydrogels that had a high aldehyde content. Based on these considerations, the lower limits of average N_x for 100CMC and 100Dex are 3.84 and 1.13, respectively if all

aldehyde groups (the limiting reagent for cross-link formation) are consumed. These results suggest that the overall crosslink content of the hydrogel may be controlled using the same modular approach by mixing reactive precursors with different degrees of aldehyde (or hydrazide) functionalization. Measurements of N_x performed at 25 °C (Supporting Information, Table 4.S1) show the lack of dependence of N_x on incubation temperature, demonstrating that gel parameters are determined by the properties of the precursors used in their fabrication.

Modular Hydrogel Thermoresponsiveness: Both the magnitude of swelling-deswelling transition as well as the reversibility of the thermal phase transition can be tuned based on the mixture of the reactive polymers used to prepare the hydrogel. Figure 4.4 shows swelling and deswelling responses of poly(NIPAM)/oxCMC/oxDex hydrogels with different oxCMC/oxDex ratios upon repeated thermal cycling above (37°C) and below (25°C) the lower critical solution temperature of poly(NIPAM) (32°C). Hydrogels prepared with 100% oxCMC exhibited essentially zero phase transition upon thermal cycling, with continuous swelling observed over time independent of temperature. As such, it is possible to "turn off" the ability of these hydrogel systems to undergo a reversible volume change by using a highly hygroscopic polymer to prepare the hydrogel. Alternately, hydrogels prepared with 100% oxDex exhibited a small but reversible phase transition. Interestingly, hydrogels with intermediate oxCMC:oxDex ratios (25CMC/75Dex) exhibit significantly higher reversible swelling/deswelling responses than hydrogels prepared only with oxDex despite the significantly higher hygroscopicity of the 25CMC/75Dex hydrogel. 25CMC/75Dex de-swells to a maximum of -29%

following incubation at 37 °C and re-swell by ~40 % after incubation at 25 °C for a minimum of one day; 100Dex under the same conditions showed a maximum de-swelling of -75 % when heated at 37 °C but re-swelled by only ~10 % on subsequent cooling (Fig. 4.4). These results are qualitatively similar to those acquired when 30 minute thermal cycles were conducted (see Supporting Information, Figure 4.S1), although the total magnitude of both deswelling and swelling (recovery) is significantly smaller given the shorter cycle times used. This observation can be rationalized based on the ability of the CMC component of the hydrogel to retain sufficient water inside the hydrogel phase such that fewer hydrogen bonds form between adjacent polymer chains in the collapsed state; as a result, water can more easily diffuse into the collapsed hydrogel and reversible swelling/deswelling transitions can be achieved (at least on the timescale of the experiment). As such, by combining different reactive precursors in a modular fashion, the hydrophilic/hydrophobic balance of the hydrogel can be optimized to yield thermoresponsive hydrogels that reversibly (or non-reversibly) swell and deswell to different degrees relative to their initial state.

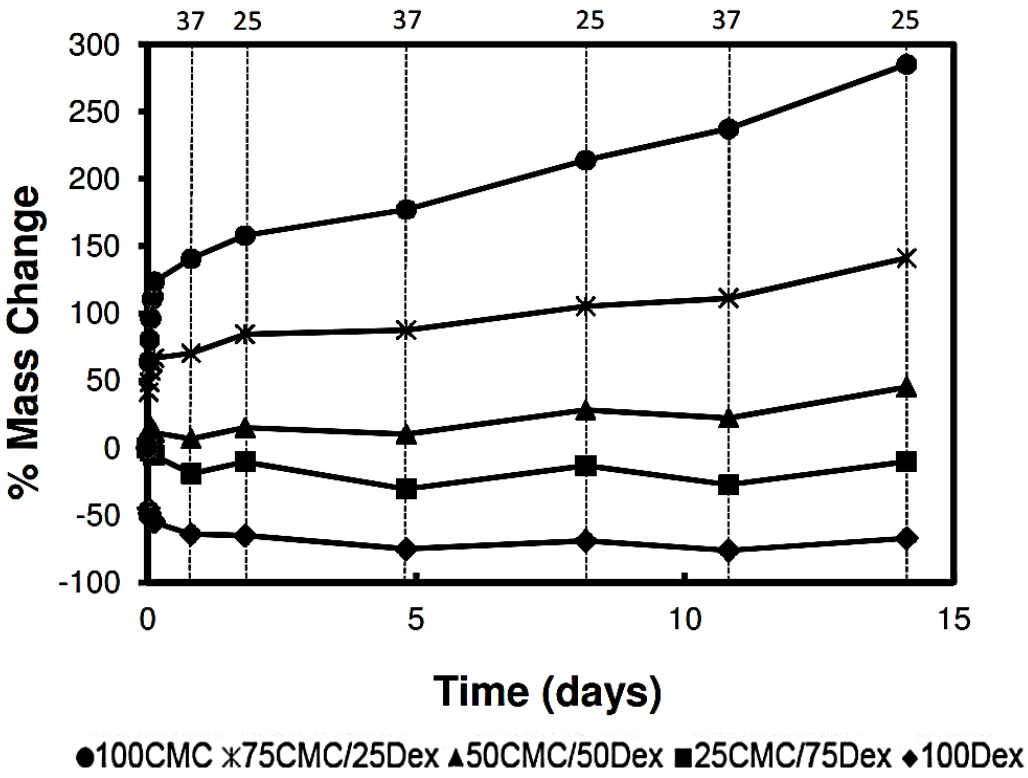

Figure 4.4. Variability in hydrogel thermosensitivity in poly(NIPAM)/oxCMC/oxDex hydrogels as a function of oxCMC and oxDex content. Vertical dashed lines indicate the incubation temperature (in Celsius) following the previous data point.

Incubation of the same hydrogels in 10mM pH 3 citrate buffer reduces the overall magnitude of hydrogel swelling observed in gels made with primarily oxCMC, which contains –COOH groups that are protonated at pH 3 but ionized at pH 7.4 in PBS; however, oxCMC-rich hydrogels still do not undergo a significant volume phase transition, even in the absence of charge-related swelling contributions (see Supporting Information, Figure 4.S2). In contrast, neither the overall swelling nor the thermoresponsive behavior of the 100Dex gel is significantly affected by pH (Figure 4.S2). The high overall degree of swelling and zero thermoresponsivity maintained in

oxCMC-rich hydrogels even in the protonated state is indicative of the significantly more hygroscopic character of CMC relative to dextran, consistent with χ parameter estimates in the protonated state[32]. Note that the excess aldehyde functionality of dextran used in these gels does not significantly affect the recovery of gel from its fully collapsed state. Dextran functionalized with approximately half of the total number of aldehyde groups (20 ± 3 mol%, within error of the degree of functionalization of the oxCMC used in this study) exhibits both swelling and thermosensitivity properties within <10% of the degrees of swelling observed with the 37 ± 6 mol% dextran reported herein, while oxCMC and oxDex-rich hydrogels exhibit a >300% difference in swelling as a function of overall composition (Figure 4.S3). Thus, the modular control over hydrogel properties is a driven primarily by composition of the precursor polymers rather than any differences in the number of functional reactive sites in the precursor polymers.

Modular Hydrogel Elasticity: By mixing precursor or reactive polymers with different degrees of functionalization and/or different hygroscopicities, the mechanical properties of the injectable hydrogels can be tuned in a modular fashion based on the reactive polymers selected. Figure 4.5 shows the change in *G'* (Fig. 4.5a) and the *G'/G"* ratio (Fig. 4.5b) as a function of oscillation frequency for hydrogels prepared by mixing poly(NIPAM)-hydrazide with different ratios of oxCMC and oxDex.

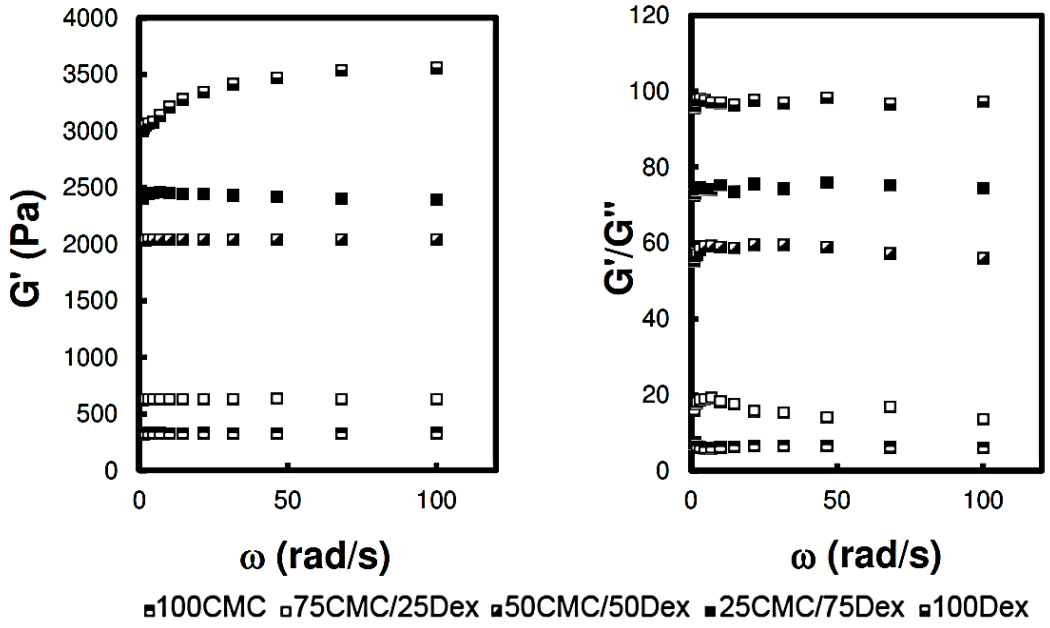

Figure 4.5. Modular rheology of poly(NIPAM)-hydrazide/oxDex/oxCMC injectable hydrogels (a) elastic modulus G' as a function of frequency; (b) G'/G" ratio as a function of frequency.

As the percentage of oxDex in the hydrogel increases, the G'_p value of the hydrogel increases (Fig. 4.5a) while the *G'/G"* ratio decreases (Fig. 4.5b). This behavior can be understood by the competing effects of water binding versus chemical crosslinking as the ratio between oxDex and oxCMC is changed. Hydrogels prepared with higher oxDex fractions have higher crosslink densities (as predicted both by Flory-Huggins theory (Table 4.2) and rubber elasticity theory (Table 4.3)) and thus exhibit both higher *G'* values and higher *G'/ G"* ratios indicative of the higher elasticities of such hydrogels. Table 4.3 also indicates that the extent of shear thinning that occurs as more stress is applied to the hydrogels increases with increasing oxCMC content (see Supporting Information, Figure 4.S4). This trend is consistent with both the lower cross-link density and higher degree of water structuring in oxCMC-rich hydrogels, facilitating improved

chain alignment and greater water structure disruption as higher shear rates are applied. In this way, by mixing different ratios of polymers with different cross-linking and water binding properties, hydrogels with higher or lower elasticities and shear thinning properties can be designed by simple mixing of different reactive components.

Table 4.3. Network parameters of poly(NIPAM)-hydrazide/oxDex/oxCMC hydrogels. Plateau moduli values represent the average and standard deviation of all G'data on the plateau for each hydrogel tested. The cross-link density is estimated based on rubber elasticity theory (Equation). The shear thinning ratio data represents ratio of the complex viscosity of the hydrogels changes between the highest frequency tested (100 rad/s) and the lowest frequency tested (0.1 rad/s).

Sample	Plateau modulus G'_p (Pa)	Cross-link density (x 10^{17} cm^{-3})	Shear thinning ratio (η^* (100 rad/s) / η^* (0.1 rad/s))
100CMC	335 ± 15	0.82 ± 0.04	7.4
75CMC/25Dex	665 ± 10	1.62 ± 0.02	3.7
50CMC/50Dex	2000 ± 20	4.86 ± 0.05	2.9
25CMC/75Dex	2435 ± 20	5.92 ± 0.05	2.5
100Dex	3210 ± 15	7.80 ± 0.04	2.2

Modular Hydrogel Degradation Kinetics: Hydrazone bonds can be cleaved via an acid catalyzed hydrolysis process dependent on the concentration of the acid catalyst and the accessibility of the catalyst to the hydrolysis site22. Figure 4.6 shows that the degradation kinetics of injectable hydrogels can be modulated by changing the composition of the reactive polymers used, while Table 4.4 reports the pseudo first-order rate constants for the degradation of modular hydrogels in varying concentrations of hydrochloric acid along with the time required to degrade half of the hydrazone bonds in the hydrogel (see Supporting Information, Figure 4.S5 for kinetic data at other acid concentrations).

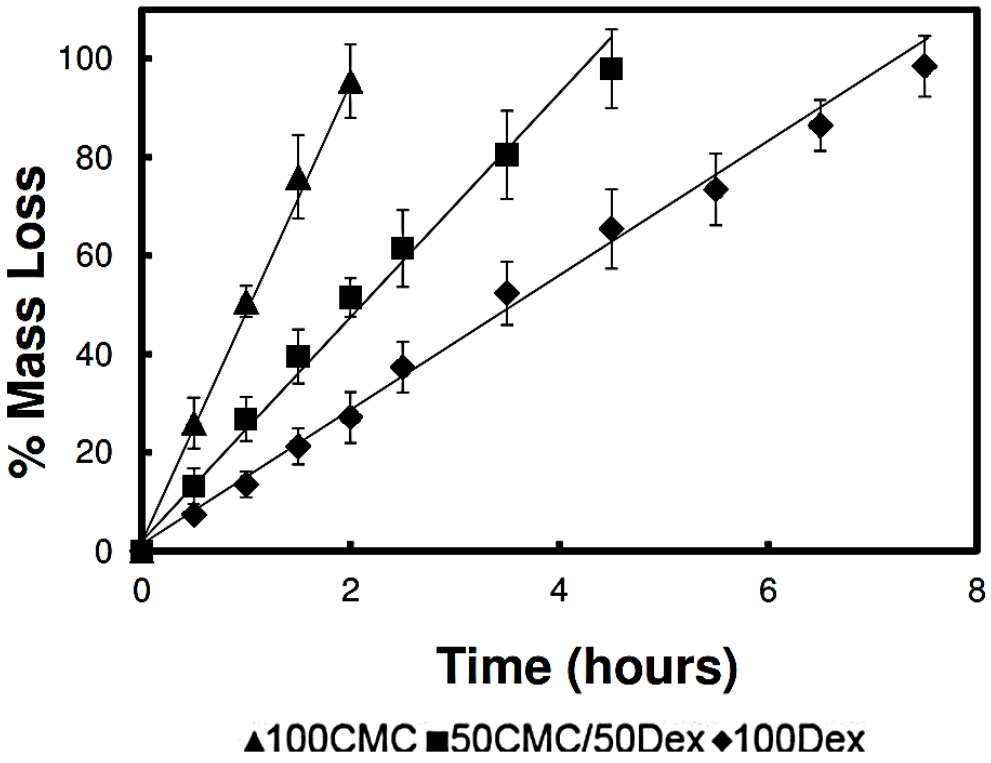

Figure 4.6. Percentage mass loss (via hydrolysis) for 100CMC, 50CMC/50Dex, and 100Dex hydrogels when exposed to 0.1 M HCl as a function of time.

Table 4.4. Degradation rate constants and half-lives of 100CMC, 50CMC/50Dex, and 100Dex hydrogels in various concentrations of hydrochloric acid.

Sample	0.1 M HCl		0.5 M HCl		1 M HCl	
	k' (s^{-1})	$t_{0.5}$ (hrs)	k' (s^{-1})	$t_{0.5}$ (hrs)	k' (s^{-1})	$t_{0.5}$ (hrs)
100CMC	0.83	1.02	1.37	0.74	1.62	0.47
50CMC/50Dex	0.36	2.16	1.04	1.03	1.39	0.55
100Dex	0.24	3.67	0.70	1.61	0.87	0.78

The degradation rate of the hydrogel increased (and thus the hydrolytic half-life of the hydrogel decreased) as the concentration of H^+ used for the hydrolysis was increased and ratio of oxCMC used to prepare the hydrogel was increased. The identified H^+ concentration dependence confirms that the acid-catalyzed hydrazone bond hydrolysis is

driving hydrogel degradation with all hydrogel compositions used. The increased hydrolysis rate in oxCMC-rich hydrogels can be correlated with the higher overall swelling observed in oxCMC-rich hydrogels, indicative of both a lower overall cross-link density (i.e. fewer bonds need to be cleaved to remove a single polymer chain from the hydrogel) and a higher mass transport rate of the proton catalyst into the hydrogel. The rate of enzymatic degradation can similarly be controlled by using a modular design approach by preparing hydrogels consisting of mixtures of enzymatically-degradable and non-degradable building blocks. As an example, enzymatic degradation studies of hydrogels prepared using oxCMC (100CMC) and oxHA (100HA) show that only the latter undergoes hydrolytic degradation, due to the substrate specificity of hyaluronidase for HA (Figure 4.7).

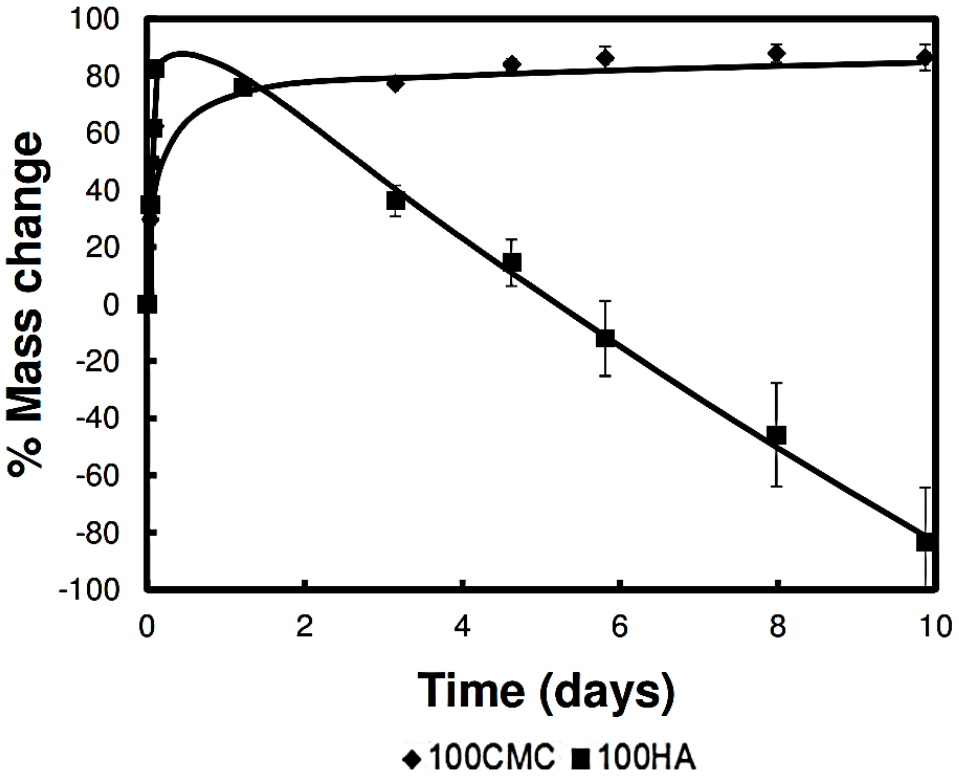

Figure 4.7. Mass change in 100CMC and 100HA hydrogels as a function of time in the presence of 0.1 mg/mL hyaluronidase in phosphate buffered saline (pH 7.4).

Of note, in the absence of hyaluronidase, both 100CMC and 100HA hydrogels exhibited similar swelling profiles as a function of time (Fig. 4.2); together, these results suggest that hydrogel swelling and hydrogel degradation can be independently tuned by varying the ratio of oxCMC and oxHA used to prepare the hydrogels.

Modular Drug Affinity: Given the cationic charge of bupivacaine at physiological pH, hydrogels rich in anionic oxCMC should exhibit higher affinity for bupivacaine given the potential for electrostatic interactions between the polymer and the drug. Indeed, Figure 4.8 indicates that the partition coefficient of bupivacaine into hydrogels with varying

oxCMC:oxDex ratios increases with increasing oxCMC content, consistent with an ionic uptake mechanism. When all drug-loaded hydrogels were subsequently immersed in fresh PBS, drug release followed a burst profile, with a rapid release of drug observed followed a plateau in the total drug content inside the hydrogel (raw drug release data available in Supporting Information, Figure 4.S6). Figure 4.8 shows that the magnitude of this burst can be modularly controlled depending on the constituent reactive polymers used to prepare the hydrogel.

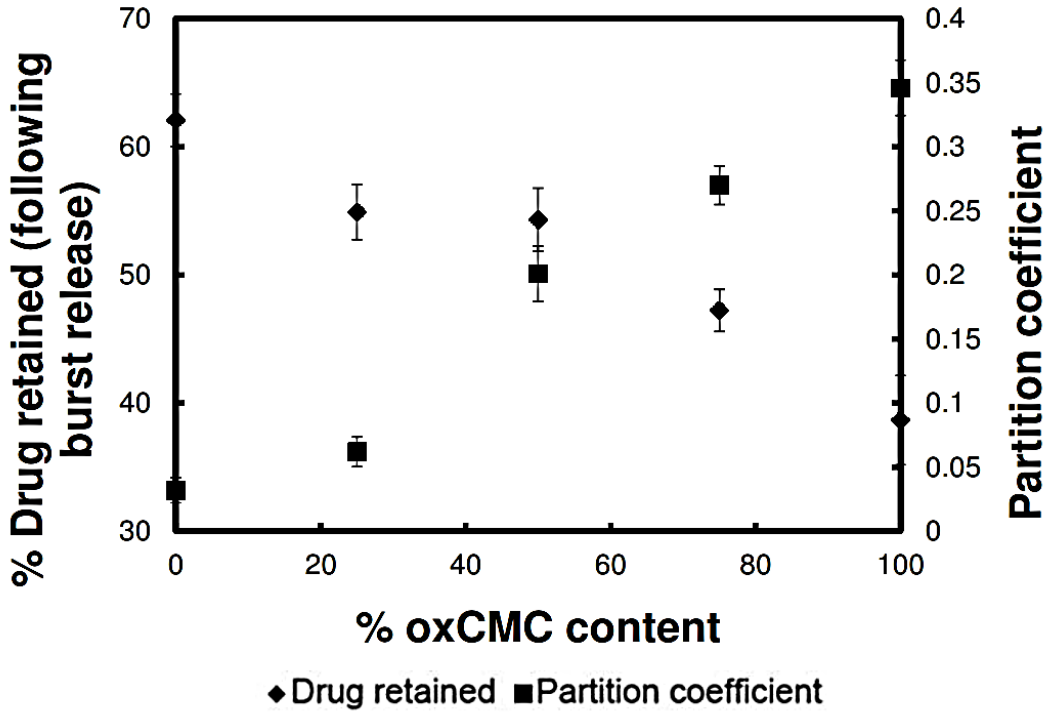

Figure 4.8. Bupivacaine retention in hydrogel after burst release and bupivacaine partition coefficient (hydrogel phase/PBS) for poly(NIPAM)-hydrazide/oxCMC/oxDex hydrogels with varying oxCMC/oxDex contents.

Drug entrapment inside the hydrogel may be promoted sterically via hydrogel deswelling (reducing the pore size and thus the diffusion coefficient inside the hydrogel) or

chemically based on the presence of affinity functional groups in the hydrogel matrix that will form ion pairs with the drug. The balance of physical versus chemical entrapment of bupivacaine in these modular hydrogel systems is reflected in the 100Dex hydrogel data. Despite the lower chemical affinity for bupivacaine in hydrogels prepared with higher oxDex contents, hydrogels containing higher ratios of oxDex:oxCMC retained more drug than hydrogels with higher oxCMC contents. Correspondingly, the calculated average pore size in this hydrogel is on the same order of magnitude as the molecular diameter of bupivacaine (~1-2nm, Table 4.2), suggesting physical entrapment may be an important contributor to drug retention behavior in this hydrogel. The competing steric and chemical effects are also evident in the drug retention data at intermediate oxCMC:oxDex ratios; both 50CMC/50Dex and 25CMC/75Dex hydrogels show the same level of drug entrapment, suggesting that the net drug retention effect represents a balance between both mechanisms of drug retention. Overall, these observations suggest that steric effects stemming from the large decrease in the free volume within the hydrogel matrix following hydrophobic collapse of the dextran-rich networks (Figure 4.3) primarily regulate drug retention in poly(NIPAM)/oxDex/oxCMC hydrogel systems that undergo large deswelling volume phase transitions while chemical affinity effects (i.e. drug-hydrogel interactions) primarily regulate drug retention in hydrogel systems that swell over time.

4. Discussion

In this study, we have demonstrated that injectable hydrogels with modular, mix-and match properties can be generated by mixing different numbers and/or ratios of a library of reactive synthetic oligomers (poly(NIPAM)) and carbohydrates (CMC, Dex, MeCe, and HA) functionalized with hydrazide and aldehyde groups respectively. Relative to conventional techniques for generating hydrogels based on mixtures of synthetic and natural polymers, this approach results in hydrogels that gel rapidly (in all cases <1 minute) by simple co-extrusion or mixing at room temperature, without requiring the application of an additional energy source (heating, UV irradiation), small molecule cross-linkers, or conjugation between the synthetic and natural polymer components prior to gelation. As such, this method is highly amenable to use in vivo, as covalently cross-linked, mechanically-robust hydrogels can be generated rapidly via a relatively non-invasive injection technique. Protein drug delivery may be a particular application of interest, as the protein would not be exposed to UV irradiation or heat and thus would be less likely to be denatured during the gelation process.

Swelling, rheology, thermoresponsivity, and degradation kinetics of hydrogels produced by mixing various reactive polymers together exhibit average properties in terms of hygroscopicity, cross-link density, and phase transition temperature. Indeed, mixing various ratios of oxCMC and oxDex together with poly(NIPAM) resulted in hydrogel swelling responses that could be predicted using the rule of mixtures. Other properties demonstrated consistent trends as a function of carbohydrate content, although the

changes observed were not always linear due to competing mechanisms (for example, the competing effects of water binding capacity versus cross-link density in determining rheological properties). Using this approach, by treating the precursor components as independent modules whose influence over the physical properties of the hydrogel may be considered additive, it is possible to fine-tune hydrogel properties to optimize hydrogel behavior for a range of potential applications. Of particular interest, this modular approach permits one hydrogel property to be tuned independently of another property in many cases; for example, 100CMC and 100HA hydrogels both swell to the same degree under physiological conditions but exhibit different degradation profiles in the presence of native enzymes (e.g. hyaluronidase).

The ability to precisely modulate hydrogel properties is attractive in a number of potential biomedical applications. In particular, precise control over hydrogel swelling in physiological fluids is frequently required for optimum hydrogel performance in vivo. In tissue engineering applications, it is frequently desirable to control the degree of cell spreading through customization of the gel's void space or to modulate the rate or molecular weight cut-off of nutrient diffusion into the hydrogel matrix and/or cellular waste out of the hydrogel matrix[35]. In other applications, the generation of zero-swelling hydrogels is essential; for example, in ophthalmic applications like vitreous humor substitutes or retinal drug delivery vehicles, hydrogel swelling may increase intraocular pressure analogously to glaucoma, potentially introducing a new clinical problem in the course of treating another problem. Control over hydrogel mechanics can also be essential for effective use of hydrogels in vivo. In the context of cell spreading, the rigidity of a

polymeric scaffold has been shown to influence the rate of cell migration through the scaffold[36]. In the particular context of spinal repair, the mechanical stiffness of hydrogels has been shown to play an important role in the extension of dorsal root ganglia within three dimension cell cultures[37]. In other applications such as synovial fluid replacement, the shear-thinning properties of the hydrogel are critical for effectively lubricating the joint while still promoting facile movement and sufficient mechanical support at rest.[38]

Similarly, hydrogels with the same physical properties but unique biological properties are frequently of interest. For example, hyaluronic acid is known to be a key extracellular matrix material in early wound healing, promoting cell spreading[39]. Since 100HA hydrogels swell to a similar degree to that of 100CMC hydrogels (Fig. 4.1), the synthesis of hydrogels using combinations of CMC and HA would result in hydrogels with the same swelling kinetics and thermodynamics but different cell responses. Similar tuning of cell adhesion or stem cell differentiation could be envisioned using the same approach; we will investigate the cellular responses to modular hydrogels in a future manuscript. In any of these cases, multiple target hydrogel properties may be predicted and controlled by mixing the right ratio and right types of library polymer "modules" together. In particular, given that hydrogels can be formed at ambient conditions by simple mixing of reactive polymers, this chemistry is highly amenable to high-throughput screening assays to combinatorially assess the cell responses to a variety of different hydrogel materials.

The demonstrated potential to independently tune hydrogel degradation (via control over hydrolysis and/or enzymatic cleavage), hydrogel pore size (via control over the cross-link density), and polymer-drug interactions (via control and the chemistry of the hydrogel)

also offers key potential advantages in drug delivery applications. In this respect, the same kinetic drug release profile could in theory be achieved in multiple ways by taking advantage of the multiple methods of drug release available (i.e. bulk hydrogel erosion, diffusion, and partitioning) available in these injectable modular hydrogel systems. As such, other selected properties of the hydrogel maybe simultaneously optimized with drug release kinetics by mixing different kinds or different ratios of reactive gel precursors.

5. Conclusions

We have demonstrated a facile approach for synthesizing "modular" hydrogels based on a desired mixture of synthetic or natural polymers via simple mixing of reactive polymer precursors, using hydrazide-aldehyde chemistry to generate rapidly in situ-gelling hydrogel systems. Provided that the precursors are miscible with each other, different numbers and/or ratios of reactive polymers may be mixed together to manipulate hydrogel swelling, thermosensitivity, degradation, or mechanics (in many cases independently of each other) as desired. Indeed, in many cases, changing the ratio of different precursor polymers used to generate the hydrogel affects gel properties in a manner that is approximately additive (relative to the precursor properties themselves) with respect to the relative concentrations of the precursor polymers used to form the polymer network. In this way, the physical, mechanical, and biological properties of the hydrogel can be tuned by simple mixing of different functional components. We anticipate that this method has particular promise to design highly customized hydrogels for targeted biomedical applications that could be screened in a high-throughput manner

without requiring the use of often toxic small molecule cross-linkers or thermal or UV initiation of gelation.

Acknowledgments: The assistance of Benjamin Greenlay and Robert Fuller is acknowledged for their help with material characterization. The Natural Science and Engineering Research Council of Canada (NSERC) and 20/20: NSERC Ophthalmic Materials Research Network is thanked for funding this work.

References

(1) Wang, S.; Zhang, Y.; Wang, H.; Yin, G.; Dong, Z. *Biomacromolecules* **2009**, *10*, 2240-4.

(2) Lee, K. Y.; Mooney, D. *J. Chem. Rev.* **2001**, *101*, 1869-1880.

(3) Fitzpatrick, S. D.; Jafar Mazumder, M. A.; Lasowski, F.; Fitzpatrick, L. E.; Sheardown, H. *Biomacromolecules* **2010**, *11*, 2261-7.

(4) Rosiak, J. M.; Yoshii, F. *Nuclear Instruments and Methods in Physics Research Section B: Beam Interactions with Materials and Atoms* **1999**, *151*, 56-64.

(5) Ito, T.; Yeo, Y.; Highley, C. B.; Bellas, E.; Kohane, D. S. *Biomaterials* **2007**, *28*, 3418-26.

(6) van der Linden, H. J.; Herber, S.; Olthuis, W.; Bergveld, P. *The Analyst* **2003**, *128*, 325-331.

(7) Valuev, I. L.; Vanchugova, L. V.; Valuev, L. I. *Polymer Science Series A* **2011**, *53*, 385-389.

(8) Hoare, T. R.; Kohane, D. S. *Polymer* **2008**, *49*, 1993-2007.

(9) Amsden, B. *Macromolecules* **1998**, *31*, 8382-8395.

(10) Joy, M. B.; Dodgson, K. S.; Olavesen, A. H.; Gacesa, P. *Biochim. Biophys. Acta* **1985**, *838*, 257-63.

(11) Ferreira, L.; Gil, M. H.; Cabrita, A. M. S.; Dordick, J. S. *Biomaterials* **2005**, *26*, 4707-16.

(12) Ehrenfreund-Kleinman, T.; Domb, A. J. .; Golenser, J. *Scaffolding In Tissue Engineering CRCnetBASE - Polysaccharide Scaffoldsfor Tissue Engineering*; Elisseeff, J., Ed.; CRC Press, **2006**; pp. 27-44.

(13) Shin, H.; Nichol, J. W.; Khademhosseini, A. *Acta Biomaterialia* **2011**, *7*, 106-14.

(14) Brannon-Peppas, L. *Chemical Engineering* **1991**, *46*, 715-722.

(15) Naddaf, A. A.; Tsibranska, I.; Bart, H. J. *Chemical Engineering and Processing: Process Intensification* **2010**, *49*, 581-588.

(16) Hoare, T.; Timko, B. P.; Santamaria, J.; Goya, G. F.; Irusta, S.; Lau, S.; Stefanescu, C. F.; Lin, D.; Langer, R.; Kohane, D. S. *ACS Nano Lett.* **2011**, *11*, 1395-400.

(17) Olsen, B. D.; Kornfield, J. A.; Tirrell, D. A. *Macromolecules* **2010**, *43*, 9094-9099.

(18) Hiemstra, C.; van der Aa, L. J.; Zhong, Z.; Dijkstra, P. J.; Feijen, J. *Macromolecules* **2007**, *40*, 1165-1173.

(19) Nishi, K. K.; Jayakrishnan, A. *Biomacromolecules* **2007**, *8*, 84-90.

(20) Bulpitt, P.; Aeschlimann, D. *J. Biomed Mat. Res.* **1999**, *47*, 152-69.

(21) Ifkovits, J. L.; Burdick, J. A. *Tissue Eng.* **2007**, *13*, 2369-85.

(22) Vetrík, M.; Prádný, M.; Hrubý, M.; Michálek, *J. Polymer Degradation and Stability* **2011**, *96*, 756-759.

(23) Nimmo, C. M.; Owen, S. C.; Shoichet, M. S. *Biomacromolecules* **2011**, *12*, 824-30.
(24) Baier Leach, J.; Bivens, K. A.; Patrick, C. W.; Schmidt, C. E. *Biotech. Bioeng.* **2003**, *82*, 578-89.
(25) Chen, J.; Yi, J.; Zhang, L. *Polymer* **2010**, *117*, 1631-1637.
(26) Schillemans, J. P.; Verheyen, E.; Barendregt,A.; Hennink, W. E.; Van Nostrum, C. F. *J. Controlled Release* **2011**, *150*, 266-71.
(27) Chang, C.; Duan, B.; Cai, J.; Zhang, L. *Eur. Polym. J.* **2010**, *46*, 92-100.
(28) Barbucci, R.; Magnani, A.; Consumi, M. *Macromolecules* **2000**, *33*, 7475-7480.
(29) Dinc, S. *Macromol. Chem. Phys.* **2002**, *203*, 1460-1465.
(30) Maia, J.; Ferreira, L.; Carvalho, R.; Ramos, M. A.; Gil, M. H. *Polymer* **2005**, *46*, 9604-9614.
(31) Flory, P. J. Principles of Polymer Chemistry; *Cornell University Press*, **1953**; p. 672.
(32) Hansen, C. M.; Beerbower, A. Solubility Parameters in Kirk-Othmer Encyclopedia of Chemical Technology, Suppl. *Interscience* **1971**, 889-910.
(33) Lawal, O. S.; Storz, J.; Storz, H.; Lohmann, D.; Lechner, D.; Kulicke, W. M. *Eur. Polym. J.* **2009**, *45*, 3399-3408.
(34) Dealy, J. M.; Larson, R. G. Structure and Rheology of Molten Polymers: From Structure to Flow Behavior and Back Again; *Hanser Verlag*, **2006**; pp. 152-158.
(35) Slaughter, B. V.; Khurshid, S. S.; Fisher, O.Z.; Khademhosseini, A.; Peppas, N. *Adv. Mat.* **2009**, *21*, 3307-29.
(36) Engler, A.; Sen, S.; Sweeney, H.; Discher, D. *Cell* **2006**, *126*, 667-689.
(37) Balgude, A. *Biomaterials* **2001**, *22*, 1077-1084.
(38) Barbucci, R.; Lamponi, S.; Borzacchiello, A.;Ambrosio, L.; Fini, M.; Torricelli, P.; Giardino, R. *Biomaterials* **2002**, *23*, 4503-13.
(39) Lei, Y.; Gojgini, S.; Lam, J.; Segura, T. *Biomaterials* **2011**, *32*, 39-47.

CHAPTER 4 - SUPPORTING INFORMATION

INJECTABLE, MIXED NATURAL-SYNTHETIC POLYMER HYDROGELS WITH MODULAR PROPERTIES

Authors: Mathew Patenaude and Todd Hoare

Publication Information: Biomacromolecules 13(2), 369-378

Accepted Date: 17 January 2012

Table 4.S1. Flory-Huggins interaction constant (from group contribution theory), polymer mass fractions at equilibrium swelling (measured), and average number of monomer units between crosslinks (from Flory-Huggins theory) for modular injectable hydrogels prepared with poly(NIPAM)-hydrazide and mixtures of oxCMC and oxDex. Parameters were determined based on swelling data at 25°C.

Hydrogel	χ	ϕ_0	ϕ_E	N_x (avg.)
100CMC	0.452	0.0494	0.0163	10.057
75CMC/25Dex	0.469	0.05	0.0253	8.074
50CMC/50Dex	0.531	0.0503	0.0431	4.884
25CMC/75Dex	0.776	0.05065	0.0482	3.537
100Dex	0.998	0.051	0.1011	1.339

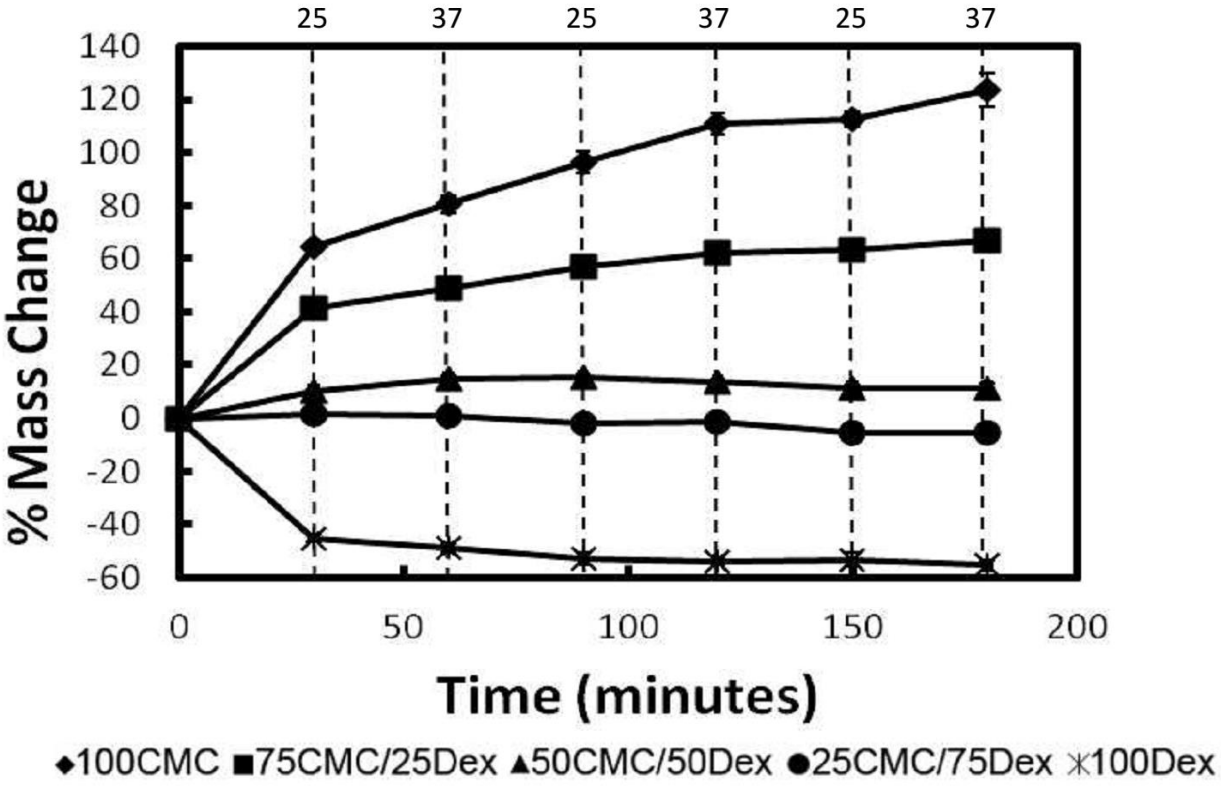

Figure 4.S1. Thermosensitivity of modular hydrogels under 30 minute heating (37°C)-cooling (25°C) cycles in PBS (pH 7.4). Vertical dashed lines indicate the incubation temperature following the previous data point.

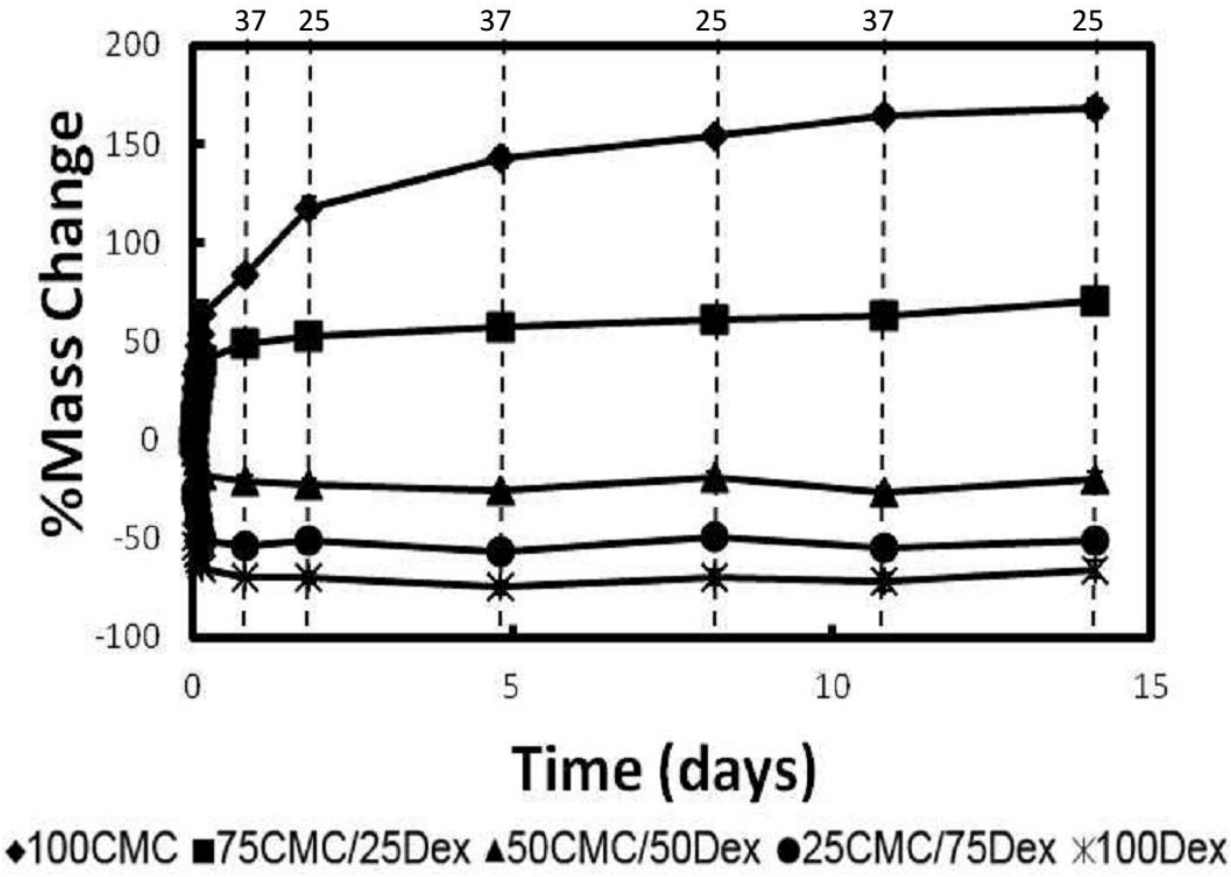

Figure 4.S2. Thermosensitivity of poly(NIPAM)/oxCMC/oxDex hydrogels as a function of oxCMC and oxDex content under multiple heating (37°C)-cooling(25°C) cycles in 10 mM pH 3 citrate buffer. Vertical dashed lines indicate the incubation temperature following the previous data point.

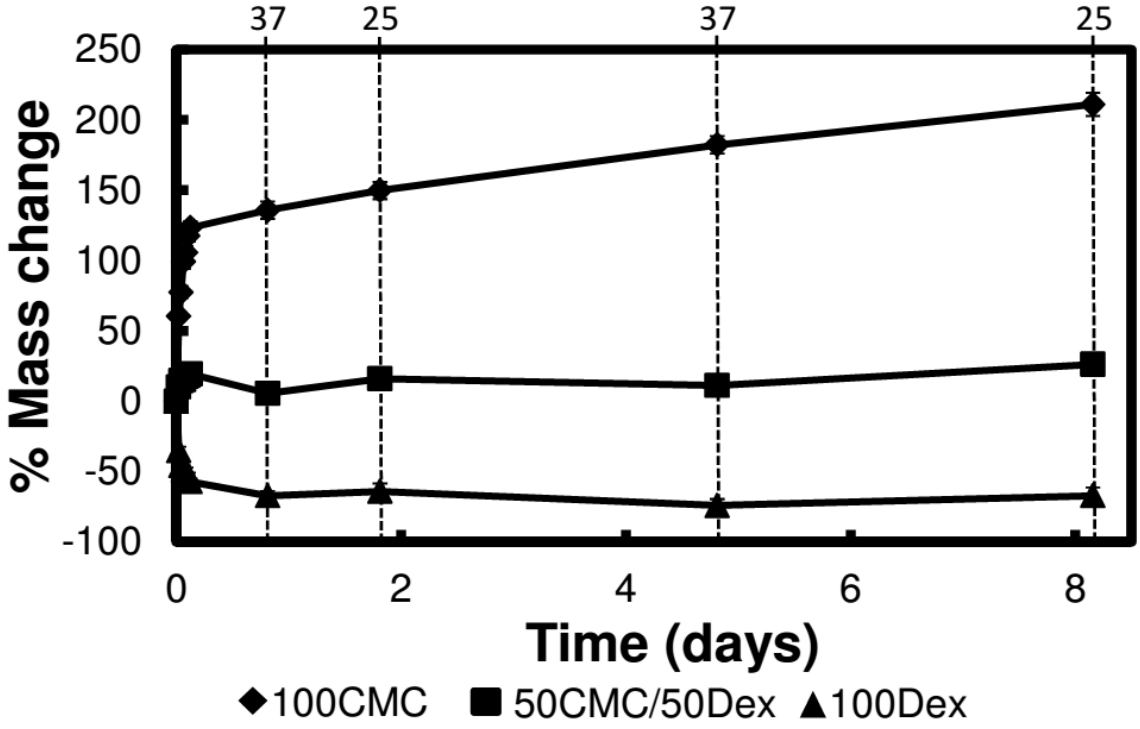

Figure 4.S3. Thermosensitivity of poly(NIPAM)/oxCMC/oxDex hydrogels as a function of oxCMC and oxDex content under multiple heating (37°C)-cooling(25°C) cycles in 10 mM pH 3 citrate buffer. Dextran used in the fabrication of these hydrogels possesses a 20 ± 3% degree of oxidation, resulting in oxDex possessing the same number of aldehyde groups (within experimental error) as oxCMC. Vertical dashed lines indicate the incubation temperature following the previous data point.

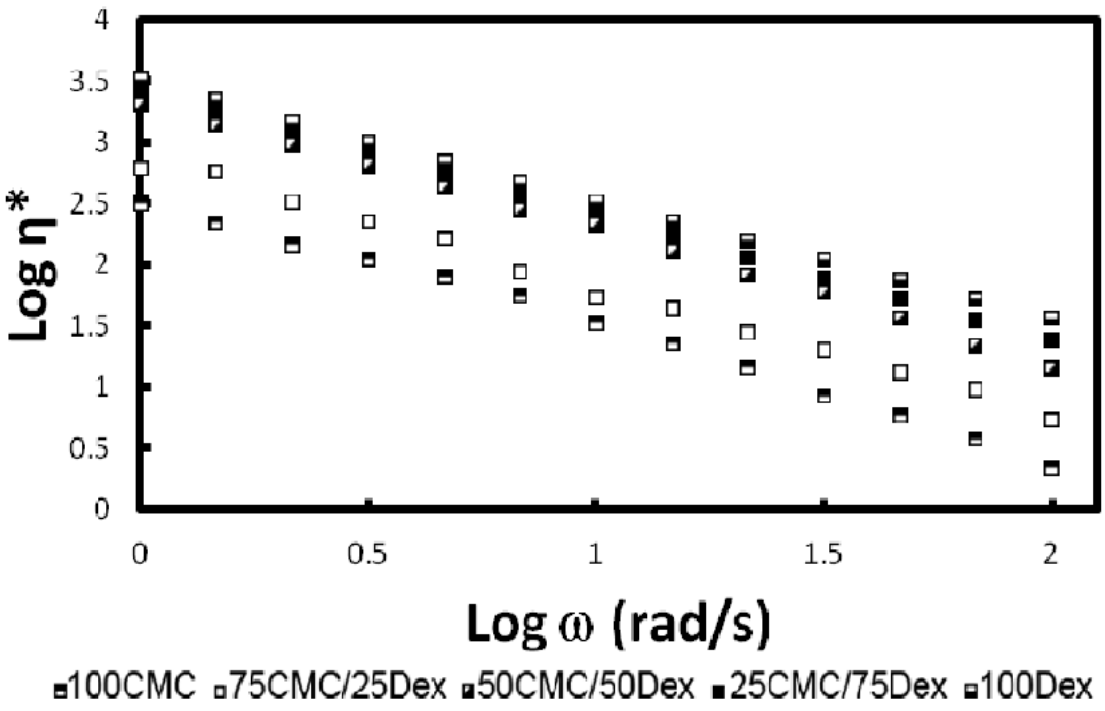

Figure 4.S4. Complex viscosity versus shear frequency for modular hydrogels.

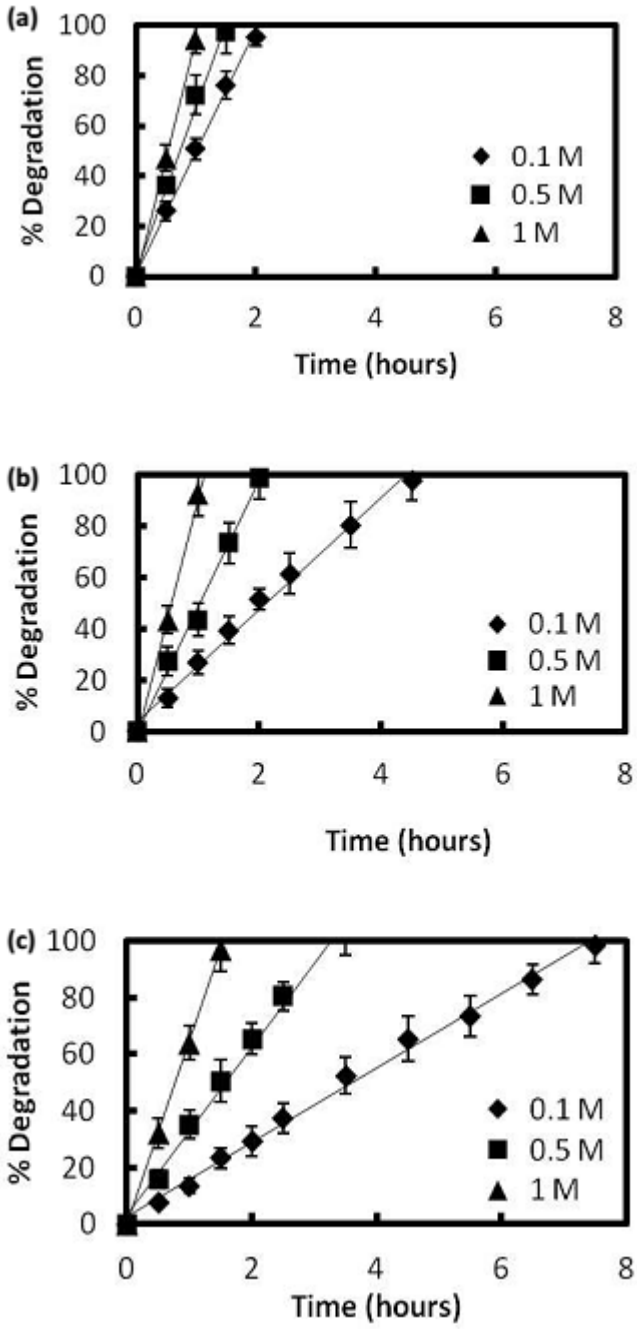

Figure 4.S5. Hydrolytic degradation of modular hydrogels (measured by mass loss in the hydrogel phase) in the presence of varying concentrations of hydrochloric acid: (a) 100CMC; (b) 50CMC/50Dex; (c) 100Dex.

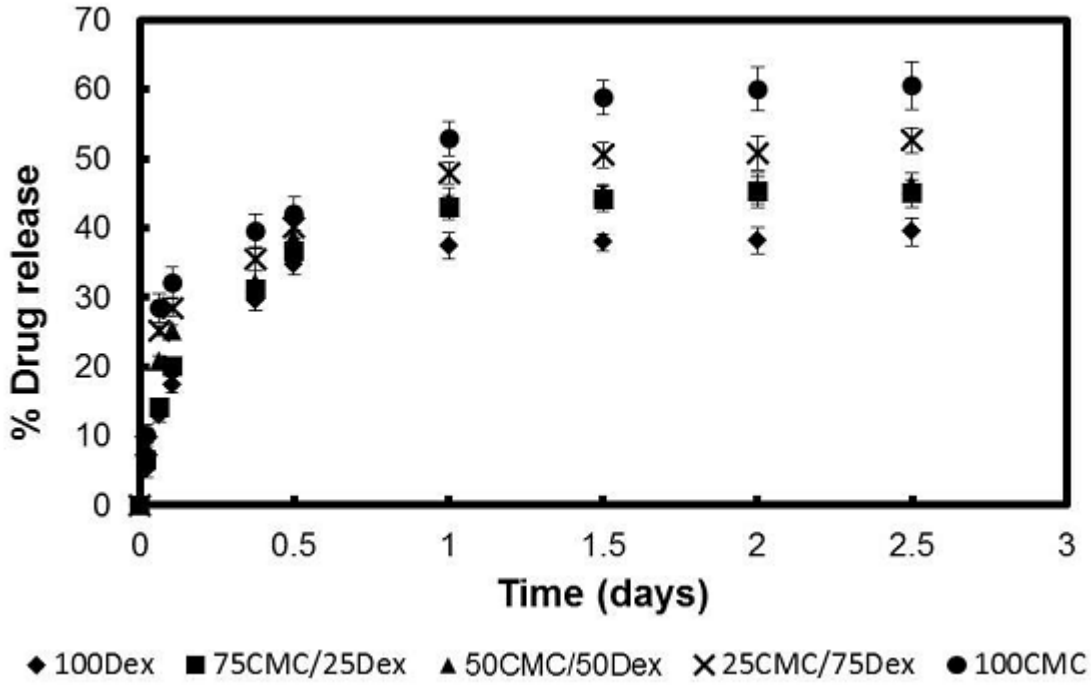

Figure 4.S6. Kinetic release profile of bupivacaine-HCl from hydrogels as a function of time and polysaccharide content. Data points for 75CMC/25Dexand 50CMC/50Dex overlap.

CHAPTER 5

INJECTABLE HYDROGELS WITH IN SITU-FORMING HYDROPHOBIC DOMAINS: OLIGO(DL-LACTIDE) MODIFIED POLY(OLIGOETHYLENE GLYCOL METHACRYLATE) HYDROGELS

Authors: Niels M.B. Smeets, Mathew Patenaude, Dennis Kinio, Francis Yavitt, Emilia Bakaic, Fei Chi Yang, Maikel Rheinstädter and Todd Hoare

Publication Information: Submitted to Journal of Polymer Chemistry

Submission Date: June, 2014

ABSTRACT

Injectable, *in situ*-gelling nanostructured hydrogels have been prepared from hydrazide and aldehyde-functionalized polymer precursors based on a copolymer of oligo(ethylene glycol) methacrylate (OEGMA) and an oligo(lactic acid) macromonomer (OLA) with varying lactic acid chain lengths. The resulting hydrogels contain a mix of chemical (hydrazone bond formation between hydrazide and aldehyde groups) and physical (hydrophobic interactions between OLA chains) cross-links which form competitively as a function of the OLA chain length and density. An increase in the OLA chain length and density results in the formation of more physical cross-links and fewer chemical cross-links. Tuning the relative prevalence of physical and chemical cross-link formation

facilitated largely independent tuning of gel mechanics relative to gel swelling and degradation. Small-angle neutron scattering of these OLA-containing hydrogels reveals a microstructure consisting of associative hydrophobic domains, based on an increased scattering intensity and decreased blob size relative to that observed for POEGMA hydrogels prepared without the OLA comonomer. The presence of hydrophobic OLA domains increases the uptake and slows the release of bovine serum albumin, a protein well-known to associate with hydrophobic domains. Coupled with the observed cytocompatibility of the reactive precursor polymers used to prepare the hydrogels, we anticipate significant potential applications of these hydrogels for the prolonged release of hydrophobic cargoes.

1. Introduction

Poly(ethylene glycol) (PEG) is a hydrophilic, non-immunogenic and non-cytotoxic polymer that has found wide-spread application in the design of biomaterials for e.g. controlled release of therapeutics and tissue regeneration.[1–4] The use of PEG is particularly attractive as this polymer significantly reduces protein adsorption and consequently cell adhesion, imparting "stealth" capability to mask any underlying biomaterial (e.g. nanoparticles,[5–7] core-shell micelles,[8,9] polymeric surfaces[10] or even hydrogels[1,11]) from the host's immune system.[5,12,13] From a controlled release perspective, PEG hydrogels have emerged as potential matrices for release of both small molecule and macromolecular therapeutics given these inherent advantages of PEG-based materials *in vivo*.[1,11] However, the use of PEG hydrogels in such applications has been limited by their high degree of swelling (and associated limited mechanical strength) and weak drug-hydrogel interactions that result in either fast drug release (in the case of hydrophilic drugs) or poor drug loading (in the case of hydrophobic drugs). Given that conventional PEG hydrogels are prepared from step-growth polymerization of α,ω functionalized PEG macromonomers that cross-link via chain ends,[14–30] chemical modification of the hydrogels to, for example, limit swelling or introduce drug affinity groups to enhance drug-hydrogel interactions is synthetically challenging, at least without sacrificing potential cross-linking sites within the hydrogel that can further exacerbate the challenge of controlling hydrogel swelling.[27,29] Most of the cross-linking reactions used also result in the formation of non-degradable

bonds, making clearance of the hydrogel following use problematic.[31] As such, while some successful examples of the use of PEG-based hydrogels for delivering proteins have been reported,[32–34] the full potential of using PEG-based materials for drug delivery has yet to be unlocked.

The weaknesses of PEG in terms of controlled release applications (i.e. degradability and poor bioavailability of hydrophobic therapeutics) can be addressed by combining PEG with hydrophobic, biocompatible, and bioresorbable polymers such as poly(lactic acid) (PLA), poly(glycolic acid), (PGA) or their copolymer poly(lactic acid-co-glycolic acid) (PLGA).[35,36] The design of nanoparticle drug delivery vehicles in particular has benefitted from this approach, wherein PEG-PLA or poly(oligoethylene glycol methacrylate)-PLA (POEGMA-PLA) block copolymers can be assembled into micelles or vesicles that can carry a hydrophobic payload in the hydrophobic PLA core while evading the host's immune system via the hydrophilic PEG corona.[37] This approach has also been extended to PEG hydrogels through the use of diacrylated PLA-*b*-PEG-*b*-PLA cross-linkers[38–44] and stereocomplexation between PEG-poly(L-lactic acid) (PEG-PLLA) and PEG-poly(D-lactic acid) (PEG-PDLA) block-copolymers.[45–48] Recently, Fan and co-workers combined both approaches, using stereocomplexed PLLA and PDLA macromonomers as cross-linkers for hydrogel synthesis.[49] As a result of their controllable physicochemical properties such as the hydrogel permeability, drug loading, and degradation rate,[39,41] PEG-PLA hydrogels have been investigated as matrices for controlled release[40,50] as well as temporary scaffolds for tissue engineering.[51] However, given that the hydrophobic PLA/PGA phase often serves as both the hydrophobic drug depot and the cross-linking site in such

hydrogels, independent tuning of cross-link density, drug affinity, and hydrogel degradation in such systems is inherently challenging.

Recently, we have reported the preparation of injectable, *in situ* covalently cross-linked POEGMA hydrogels that display all the desired biointerfacial properties of PEG (i.e. protein and cell repellency, non-toxicity, and minimal inflammatory responses *in vivo*).[52,53] Hydrogel formation occurs through the formation of dynamic covalent hydrazone bonds,[54,55] which allows for *in vivo* gelation as well as hydrolytic degradation and ultimate clearance of the POEGMA precursors.[52] Copolymerization of oligo(ethylene glycol methacrylate) monomers (OEGMA) of varying ethylene oxide side chain lengths (*n*) and/or (meth)acrylate monomers with various side chain functionalities allows for facile control over the lower-critical solution temperature (LCST)[56–58] as well as the functionality of the POEGMA precursors, giving access to POEGMA hydrogels with a broad range of physiochemical properties and drug affinities via simple free radical copolymerization.[52,53] While these injectable POEGMA hydrogels address many of the challenges associated with PEG hydrogels (degradability, independent control over swelling and mechanical properties, and facile polymer functionalization), hydrogels based on POEGMA have analogous swelling and interfacial properties to PEG hydrogels, making them unlikely candidates to address the issues of fast release of proteins or low uptake of hydrophobic drugs associated with PEG hydrogels.

Herein, we aim to improve the capacity of POEGMA hydrogels for drug delivery by functionalizing hydrogel precursor polymers with PLA via copolymerization of pre-synthesized oligo (D,L-lactide) macromonomers (OLA)[59] with OEGMA during the

polymer precursor synthesis (Scheme 5.1). Our approach differs from most found in the literature given that we do not explicitly use the OLA grafts for the purpose of cross-linking; instead, cross-linking is driven primarily by hydrazone bond formation between the hydrazide and aldehyde-functionalized polymer precursors. As such, the PLA residues will be (at least partially, within the context of the cross-linked network formed) free to self-assemble during gelation via hydrophobic association to form a nanostructured hydrogel with nanodomains governed by the mole fraction and side-chain length of the OLA co-monomers. The results show that the incorporated OLA co-monomers significantly alter the physiochemical properties (i.e. hydrogel swelling, mechanical strength and degradation) of the POEGMA hydrogels. Furthermore, loading and release of bovine serum albumin (BSA), a model protein which associates with hydrophobic domains,[60] showed a strong dependence on the mole fraction of PLA in the hydrogel, suggesting that functionalized poly(OEGMA-co-OLA) precursors may offer a versatile route towards the synthesis of injectable hydrogels with the potential for sustained release.

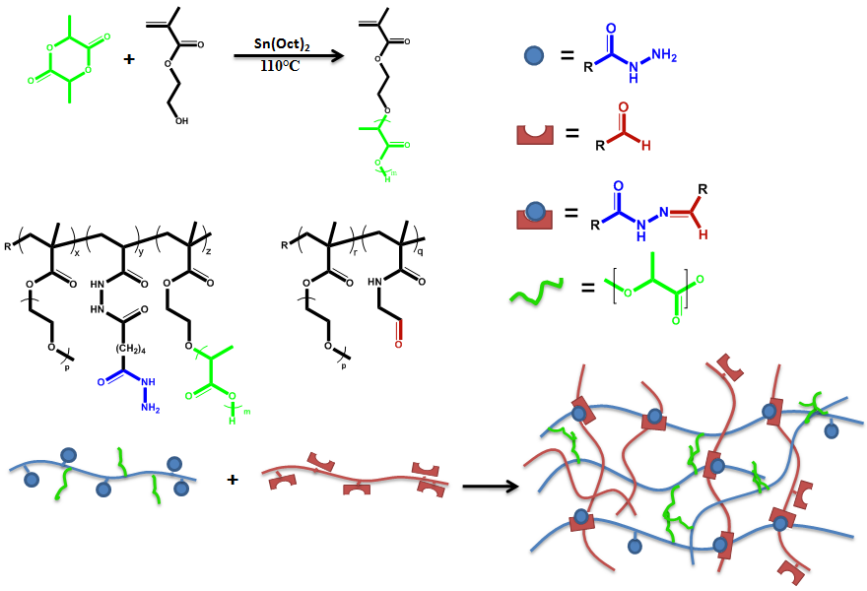

Scheme 5.1. Schematic representation of the synthesis of OLA macromonomers, POH-OLA and POA hydrogel precursors and hydrophobically-modified PO-OLA hydrogels

2. Experimental

Di(ethylene glycol) methyl ether methacrylate ($M(EO)_2MA$, Sigma Aldrich, 95%) and oligo(ethylene glycol) methyl ether methacrylate ($OEGMA_{475}$, Sigma Aldrich, 95%) were purified by passing each monomer through a column of basic aluminum oxide (Sigma Aldrich, type CG-20) to remove the methyl ether hydroquinone (MEHQ) and butylated hydroxytoluene (BHT) inhibitors. 2,2-azobisisobutryic acid dimethyl ester (AIBMe, Wako Chemicals, 98.5%), 2-hydroxyethyl methacrylate (HEMA, Sigma Aldrich, 99%) acrylic acid (AA, Sigma Aldrich, 99%), adipic acid dihydrazyde (ADH, Alfa Aesar, 98%), D,L-lactide (Sigma Aldrich), tin(II) 2-ethylhexanoate (Sigma Aldrich, 95%), 2-hydroxymethacrylate (Sigma Aldrich, >97%) (*N*'-ethyl-*N*-(3-dimethylaminopropyl)-carbodiimide (EDC, Sigma Aldrich, commercial grade) and thioglycolic acid (TGA, Sigma Aldrich, ≥99.8%) were used as received. *N*-(2,2-dimethoxyethyl)methacrylamide

(DMEMAm) was synthesized as reported previously.[52] For all experiments, Milli-Q grade distilled deionized water (DIW) was used. Dimethyl sulfoxide (DMSO, reagent grade) was purchased from Caledon Laboratory Chemicals (Georgetown, ON). Hydrochloric acid (1M) was received from LabChem Inc. (Pittsburgh, PA). 3T3 mouse cells were obtained from Cedarlane Laboratories (Burlington, ON). Cell proliferation and recovery media contents including Dulbecco's Modified Eagle Medium-high glucose (DMEM), fetal bovine serum (FBS), horse serum (HS), and penicillin streptomycin (PS) as well as trypsin-EDTA were purchased from Invitrogen Canada (Burlington, ON).

Table 5.1. Chemical synthesis of the POH-OLA hydrazide-functionalized polymers

	m [-]	$OEGMA_{475}$ [g]	OLA [g]	AA [μL]	AIBMe [mg]
POH	-	4.0	0.0	286	35
$POH\text{-}OLA_{4\text{-}10}$	4	2.5	0.37	181	35
$POH\text{-}OLA_{8\text{-}10}$	8	2.5	0.62	181	35
$POH\text{-}OLA_{8\text{-}20}$	8	2.0	1.20	171	35
$POH\text{-}OLA_{8\text{-}30}$	8	1.2	1.32	129	18
$POH\text{-}OLA_{16\text{-}10}$	16	2.5	1.12	181	35

Synthesis of oligo(DL-lactide) macromonomers (OLA): Synthesis of the OLA macromonomers with m = 4, 8 and 16 lactide repeat units was carried out according to the method of Ishikawa et al.[59] DL-lactide (m = 4: 5 g, 34.7 mmol; m = 8: 10 g, 69 mmol; m = 16: 20 g, 138 mmol) was placed in a 100 mL one-neck round bottom flask and dried overnight under vacuum. HEMA (2.1 mL, 17.3 mmol) and tin(II) 2-ethylhexanoate (32 μL, 0.1 μmol) were then added to the flask, and the mixture was deoxygenated by a repeated vacuum-nitrogen cycle. Subsequently, the reaction mixture was heated to 110 °C under vacuum for 3 hours with stirring. The crude product was dissolved in anhydrous chloroform

and washed with 1 M HCl. The organic phase was then washed with deionized water, isolated, and residual chloroform removed using a rotary evaporator operating under vacuum. Yield varied from 85-90% based on the added amount of DL-lactide. ^{1}H-NMR (600 MHz, $CDCl_3$, *m* = 8 monomer): δ = 1.38-1.63 ppm (24H, CH-$\underline{CH_3}$), δ = 1.94 ppm (3H, CH_2=C$\underline{CH_3}$), δ = 2.79 ppm (1H, OH), δ = 4.26-4.39 ppm (4H, O$\underline{CH_2}$-$\underline{CH_2}$), δ = 4.39-4.51 ppm (1H, $\underline{CH}$-(OH)CH_3), δ = 5.08-5.29 ppm (7H, C(=O)-$\underline{CH}$), δ = 5.58 ppm (1H, $\underline{CH_2}$=C), δ = 6.10 ppm (1H, $\underline{CH_2}$=C); longer macromonomers had similar peak positions but different integrations corresponding to their specific length.

Synthesis of hydrazide functionalized poly(oligoethylene glycol methacrylate-co-oligo DL-lactide) (POH-OLA): An extensive synthesis protocol for hydrazide-functionalized POEGMA polymers was reported previously.[52] Recipes for the hydrazide-functionalized polymers used in this work are given in Table 5.1 and identified via the code POH-OLAm-z where m is the theoretical number of lactide repeat units and z is the theoretical mole percentage of the OLA macromonomer incorporated into the polymer. As an example (Table 5.1, entry POH-OLA8-20), AIBMe (37 mg, 0.14 mmol), OEGMA475 (2.0 g, 4.2 mmol), OLA (m = 8, 1.2 g, 1.7 mmol) and AA (171 μL, 2.49 mmol, corresponding to ~30mol% in each hydrazide-functionalized copolymer) were all dissolved in dioxane (20 mL). Polymerization was continued for 4 hours at 75°C, after which the polymer was purified and isolated. Subsequently, the carboxylic acid groups of polymer were converted to hydrazide groups at high yield (~90-95%) via the carbodiimide-mediated conjugation of

a large excess of adipic acid dihydrazide. The functionalized polymers were purified by dialysis and lyophilized for storage.

Synthesis of poly(oligo ethylene glycol methacrylate-co-DMEMAm) (POA): An extensive synthesis protocol for aldehyde-functionalized POEGMA polymers was reported previously.52 Briefly, AIBMe (32 mg, 0.14 mmol), OEGMA475 (4.00 g, 8.4 mmol), DMEMAm (0.60 g, 3.5 mmol) and TGA (1.0 μL, 0.02 mmol) were dissolved in dioxane (20 mL) and polymerized at 75°C for 4 hours. Subsequently, the polymer was isolated by rotary evaporation and dissolved in 100 mL 0.5 M HCl for 24 hours to convert the acetals to the reactive aldehydes. The functionalized polymers were purified by dialysis and lyophilized for storage.

Chemical Characterization: Aqueous size exclusion chromatography (SEC) was performed using a Waters 515 HPLC pump, Waters 717 Plus autosampler, three Ultrahydrogel columns (30 cm × 7.8 mm i.d.; exclusion limits: 0–3 kDa, 0–50 kDa, 2–300 kDa) and a Waters 2414 refractive index detector. A mobile phase consisting of 0.3 M sodium nitrate and 0.05 M phosphate buffer (pH 7) at a flow rate of 0.8 mL/min was used for all polymers analyzed, and the system was calibrated with narrowly-dispersed poly(ethylene glycol) standards ranging from 106 to 584×103 g/mol (Waters). 1H-NMR was performed on a Bruker AVANCE 600 MHz spectrometer using deuterated chloroform as the solvent. The acrylic acid content of the polymers was determined using base-into-acid conductometric titration (ManTech Associates) using 50 mg of polymer dissolved in 50 mL of 1 mM NaCl as the analysis sample and 0.1 M NaOH as the titrant. Particle size

analysis and the determination of the critical association concentration were performed using a Brookhaven NanoBrook 90Plus particle size analyzer. Polymer solutions were measured as 150 mg/mL and 20 mg/mL solutions in PBS at 22°C using a disposable cuvette. Particle size data reported is based on the intensity average size distribution (n = 3). A Variant Cary Bio 100 UV-vis spectrophotometer was used to measure the LCST. The polymers were dissolved at a concentration of 1 mg/mL in PBS (pH = 7.4) and the absorbance of the polymer solution was recorded at a wavelength of 500 nm at every 0.5°C over a temperature range of 10°C to 80°C, with the temperature ramped at a rate of 1°C/min.

Critical association concentration (CAC): The critical association concentration (CAC) was determined by measuring the light scattering intensity as a function of the precursor concentration. Hydrazide functionalized precursor polymer (POH-OLA) solutions ranging from 5×10-5 mg/mL (~10-9 mM) to 20 mg/mL (~10-3 mM) in 10 mM PBS were prepared and measured at 22°C using a disposable cuvette. The scattering intensity, expressed as the count rate per second (kcps), was averaged over 3 individual measurements each consisting of 12 runs. The scattering intensity as a function of the precursor concentration is plotted as a log-log plot, where CAC is defined as the intersection of two best linear fits (R2 > 0.98) describing the count rate below and above the CAC. Error bars represent the cumulative error associated with slope and intercept fitting.

Hydrogel preparation: The different POEGMA hydrogels were prepared via co-extrusion of hydrazide-functionalized (POH-OLA) and aldehyde-functionalized (POA) precursors

dissolved in 10 mM PBS. Both polymer precursor solutions were intimately mixed upon injection using a double barrel syringe fitted with a static mixer at the outlet (Medmix Systems). Hydrogel disks for all in vitro testing were prepared by extrusion of the reactive polymer precursors through the double barrel syringe into cylindrical silicone rubber molds (diameter = 7 mm, volume = 300 μL) and incubated at room temperature for at least 12 hours to ensure complete gelation prior to further testing.

Table 5.2. Chemical analysis of the hydrogel precursors

	Functionality [-]	m^a [-]	OLA (Theo)[b] [mol%]	OLA(Exp)[c] [mol%]	Hydrazide or Aldehyde [mol%]	M_n[d] [10^3 g/mol]	$Đ$ [e] [-]	N_f [f] [-]	N_{OLA}[g] [-]	CAC.[h] [10^{-6} mM]
POH	Hydrazide	-	0	-	27.2	18.1	2.85	15	-	N/A
POH-OLA$_{4\text{-}10}$	Hydrazide	4.4	10	6.0	27.4	19.0	3.38	16	3	1.9 ± 0.3
POH-OLA$_{8\text{-}10}$	Hydrazide	8.5	10	6.4	27.8	16.6	3.42	12	3	7.2 ± 0.4
POH-OLA$_{8\text{-}20}$	Hydrazide	8.5	20	14.0	28.5	16.7	2.93	11	6	6.4 ± 0.5
POH-OLA$_{8\text{-}30}$	Hydrazide	8.5	30	30.0	28.1	16.3	2.41	11	12	5.5 ± 0.5
POH-OLA$_{16\text{-}10}$	Hydrazide	16.8	10	4.5	28.8	27.9	3.38	18	3	2.6 ± 0.2
POA	Aldehyde	-	-	-	28.1	19.6	2.74	12	-	N/A

[a] Average number of LA repeat units in OLA macromonomer as determined from ^{1}H-NMR, [b] Theoretical OLA mol fraction. [c] Experimental OLA mol fraction as determined from ^{1}H-NMR, [d] Number-average molecular weight as determined from aqueous SEC, [e] Dispersity, [f] Average number of hydrazide or aldehyde groups per chain [g] average number of OLA grafts per chain. [h] Critical association concentration (CAC) as estimated from dynamic light scattering.

Hydrogel swelling: The swelling kinetics were determined at 22°C and 37°C in 10 mM PBS at pH 7.4. The hydrogels were placed into cell culture inserts that are then placed in a 12-well cell culture plate and completely submerged with PBS (4 mL/well). Hydrogel swelling was monitored until equilibrium swelling was reached (generally ~30 hours) by weighing the hydrogels after gently wicking off any non-absorbed PBS. Subsequently, the hydrogels were resubmerged in a fresh 4 mL of PBS solution until the next data point was collected. Error bars represent the standard deviation of the replicate measurements (n = 4).

Degradation kinetics: The relative degradation kinetics of the different hydrogels were determined at 37°C in 50 mM HCl. The hydrogels were placed into cell culture inserts that were subsequently placed in a 12-well cell culture plate and completely submerged with the HCl solution (4 mL per well). Hydrogel degradation was monitored until the hydrogels had completely degraded by weighing the hydrogels after gently wicking off any non-absorbed PBS. Subsequently, the hydrogels were resubmerged in fresh 50 mM HCl solution (4 mL/well) until the next data point was collected. Error bars represent the standard deviation of the replicate measurements (n = 4).

Hydrogel rheology: The rheological properties of the hydrogels were measured using an ARES rheometer (TA Instruments) operating under parallel-plate geometry with a plate diameter of 7 mm and a plate spacing of 1 mm. Rheological properties were measured by first conducting a strain sweep from 0.1−100% strain at 1 Hz to identify the linear viscoelastic range of the hydrogels. A strain was then selected from the middle of this linear range and set as a constant to perform a frequency sweep from 1 to 100 rad/s to measure shear elastic (G′) and loss (G″) moduli. All measurements were conducted at 22 °C and in triplicate, with error bars representing the standard deviation of the replicate measurements (n = 3).

Small angle neutron scattering (SANS): SANS experiments were conducted using the 30 m SANS NG3 at the NIST Center for Neutron Research (NCNR), Gaithersburg, MD, USA. Sample-to-detector distances of 1 m, 4 m, and 13 m were used at neutron wavelengths of 6 Å. In addition, lenses were used at a wavelength of 8.4 Å for the 13 m distance. Prior to SANS experiments, precursor solutions were prepared at 150 mg/mL in 10 mM phosphate

buffered D_2O to facilitate scattering contrast. Hydrogels (~300 μL of hydrogel) were subsequently prepared using a double barrel syringe, directly into a demountable 4.32 × 3.49 × 2.16 cm3 sample cell with an internal gap thickness of 1 mm, requiring Polymers extruded into sample cells were left to completely gel for 12 hours prior to analysis. The low q range data was acquired by counting for 15 minutes using the 13 m detection distance followed by 20 minutes using the 13 m distance with lens. The medium q range was collected using a 4 m detection distance, counting for 5 minutes. The high q range was collected using a 1 m detection distance, counting for 2 minutes. The four ranges of data collected were merged using the NCNR's data reduction tool (DAVE).61 The individual scattering intensity (I(q)) plots (Eq. 1) were fitted using a sum of the Ornstein-Zernike function (Eg. 2) and the squared-Lorentzian (or Debye Bueche) function (Eq. 3), as reported previously for hydrogels,[62,63] to obtain estimates of the correlation length of the network (ξ) and the characteristic size of inhomogeneities (Ξ).

$$I(q) = \frac{\Delta\rho^2 RT\phi^2}{N_A M_{OS}}\left[\frac{I_{oz}(0)}{1+\xi^2 q^2} + \frac{I_{SL}(0)}{(1+\Xi^2 q^2)^2}\right] \quad (1)$$

$$I_{oz}(q) = \frac{I_{oz}(0)}{1+\xi^2 q^2} \quad (2)$$

$$I_{SL}(q) = \frac{I_{SL}(0)}{(1+\Xi^2 q^2)^2} \quad (3)$$

In Eq. 1-3, q is the scattering vector, I_{oz}(q) the scattering term from the Ornstein-Zernicke function, I_{SL}(q) the scattering term from the squared-Lorentzian function, $\Delta\rho^2$ the

scattering length density difference squared, φ the volume fraction of the solute, N_A Avogadro's number, R the universal gas constant, T the temperature and M_{OS} the osmotic modulus.

Protein Loading: Protein loading was determined by incubating hydrogels in a 500 μg/mL solution of FITC-BSA at 37 °C in 10 mM PBS (pH 7.4). The hydrogels were placed into cell culture inserts that were subsequently placed in a 12-well cell culture plate and completely submerged with the FITC-BSA solution (4 mL per well). These plates were then covered, placed in an incubator at 37 °C, and shaken for 48 hours in darkness. FITC-BSA drug loading was determined from the difference in fluorescence intensity between the loading solution (500 μg/mL) and the loading solution after 48 hours of incubation, using 495 nm and 519 nm as the excitation and emission wavelengths, respectively. Absorbances were subsequently converted to concentrations using a calibration curve prepared for FITC-BSA at known concentrations ($R^2 = 0.99$). Error bars represent the standard deviation of the replicate measurements (n = 4).

Protein release kinetics: Release kinetics were determined by incubating FITC-BSA-loaded hydrogels (described above) in 10 mM PBS at pH = 7.4 at 37°C (4 mL/well). These plates were incubated at 37 ºC in darkness and sampled at pre-determined intervals, with PBS replaced with fresh buffer following every sampling point to maintain infinite sink conditions during the full release time period. Release concentrations were monitored by fluorescence as described above for protein loading. Error bars represent the standard deviation of the replicate measurements ($n = 4$).

In vitro cytotoxicity: The cytocompatibility of polymer precursors and hydrogels was assessed using a MTT assay. NIH 3T3 fibroblasts were plated at density of 1.0×10^4 cells per well in a 24-well plate and maintained in DMEM media supplemented with 10% FBS and 1% penicillin. Polymer concentrations ranging from 200 to 2000 μg/mL were transferred into wells with cultured cells and incubated for 24 hours. Cell viability was then characterized using a modified MTT assay. The absorbance of the MTT solution was read using a Biorad microplate reader (model 550) at 570 nm and normalized against a 630 nm baseline to account for non-specific scattering. Error bars represent the standard deviation of the measured cell viability percentages (n = 4).

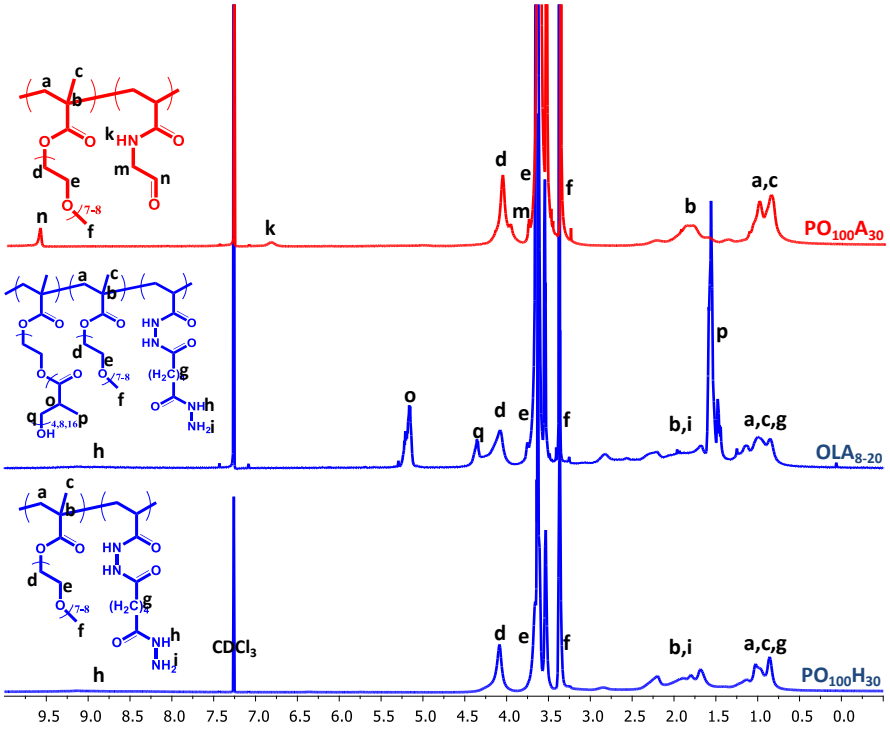

Fig. 5.1. ^{1}H-NMR (600 MHz) analysis on the hydrazide, aldehyde and oligo(D,L-lactide) functionalized poly(oligoethylene glycol methacrylate) in $CDCl_3$.

3. Results and Discussion

Synthesis of the OLA macromonomers and hydrogel precursors: Oligo(D,L-lactide) macromonomers (OLA_m) were prepared from the stanneous(II) octanoate ($Sn(Oct)_2$)-catalyzed ring opening polymerization (ROP) of D,L lactide (LA) initiated by 2-hydroxyethyl methacrylate (HEMA)[59] (Scheme 5.1). OLA macromonomers with LA chain lengths (*m*) of *m* = 4, 8 and 16 repeat units were targeted by changing the ratio of LA to HEMA. ^{1}H-NMR analysis shown in Table 5.2 confirms that the theoretical and experimental values for *m* are in good agreement, consistent with prior literature.[59]

The OLA macromonomers were copolymerized with oligo(ethylene glycol methacrylate) ($OEGMA_{475}$) and acrylic acid (AA), and the carboxyl groups of the polymer subsequently functionalized with adipic acid dihydrazide (ADH) using carbodiimide (EDC) coupling[52] to synthesize hydrazide-functionalized precursors (Scheme 5.1). The poly(oligoethylene glycol methacrylate-*co*-adipic acid dihydrazide-*co*-oligo(D,L-lactide) methacrylate) ($POH\text{-}OLA_{m\text{-}z}$) precursors are labelled according to their theoretical OLA chain length (*m* = 4, 8 and 16) and the theoretical mol fraction of OLA grafts in the precursor composition (*z* = 10, 20 and 30 mol%). Characteristic ^{1}H-NMR (600 MHz in $CDCl_3$) spectra for POH (= $PO_{100}H_{30}$ from our previous work[52]) and $POH\text{-}OLA_{8\text{-}20}$ are shown in Fig. 5.1, confirming the presence of both hydrazide (peak h, δ ~ 9.2 ppm, NH-N$\underline{H_2}$) and OLA (peak o, δ = 5.12-5.26 ppm, C(O)C$\underline{H}$(CH_3)O) groups in the functionalized copolymer.

The degree of OLA macromonomer incorporation varies depending on the OLA side chain length. For precursor polymers synthesized with *z* = 10 mol%, OLA_4 and OLA_8 incorporate to a higher extent than OLA_{16}. The increasing side chain length significantly increases the viscosity of the OLA macromonomer, inducing both diffusional and steric limitations on the copolymerization kinetics. All OLA functionalized precursors have number-average molecular weights (M_n) of ~20 $\times 10^3$ g/mol and relatively broad molecular weight distributions (MWDs) (Table 5.2). The relatively high values for the disperisity ($Đ$) can at least in part be attributed to the fact that size exclusion chromatography (SEC) is performed using linear poly(ethylene glycol) standards whereas the POH-OLA polymers are in reality dense brush co-polymers as a result of the long ethylene oxide and lactic acid side chains. The average number of OLA macromonomers incorporated per hydrogel precursor

polymer chain (N_{OLA}) was calculated from the OLA mole fraction measured via NMR and increases systematically from 3 (for 10 mol% OLA) to 6 (for 20 mol% OLA) to 12 (for 30 mol% OLA), largely independent of the OLA chain length (Table 5.1). Note that, although OLA_{16} copolymerizes less efficiently when compared to the other macromonomers, the lower degree of incorporation is off-set by the somewhat higher M_n of the POH-$OLA_{16\text{-}10}$ polymer. Similar to the POH precursor,[52] none of the POH-OLA precursors display a cloud point or lower-critical solution temperature (LCST) in 10 mM PBS up to 80°C, despite the contribution of the OLA residues to the hydrophilic-hydrophobic balance of the polymer. Each hydrazide functionalized precursor polymer contains approximately 30 mol% reactive groups, resulting in an approximately equal average number of hydrazide groups per polymer chain (N_f) of 14 ± 3 among all precursor polymers prepared (i.e. the number of potential reactive functional groups for cross-linking is approximately equal in each precursor polymer). An aldehyde functionalized poly(oligoethylene glycol methacrylate) precursor POA (= $PO_{100}A_{30}$ from our previous publications[52]) was synthesized via statistical copolymerization of $OEGMA_{475}$ and (*N*-(2,2-dimethoxyethyl)methacrylamide, DMEMAm) followed by acid catalyzed deprotection of the acetal[53] (Scheme 5.1). The degree of aldehyde functionalization was calculated based on the integrals of the signals at δ = 9.58 ppm (C<u>H</u>O) and δ = 3.36 ppm (O-C<u>H_3</u>) (Fig. 5.1).

To investigate the solution properties of the precursor polymers, solutions of the hydrazide (POH-$OLA_{m\text{-}z}$) and aldehyde (POA) functionalized precursors were prepared at concentrations of 150 mg/mL in 10 mM PBS (analogous to the pre-gel concentrations to be used). At this concentration, all OLA functionalized precursors yield opaque solutions,

which we attribute to aggregate formation driven by hydrophobic interactions between the OLA chains often used to drive macroscopic gelation via physical interactions. Self-association of OLA residues would lead to the formation of hydrophobic domains that could serve to (a) supplement the cross-link density of the hydrazone cross- linked hydrogels and (b) facilitate uptake and slow release of hydrophobic drugs or proteins from the hydrogel matrix.

The critical association concentration (CAC) was determined using dynamic light scattering, as previously reported for hydrophobically modified or amphiphilic block copolymers.[64] POH-OLA precursors yield a marked increase in the scattered light intensity as the precursor concentration is increased from 5×10^{-5} mg/mL (10^{-9} mM) to 20 mg/mL (10^{-3} mM) (Fig. 5.2). Conversely, the unmodified POH precursor shows only a marginal increase in the scattered light intensity over the same concentration range. The CACs of the POH-OLA precursors are all estimated to be range of $1\text{-}7\times10^{-6}$ mM, corresponding to 0.02-0.12 mg/mL (Fig. 5.2). Despite the differences between the POH-OLA precursors, no clear correlation between the CAC and m and N_{OLA} was observed, aside from a decrease in CAC as the mole fraction of PLA_8 in the copolymer is increased (Table 5.2). However, all precursor polymer solutions used for hydrogel formation (150 mg/mL) lie well above the CAC of all POH-OLA precursors, such that hydrophobic domain formation is expected to occur in parallel to covalent gelation of the hydrogels.

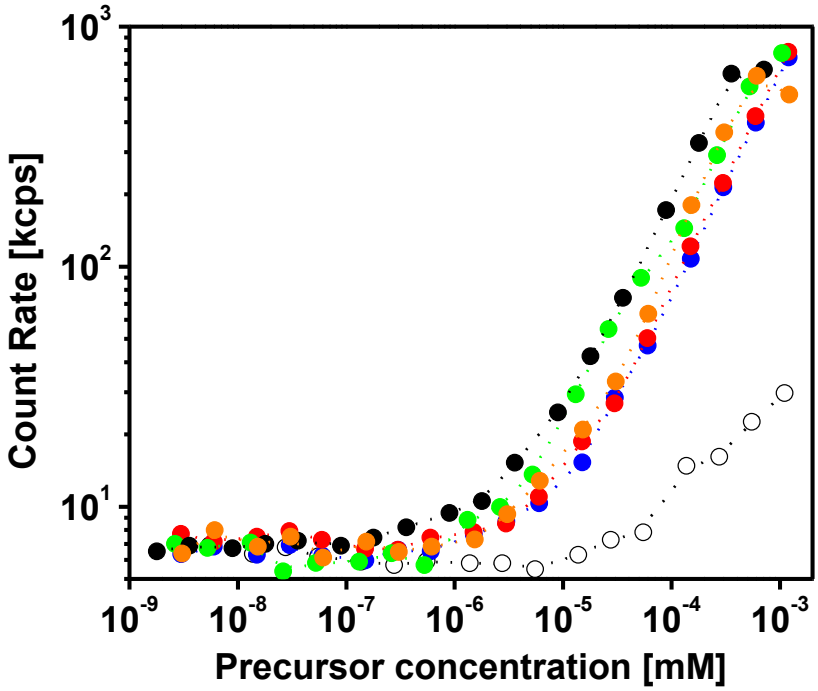

Fig. 5.2. Scattering intensity of POH-OLA polymers as a function of the polymer concentration in 10 mM as determined from dynamic light scattering. (○, white) POH, (●, blue) POH-OLA$_{8\text{-}10}$, (●, red) POH-OLA$_{8\text{-}20}$, (●, orange) POH-OLA$_{10\text{-}30}$, (●, green) POH-OLA$_{4\text{-}10}$ and (●, black POH-OLA$_{16\text{-}10}$.

Dynamic light scattering experiments on the undiluted precursor solutions (150 mg/mL) further confirmed the presence of large aggregates in the micron-size range; dilution of the precursor solutions to 20 mg/mL reduced the aggregate size to 100-500 nm but retained a high scattering intensity indicative of a high aggregate concentration. Interestingly, functionalizing the POH-OLA precursors up to 30 mol% OLA (m = 8) did not yield macroscopic hydrogels despite the physical aggregation of the precursor polymers observed via light scattering.

Hydrogel formation: Hydrazide functionalized POH-OLA and aldehyde functionalized POA precursor solutions (150 mg/mL, in 10 mM PBS) were co-extruded using a double-

barrel syringe to prepare hydrogels. For comparison, a POEGMA hydrogel without any OLA macromonomer was prepared by co-extruding POH and POA. PO-g-OLA hydrogels were successfully prepared for POH-OLA precursors containing up to 20 mol% OLA. PO-g-$OLA_{4\text{-}10}$ and PO-g-$OLA_{8\text{-}10}$ hydrogels required ~45 min to gel, similar to the unmodified PO hydrogel; PO-g-$OLA_{16,10}$ and PO-g-$OLA_{8\text{-}20}$ hydrogels gelled in 20 min and 1 h, respectively (see Table 5.3). In contrast, when POH-$OLA_{8\text{-}30}$ was used as the hydrazide-containing precursor polymer, no gelation whatsoever occurred up to 48 hours. This suggests that for a given *m*, macroscopic gelation becomes progressively slower and is eventually inhibited as the fraction of OLA in the precursor polymers increases, despite the increased hydrophobic associations present. We therefore hypothesize that covalent gelation of these precursor polymers can only occur if the precursor polymers have sufficient mobility following OLA-driven self-assembly to facilitate sufficiently high densities of hydrazone bond formation.

Physiochemical properties of the hydrogels: Hydrogel swelling kinetics were monitored by submerging the PO-OLA hydrogels in 10 mM PBS for 30 hours at 22°C and 37°C (Fig. 3). Similar to PEG hydrogels, the POEGMA hydrogel prepared without OLA quickly adsorbs water, reaching an equilibrium mass-based swelling ratio (Q_m) of 18.5±0.5 (at 22°C) and 16.1±0.0 (at 37°C) after 6 hours of incubation. In comparison, the OLA containing hydrogels swell considerably slower and reach significantly lower equilibrium Q_m values (Table 5.3). The lower degree of swelling when compared to the unmodified POEGMA hydrogel may be attributable to the higher hydrophobicity of the hydrogels containing OLA

grafts and/or physical cross-link formation within the hydrogel as a result of intermolecular OLA graft interactions. However, the magnitude of the swelling achieved in PO-OLA hydrogels is directly correlated to the overall weight fraction of OLA residues in the hydrogels; PO-OLA$_{4\text{-}10}$ and PO-OLA$_{8\text{-}10}$ hydrogels contain the lowest weight fraction of OLA (0.95 and 1.57 wt%, respectively, based on the initial hydrogel weight) and reach the lowest Q_m values after swelling for 30 hours while the PO-OLA$_{8\text{-}20}$ hydrogel (containing the highest OLA fraction of 3.24 wt%) swells to higher Q_m value. Since the overall hydrophobicity of hydrogels increases with the OLA content (*z*), this result can only be explained if the effective degree of intermolecular chemical cross-linking is lower in hydrogels prepared with higher OLA contents.

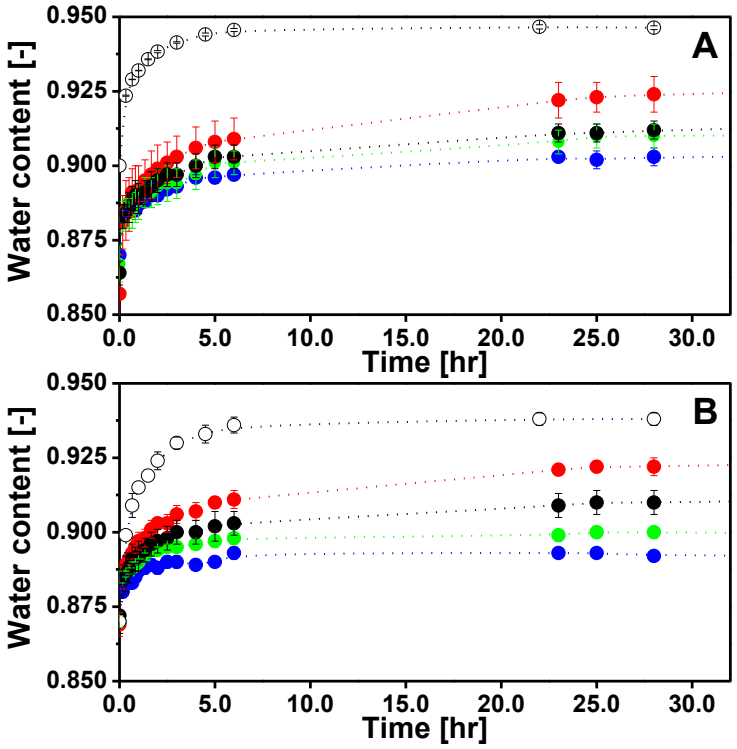

Fig. 5.3. Swelling kinetics of PO-OLA hydrogels in 10 mM PBS at 22°C (A) and 37°C (B). (○, white) PO, (●, blue) PO-OLA$_{8\text{-}10}$, (●, red) PO-OLA$_{8\text{-}20}$, (●, green) PO-OLA$_{4\text{-}10}$, (●, black) PO-OLA$_{16\text{-}10}$.

The dynamic hydrazone bond is reversible in aqueous media and in particular in the presence of acidic protons. Hydrogel degradation was evaluated in accelerated conditions in 50 mM HCl to provide comparative degradation profiles among the different hydrogels prepared (Fig. 5.4A). Note that both the hydrazone bonds as well as the PLA side-chains can degrade under these conditions, such that both chemical and physical cross-links are expected to be cleaved. The unmodified POEGMA hydrogel initially swells as hydrazone bonds are broken and the cross-link density of the hydrogel decreases. Subsequently, the normalized weight of the hydrogel gradually decreases as polymer chains erode from the bulk hydrogel, with complete degradation of the hydrogel reached within 150 min. With exception of the PO-$OLA_{8\text{-}20}$ hydrogel, all PO-OLA hydrogels show similar degradation behavior and degrade slower than the POEGMA hydrogel, requiring ~240 min to completely degrade (Fig. 5.4A). This result suggests that the chemical cross-link density for these hydrogels is similar and the variance in OLA graft chain length has little effect on the rate of degradation. For the PO-$OLA_{8\text{-}20}$ hydrogel, no initial swelling is observed and the hydrogel degrades rapidly, with complete degradation observed within 45 minutes. This result suggests that the hydrazone cross-link density in PO-$OLA_{8\text{-}20}$ is significantly lower than that in the other hydrogels despite the equivalent number of hydrazide reactive functional groups present within the hydrogel precursor solutions between all gels evaluated (Table 5.2).

The elastic storage modulus (G') and the average number of cross-links per unit volume of hydrogel (ν) were determined from rheological measurements (Fig. 5.4B and Table 5.3).

Compared to the unmodified POEGMA hydrogel, all PO-OLA hydrogels show higher *G*' values and, consequently, a higher average degree of cross-linking. Increasing the OLA weight fraction from 0 wt% to 3.24 wt% increases the plateau *G*' from 0.52 kPa to 3.37 kPa (Table 5.3). As the OLA graft chain length increases from $m = 4$ to $m = 8$, *G*' increases from 2.04±0.17 to 5.20±0.47 kPa due to stronger associations between the OLA grafts at higher *m*. Increasing *m* to 16 seems to have little effect on the absolute value of *G*'; however, it does alter the shear-dependent rheological behaviour of the gels (Fig. 5.4B). For example, the *G*' versus shear frequency profile of a hydrogel prepared with PO-$OLA_{16\text{-}10}$ (the longest OLA chain used in this work) shows a significant frequency dependence that is absent in gels prepared with shorter OLA chain length macromonomers or without any OLA macromonomers (Fig. 5.4B). Again, this result indicates that shear-dependent physical cross-links can form in addition to covalent cross-links in the PO-OLA hydrogels, with the number of repeat units in the OLA macromonomer determining the efficacy of intermolecular cross-linking (longer OLA chain lengths, affecting the rheology versus shear) versus intramolecular cross-linking (shorter OLA chain lengths, not impacting the rheology versus shear).

Table 5.3. Properties of the OLA-functionalized hydorgels (PO-OLA)

	m[a] [-]	OLA[b] [wt%]	t_{gel} [min]	Q_m (22°C)[c] [-]	Q_m (37°C)[d] [-]	*G*' [kPa]	v [e] [10^{17} cm^{-3}]
PO	-	0.0	46	18.5±0.5	16.1±0.0	0.52±0.01	1.28±0.02
PO-$OLA_{4\text{-}10}$	4	0.95	55	11.4±0.1	9.9±0.1	0.83±0.07	2.04±0.17
PO-$OLA_{8\text{-}10}$	8	1.57	40	10.4±0.5	9.3±0.2	2.35±0.13	5.79±0.32
PO-$OLA_{8\text{-}20}$	8	3.24	62	15.0±0.7	13.3±0.2	3.37±0.15	8.30±0.37
PO-$OLA_{16\text{-}10}$	16	1.72	23	12.2±0.2	11.1±0.2	2.11±0.19	5.20±0.47

[a] All hydrogels prepared by co-extruding 150 mg/mL precursor solutions in 10 mM PBS. [a] Theoretical OLA chain length, [b] OLA weight fraction in the hydrogels at 22°C, [d] volumetric swell ratio determined at 37°C, [c]

the average cross-link density.

From the results presented in Figs. 5.3 and 5.4, we can conclude that cross-linking in PO-OLA hydrogels is combination of two factors: (i) chemical cross-linking through the formation of hydrazone bonds and (ii) physical cross-linking between the hydrophobic OLA grafts. Furthermore, chemical and physical cross-linking in the PO-OLA hydrogels are competing cross-link mechanisms, as the loss of conformational mobility of the polymer chains upon OLA self-association restricts chemical cross-link density. This competing effect is best illustrated by PO-$OLA_{8\text{-}20}$, which swells to a higher Q_m (Table 5.3) and degrades significantly faster than the other hydrogels (Fig. 5.4A) (i.e. it has a lower covalent cross-link density) yet has the highest G' of any tested hydrogel (Fig. 5.4B) (i.e. it has a high physical cross-link density, owing to its highest total mole fraction of LA repeat units among all tested hydrogels as per Table 5.3). In this way, by exploiting competing cross-link formation mechanisms, hydrogel swelling (Q_m) and mechanical strength (G') can be decoupled, as the physical cross-links add to the mechanical strength but interfere with chemical cross-linking. Increasing the OLA graft density from $N_{OLA} = 3$ to $N_{OLA} = 6$ significantly enhances physical cross-linking and, correspondingly, lowers chemical cross-linking, while increasing the OLA chain length from $m = 4$ to $m = 16$ (at roughly equimolar concentrations) has a minimal effect on the chemical cross-link density (and thus the swelling and degradation kinetics) but increases the plateau modulus of the hydrogel, with longer grafts likely promoting both stronger hydrophobic associations as well as more intermolecular versus intramolecular interactions.

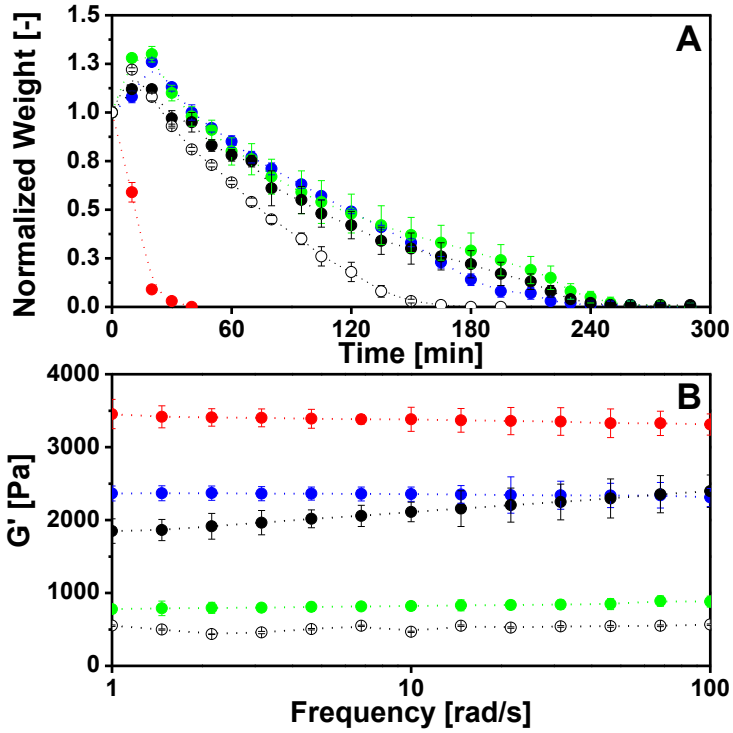

Fig. 5.4. Degradation kinetics in 50 mM HCl at 37°C (A) and elastic storage modulus (B) of PO-OLA hydrogels. (○, white) PO, (●, blue) PO-OLA$_{8\text{-}10}$, (●, red) PO-OLA$_{8\text{-}20}$, (●, green) PO-OLA$_{4\text{-}10}$, (●, black) PO-OLA$_{16\text{-}10}$.

Microstructure of the hydrogels: To support the hypotheses above regarding the effects of the dual chemical/physical cross-linking mechanisms in PO-OLA hydrogels on the hydrogel physicochemical properties, the internal morphologies of the hydrogels were probed. Analogous to the POH-OLA precursor solutions, the PO-OLA hydrogels are translucent and thus show signs of domain formation on a macroscopic scale (insets, Fig. 5.5). The small angle neutron scattering (SANS) intensity functions of the injectable PO-OLA hydrogels prepared at 150 mg/mL precursor concentration (polymer weight fraction of 0.13 w/w%) are shown in Figure 5.5. Comparing the scattering intensity (I(q)) results between the different PO-OLA hydrogels (Fig. 5.5A), structure formation occurs over two

different length scales. At the nanometer scale (~10^{-2} Å^{-1} to 10^{0} Å^{-1}), the functions display a broad shoulder; at the micrometer scale (~10^{-3} Å^{-1} to 10^{-2} Å^{-1}), the functions exhibit a power law scattering regime. Of note, the four PO-OLA hydrogels scatter significantly more at $q < 10^{-2}$ Å^{-1} when compared to the PO hydrogel. A similar increase in I(q) is observed for chemically cross-linked poly(acrylamide) (PAAm) hydrogels with increasing cross-link density.[65,66] Consequently, the increased scattering at $q < 10^{-2}$ Å^{-1} for the PO-OLA hydrogels suggests the presence of additional cross-linking, likely attributable to hydrophobic associations between the OLA side-chains. The hydrophobic associations add to concentration fluctuations which are 'frozen' into the hydrogel morphology upon random chemical cross-linking.[67] Concentration fluctuations are likely induced in these hydrogels by the presence of self-assembled polymer aggregates prior to co-extrusion that are subsequently immobilized into the hydrogel via covalent cross-linking. The progression in I(q) shows that there is no clear trend in I(q) as a function of the OLA graft content in the hydrogel, likely attributable to the competing effects of chemical and physical cross-linking in these hydrogels described earlier. Interestingly, the PO-OLA$_{4\text{-}10}$ and PO-OLA$_{8\text{-}20}$ hydrogel SANS functions show significant structural similarity at $q < 10^{-2}$ Å^{-1} despite indications from the physical gel property measurements that PO-g-OLA$_{4\text{-}10}$ is predominantly chemically cross-linked while physical cross-linking dominates in the PO-OLA$_{8\text{-}20}$ hydrogel. In comparison, the PO hydrogel that contains no OLA (and thus does not contain hydrophobic domains) scatters significantly less than any of the PO-OLA hydrogels and is thus more homogeneous, as expected.

Table 5.4. Structure properties of PO-OLA hydrogels as determined by SANS

	d [a] [Å]	ξ [b] [Å]	Ξ [c] [Å]
PO	110	20.0±0.3	905
PO-OLA$_{4\text{-}10}$	84	19.1±0.4	607
PO-OLA$_{8\text{-}10}$	120	25.7±0.4	531
PO-OLA$_{8\text{-}20}$	86	24.4±0.4	614
PO-OLA$_{16\text{-}10}$	175	36.8±0.5	598

[a] Average distance between scattering intensities (d = 2π/q), [b] Correlationl length of the network, [c] Characteristic size of network inhomogeneities.

The correlation length of the network increases with increasing OLA graft density from 20±0.3 Å for PO to 36.8±0.5 Å for PO-OLA$_{16\text{-}10}$. As the OLA graft density increases, hydrophobic associations between polymer chains promote intramolecular cross-linking that sterically inhibits intermolecular cross-linking and results in an increase in the correlation length of the network.[68] Correspondingly, the characteristic size of inhomogeneities decreases significantly upon the introduction of OLA grafts, from Ξ = 905 Å for PO to ~550-600 Å for the PO-OLA hydrogels. This trend is coupled with an observed decrease in the distance between inhomogeneities from d = 110 Å for the PO hydrogel to d ~85 Å for PO-OLA$_{8\text{-}20}$ and PO-OLA$_{4\text{-}10}$, indicating that the hydrophobic associations between the OLA grafts promote the formation of more and smaller domains. Interestingly, when a longer m = 16 graft length is used, the distance between inhomogeneities increases to d = 175 Å while the size of the inhomogeneities remains similar to the other PO-OLA hydrogels; this result suggests the presence of denser domains consistent with the formation stronger hydrophobic interactions. However, there is no clear trend in the size of inhomogeneities between the different PO-OLA hydrogels, likely due to the competing effects of chemical and physical cross-linking in these systems (i.e. hydrogels with higher

self-associations also have lower covalent cross-link densities).

The indirect evidence of macroscopic structure formation based on the optical appearance (insets Fig. 5.5), coupled with the SANS analysis (Fig. 5.5) further suggests the importance of hydrophobic aggregation in defining the microstructure of the PO-OLA hydrogels. Most SANS studies reported thus far on PEG hydrogels focus on chemically cross-linked PEG diacrylates[62] or physically cross-linked PLA-PEG-PLA triblock-copolymers.[69] The hydrogel system reported here combines chemical and physical cross-linking, with the physical cross-link density directly influencing the capacity of the polymers to form a covalently cross-linked network.

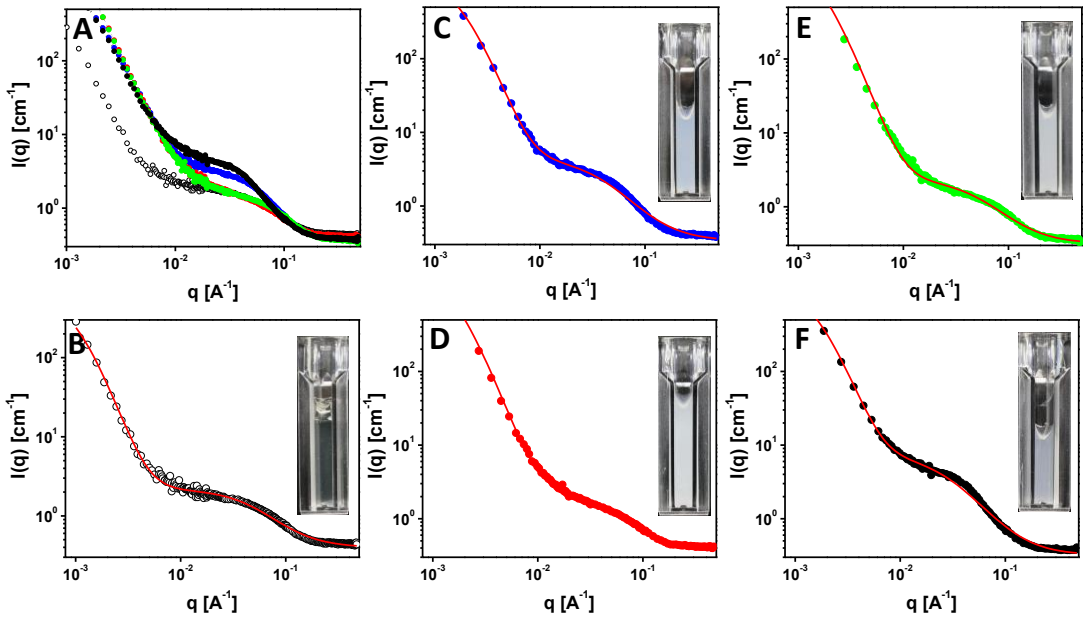

Fig. 5.5. (A) Small angle neutron scattering (SANS) scattering intensity as a function of the scattering vector (q) for (○, white) PO, (●, blue) PO-OLA$_{8\text{-}10}$, (●, red) PO-OLA$_{8\text{-}20}$, (●, green) PO-OLA$_{4\text{-}10}$, (●, black) PO-OLA$_{16\text{-}10}$. (B-F) The individual scattering functions (black points) and the fit obtained with the combined Ornstein-Zernike and squared Lorentzian functions (red line) for PO (B), PO-OLA$_{8\text{-}10}$ (C), PO-OLA$_{8\text{-}20}$ (D), PO-OLA$_{4\text{-}10}$ (E) and PO-OLA$_{16\text{-}10}$ (F). Insets show the optical appearance of the PO-OLA hydrogels prepared at 150 mg/mL in PBS.

Drug loading and release: To demonstrate the potential of the PO-OLA hydrogels as injectable hydrogels containing hydrophobic domains for applications in drug delivery, the loading efficiency (Fig. 5.6) and release kinetics (Fig. 5.7) of a model protein were determined *in vitro*. Bovine serum albumin (BSA) was chosen as the model protein as it is a moderate molecular weight protein (67 kDa) that is well-known to associate with hydrophobic domains.[70,71]

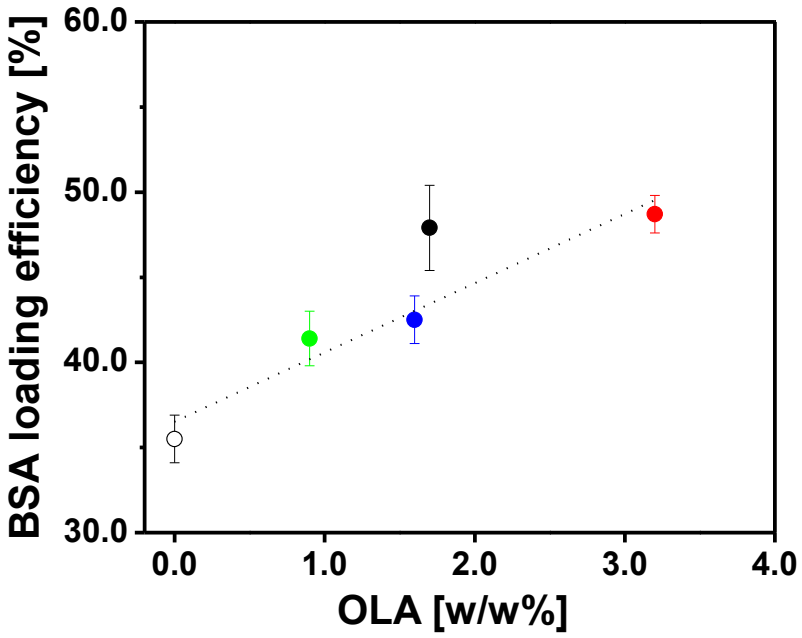

Fig. 5.6. Bovine serum albumin (BSA) loading efficiency of PO-OLA hydrogels. (○, white) PO, (●, blue) PO-OLA$_{8\text{-}10}$, (●, red) PO-OLA$_{8\text{-}20}$, (●, green) PO-OLA$_{4\text{-}10}$, (●, black) PO-OLA$_{16\text{-}10}$.

BSA partitioning experiments were performed to quantify the affinity of each hydrogel matrix for BSA (Fig. 5.6). Hydrogels were incubated in a 500 μg/mL BSA solution prepared in 10 mM PBS at 37°C for 48 hours. The unmodified PO hydrogel shows the lowest affinity for BSA, with 35.5±1.4% of added BSA loaded into the gel phase. The presence of OLA grafts significantly improves the loading efficiency, with the degree of drug uptake increasing linearly with the weight fraction of lactic acid repeat units in the for hydrogels prepared with $m = 4$ and $m = 8$ ($R^2 = 0.979$ for the fit shown in Fig. 5.6, excluding the black data point for PO-OLA$_{16\text{-}10}$). The loading efficiency of PO-OLA$_{16\text{-}10}$, however, is significantly higher than what would be expected based on the weight fraction of OLA in the hydrogel, suggesting that the long OLA chains (m = 16) form more hydrophobic

domains than the shorter (m = 4 and 8) hydrophobic domains (consistent with the SANS data indicating the presence of more compact inhomogeneities with this hydrogel).

BSA release from the loaded PO-OLA hydrogels was subsequently evaluated *in vitro,* with the results shown in Fig. 5.7. While release is shown only for the first 48 hours for clarity, the plateau values achieved persisted up to 3 weeks of incubation. The unmodified PO hydrogel shows a quick burst release and releases 99% of the loaded amount of BSA in the first 3 hours of incubation. This result is consistent with drug loading experiments that showed that these hydrogels have the lowest affinity for the protein (Figure 5.7) as well as the largest degree of swelling (Fig. 5.3), resulting in a gel matrix with a large mesh size (rapid diffusion) and minimal protein affinity; this is comparable to conventional PEG hydrogels.[11,72] In comparison, when OLA is incorporated into the hydrogel, a significantly slower burst release is observed over the first 3 hours of incubation and sustained release is achieved following the initial burst, plateauing only after ~120 hours (Fig. 5.7). The magnitude of burst release decreases as the amount of OLA in the hydrogel is increased; as the total weight fraction of OLA was increased from 0.95 wt% (PO-OLA$_{4\text{-}10}$) to 3.24 wt% (PO-OLA$_{8\text{-}20}$), the burst release over the first 3 hours was decreased from 73.6 ± 2.4% to 34.6 ± 4.5%. The relative release kinetics are also influenced by the length of the OLA macromonomer, with release rates increasing in the order m = 4 > m = 8 > m = 16 for a fixed mole fraction of OLA macromonomer (z = 10 mol%). This latter result is consistent with the protein uptake experiments in that the higher affinity hydrogels release protein more slowly. It should also be emphasized that the relative release kinetics cannot be explained solely by swelling differences between the hydrogels; for example, the PO-

$OLA_{8\text{-}20}$ hydrogel swells the most at 37°C among the PO-OLA hydrogels (Fig. 5.3) but shows the slowest drug release kinetics (Fig. 5.7). Therefore, the difference in release kinetics is primarily attributable to the enhancement in protein-hydrogel interactions due to the presence of hydrophobic OLA side-chains. It is expected that further functionalization of the hydrazide precursor or an increase in the precursor concentration can further improve the drug release kinetics, ultimately aiming towards a minimal burst release followed by long-term sustained release. Furthermore, as neither the POH nor any of the POH-OLA precursors are cytotoxic up to a concentration of 2000 μg/mL (as determined from a MTT assay on 3T3 mouse fibroblasts, Fig. 5.8) and the hydrogels are completely degradable (Fig. 5.4A), these injectable hydrogels offer significant potential for *in vivo* drug release applications.

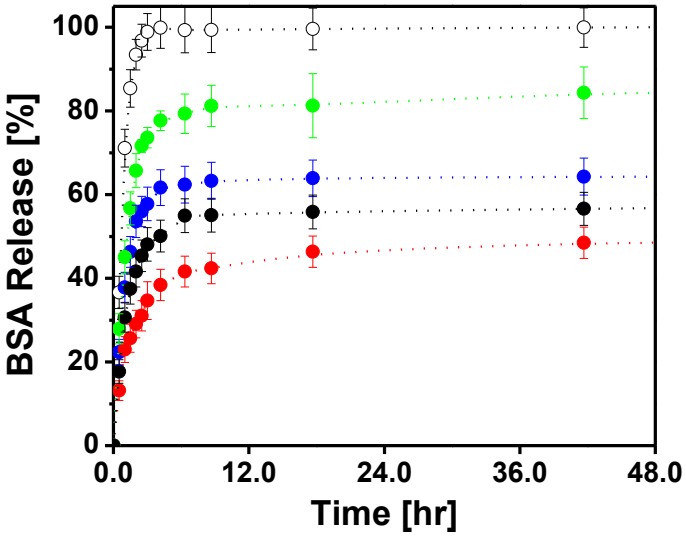

Fig. 5.7. Cumulative bovine serum albumin (BSA) release over the first 2 days for PO-OLA hydrogels. (○, white) PO, (●, blue) PO-OLA$_{8\text{-}10}$, (●, red) PO-OLA$_{8\text{-}20}$, (●, green) PO-OLA$_{4\text{-}10}$, (●, black) PO-OLA$_{16\text{-}10}$.

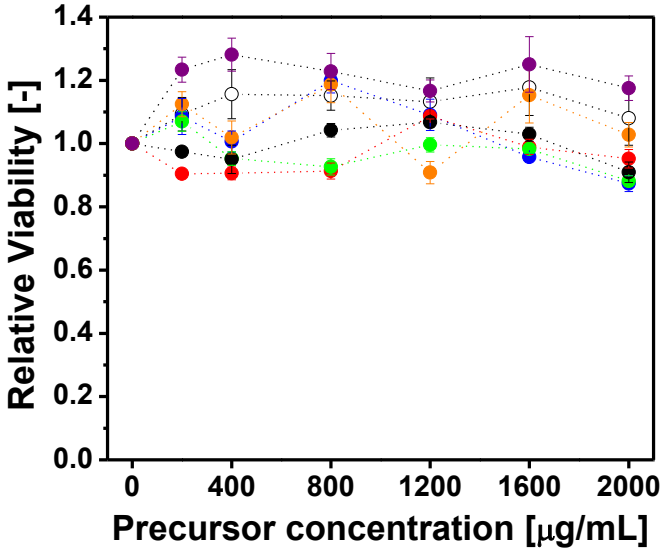

Fig. 5.8. Cytotoxicity of the polymer precursors and degradation products via MTT assay on 3T3 mouse fibroblasts. (○, white) POH, (●, purple) POA, (●, blue) POH-OLA$_{8\text{-}10}$, (●, red) POH-OLA$_{8\text{-}20}$, (●, orange) POH-OLA$_{10\text{-}30}$, (●, green) POH-OLA$_{4\text{-}10}$ and (●, black) POH-OLA$_{16\text{-}10}$.

4. Conclusions

Oligo(lactic acid) macromonomers have been successfully incorporated into hydrazide-functionalized poly(oligoethylene glycol methacrylate (POEGMA) reactive precursor polymers to facilitate the formation of injectable PO-OLA hydrogels upon mixing with an aldehyde-functionalized POEGMA precursor. The resulting hydrogels are cross-linked via a combination of chemical (hydrazone bond formation) and physical (OLA side-chain self-association) mechanisms, with the competition between the two mechanisms (i.e. increased physical cross-linking results in reduced chemical cross-linking) leading to significant differences in the swelling, mechanical, and degradation properties of the resulting hydrogels. Of particular interest, gel swelling, mechanics, and degradation rate can be independently tuned according to the balance between physical and chemical cross-link formation. Small angle neutron scattering confirms the presence of associative hydrophobic domains inside the hydrogels prepared with OLA macromonomers, with OLA-containing hydrogels exhibiting significantly higher scattering intensities, smaller inhomogeneity sizes, and smaller distances between inhomogeneities relative to hydrogels prepared without OLA macromonomer. The presence of the resulting hydrophobic domains facilitates significantly enhanced loading, reduced burst release, and prolonged sustained release of bovine serum albumin, with protein binding and release directly related to both the length and the density of OLA side-chains present in the hydrogel. Given the *in situ* gelation properties of these materials, the ready tunability of hydrogel properties based on the amount and length of OLA side-chains present, and the degradability of both the chemical and physical cross-linking networks formed within these gels, PO-OLA

hydrogels hold significant promise for sustained delivery of hydrophobic or macromolecular therapeutics.

Acknowledgements

Funding from 20/20: NSERC Ophthalmic Materials Research Network, the Ontario Ministry of Research and Innovation Postdoctoral Fellowship program (NMBS) is gratefully acknowledged. We acknowledge the National Institute of Standards and Technology, U.S. Department of Commerce, in providing the neutron research facilities used in this work as well as Dr. Boualem Hammouda at NCNR for his assistance with the SANS experiments. Certain commercial equipment, instruments, or materials are identified in this paper to foster understanding. Such identification does not imply recommendation or endorsement by the National Institute of Standards and Technology, nor does it imply that the materials or equipment identified are necessarily the best available for the purpose. Furthermore, we acknowledge Jacqueline Chau for her assistance with critical aggregation concentration measurements.

References

1. C. C. Lin and K. S. Anseth, *Pharm. Res.*, **2009**, 26, 631–643.
2. J. L. Drury and D. J. Mooney, *Biomaterials*, **2003**, 24, 4337–4351.
3. N. A. Peppas, J. Z. Hilt, A. Khademhosseini, and R. Langer, *Adv. Mater.*, **2006**, 18, 1345–1360.
4. B. D. Ratner and S. J. Bryant, *Annu. Rev. Biomed. Eng.*, **2004**, 6, 41–75.
5. J. V. Jokerst, T. Lobovkina, R. N. Zare, and S. S. Gambhir, *Nanomedicine*, **2011**, 6, 715–728.
6. H. Otsuka, Y. Nagasaki, and K. Kataoka, *Adv. Drug Deliv. Rev.*, **2012**, 64, 246–255.
7. U. Wattendorf and H. P. Merkle, *J. Pharm. Sci.*, **2008**, 97, 4655–4669.
8. K. Kataoka, A. Harada, and Y. Nagasaki, *Adv. Drug Deliv. Rev.*, **2012**, 64, 37–48.
9. A. Rösler, G. W. M. Vandermeulen, and H.-A. Klok, *Adv. Drug Deliv. Rev.*, **2012**, 64, 270–279.
10. S. Krishnan, C. J. Weinman, and C. K. Ober, *J. Mater. Chem.*, **2008**, 18, 3405–3413.
11. N. A. Peppas, K. B. Keys, M. Torres-Lugo, and A. M. Lowman, *J. Control. Release*, **1999**, 62, 81–87.
12. S. M. Ryan, G. Mantovani, X. Wang, D. M. Haddleton, and D. J. Brayden, *Expert Opin. Drug Deliv.*, **2008**, **5**, 371–383.
13. F. M. Veronese, *Biomaterials*, **2001**, 22, 405–417.
14. C. R. Nuttelman, M. A. Rice, A. E. Rydholm, C. N. Salinas, D. N. Shah, and K. S. Anseth, *Prog. Polym. Sci.*, **2008**, 33, 167–179.
15. J. D. McCall and K. S. Anseth, *Biomacromolecules*, **2012**, 13, 2410–2417.
16. A. A. Aimetti, A. J. Machen, and K. S. Anseth, *Biomaterials*, **2009**, 30, 6048–6054.
17. Y. Fu and W. J. Kao, *J. Biomed. Mater. Res. A*, **2011**, 98, 201–211.
18. M. P. Lutolf and J. A. Hubbell, *Biomacromolecules*, **2003**, 4, 713–722.
19. S. P. Zustiak and J. B. Leach, *Biomacromolecules*, **2010**, 11, 1348–1357.
20. J. J. Roberts and S. J. Bryant, *Biomaterials*, **2013**, 34, 9969–9979.
21. E. A. Phelps, N. O. Enemchukwu, V. F. Fiore, J. C. Sy, N. Murthy, T. a Sulchek, T. H. Barker, and A. J. García, *Adv. Mater.*, **2012**, 24, 64–70.
22. M. W. Toepke, N. A. Impellitteri, J. M. Theisen, and W. L. Murphy, *Macromol. Mater. Eng.*, **2013**, 298, 699–703.
23. N. Cengiz, J. Rao, A. Sanyal, and A. Khan, *Chem. Commun.*, **2013**, **49**, 11191–11193.
24. B. D. Polizzotti, B. D. Fairbanks, and K. S. Anseth, *Biomacromolecules*, **2008**, 9, 1084–1087.

25. M. Malkoch, R. Vestberg, N. Gupta, L. Mespouille, P. Dubois, A. F. Mason, J. L. Hedrick, Q. Liao, C. W. Frank, K. Kingsbury, and C. J. Hawker, *Chem. Commun.*, **2006**, 24, 2774–2776.
26. R. T. Chen, S. Marchesan, R. A. Evans, K. E. Styan, G. K. Such, A. Postma, K. M. McLean, B. W. Muir, and F. Caruso, *Biomacromolecules*, **2012**, 13, 889–895.
27. K. C. Koehler, K. S. Anseth, and C. N. Bowman, *Biomacromolecules*, **2013**, 14, 538–547.
28. D. L. Alge, M. A. Azagarsamy, D. F. Donohue, and K. S. Anseth, *Biomacromolecules*, **2013**, 14, 949–53.
29. G. N. Grover, J. Lam, T. H. Nguyen, T. Segura, and H. D. Maynard, *Biomacromolecules*, **2012**, 13, 3013–3017.
30. H. Saito, A. S. Hoffman, and H. I. Ogawa, *J. Bioact. Compat. Polym.*, **2007**, 22, 589–601.
31. M. Patenaude, N. M. B. Smeets, and T. Hoare, *Macromol. Rapid Commun.*, **2014**, 35, 598–617.
32. X. Zhao and J. M. Harris, *J. Pharm. Sci.*, **1998**, 87, 1450–1458.
33. B. Kim and N. A. Peppas, *Int. J. Pharm.*, **2003**, 266, 29–37.
34. J. A. Burdick, M. N. Mason, A. D. Hinman, K. Thorne, and K. S. Anseth, *J. Control. Release*, **2002**, 83, 53–63.
35. A. J. R. Lasprilla, G. A. R. Martinez, B. H. Lunelli, A. L. Jardini, and R. M. Filho, *Biotechnol. Adv.*, **2012**, 30, 321–328.
36. J. M. Anderson and M. S. Shive, *Adv. Drug Deliv. Rev.*, **2012**, 64, 72–82.
37. J. K. Oh, *Soft Matter*, **2011**, 7, 5096–5108.
38. A. S. Sawhney, C. P. Pathak, and J. A. Hubbell, *Macromolecules*, **1993**, 26, 581–587.
39. A. T. Metters, K. S. Anseth, and C. N. Bowman, *Polymer*, **2000**, 41, 3993–4004.
40. A. T. Metters, K. S. Anseth, and C. N. Bowman, *J. Phys. Chem. B*, **2001**, 105, 8069–8076.
41. A. Metters and J. Hubbell, *Biomacromolecules*, **2005**, 6, 290–230
42. K. S. Anseth, A. T. Metters, S. J. Bryant, P. J. Martens, J. H. Elisseeff, and C. N. Bowman, *J. Control. Release*, **2002**, 78, 199–209.
43. N. M. Shah, M. D. Pool, and A. T. Metters, *Biomacromolecules*, **2006**, **7**, 3171–3177.
44. I. Barakat, P. Dubois, R. Jérôme, P. Teyssié, and E. Goethals, *J. Polym. Sci. Part A Polym. Chem.*, **1994**, 32, 2099–2110.
45. S. J. Buwalda, P. J. Dijkstra, and J. Feijen, *Macromol. Chem. Phys.*, **2012**, 213, 766–775.
46. S. J. Buwalda, L. Calucci, C. Forte, P. J. Dijkstra, and J. Feijen, *Polymer*, **2012**, 53, 2809–2817.
47. C. Hiemstra, Z. Zhong, L. Li, P. J. Dijkstra, and J. Feijen, *Biomacromolecules*, **2006**, **7**, 2790–2795.

48. D. G. Abebe and T. Fujiwara, *Biomacromolecules*, **2012**, 13, 1828–1836.
49. X. Fan, M. Wang, D. Yuan, and C. He, *Langmuir*, **2014**, 46, 14307–14313.
50. M. N. Mason, A. T. Metters, C. N. Bowman, and K. S. Anseth, *Macromolecules*, **2001**, 34, 4630–4635.
51. S. J. Bryant and K. S. Anseth, *J. Biomed. Mater. Res. A*, **2003**, 64, 70–79.
52. N. M. B. Smeets, E. Bakaic, M. Patenaude, and T. Hoare, *Chem. Commun.*, **2014**, 50, 3306–3309.
53. N. M. B. Smeets, E. Bakaic, M. Patenaude, and T. Hoare, 2014. 10.1016/j.actbio.2014.05.035
54. A. W. Jackson and D. a. Fulton, *Polym. Chem.*, **2013**, 4, 31–45.
55. J.-M. Lehn, *Aust. J. Chem.*, **2010**, 63, 611–623.
56. J.-F. Lutz, *Adv. Mater.*, **2011**, 23, 2237–2243.
57. J.-F. Lutz and A. Hoth, *Macromolecules*, **2006**, 39, 893–896.
58. S. Sun and P. Wu, *Macromolecules*, **2013**, 46, 236–246.
59. K. Ishimoto, M. Arimoto, T. Okuda, S. Yamaguchi, Y. Aso, H. Ohara, S. Kobayashi, M. Ishii, K. Morita, H. Yamashita, and N. Yabuuchi, *Biomacromolecules*, **2012**, 13, 3757–3768.
60. Y. An, L. Zhang, S. Xiong, S. Wu, M. Xu, and Z. Xu, *Colloids Surf. B. Biointerfaces*, **2012**, 92, 246–253.
61. R. T. Azuah, L. R. Kneller, Y. Qui, P. L. W. Tregenna-Piggott, C. M. Brown, J. R. D. Copley, and J. Dimeo, *J. Res. Natl. Inst. Stan. Technol.*, **2009**, 114, 341–358.
62. S. Lin-gibson, R. L. Jones, N. R. Washburn, and F. Horkay, *Macromolecules*, **2005**, 7, 2897–2902.
63. T. Matsunaga, T. Sakai, Y. Akagi, U. Chung, and M. Shibayama, *Macromolecules*, **2009**, 10, 1344–1351.
64. Ö. Topel, B. A. Çakır, L. Budama, and N. Hoda, *J. Mol. Liq.*, **2013**, 177, 40–43.
65. M. Shibayama, *Macromol. Chem. Phys.*, **1998**, 30, 1–30.
66. S. Mallam, *Macromolecules*, **1989**, 4, 3356–3361.
67. M. Shibayama, *Polym. J.*, **2010**, 43, 18–34.
68. N. S. Davidson, R. W. Richards, and A. Maconnachiet, *Macromolecules*, **1986**, 2, 434–441.
69. S. K. Agrawal, N. Sanabria-Delong, P. R. Jemian, G. N. Tew, and S. R. Bhatia, *Langmuir*, **2007**, 23, 5039–5044.
70. S. C. Semple, A. Chonn, and P. R. Cullis, *Adv. Drug Deliv. Rev.*, **1998**, 32, 3–17.
71. A. Chonn, S. C. Semple, and P. R. Cullis, *J. Biol. Chem.*, **1992**, 267, 18759–18765.
72. L. B45:B105M. Weber, C. G. Lopez, and K. S. Anseth, J. Biomed. Mater. Res. A, **2009**, 90, 720–9.

SUMMARY AND RECOMMENDATIONS FOR FUTURE WORK

Summary of Thesis. Chapter 1 of this thesis provides an exhaustive overview of the different covalent *in situ* cross-linking chemistries employed to date as described in the literature. In this contribution, I specifically chose to focus on chemistries that can be used to develop co-injectable pre-functionalized polymeric precursors that can spontaneously form intermolecular chemical cross-links for rapid *in situ* gel formation.

Chapter 2 describes the development of an *in situ* forming hydrogel system based on PNIPAM. Once formed, these hydrogels retain the environmentally responsive (i.e. temperature dependent) physical properties of conventional PNIPAM gels. The selection of hydrazone cross-linking chemistry was made deliberately in order to afford gels that would form rapidly and yet degrade slowly over a clinically relevant time frame (over a period of months). *In vitro* studies have shown that the precursors (i.e. degradation products) of these gels are well tolerated by 3T3 mouse fibroblasts as well as human retinal epithelial cells, even at very high concentrations that are well outside of the range that would be experienced in a real application of these materials.

Chapter 3 focuses on fine-tuning a number of the physical properties of the hydrogels described in Chapter 2 by replacing more reactive aldehydes with less reactive ketones as the electrophilic moieties in the cross-linking chemistry. The work in Chapter 2 describes hydrogels that form very rapidly (< 10 seconds) following coextrusion of 6 wt% (m/v) aqueous solutions of aldehyde and hydrazide functionalized PNIPAM precursors. The resulting gels are opaque at room temperature, implying the presence of heterogeneities

within the hydrogels that are capable of scattering light. Beyond their effect on the gels' optical properties, it is possible that these regions of heterogeneity could lead to irreproducible cell differentiation or drug delivery properties if employed in those applications. By using slower cross-linking ketones, the rate of gel formation was decreased, providing polymer chains with ample time to evenly diffuse through the gel matrix prior to cross-linking and thereby enabling fabrication of hydrogels with more uniform matrices. By varying the ratio of ketone to aldehyde functionalities in the electrophilic PNIPAM precursor polymers, gel formation and degradation kinetics, gel mechanical properties, and the degree of gel opacity can all be controlled. Most substantially, by increasing the total electrophile content of polymer precursors functionalized exclusively with ketone groups (i.e. no aldehydes present), it is possible to retain a number of the properties of the gels described in Chapter 2 (specifically, mechanical properties) while increasing the optical transparency of the gels compared with those made from aldehyde-only electrophilic precursor chains. Furthermore, the higher electrophilic ketone pre-polymers were demonstrated to be better tolerated than conventional aldehyde-only electrophilic PNIPAM chains.

Chapter 4 of this thesis describes some of the earliest work undertaken during the tenure of my Ph.D. This work expands upon the basic conventional PNIPAM hydrogels described in Chapter 2 by incorporating different ratios of charged and uncharged polysaccharides as the electrophilic precursor polymers constituting the hydrogel matrices. By employing this "modular", mix-and-match approach to hydrogel design, specifically by varying the ratio of aldehyde-functionalized dextran (an uncharged

polysaccharide) and aldehyde-functionalized carboxymethyl cellulose (a polyanionic polysaccharide) precursors used to prepare the hydrogels, a number of hydrogel properties including gel swelling, degradation, drug partitioning and loading, and mechanical properties could be precisely tuned, in many cases in predictable ways based on the simple rule of mixtures relative to the pure component hydrogel properties. This approach facilitates the *a priori* design of hydrogels with well-defined properties by simple mixing of reactive precursors instead of requiring new chemistry.

Chapter 5 describes the rational design of hydrogel precursor polymers for a specific target application, in this case the delivery of hydrophobic or hydrophobic-associative therapeutic targets typically difficult to deliver effectively with hydrogels. In this case, the reactive precursors were prepared using a methacrylate (monomeric, polymerizable) analogues of polyethylene glycol (POEGMA) and poly(lactic acid) (POLA) with varying PLA chain lengths for the controlled release of protein drugs. Loading of the fat-carrying protein bovine serum albumin as well as the swelling and mechanics of the hydrogel could be tuned depending on both the overall content of PLA inside the hydrogel and the length of each PLA side-chain. This approach represents a unique strategy to impart well-defined chemical domains directly into hydrogels that can self-assemble on the same time scale as gelation, leading to potentially new and useful morphologies.

Future work. Much of the work described in this thesis focuses on the development of injectable hydrogels that can be tuned to fit a number of biomaterials applications. Moving forward, I would like to expand beyond the manipulation the hydrogels' physical properties and focus on therapeutic applications, particularly drug delivery. PNIPAM has gained a great deal of interest in the literature because of its ability to potentially entrap pre-loaded drug, creating a diffusional barrier to therapeutic release; however, in application, PNIPAM's collapse at physiological temperatures tends to result in a mass efflux of pre-loaded drug toward the surrounding environment, limiting the ability of these hydrogels to be effectively pre-loaded with drug for long term therapeutic effect. In order to address this, I am currently working in collaboration with Rachelle Kleinberger on generating poly(N-hydroxyethylacrylamide)-*b*-poly(N-isopropylacrylamide) precursor copolymers synthesized using reversible addition-fragmentation chain transfer (RAFT) polymerization. In these systems, complimentary PNIPAM chains will be given either electrophilic or nucleophilic functionality as described in Chapter 2. Once co-extruded *in vivo*, we anticipate that these systems will rapidly form hydrazone cross-linked hydrogels but with entrapped hydrophilic poly(N-hydroxyethylacrylamide) chains immobilized throughout the matrix that can provide an affinity domain for pre-loaded hydrophilic drug. Such a morphology should reduce burst effect and thus significantly improve the release kinetics of therapeutics loaded into PNIPAM hydrogels, which are an otherwise attractive biomaterial.

Chapter 4's work on modular mixed natural-synthetic hydrogels was carried out without assessing *in vivo* biological activity toward the material. Given the ability to tune a

number of gel parameters, which are largely based on differences in negative charge content within the different gels offered by CMC, we may be able to exercise control over cell fate/migration in the presence of these gels following introduction. I believe that this work would be a significant contribution to the rational design of hydrogels for tissue engineering applications.

The work carried out in Chapter 5 dealt with the loading and release of BSA, a large molecule, from gels functionalized with PLA moieties, which act as hydrophobic reservoirs. In future work, we may explore the release of small molecule hydrophobic drugs from such a system (such as dexamethasone).

In general, it would be interesting to establish routes of elimination of synthetic polymers within the body. We have designed our systems to biodegrade, but it is important to establish the ultimate fate of these materials in order for them to attain clinical relevance.